2013-05-13

Elucidating the Molecular Mechanism of CYLD-Mediated Necrosis: A Dissertation

David M. Moquin
University of Massachusetts Medical School Worcester

ELUCIDATING THE MOLECULAR MECHANISM OF CYLD-MEDIATED NECROSIS

A Dissertation Presented

By

David Mark Moquin

Submitted to the Faculty of the
University of Massachusetts Graduate School of Biomedical Sciences, Worcester
in partial fulfillment of the requirements for the degree of

DOCTOR OF PHILOSOPHY

May 13, 2013

IMMUNOLOGY VIROLOGY PATHOLOGY PROGRAM

ELUCIDATING THE MOLECULAR MECHANISM OF CYLD-MEDIATED NECROSIS

A Dissertation Presented
By

David Mark Moquin

The signatures of the Dissertation Defense Committee signify completion and approval as to style and content of the Dissertation

_____
Francis Ka-Ming Chan Ph.D., Thesis Advisor

_____
Jason Chen Ph.D., Member of Committee

_____
Kenneth Rock M.D., Member of Committee

_____
Neal Silverman Ph.D., Member of Committee

_____
Ralph Budd M.D., Member of Committee

The signature of the Chair of the Committee signifies that the written dissertation meets the requirements of the Dissertation Committee

_____
Leslie Berg Ph.D., Chair of Committee

The signature of the Dean of the Graduate School of Biomedical Sciences signifies that the student has met all graduation requirements of the school. (Signature)

_____
Anthony Carruthers, Ph.D.,
Dean of the Graduate School of Biomedical Sciences

Immunology Virology Pathology

May 13, 2013

"I went to the woods because I wished to live deliberately, to front only the essential facts of life, and see if I could not learn what it had to teach, and not, when I came to die, discover that I had not lived. I did not wish to live what was not life, living is so dear; nor did I wish to practise resignation, unless it was quite necessary. I wanted to live deep and suck out all the marrow of life, to live so sturdily and Spartan- like as to put to rout all that was not life, to cut a broad swath and shave close, to drive life into a corner, and reduce it to its lowest terms, and, if it proved to be mean, why then to get the whole and genuine meanness of it, and publish its meanness to the world; or if it were sublime, to know it by experience, and be able to give a true account of it in my next excursion."—
Henry David Thoreau (an excerpt from Walden)

This work is dedicated to my beloved grandmother Mary S. Bouffard (3/11/37-5/21/13)

Acknowledgements

I would first and foremost like to thank my thesis advisor Dr. Francis Chan. Over the years he has been a very diligent mentor and has greatly impacted my development as a scientist. Working with Francis has undoubtedly helped me become a better learner, which has not only helped with my confidence, but has also helped me become a happier person. Some of the most indelible and potent learning experiences I have had were during group meetings when Francis would share his scientific approaches to addressing a wide range of questions. I consider it an honor to have had the opportunity to learn from such a gifted scientist, and I'm extremely grateful for all of his support throughout the years. I would also like to thank other members of the Chan lab both present and past: Kenta Moriwaki, Thomas McQuade, Sakthi Balaji, and YoungSik Cho. I truly enjoyed working with and learning from these individuals.

I would also like to thank the members of my thesis advisory committee, Leslie Berg, Neal Silverman, Kenneth Rock, and Jason Chen for taking time out of their busy schedules to help guide me in the right direction. I would also like to thank Ralph Budd for agreeing to be my outside dissertation committee member and the accompanying sacrifice in time he has had to make.

I have a number of friends and colleagues at UMass that I would like to thank for being supportive in many ways over the years. I would specifically like to thank: Varun Kapoor, HyunMu Shin, Stina Urban, Ribhu Nayar, Greg Orlowski, Milan Patel, Tia Bumpus, Laurie Kenney, Amanda Prince, and Peter Trenh. These people significantly contributed to the positive experience I had during my time at UMass, and I will miss all of them.

Finally, I would like to thank my family for always rooting for me, caring about the pursuit of my dreams, and endless support over the years. The successful completion of this work would not have been possible without their presence in my life. I have very fond memories from my childhood, which have provided me with one of the highest forms of education available.

TABLE OF CONTENTS

Title i

Signature Page ii

Acknowledgements iv

Table of Contents vi

List of Figures ix

List of Tables xi

ABSTRACT xii

PREFACE TO CHAPTER I 1

INTRODUCTION 2

A brief comparison between apoptosis and programmed necrosis 3

Biological relevance of programmed necrosis 6

Signaling mechanisms required for programmed necrosis 15

RIP1 ubiquitination and transition to the DISC 29

CYLD in the context of myriad biological processes 42

Current understanding of CYLD in cell death signaling 49

Thesis objective 51

PREFACE TO CHAPTER II 54

CHAPTER II: Identifying new regulators of programmed necrosis 55

Introduction 56

Results

CYLD and FUS1 are putative regulators of necrosis 58

Discussion 65

Materials and methods 69

PREFACE TO CHAPTER III 71

CHAPTER III: Characterization of the requirement of CYLD in necrosis 72

Introduction 73

Results

CYLD promotes but is not essential for TNFα-induced programmed necrosis 77

CYLD is dispensable in other cell death pathways 78

Discussion 91

Materials and methods 95

Preface to CHAPTER IV 98

Introduction 100

Results

CYLD does not control RIP1 ubiquitination within the TNFR-1 complex 104

Deubiquitination of RIP1 by CYLD facilitates programmed necrosis 105

CYLD regulates RIP1 ubiquitination in a spatially and temporally distinct compartment 107

CYLD controls the kinetics of necrosome formation and activation 108

Ubiquitination hinders RIP1 autophosphorylation 111

Phosphorylated CYLD associates with RIP1 during necrosis 112

CYLD interaction with RIP1 is indirect 113

Discussion 137

Materials and Methods 142

PREFACE TO CHAPTER V 147

CHAPTER V: DISCUSSION 148

Overview 149

The involvement of CYLD in TNFα-induced cell death 150

CYLD-mediated regulation of the necrosome 154

RIP1 ubiquitination in the necrosome 157

Implications of CYLD phosphorylation 161

PREFACE TO APPENDIX 170

APPENDIX: Cancer gene siRNA library screen data 171

A compilation of the screen data 172

References 223

LIST OF FIGURES

Figure 1.1 Current model of necrosis signaling pathway 26

Figure 1.2 Factors that regulate RIP1 ubiquitination and cell death.....32

Figure 1.3 SMAC mimetic mechanism for enhancesment of cell death 33

Figure 1.4 Current model of CYLD-mediated necrosis.....53

Figure 2.1 Tumor suppressor plate 1b 61

Figure 3.1 Partial protection against TNFα-induced necrosis by CYLD siRNAs 81

Figure 3.2 Residual TNFα-induced necrosis and apoptosis in $CYLD^{-/-}$ MEFs.....83

Figure 3.3 CYLD is not involved in other death inducing stimuli in MEFs 85

Figure 3.4 RIP1-dependent necrosis occurs in $CYLD^{-/-}$ MEFs 87

Figure 3.5 CYLD impacts TNFα-induced ROS production.....89

Figure 4.1 CYLD does not regulate RIP1 ubiquitination in the TNFR-1 complex.....115

Figure 4.2 CYLD deubiquitinase activity and CG3 are required for TNFα-induced necrosis 117

Figure 4.3 Poly-ubiquitinated RIP1 is the major substrate for CYLD in TNFα-induced necrosis 119

Figure 4.4 CYLD regulates the ubiquitination status of RIP1 in the necrosome 121

Figure 4.5 CYLD regulates the kinetics of RIP1-RIP3 necrosome assembly 123

Figure 4.6 CYLD regulates the kinetics of assembly for multiple components of the necrosome 125

Figure 4.7 Impaired RIP1 and RIP3 phosphorylation in the absence of CYLD.....127

Figure 4.8 Induction of RIP1 associated kinase activity in the NP-40 insoluble compartment 129

Figure 4.9 Poly-ubiquitinated RIP1 is a poor substrate for autophosphorylation.....131

Figure 4.10 RIP1 kinase dependent phosphorylation of CYLD during TNFα-induced necrosis 133

Figure 4.11 CYLD does not directly bind to RIP1 or RIP3.....135

Figure 5.1 Revised model for CYLD-mediated necrosis.....165

Figure 5.2 Tentative model for overlapping pro-necrotic and pro-apoptotic function of CYLD.....166

Figure 5.3 Potential impact of hyperubiquitinated RIP1 167

Figure 5.4 Potential effects of CYLD phosphorylation.....168

Figure 5.5 Potential CYLD phosphorylation mechanism in the context of TNFR-1 signaling.....169

LIST OF TABLES

Table 2.1A-C Putative regulators of necrosis from the initial screen……62

ABSTRACT

TNFα-induced programmed necrosis is a caspase-independent cell death program that is contingent upon the formation of a multiprotein complex termed the necrosome. The association of two of the components of the necrosome, receptor interacting protein 1 (RIP1) and RIP3, is a critical and signature molecular event during necrosis. Within this complex, both RIP1 and RIP3 are phosphorylated which are consequential for transmission of the pro-necrotic signal. Namely, it has been demonstrated that RIP3 phosphorylation is required for binding to downstream substrates. Nevertheless, the regulatory mechanisms governing necrosome activation remain unclear. Since necrosis is implicated in a variety of different diseases, understanding the biochemical signaling pathway can potentially yield future drug targets. I was interested in identifying other regulators of necrosis in hope of gaining a better understanding of the necrosis signaling pathway and regulators of the necrosome. To address this, I screened a cancer gene siRNA library in a cell line sensitive to necrosis. From this, I independently identified CYLD as a positive regulator of necrosis. Previous studies suggest that deubiquitination of RIP1 in the TNF receptor (TNFR)-1 signaling complex is a prerequisite for transition of RIP1 into the cytosol and assembly of the RIP1-RIP3 necrosome. The deubiquitinase cylindromatosis (CYLD) is presumed to promote programmed necrosis by facilitating RIP1 deubiquitination in this membrane receptor complex. Surprisingly, I found that TNFα could induce RIP1-dependent necrosis in $CYLD^{-/-}$ cells. I show that CYLD does not regulate RIP1 ubiquitination at the receptor complex. Strikingly, assembly of the RIP1-RIP3 necrosome was delayed, but not abolished in the absence of CYLD. In addition to the TNFR-1 complex, I found that RIP1 within the necrosome was also

ubiquitinated. In the absence of CYLD, RIP1 ubiquitination in the NP-40 insoluble necrosome was greatly increased. Increased RIP1 ubiquitination correlated with impaired RIP1 and RIP3 phosphorylation, a signature of kinase activation. My results show that CYLD regulates RIP1 ubiquitination in the NP-40 insoluble necrosome, but not in the TNFR-1 signaling complex. Contrary to the current model, CYLD is not essential for necrosome assembly. Rather, it facilitates RIP1 and RIP3 activation within the necrosome and the corollary is enhancement of necrosome functionality and subsequent necrosis. My results therefore indicate that CYLD exerts its pro-necrotic function in the NP-40 insoluble necrosome, and illuminates the mechanism of necrosome activation.

PREFACE TO CHAPTER I

List of author contributions:

David Moquin: All of the work in this chapter

CHAPTER I: Introduction

A brief comparison between apoptosis and programmed necrosis

Programmed cell death is a critical function for the maintenance of cellular homeostasis. Indeed, the emergence of multicellular organisms was likely contingent upon development of cell suicide programs to eliminate superfluous cells, damaged cells, pathogen infected cells, and transformed cells. It is not surprising that cell death is a lynchpin in a multitude of both physiological and patho-physiological contexts. The requirement of programmed cell death begins during embryogenesis and persists throughout the organism's lifetime. Indeed there are numerous examples of disastrous consequences attributed to the perturbation of cell death programs. For instance, loss of function mutations in the death receptor Fas (CD95), are responsible for causing autoimmune lymphoproliferative syndrome (ALPS). The clinical manifestations of this disease include splenomegaly, lymphadenopathy, accumulation of an atypical mature T cell population that is double negative, autoimmunity, and increased probability of hematological tumors (Oliveira et al., 2008).

Over the years apoptosis has become synonymous with programmed cell death while necrosis has been associated with an unregulated form of cell death. This is logical considering apoptosis was the first name coined for programmed cell death and later was the first to be defined both genetically and biochemically (Kerr et al., 1972; Vaux et al., 1988; Yuan et al., 1992). However, even to this day many scientists still think of necrosis as an accidental form of cell death rather than programmed. Over the past several years mounting evidence has resulted in an increasing recognition of necrosis as a programmed form of cell death. Depending on the group, it is either referred to as "programmed

necrosis" or "necroptosis", which will hereafter be referred to as necrosis in the rest of this document (Chan et al., 2003; Degterev et al., 2005).

One of the first studies suggesting that necrosis was programmed was in 1988. This group tested a variety of cell-lines for sensitivity to TNFα-induced cell death and used time-lapse videos in conjunction with chromium release or tritiated thymidine release assays to define loss of plasma membrane integrity or nuclear disintegration, respectively. This study demonstrated that TNFα induced different types of cell death depending on the cell-line. Some cells underwent cell death with apoptotic morphology and others underwent cell death with necrotic morphology (Laster et al. 1988). Another seminal finding, which supported necrosis qualifying as a type of programmed cell death, was that caspase-inhibition enhances TNFα-induced reactive oxygen species (ROS) production and necrotic cell death in the murine fibrosarcoma cell-line L929. Importantly, cell death was completely blocked when treated with a ROS scavenger. This established that necrosis is a caspase-independent cell death program and requires the generation of ROS for execution. It also provided evidence that the necrosis signaling pathway is distinct from the apoptosis, which requires caspases (Vercammen et al., 1998).

Over the past several years it has been revealed that necrosis can be initiated by a variety of different stimuli such as death receptors, pattern recognition receptors, virus infection, chemotherapeutic agents, and oxidative stress. Hence, one of the major goals of the field has been to determine the core components of the necrotic machinery or independent signaling pathways that lead to the same type of cellular demise

(Vandenabeele et al., 2010; Vanlangenakker et al., 2012). The discovery that the serine threonine kinases Receptor Interacting Protein 1 and 3 (RIP1/RIP3) are required for TNFα-induced necrosis provided the incipient illumination of the biochemical pathway (Chan et al., 2003; Cho et al., 2009, He et al., 2009; Holler et al., 2000; Zang et al., 2009). The molecular details will be covered later in this chapter.

An accurate epithet of programmed necrosis is "Explosive cell death." As mentioned earlier, necrosis is a caspase-independent form of cell death. Necrotic cells exhibit signs of both organelle and cellular swelling (oncosis), increased translucence of cytoplasm, irregular chromatin condensation, and eventually loss of plasma membrane integrity and release of the cellular contents into the surrounding extracellular environment (Vandenabeele et al., 2010). Importantly, necrosis is a pro-inflammatory form of cell death because of the release of danger associated molecular patterns (DAMPs) such as Monosodium urate (MSU) microcrystals, ATP, and HMGB1. The ramifications of the release of DAMPs from necrotic cells are activation of both the innate and adaptive immune responses. DAMPs elicit dendritic cell activation and subsequent homing to the lymph node where adaptive immune responses to dead cell associated antigens can be initiated. Furthermore, DAMPS can also influence the production of cytokines such as the case with MSU and IL-1 production. IL-1 signaling is particularly important in the inflammatory response initiated by dead cells (Rock et al., 2011).

A suitable epithet of apoptosis is "Bubbly cell death." Apoptosis is a caspase-dependent pathway triggered by a myriad of stimuli such as death receptors, growth

factor withdrawal, cellular stress, and viral infection. Caspases are cysteine proteases that cleave after aspartate residues. They are zymogens, which get activated by signals leading to autoprocessing of apical or initiator caspases followed by a proteolytic casade. Namely, these caspases cleave and activate executioner caspases that target multiple cellular proteins for cleavage, which leads to apoptotic cell death (Boatright et al., 2003). Unlike necrotic cells, apoptotic cells maintain plasma membrane integrity, but lose control over separating components between the inner leaflet and outer leaflet of the plasma membrane. Namely, phosphatidylserine, which is normally restricted to the inner leaflet of the plasma membrane, is also found in the outer leaflet during apoptosis. This acts as an "eat me" signal for professional phagocytic cells (Fadok et al., 1992). Apoptotic cells also round up and exhibit pyknosis, which is loss of cell volume. The plasma membrane blebs, and packages intact organelles inside; thereby, facilitating the phagocytic process. Therefore, under normal conditions apoptotic cells are cleared. Apoptotic cells are also morphologically characterized by chromatic condensation, and DNA fragmentation (karyorrhexis) due to caspase activated deoxyribonuclease (CAD) (Enari et al., 1998; Wyllie et al., 1980). Prior to caspase activation, CAD is latent in the cytosol via interaction with inhibitor of caspase activated deoxyribonuclease (ICAD). During apoptosis, activated caspases cleave ICAD, thereby liberating CAD to translocate to the nucleus and degrade DNA (Enari et al., 1998).

Biological relevance of programmed necrosis

The most compelling evidence for a physiological circumstance when necrosis is important is during viral infection. Conceptually, the most straightforward function of necrosis is to eliminate cells infected with viruses, which have successfully subverted apoptosis, the default cell death program (Challa et al., 2010). One of the first examples of necrosis functioning in a viral context was demonstrated with vaccinia virus infection. Mouse fibroblasts infected with vaccinia virus become sensitized to TNFα-induced necrosis. Vaccinia virus encodes the caspase inhibitor B13R/Spi2. Interestingly, mutant vaccinia virus lacking this caspase inhibitor was shown to be defective in stimulating mouse fibroblasts to undergo TNFα-induced necrosis (Li et al., 2000). This suggested that necrosis is a second cell suicide program to eliminate viral propagation. Importantly, both T cells and MEFs deficient of RIP3 were protected from TNFα-induced necrosis during vaccinia virus infection. Furthermore, RIP3 deficient mice have impaired control over vaccinia virus infection as indicated by an increase in viral titer and death. Hence, RIP3-mediated necrosis plays a role in controlling vaccinia virus infection with the driver being TNFα (Cho et al., 2009).

In addition to vaccinia virus infection, studies have shown that necrosis also plays an anti-viral role during murine cytomegalovirus (MCMV) infection. Interestingly, MCMV is able to inhibit death receptor and PRR induced NFκB activation, apoptosis, and necrosis through viral inhibitor of RIP1 activation (vIRA), which is a protein encoded by the M45 gene (Mack et al., 2008; Upton et al., 2008; Upton et al., 2010; Upton et al., 2012). vIRA contains a RIP Homotypic interaction Motif (RHIM), which allows binding and inhibition of RIP1 and RIP3 function (Upton et al., 2008). RIP1/RIP3

both contain a RHIM, which allows their association and is required for their TNFα driven pro-necrotic function (Cho et al., 2009). vIRA binding to RIP1 is required for its suppression of both TNFα and TRIF dependent apoptosis (Upton et al., 2008). vIRA can also block TNFα-induced necrosis and TLR3-induced NFκB activation (Mack et al., 2008). Recombinant viruses containing M45, with mutations in the RHIM (M45mutRHIM) that abolish binding, were unable to control necrosis and therefore resulted in severe attenuation of the strains. Importantly, infection of RIP3 knock-mice restored virulence of the recombinant virus demonstrating that RIP3-mediated necrosis is an important anti-viral mechanism in the context of MCMV infection (Upton et al., 2010). Unlike death receptor induced-necrosis, MCMV mediated necrosis is RIP1-independent. This was clarified when it was demonstrated that RIP3 forms RHIM-mediated interactions with the cytosolic DNA-dependent activator of interferon regulatory factors (DAI) sensor, presumably circumventing the requirement of RIP1 for RIP3 activation. Similar to infection of RIP3 knock-out mice, recombinant MCMV M45mutRHIM infection is no longer attenuated in DAI knock-out mice. This highly suggests that vIRA normally suppresses DAI mediated necrosis through RHIM-mediated interactions with DAI and RIP3. Since it is well established that RIP1 is upstream of RIP3 kinase activation in death receptor induced necrosis, this study provides evidence that other RHIM containing upstream activators of RIP3 can substitute for RIP1 (Upton et al., 2010; Upton et al., 2012). MCMV also encodes viral inhibitor of caspase-8 activation (vICA) as well as other inhibitors of programmed cell death demonstrating that other types of cell death must be evaded by MCMV (Skaletskaya et al., 2001).

There is also evidence that necrosis can be inimical to the health of the organism in certain contexts. For example, it is well known that necrotic cell death of neurons is a later stage consequence of ischemic reperfusion, making it an attractive target for therapeutic intervention. Several years ago Junying Yuan's group screened a small chemical inhibitor library for necrosis, and identified the allosteric inhibitor of RIP1 kinase activity, Necrostatin-1 (Nec-1) (Degterev et al., 2005; Degterev et al., 2008). Through structural activity relationship necroptosis assays they determined that alterations of specific chemical groups of Nec-1, which abrogated the anti-necrosis activity also abrogated Nec-1 inhibition of RIP1 kinases activity. Furthermore, analogs with a reduced IC_{50} in necroptosis cell death assays also demonstrated enhanced inhibition of RIP1 kinase activity. This provided compelling evidence that the anti-necrosis activity of Nec-1 is attributed to inhibition of RIP1 kinase activity. In a mouse model of ischemia brain injury, Nec-1 treatment alleviated infarct volume (Degterev et al., 2005). Altogether, this study was the first to demonstrate that the necrosis pathway can be targeted for therapeutic intervention by inhibition of a critical kinase.

In line with the requirement of RIP1 kinase activity to potentiate death receptor driven necrosis, auto-phosphorylation of RIP1 at Serine 161 is also required. Indeed, cells harboring a serine to alanine mutation at amino acid position 161 of RIP1, which abrogates auto-phosphorylation, have attenuated necrosis. In fact, thus far all of the RIP1 auto-phosphorylation sites identified are contained within the N-terminal kinase domain of RIP1. This suggests that auto-phosphorylation may regulate RIP1 kinase activity. Indeed, mutant RIP1 S161A has impaired kinase activity *in vitro*. This residue is within

the activation segment (T-loop), which occludes ATP access of the catalytic cleft. Through molecular modeling this group proposed that Nec-1 inhibits RIP1 kinase activity through stabilizing the inactive conformation of the T-loop. Indeed, the phospho-mimetic mutant RIP1 S161E that theoretically destabilizes the inactive state of the T-loop is no longer sensitive to Nec-1 inhibition in both kinase assays and necroptosis assays (Degterev et al., 2008).

Necrosis can also have a multitude of deleterious effects when components of the apoptotic machinery are absent. A number of studies have pointed to the requirement of components of the apoptotic machinery in actively suppressing necrosis in different cellular contexts. Reports have indicated that T cell specific deletion of key regulators of death receptor induced-apoptosis such as FADD and Capase-8 results in a proliferation defect (Ch'en et al., 2011; Lu et al. 2011). This is contrary to the expectation of the loss of pro-death regulators. This phenotype is explained by the pro-survival role of these apoptosis regulators, which is attributed to negative regulation of necrosis. Namely, T cell stimulation results in the cleavage and inactivation of RIP1/RIP3 by the pro-apoptotic proteins. In T cells replete with FADD/Caspase-8 the necrosis pathway is actively suppressed. In agreement with this model, reconstitution of RIP1 deficient Jurkat T cells with a cleavage resistant mutant RIP1 shifts TNFα-driven cell death from apoptosis to necrosis. This provides evidence that caspase mediated cleavage of RIP1 negatively regulates its pro-necrotic function in T cells. Furthermore, using an *in vivo* mouse system with conditional expression of a dominant negative form of FADD (FADDdd) in T cells it was demonstrated that the proliferation defect could be rescued by

crossing the mice to RIP3 knock-mice (Lu et al., 2011). Similarly, T cells from mice with a conditional knock-out of FADD or Caspase-8 were rescued from a proliferation defect via treatment with Nec-1 or genetic ablation of RIP3, respectively (Ch'en et al., 2011; Osborn et al., 2010). Altogether these studies demonstrated that the apoptotic regulators FADD and caspase-8 are required to actively suppress necrosis during T cell stimulation. Furthermore, these double-knockout mice with rescued T cell proliferation developed lymphoadenopathy indicating that these cell death regulators are important for maintenance of T cell homeostasis (Lu et al., 2011).

The requirement of the apoptotic machinery for actively suppressing the necrosis program was also found to be important during other physiological contexts such as embryogenesis and colon epithelial cell homeostasis. Mice that are deficient of either FADD, Caspase-8, cFLIP are embryonic lethal. This is seemingly counterintuitive considering that FADD and Caspase-8 are pro-apoptotic proteins and therefore the removal of such proteins should in theory promote cell survival. Several groups provided an answer to this conundrum through establishing the importance of these proteins as negative regulators of excess necrosis during embryogenesis. Namely, developing double knock-out mice that lacked both FADD/RIP1 or caspase-8/RIP3 was able to rescue the embryonic lethality of the FADD or caspase-8 single knock-outs (Kaiser et al., 2011; Oberst et al., 2011; Zhang et al., 2011). However, the embryonic lethality of cFLIP knock-out embryos cannot be rescued by developing cFLIP/RIP3 double knock-out mice because they are also embryonic lethal. Astonishingly, cFLIP/RIP3/FADD triple knock-out mice are viable. This is attributed to the fact that cFLIP(L) inhibits both apoptosis

and necrosis and therefore the cFLIP/RIP3 double knock-out embryos undergo extensive apoptosis during embryogenesis, hence they are still embryonic lethal (Dillon et al., 2012).

cFLIP(L) and caspase-8 form a heterodimeric complex that is required for necrosis suppression during embryogenesis (Oberst et al., 2011). One of the initial reports leading to this discovery was that bacterial artificial chromosome (BAC) transgene expression of a mutant caspase-8, which is resistant to cleavage between the large and small subunits, is sufficient to rescue the lethality of caspase-8 knock-out embryos (Kang et al., 2008). The caspase-8 cleavage mutant is unable to form active homodimers, which are required for promoting apoptosis. Interestingly, through *in vitro* cleavage assays it was demonstrated that although the cleavage resistant mutant was unable to form active homodimers, when force heterodimerized with $cFLIP_L$ it still maintained the potential to cleave RIP1. Although, the Caspase-8 cleavage mutant lost its pro-apoptotic function, it still maintained its anti-necrotic function in a cFLIP-dependent manner. Since active caspase-8 homodimers are required for mediating apoptosis this study demonstrated that the pro-apoptotic and anti-necrotic (pro-survival) function of caspase-8 are not inextricably linked. Importantly, the formation of cFLIP(L)/caspase-8 complexes is required during embryogenesis in order to actively suppress necrosis by cleaving RIP1 and RIP3. In agreement with T cell conditional knock-out studies, early on the RIP3/caspase-8 double knock-out mice have normal mature T cells; however, older mice develop phenotypic aspects of the lympho-proliferative disorder found in patients and mice that have functionally impairing

mutations of Fas or FasL. Namely, this results in the accumulation of B220+CD3+CD4-CD8- cells (Lu et al., 2011; Oberst et al., 2011).

Similar to embryogenesis, conditional deletion of FADD in intestinal epithelial cells leads to excess necrosis. The corollary of excess necrosis is loss of colon integrity, the development of spontaneous colitis, enteritis of the small intestine, and loss of paneth cells. Several lines of evidence support the notion that excess necrosis is the culprit. First, FADD deletion in intestinal epithelial cells leads to non-apoptotic death of crypt epithelial cells as determined by the lack of active caspase-3 staining in the epithelium. Second, the morphology of the cell death, as revealed by electron microscopy, was necrotic. Third, crossing the FADD conditional knock-out mice to the RIP3 or cylindromatosis (CYLD) knock-out mice was able to rescue the colitis phenotype. As these are both regulators of necrosis, it strongly suggests that the epithelial cell non-apoptotic death was indeed necrosis. However, the phenotype was only partially rescued by crossing the mice to TNFα knock-out mice. This may be attributed to the fact that other ligands can give rise to necrosis. The colitis phenotype could be reverted in a germ free environment, or crossing with MYD88 KO mice, which is an important regulator downstream of many Toll-Like Receptors (TLRs). This supports the notion that FADD is required to actively suppress necrosis of colon epithelial cells; loss of FADD results in excessive necrosis, loss of colon integrity, leading to invasion of the mucosa with the gut microflora, which activates TLR-driven production of pro-inflammatory cytokines, and ultimately chronic inflammation (Welz et al., 2011).

In the FADD conditional knock-out system there were some differences in the molecular determinants of pathology in the large intestine and small intestine. FADD conditional knock-out mice developed enteritis (small intestine inflammation), compromised small intestine architecture, and loss of paneth cells, which could be rescued by RIP3 deficiency. However, unlike the colitis phenotype this could not be rescued by crossing to CYLD knock-out mice or a germ free environment. These differences in molecular requirements for necrosis driven disease pathogenesis may be attributed to differential stimuli driving cell death in the colon as opposed to cell death in the small intestine (Welz et al., 2011). As mentioned above, in certain contexts of necrosis induction, regulators such as RIP1 are dispensable. It is therefore conceivable that in these cases CYLD is also dispensable since RIP1 is the primary target of CYLD in the context of necrosis. This will be addressed in length later in the thesis. It is also possible that there might be differential expression of compensatory RIP1 deubiquitinases in the large and small intestine. This may account for the observed essential requirement and non-essential requirement for necrosis in the different compartments.

Similar to FADD conditional deletion in epithelial cells, caspase-8 deletion in epithelial cells leads to spontaneous ileitis and loss of paneth cells with necrotic morphology. Interestingly, biopsies from the small intestines of Crohn's disease patients exhibit necrotic morphology and loss of paneth cells. This suggests that necrosis may indeed be involved in driving the pathogenesis of Crohn's disease; however, the specific causes of excessive necrosis and subsequent loss of paneth cells is unknown (Gunther et al., 2011). One possibility is that certain viral infections may inactive the pro-

apoptotic/anti-necrotic machinery in intestinal epithelial cells, and this may drive excess necrosis and disease.

Similar to necrosis, apoptosis can also be deleterious to intestinal epithelium barrier integrity when critical negative regulators are absent. Conditional deletion of NFκB Essential Modifier (NEMO) in intestinal epithelial cells also leads to a spontaneous colitis phenotype. NEMO is the regulatory subunit of the IKK complex, which is required for TNFα driven NFκB activation. Hence, deletion of NEMO in intestinal epithelial cells impairs NFκB activation, leading to apoptotic cell death of epithelial cells, loss of colon integrity, invasion of mucosa with gut microflora, and chronic inflammation (Nenci et al., 2007). It has also been demonstrated that NEMO negatively regulates apoptosis in an NFκB-independent manner (Legarda-addison et al., 2009). Unlike the FADD conditional knock-out, crossing to mice devoid of CYLD does not rescue the phenotype. One possibility for the dispensability of CYLD in this apoptotic pathway may be attributed to the possibility that NEMO is the primary target of CYLD in the context of TNFα-induced apoptosis. This concept will be discussed in further detail later. The colitis phenotype could also be rescued by crossing to TNFR-1 knock-mice demonstrating that cell death is primarily TNFα driven in this system (Nenci et al., 2007).

Signaling mechanisms required for programmed necrosis

Trimeric TNFα engagement of pre-assembled TNFR-1 homotrimers leads to the activation of different cellular programs resulting in potentially diametrically opposed

cell fates (Chan et al., 2000). Spatially, temporarily, and compositionally distinct complexes delineate the varying programs. Within minutes of TNFα stimulation, a TNFR-1 associated complex (Complex I) forms, resulting in NFκB activation and cell survival. Several proteins compose this complex. The death domain (DD) containing proteins TRADD and RIP1 are recruited to the complex, and interact with TNFR-1 DD domains in the cytoplasmic tail. TRADD is required for NFκB activation and apoptosis, while it is dispensable for necrosis (Zheng et al., 2006). During SMAC mimetic sensitization to TNFα-induced apoptosis TRADD actually appears to have a negative regulatory role (Wang et al., 2008). The adapter and E3 ligase protein TRAF2 as well as the E3 ligases c-IAP1/2 are also recruited to Complex I. TRAF2 is required for recruitment of cIAP1/2 via its cIAP1/2 interacting motif (CIM) (Vince et al., 2009). RIP1 gets polyubiquitinated within the complex, which acts as a docking site for both the IKK complex and the IKK activating complex, which is composed of Tak1/Tab2/3 (Ea et al., 2006; Kanayama et al., 2004). cIAP1/2 are responsible for RIP1 polyubiquitination and NFκB activation, while the TRAF2 RING domain is dispensable (Vince et al., 2009).

Later during stimulation, Complex I transitions into a cytosolic complex (Complex II) lacking TNFR-1, which is the location of caspase-8 activation and initiation of the apoptosis program (Micheau et al., 2003). The regulatory mechanisms of RIP1 transition into Complex II will be extensively covered later. Caspase-8 activation requires the adaptor protein FADD. During caspase inhibition, the kinases Receptor Interacting Protein 1 and 3 (RIP1/RIP3) associate, and give rise to the formation of a complex dubbed the "necrosome." Components of the apoptotic-mediating Complex II

are also found in the necrosome. This suggests that during caspase inhibition additional pro-necrotic proteins, such as RIP3, are recruited to Complex II and thereby give rise to the necrosome (Cho et al., 2009; He et al., 2009; Zhang et al., 2009).

The first headway in defining the biochemical pathway leading to cellular demise by necrosis was made over a decade ago with the discovery that RIP1 is required. RIP1 is a serine-threonine kinase, and its pro-necrotic function requires its kinase activity. It was demonstrated that RIP1 is required for necrosis induced by the death receptors Fas, TRAIL-R, and TNFR-1 (Holler et al., 2000). The role of RIP1 in TNFR-1 signaling will be extensively covered in the following section.

The role of the adaptor protein Fas Associated protein with Death Domain (FADD) in death receptor induced necrosis depends on the specific death receptor engaged. FADD contains both a death effector domain (DED) and a death domain (DD) and is required for caspase-8 recruitment to TRAIL receptor, Fas, and it is a critical component of Complex II during TNFR-1 receptor signaling. Whereas TRAIL and Fas ligand induced necrosis require FADD, TNFα-induced necrosis is enhanced in the absence of FADD (Chan et al., 2003; Holler et al., 2000). Consistent with the role of FADD during FasL-induced necrosis, Jurkat cells deficient of caspase-8, which are resistant to apoptosis, can be sensitized to necrotic cell death by forced dimerization of FADD (Kawahara et al., 1998). Forced dimerization of FADD or its DD in L929 cells induces RIP1-dependent necrosis, whereas forced dimerization of FADD DED induces apoptosis. Removal of RIP1 shifts the FADD dimerization induced necrosis to apoptosis.

Conversely, forced dimerization of FADD DED can be shifted from apoptosis to necrosis upon treatment with zVAD through recruitment of RIP1 (Vanden Berghe et al., 2004).

The requirement of RIP3 in TNFα-induced necrosis was independently discovered by three groups. All groups screened siRNA libraries in necrosis sensitive cell lines and ascertained which genes when knocked-down confer protection (Cho et al., 2009; He et al., 2009; Zhang et al., 2009). It was discovered that RIP3 associates with RIP1 and other components of Complex II only in instances when caspases are inhibited. Therefore, RIP3 association with RIP1 is a signature biochemical event that occurs only during necrosis and not apoptosis. The association between RIP1 and RIP3 was also demonstrated to be consequential for cellular demise via necrosis. Both RIP1 and RIP3 contain RHIM domains, which are required for their association and necrosis. Namely, cells expressing RHIM mutants of either RIP1 or RIP3 were unable to transduce the pro-necrotic signal. The enzymatic activity of both kinases is also required for their pro-necrotic function (Cho et al., 2003; He et al., 2009). RIP1 is the upstream kinase as its enzymatic activity is required for its association with RIP3, but the kinase activity of RIP3 is not required for its association with RIP1. In fact, it was demonstrated that kinase inactive RIP3 can act as a dominant negative when transfected in cells containing endogenous WT RIP3, presumably by associating with RIP1 and poisoning the necrosome (He et al., 2009). In addition to association between RIP1 and RIP3, both proteins are phosphorylated specifically during necrosis. Phosphorylation of RIP1 requires the presence of RIP3, as RIP3 knock-out MEFs do not exhibit phosphorylated RIP1 during necrosis stimulation. Conversely, phosphorylation of RIP3 requires RIP1

kinase activity, as Nec-1 blocks RIP3 phosphorylation during necrosis. This highlights the intricate nature of potential auto-phosphorylation and trans-phosphorylation events between RIP1 and RIP3 that occur during necrosis. *In vitro* kinase assays suggests that RIP3 can trans-phosphorylate RIP1, but the converse was not observed (Cho et al., 2009). One of the phosphorylation sites of RIP3 was identified as serine 199; however, the functional requirement of this phosphorylation event during necrosis was not addressed. The phosphorylation event requires its own kinase activity, as RIP3 phosphorylation was not observed in complexes between kinase inactive RIP3 and RIP1 during necrosis signaling (He et al., 2009). Clearly, more careful work needs to be conducted in order to truly understand the hierarchy of these phosphorylation events, and their functional impact on the necrosis signaling pathway.

RIP3 is a necrosis specific regulator. Consistent with the biochemical data, RIP3 knock-down does not confer protection against TNFα-induced apoptosis. Since RIP1 is involved in TNFα-induced apoptosis when cells are treated with SMAC mimetic, RIP3 possibly constitutes the divergence point of the biochemical pathway between necrosis and apoptosis (Cho et al., 2009; He et al., 2009; Wang et al., 2008). The expression level of RIP3 directly correlates with the level of necrosis in a panel of cell lines. Cell lines, which lack endogenous RIP3 are resistant to TNFα-induced necrosis. Sensitivity to necrosis can be conferred by ectopic expression of WT RIP3, but not kinase dead RIP3 (He et al., 2009).

Additional components of the necrosome were recently identified. The Mixed Linage Kinase Domain Like protein (MLKL) is yet another component of the necrosome.

The first group revealing its role in necrosis discovered it by analyzing the necrosome via mass spectrometry. This group also screened a small chemical compound library to identify inhibitors of necrosis. Interestingly, an inhibitor of MLKL was identified and dubbed Necrosulfanimide. This group initially deemed MLKL as a kinase dead protein due to the lack of key amino acid residues important for phosphate binding, and magnesium ion coordination (Sun et al., 2012). Shortly after, another group screening an shRNA library targeting kinases and phosphatases also revealed the pro-necrotic function of MLKL, and demonstrated that it was indeed kinase active. However, MLKL proved to be a weaker kinase in *in vitro* assays in comparison to RIP1 and RIP3 (Zhao et al., 2012).

NSA was used to help determine the pro-necrotic molecular mechanism of MLKL. Unlike Nec-1, which blocks necrosome formation, NSA inhibits necrosis downstream of RIP1/RIP3 association. This is supported by evidence that the inhibitor actually results in enhancement of RIP1/RIP3 association and phosphorylation, in spite of the fact that it blocks death. Confocal microscopy provided further evidence that NSA blocks a step downstream of RIP1/RIP3 association. Namely, HeLa cells stably transfected with fluorescently labeled RIP3 showed the transition from diffuse cytoplasmic to the formation of discrete punctae during necrosis. These RIP3 punctae increased in size over time. In agreement with NSA blocking a molecular event downstream of RIP1/RIP3 association, treatment of these cells with NSA did not abolish the stimulus dependent formation of RIP3 punctae whereas Nec-1 treatment did. Instead, NSA eliminated the size increase in the punctae. The first clue as to the target of NSA

was revealed when MLKL was identified as an additional component of the necrosome through mass spectrometry. The functional relevance of MLKL in mediating necrosis was validated, and its molecular mechanism was investigated. Importantly, siRNA knock-down of MLKL was a pheno-copy of NSA treatment in respect to the enhancement of RIP1/RIP3 association and the abolishment of RIP3 punctae growth during necrosis (Sun et al., 2012; Zhao et al., 2012). This prompted the hypothesis that NSA targeted MLK.

Indeed, it was demonstrated that NSA forms a covalent attachment to cysteine 86 of MLKL, and this residue is required for the necrosis suppressive effect of NSA. *In vitro* kinase assays revealed that RIP3 can directly phosphorylate MLKL at threonine 357 and serine 358. Compound mutants of both phosphorylation acceptor sites abolished the pro-necrotic function of MLKL. The phospho-mimetics of MLKL were functional in necrosis, and NSA could still block necrosis in cells stably transfected with them. This suggests that the mechanism of NSA inhibition is independent of MLKL phosphorylation. This is in agreement with data showing that NSA forms a covalent bond with MLKL in the N-terminal Coiled-Coil (CC) domain and the phosphorylation sites are in the C-terminal kinase like domain (Sun et al., 2012). The mechanism of NSA suppression was revealed to be inhibition of recruitment of another component of the necrosome PGAMS (Wang et al., 2012).

Akin to the requirement of RIP1 kinase activity for association with RIP3, it was demonstrated that RIP3 kinase activity is required for association with its substrate MLKL. It was also revealed that RIP3 undergoes auto-phosphorylation at serine 227 and

this modification is required for its pro-necrotic function and association with MLKL similar to RIP3 kinase activity (Sun et al., 2011). In co-transfection experiments it was demonstrated that RIP3 is required for MLKL and RIP1 association. This supports a model where MLKL is recruited to the necrosome via its association with RIP3. Furthermore, the weak kinase activity of MLKL appears to be required for its pro-necrotic function, as a kinase dead mutant MLKL is insufficient to restore necrosis in cells with MLKL knocked-down. The potential targets of MLKL have not been identified yet. It was also demonstrated that MLKL is required for the late phase of JNK activation and ROS production during necrosis in HT-29 cells; however, both of these molecular events are dispensable for necrosis in this cell type. In other cells types evidence suggests that JNK activation and ROS production are required for necrosis. Nevertheless, MLKL must be targeting something other than JNK and ROS production in HT-29 cells to transduce the pro-necrotic signal (Zhao et al., 2012).

In addition to MLKL, the mitochondrial phosphoglycerate mutase/protein phosphatase (PGAM5) was found to be a component of the necrosome. Due to alternative splicing, PGAM5 has two isoforms, PGAM5L and PGAM5S. While PGAM5L can be found in the TritonX-100 soluble fraction, PGAM5S can only be found in the TritonX-insoluble SDS-soluble fraction. This is potentially attributed to the fact that PGAM5S has additional exposure of hydrophobic amino acids. Both isoforms are involved in necrosis and both PGAM5L/S associate with the RIP1/RIP3/MLKL complex during necrosis. As is the case with MLKL recruitment to the necrosome, PGAM5L/S require the kinase activity of RIP3 to be recruited to the necrosome. This places

PGAM5L/S downstream of RIP3 kinase activation. Indeed, *In vitro* kinase assays revealed that RIP3 can phosphosphorylate PGAM5L and the corollary of this is activation of the phosphatase activity of PGAM5L. Importantly, PGAM5 requires intact phosphatase activity in order to exert its pro-necrotic function (Wang et al., 2012).

The necrosis inhibitor NSA differentially regulates the two isoforms of PGAM5. As previously discussed, NSA covalently modifies MLKL, but the mechanism accounting for its necrosis suppressing effect was not clarified. Clues as to its mechanism were revealed when looking at necrosome association with and phosphorylation of PGAM5. NSA treatment or MLKL knock-down does not abolish PGAM5L interaction with the necrosome, nor does it block phosphorylation of PGAM5L during necrosis. This indicates that PGAM5L recruitment to the necrosome and phosphorylation is MLKL-independent. However, NSA treatment or MLKL knock-down both block PGAM5S association with the necrosome, PGAM5S phosphorylation, and mitochondrial fragmentation during necrosis. This demonstrates that NSA blocks necrosis at the step of RIP1/RIP3/MLKL/PGAM5L complex association and activation of PGAM5S. The downstream consequence of blocking this molecular event is impaired mitochondrial fragmentation (Wang et al., 2012).

The functional relevance of mitochondrial fragmentation during necrosis still needs to be clarified; however some of the mechanistic details have been worked out. PGAM5S functions upstream of mitochondrial fragmentation during necrosis. Some evidence suggests that it directly activates the mitochondrial fission machinery. Drp-1 is a mitochondrial fission enzyme that harbors GTPase activity, and can be found at the site

of mitochondrial constriction during the process. Drp-1 is functionally involved in necrosis; however its participation in the observed mitochondrial fragmentation is inferred and has not been directly addressed. Indeed, Drp-1 co-localizes with the mitochondria during necrosis, which suggests that its function in necrosis relates to the mitochondrial fragmentation process. PGAM5 mediated dephosphorylation of Drp-1 results in its dimerization, and activation of its GTPase activity, which promotes mitochondrial fission. In the absence of PGAM5S, Drp-1 does not get activated via dephosphorylation; hence it does not mediate mitochondrial fission. Whether Drp-1 is the only target of PGAM5 in the context of necrosis still needs to be worked out (Wang et al., 2012). It is conceivable that PGAM5 promotes the activation of other components of the fission machinery or negatively regulates components of the mitochondrial fusion machinery.

The phosphorylated forms of RIP1/3, PGAM5L, and Drp-1 transition into the SDS-soluble fraction during necrosis. The SDS-soluble fraction is presumably where the necrosome engages the mitochondrial constriction points. This suggests that the necrosome may indeed be recruited to mitochondria; however, microscopy studies have yet to reveal RIP3 colocalization with the mitochondria during necrosis (Wang et al., 2008). RIP3 kinase activity is required for the necrosome to transition into the SDS-soluble fraction, which places RIP3 upstream of these mitochondrial events (Wang et al., 2012). This is not surprising considering that RIP3 was shown to be upstream of ROS production during necrosis (Cho et al., 2009). Additionally, PGAM5S is required for

PGAM5L and Drp-1 transition into the SDS-soluble fraction. This places PGAM5S as the link between the necrosome and the mitochondria (Wang et al., 2012) (Fig. 1.1).

Many different stimuli trigger necrosis, and not all require activation of the necrosome. Interestingly, inducing necrosis with either the ROS generator t-butyl hydroxide (TBH), Hydrogen Peroxide, or the calcium ionophore A23187 resulted in necrosis that was independent of RIP1/3, and MLKL. In contrast to the dispensability of some of the key players in death-receptor induced necrosis, PGAM5S/L and Drp-1 were required for necrosis induced by these stimuli. This suggests that PGAM5S/L and Drp-1 function at the intersection of multiple inducers of necrosis, and can be activated by necrosome-independent mechanisms. Namely, these necrosis regulators are common to both the extrinsic death receptor mediated necrosis and intrinsic necrosis. Indeed, TBH-induced necrosis caused mitochondrial fragmentation as seen in death receptor induced necrosis. This highlights the potential importance of mitochondrial fragmentation as a common downstream event during necrosis induced by a multitude of stimuli (Wang et al., 2012).

The requirement of specific mitochondrial events for the execution phase of necrosis appears to be cell-type specific. Quenching mitochondrial ROS protects some cell-types from necrosis such as the mouse fibrosarcoma cell line L929 and MEFs, and yet confers no protection in other cell-types such as the human colon carcinoma cell line HT-29 (Lin et al., 2004; Vanlangenakker, et al., 2011; Wang et al., 2009). Other reports have demonstrated the involvement of components of the mitochondrial transition pore complex such as adenine nucleotide translocase (ANT) and cyclophilin D (CYPD), and

Figure 1.1 Current model of necrosis signaling pathway

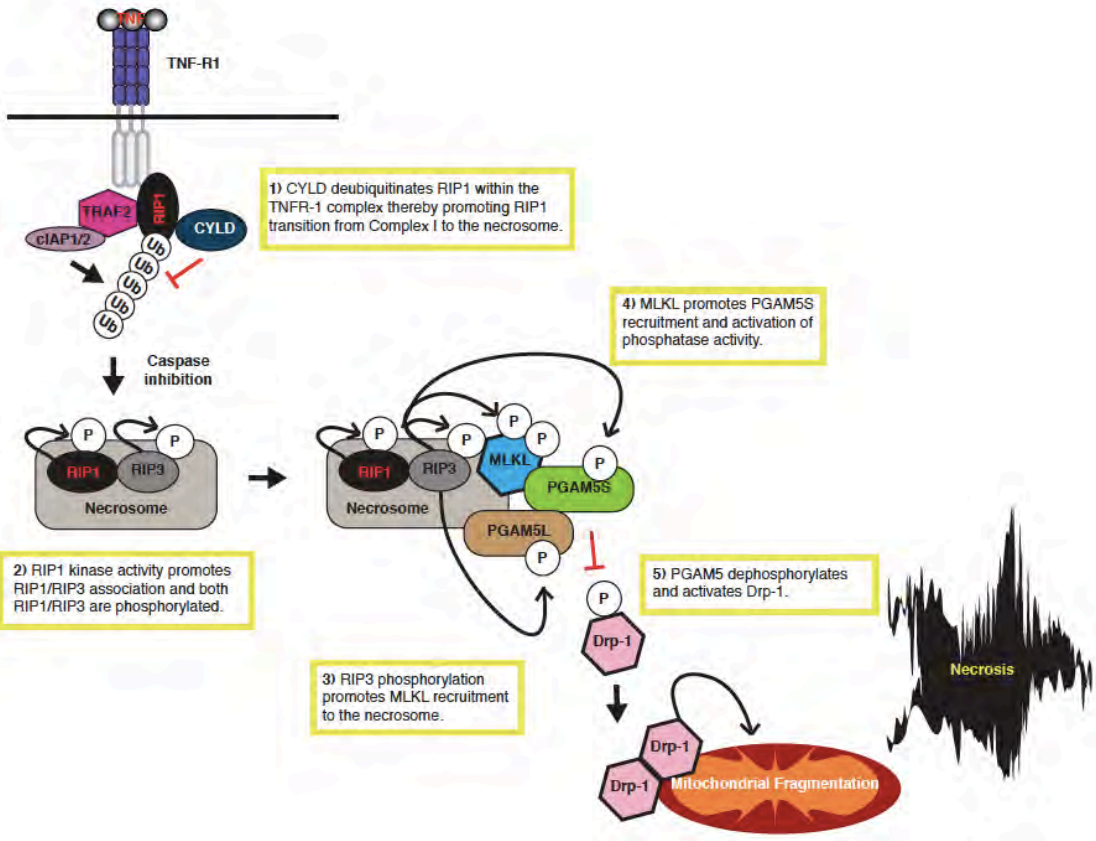

the loss of cellular ATP during necrosis. ANT regulates ADP and ATP exchange between the cytosol and mitochondria. One report demonstrates that RIP1 targets the inhibition of ANT during necrosis through disrupting its interaction with cyclophilin D. This accounts for the drop in cellular ATP levels, as ANT requires cyclophilin D for its function. Although ROS production occurred during necrosis, quenching it had no bearing on either the drop in ATP levels or necrosis in the myelomonocytic cell-line U937 and monocytic leukemia THP-1. Furthermore, mitochondrial release of cytochrome C was only observed in cells undergoing apoptosis and not necrosis (Temkin et al., 2006). Cytochrome C is an activator of the apoptosome with Caspase-9 being the apical caspase. This is consistent with the notion that apoptotic pathways mediate different mitochondrial events than the necrosis pathway and may account for the morphological differences between the two cell death programs. Clearly, a lot of questions remain as to the effector mechanisms of necrosis. Future studies should more rigorously address whether mitochondrial fragmentation is consequential for necrosis, and the mechanism behind how it leads to necrosis. Namely, does it influence ROS production, loss in cellular ATP, or some other novel mechanism?

The pro-inflammatory properties of RIP3 and other necrosis regulators extend beyond their role in necrosis. Interestingly, a recent report demonstrated that in Caspase-8 deficient dendritic cells multiple components of the necrosome promote NALP3 inflammasome activation, independent of their effects on promoting necrosis. caspase-8 deficient DCs only require the priming signal (LPS) for IL-1β secretion. Normally, DCs require an activation signal such as ATP to activate caspase-1 via the NALP3

inflammasome. This activation signal independent maturation of IL-1β was shown to require the necrosome components RIP3, MLKL, and PGAM5. Importantly, death was not observed in caspase-8 deficient DCs during LPS stimulation. This demonstrated that the pro-inflammatory properties of these necrosis regulators can also be attributed to cell death independent pathways. Interestingly, these components of the necrosome were observed in complex with the NALP3 inflammasome during LPS treatment in caspase-8 deficient DCs (Kang et al., 2013).

TNFα and other ligands that engage death receptors are not the only triggers of programmed necrosis. Recently, it was demonstrated that the TLR3 and TLR4 ligands poly(I:C) and LPS can induce necrosis (He et al., 2012; Zhang et al., 2009). These receptors belong to a family of Pattern Recognition Receptors that are important for mounting anti-microbial defenses. TLR3 functions solely through the adaptor protein TRIF, whereas TLR4 functions through both TRIF and MyD88. Interestingly, macrophages stimulated with ligands for these TLRs and caspase inhibition with zVAD, undergo necrosis that requires both TRIF and RIP3. TRIF, like RIP3, contains a RIP Homotypic Interaction Motif (RHIM). The RIP3 RHIM was demonstrated to be required for stimulus dependent RIP3/TRIF interaction. Namely, cells expressing a RHIM mutant RIP3 showed no signs of this molecular event. The requirement of TRIF's RHIM was not clarified in this study as well as the relevance of TRIF/RIP3 association in driving necrosis. In agreement with the absence of data suggesting the involvement of TRIF in TNFR-1 signaling, TNFα-induced necrosis in macrophages does not require TRIF. This demonstrates that multiple receptors can give rise to necrosis, and utilize alternative

mechanisms for RIP3 activation. Depending on the receptor used to trigger necrosis, there are differential requirements for signaling proteins. Furthermore, ROS production was demonstrated to be a molecular event required for either TLR or TNFα driven necrosis in macrophages. Both RIP3 and TRIF are required for ROS production by TLRs and only RIP3 is required for ROS production by TNFα in macrophages. Due to the dispensability of ROS for necrosis in other cell types, such as HT-29 cells, this highlights that necrosis employs death effector mechanisms that are cell-type specific (Wang et al., 2012; Zhao et al., 2012).

RIP1 ubiquitination and transition to the DISC

During TNFα signaling, RIP1 ubiquitination within Complex I is believed to negatively regulate its transition to Complex II. RIP1 ubiquitination within Complex I is required for NEMO binding and subsequent IKK activation, and therefore dictates the NFκB-dependent pro-survival function of RIP1 (Ea et al., 2006). During TNFR-1 complex formation c-IAP1/2 are recruited to the complex, and serve as functionally redundant E3 ligases responsible for ubiquitinating RIP1 (Mahoney et al., 2008; Varfolomeev et al., 2008). By promoting RIP1 ubiquitination, c-IAP1/2 aid in activating NFκB and cell survival. Specifically, in MEFs with dual knock-down of c-IAP1/2, TNFα-induced RIP1 ubiquitination within the TNFR-1 complex is impaired as well as subsequent NFκB activation. Similarly, treatment of cells with the SMAC mimetic BV6, which effectively depletes both c-IAP1/2, results in a loss of RIP1 ubiquitination within

the TNFR-1 complex, and a block in NFκB activation. In MEFs, genetic ablation of either c-IAP1 or c-IAP2 is insufficient to block activation. However, knock-down of the remaining E3 ligase c-IAP1 or c-IAP2 in the singly deficient MEFs abrogates activation. The same observations were made when addressing the anti-apoptotic function of c-IAP1/2. Knock-down of c-IAP2 in c-IAP1 deficient MEFs resulted in apoptosis while absence of only one of them has no effect. Reconstitution of c-IAP1/2 depleted cells with a catalytic inactive c-IAP1 was insufficient for restoring NFκB activation, but wild-type c-IAP1 was. This demonstrates that impaired NFκB activation was indeed attributed to the lack of E3 ligases, and that the E3 ligase enzymatic activity is required for c-IAPs function in NFκB activation. This supports the notion that both c-IAP1/2 play a functionally redundant role in promoting NFκB activation, and blunting apoptosis (Varfolomeev et al., 2008).

It is well known that cancer cells subvert the cellular machinery responsible for programmed cell death. In different types of cancer the chromosome loci harboring the anti-apoptotic genes cIAP1/2 and XIAP are amplified, mutated, or translocated. XIAP is the only anti-apoptotic protein of the group that is known to directly inhibit caspases. Namely, it binds to Caspase-9 and thereby vitiates the intrinsic mitochondrial apoptosis pathway (Eckelman et al., 2006). Normally, during the intrinsic mitochondrial apoptosis pathway, Second Mitochondria-derived Activator of Caspases (SMAC) is released from the mitochondrial intermembrane space and de-represses Caspase-9 by disrupting its association with XIAP, thereby promoting apoptosis. SMAC binds to the BIR3 domain of XIAP via a specific tetra-residue (Srinivasula et al., 2001). Many drug companies

have designed small chemical compounds, peptidomimetics, and peptides based on this tetra-residue of SMAC. These compounds are cell permeable, and have proved successful in sensitizing cancer cells to apoptosis. Although these drugs are modeled after SMAC binding to XIAP, they also effectively target c-IAP1/2 for auto-ubiquitination, degradation mediated by the proteasome, and apoptosis (Bertrand et al., 2008; Fulda et al., 2012).

The molecular details regarding the anti-apoptotic function of c-IAP1 and c-IAP2 are not restricted to their effects on promoting NFκB activation. By keeping RIP1 in an ubiquitinated state, c-IAP1/2 hinder RIP1 association with caspase-8, which blocks caspase activation and apoptosis (Fig1.2 and Fig1.3). Treatment of certain cancer cells with a SMAC mimetic compound causes auto-ubiquitination of c-IAP1/2 followed by proteasome degradation, and cell death. This is supported by data showing that SMAC mimetic co-treatment with proteasome inhibitors results in the accumulation of ubiquitinated c-IAP1/2 and abrogates caspase activation and cell death. *In vitro* ubiquitination assays reveal that SMAC mimetics directly activate the E3 ligase activity of c-IAP1/2. In the absence of its cognate E3 ligases, RIP1 is predominately in an unmodified state. Unmodified RIP1 has a higher propensity for associating with caspase-8, and results in caspase activation, and apoptosis. Since RIP1 ubiquitination is required for association with TAK1, SMAC mimetic treatment abrogates the RIP1/TAK1 association (Bertrand et al., 2008; Kanayama et al., 2004). TAK1 is not only involved in activating the IKK complex during TNFα signaling, but it has been demonstrated to negatively regulate programmed necrosis, as will be discussed in further detail

Figure 1.2 Factors that regulate RIP1 ubiquitination and cell death

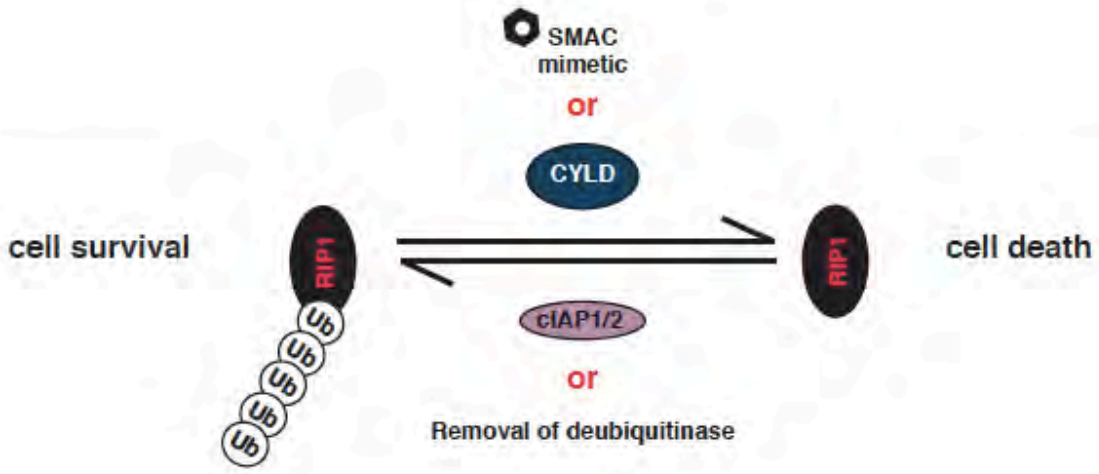

Figure 1.3 SMAC mimetic mechanism for enhancement of cell death

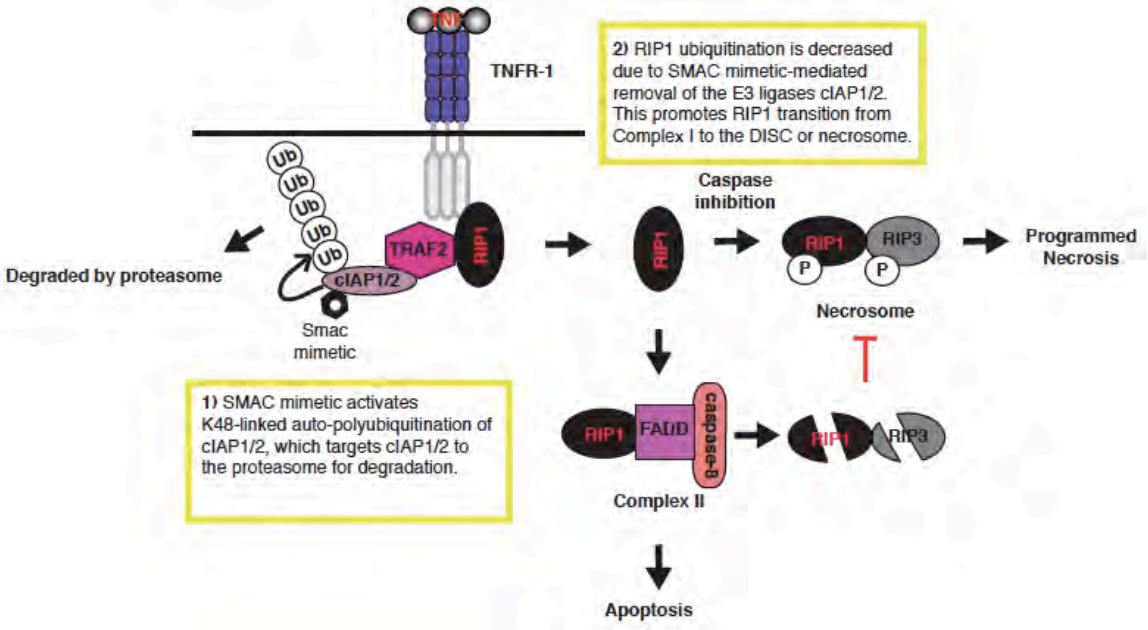

(Vanlangenakker, et al., 2011). Cancer cell death sensitization was demonstrated to require autocrine production of death receptor ligands. Prior to SMAC mimetic treatment, these cancer cells are impervious to death receptor induced death presumably due to hyper-ubiquitination of RIP1, which results in NFκB activation, upregulation of anti-apoptotic genes, and impaired RIP1 association with Caspase-8 (Bertrand et al., 2008).

In agreement with the aforementioned studies showing the anti-apoptotic function of c-IAP1/2, cells expressing an ubiquitin acceptor site mutant RIP1 (K377R) undergo enhanced Complex II formation and apoptosis (O'Donnell et al., 2007). This predicts a deubiquitinase that regulates RIP1 ubiquitination; thereby, promoting Complex I to Complex II transition. Some studies suggest that the pro-death function of CYLD is attributed to de-ubiquitination of RIP1. Namely, CYLD regulates RIP1 ubiquitination resulting in complex I to II transition, and cellular demise via apoptosis (Wang et al., 2008).

A conundrum in the TNFα induced cell death field was the fact that the components of Complex II do not require de novo gene transcription and are expressed at significant levels prior to NFκB activation, whereas many of the anti-apoptotic proteins require NFκB driven expression. This is not intuitive when considering the default TNFα-induced program is survival, but the survival components require new gene transcription whereas the pro-apoptotic proteins are constitutively expressed. This suggested the presence of additional NFκB-independent survival mechanisms to prevent unintended TNFα-driven cell death. This conundrum was solved based on work from

Adrian Ting's group on the NFκB-independent anti-apoptotic function of NEMO (Legarda-addison et al., 2009).

NEMO is also a negative regulator of Complex I to Complex II transition. Initially, it was assumed that the pro-survival effect of NEMO was attributed to its role in NFκB activation and subsequent up-regulation of pro-survival genes such as cFLIP. A report clarified that NEMO has an anti-apoptotic function independent of its function as a NFκB activator. It was observed that Jurkat T cells expressing an IκBα super repressor, in which NFκB cannot be activated showed a lesser degree of TNFα driven apoptosis enhancement than cells deficient of NEMO. This suggested that NEMO must have an additional pro-survival function independent of NFκB activation. In agreement with this hypothesis, Jurkat T cells that are deficient of NEMO and express the IκBα super repressor show enhanced apoptosis as compared to cells only expressing the IκBα super repressor. Reconstitution of the NEMO deficient/ IκBα super repressor cells with NEMO was able to repress apoptosis to the same level as cells only expressing the IκBα super repressor. The molecular events that describe this cell death phenotype are that NEMO binds to ubiquitinated RIP1 and inhibits RIP1 association with caspase-8. In other words, NEMO inhibits transition of RIP1 from Complex I to Complex II (Legarda-addison et al., 2009).

The NFκB-independent pro-survival function of NEMO extends beyond its regulation of apoptosis. NEMO deficient Jurkat cells expressing an IκBα super repressor are more sensitive to TNFα-induced necrosis. Just like in apoptosis, the necrosis

suppressive effect requires intact ubiquitin binding domains. Specifically, mutations in the ubiquitin binding domain of NEMO that eliminate its ability to bind ubiquitin, also eliminates its necrosis suppressive function. In agreement with the notion that NEMO binds to ubiquitinated RIP1 and thereby stifles necrosis, SMAC mimetic eliminated the protection observed in NEMO deficient cells reconstituted with wild-type NEMO. The explanation for this observation is that the SMAC mimetic removes cIAPs and in doing so RIP1 is in a primarily unmodified state. Since the NFκB-independent survival function of NEMO requires binding to ubiquitinated RIP1, NEMO can no longer exert its anti-necrotic effect when cells are treated with SMAC mimetic. In agreement with the requirement for NEMO binding to ubiquitinated RIP1 in order to block RIP1 transition to Complex II, cells expressing a mutant version of RIP1 (K377R), which removes a ubiquitin acceptor site, enhances TNFα-induced necrosis. As expected, the necrosis enhancing effect of SMAC mimetic treatment was not pronounced in cells expressing K377R RIP1. More evidence suggesting that RIP1 ubiquitination negatively regulates its pro-necrotic function came from experiments showing that cells expressing a dominant negative TRAF2, which have impaired RIP1 ubiquitination, also have enhanced necrosis (O'Donnell et al., 2012). Although, RIP1 ubiquitination negatively influences both apoptosis and necrosis, CYLD is dispensable for TNFα-induced apoptosis in NEMO deficient cells and yet required for necrosis in these same cells. This is explained by the observation that CYLD is rapidly degraded in NEMO deficient cells during apoptosis, which is dependent on Caspase-8 mediated cleavage of CYLD (O'Donnell et al., 2011).

It is important to note that normally RIP1 is dispensable for TNFα-induced apoptosis when cells are sensitized with either the protein translation inhibitor cycloheximide (CHX) or blockade of NFκB via stable transfection of an IκB super repressor (O'Donnell et al., 2009; Wang et al., 2008). Interestingly, this form of RIP1-independent apoptosis is highly susceptible to the negative regulation by cFLIP, which is a NFκB target gene. In fact, the requirement for NFκB inhibition in order to sensitize cells to die via TNFα-induced apoptosis is circumvented by cFLIP knockdown. The other form of TNFα-induced apoptosis occurs when cIAPs are depleted and requires RIP1 and its functional kinase activity. This form of apoptosis is more resistant to the anti-apoptotic effects of cFLIP, which has been attributed to the fact that a higher level of RIP1/Caspase-8/FADD complex formation occurs in these cells, and may override the repressive effects of cFLIP levels. Indeed, this form of apoptosis does not require NFκB inhibition as it was activated in the presence of SMAC mimetic (Wang et al., 2008). Interestingly, in cells deficient of NEMO and expressing an IκB super repressor, TNFα-induced apoptosis requires RIP1 (O'Donnell et al., 2009). This suggests that the presence or absence of NEMO dictates whether apoptosis is RIP1-independent or RIP1-dependent, respectively.

The pro-death function of RIP1 extends beyond its role in Complex II derived from TNFR-1. This RIP1-dependent complex was identified by two separate groups and termed the "Ripotosome." The groups did not use the same stimuli to induce cell death in their studies. The first group used the chemotherapeutic agent Etoposide, and wanted to determine the biochemical mechanism responsible for its cytotoxic effects on cancer

cells. They demonstrated Etoposide reduced the cellular levels of cIAP1/2 and XIAP, allowing for the formation of a RIP1-dependent complex. It was demonstrated that this complex contains RIP1/FADD/Caspase-8 and can promote either apoptosis or necrosis depending on whether caspases are inhibited. This complex shares compositional similarities with Complex II derived from the TNFR-1 pathway. Interestingly, this complex was not derived from death receptor complexes as siRNA knock-down and neutralizing antibodies for death receptors such as TNFR-1 were insufficient for blocking death. This revealed that in response to other stimuli, RIP1 could form alternative complexes that mediate cell death.

Another distinguishing feature of this complex is that it is of higher molecular weight than the one originally characterized for TNFR-1 signaling (Micheau et al., 2003). The RIP1-dependent complex that formed from Etoposide/SMAC mimetic treatment was found in 2MDa fractions from gel sizing columns. It was the RIP1 within these high molecular weight fractions that was in a complex with caspase-8, which warranted the nomenclature "Ripotosome" (Tenev et al., 2011).

The other group characterizing the "Ripotosome" used the synthetic TLR-3 ligand poly(I:C) in addition to SMAC mimetic to induce apoptosis or necrosis, depending on additional treatment with zVAD. Like the first group they demonstrated that the cell death was independent of autocrine TNFα signaling. Similarly, this group found that RIP1 was required for the formation of the "Ripotosome" which contained RIP1, Caspase-8/10, FADD, and cFLIP. They also demonstrated that TLR-3 stimulation and SMAC mimetic treatment resulted in the recruitment of the sole TLR-3 adaptor protein,

TRIF, to the complex, which has been demonstrated to mediate TLR-3 induced apoptosis as well as necrosis (He et al., 2012). As with TNFα-mediated cell death, knock-down of caspase-8 or treatment with zVAD pushed the death towards RIP3-dependent necrosis. While RIP3 is solely required for Ripotosome-mediated necrosis, both apoptosis and necrosis require RIP1. During apoptosis induced by poly(I:C) and SMAC mimetic, RIP1 appears to play a scaffolding role, as its kinase activity is dispensable, but its presence is necessary. During necrosis, the kinase activity of RIP1 is required as cell death in the presence of zVAD can be inhibited with Nec-1 treatment. Altogether, this data indicates that the Ripotosome is a death inducing hub downstream of a variety of stimuli, but distinct from the Complex II derived from TNFR-1 signaling (Feoktistova et al., 2011).

The short and long c-FLIP isoforms were shown to be functionally distinct in their regulation of the Ripotosome. The c-FLIP$_L$ isoform was shown to negatively regulate poly(I:C) induced apoptosis, while c-FLIP$_S$ promoted necrosis in addition to blocking apoptosis. Impaired apoptosis in c-FLIP$_L$ overexpressing cells was attributed to a block in Ripotosome formation. Interestingly, in cells overexpressing c-FLIP$_S$, treatment with the c-IAP antagonist caused spontaneous Ripoptosome formation and necrosis. Furthermore, in cells overexpressing c-FLIP$_S$ there was a portion of the total cellular pool of c-FLIP$_S$, caspase-8, and RIP1 in high molecular weight fractions (2 MDa); however, complex formation of these proteins only occurred in the presence of SMAC mimetic. These results provide evidence that different c-FLIP isoforms have diametrically opposed functions in respect to ripotosome-mediated cell death. Interestingly, in cells overexpressing c-FLIP$_S$, inhibiting the proteasome with MG-132

resulted in the formation of the ripotosome, which is similar to treatment with SMAC mimetic alone. In other words, this means that blocking proteasomal mediated degradation shares some of the molecular ramifications as eliminating cIAPs. This suggests that the negative regulatory role of cIAPs during ripotosome formation is possibly due to targeting a select proportion of RIP1 for proteasomal degradation that is competent for participating in ripotosome formation (Feoktistova et al., 2011). Since one report provides compelling evidence of RIP1/RIP3 amyloid fibril formation and functionality during necrosis, it is conceivable that cIAPs may function to eliminate their spontaneous formation in the cell (Li et al., 2012). Whether the ripotosome contains amyloid RIP1 or RIP3 has not been tested. This data also suggests that cell-type specific differences in the proportion of c-FLIP isoforms may dictate their sensitivity to Ripoptosome-mediated cell death both quantitatively and qualitatively.

During TNFα stimulation RIP1 is ubiquitinated with a heterogeneous group of linkage types in the TNFR-1 complex. As previously mentioned, RIP1 ubiquitination is a critical post-translational modification that brings NEMO complexes in proximity to TAK1 complexes and therefore supports IKK activation (Ea et al., 2006; Kanayama et al., 2004). One report used an ubiquitin replacement strategy to elucidate the functional requirement of K63-linked polyubiquitin chains in TNFα-induced IKK complex activation. In this report they were able to knock-down endogenous ubiquitin and replace it with ubiquitin in which the various ubiquitin acceptor site lysine residues were mutated. Via this method they determined that K63-linked polyubiquitination is dispensable for IKK activation and subsequent IκB phosphorylation. Consistent with this

data, the E2 conjugating enzyme Ubc13 was also found to be dispensable. When in complex with an E3 ligase, Ubc13 is only capable of supporting K63-linked polyubiquitin chains. However, the more promiscuous E2 UbcH5c, which aids in polyubiquitination of a variety of chain linkage types, was in fact required for TNFα-induced NFκB activation. They attributed the dispensability of K63-linked chains to the fact that RIP1 can still get ubiquitinated in NEMO complexes using this system. Furthermore, single mutations of all of the lysine residues in ubiquitin, as well as some double mutations, were still sufficient for TNFα-driven RIP1 ubiquitination. All this data strongly suggests that RIP1 can be ubiquitinated with a variety of linkage types that support its role in activating the IKK complex (Xu et al., 2009). Further investigation regarding the potential influences of different ubiquitin linkage types on RIP1-mediated cell death is merited.

The findings in the aforementioned study were bolstered by a later study, which used antibodies specific for different ubiquitin linkage types and mass spec analysis to demonstrate the heterogeneity of RIP1 ubiquitination linkage types both *in vitro* and *in vivo*. *In vitro* assays indicated, that RIP1 could be ubiquitinated with K63, K48, and K11 polyubiquitin via UbcH5c and cIAP1 and were quantified by mass spec. Furthermore, *in vivo* experiments showed that RIP1 within the TNFR-1 complex could be ubiquitinated with these various ubiquitin chain linkages that was dependent on both UbcH5 and cIAP1. Based on their findings in a yeast two hybrid study using cIAP1 as bait, they identified a variety of E2s, which it can interact with. Using a variety of stimuli, which are known to disrupt cIAP1 stability through activation of its E3 ligase activity, auto-

ubiquitination, and subsequent proteasome mediated degradation they demonstrated the requirement for UbcH5 and the dispensability of the other E2s, which can bind cIAP1. However, this does not negate the possibility that cIAP1 and other E2 enzyme pairs may function in other signaling paradigms where cIAP1 E3 ligase activity is required. Through *in vitro* binding assays it was also demonstrated that NEMO can bind to K11-linked polyubiquitin chains with a dissociation constant in the low micromolar range. These findings bolster the notion that alternative linkages may function in the TNFα signaling pathway, but any individual linkage type by itself is dispensable (Dynek et al., 2010).

CYLD in the context of a myriad of biological processes

CYLD is a tumor suppressor with de-ubiquitinating enzymatic activity (Bignell et al., 2000; Brummelkamp et al., 2003; Kovalenko et al., 2003; Trompouki et al., 2003). It's involved in a myriad of biological processes such as skin homeostasis, progression of spermatogenesis, lymphocyte development, bone development, and multiple cancer types (Jin et al., 2008; Keats et al., 2007; Massoumi et al., 2006; Reiley et al., 2006; Reiley et al., 2007; Wright et al., 2007). Furthermore, a group of overlapping autosomal dominant diseases are attributed to mutations that disrupt CYLD's enzymatic activity; namely, familial cylindromatosis (FC), multiple familial trichoepithelioma (MFT), and Brooke Spiegler syndrome (BSS). These diseases are typified by benign tumors of the face, scalp, and neck (Young et al., 2006).

The first studies that characterized the signaling function of CYLD revealed that it acts as a negative regulator of JNK and NFκB activation by de-ubiquitinating adaptor proteins such as TRAF2, TRAF6 and components of the IKK complex that function downstream of a variety of cytokines (Brummelkamp et al., 2003; Kovalenko et al., 2003; Trompouki et al., 2003). CYLD also negatively regulates the non-conical NFκB pathway thereby blocking cellular proliferation (Massoumi et al., 2006). Both *in vitro* and *in vivo* studies have revealed that CYLD deubiquitinates target proteins conjugated with K63-linked and linear polyubiquitin chains. These ubiquitin chain linkages are both topologically and functionally distinct from K48-linked chains. Unlike K48-linked polyubiquitin chains that target acceptor proteins for proteasomal degradation, K63-linked chains provide binding sites for signaling proteins (Komander et al., 2009; Wright et al., 2007).

CYLD is a negative regulator of innate anti-viral signaling pathways. Namely, CYLD suppresses the induction of type I interferons (IFN) by the cytosolic RNA sensor RIG-I. The mechanism of suppression is suggested to be through CYLD-mediated deubiquitination of RIG-I. Dendritic cells devoid of CYLD have constitutive hyperactivation of kinases that function downstream of RIGI, IKKε and TANK Binding Kinase 1 (TBK1) (Zhang et al., 2008). RIG-I is also hyperubiquitinated in dendritic cells devoid of CYLD. This suggests that the ubiquitination status of RIG-I influences its signaling capacity. Another report demonstrates that CYLD can also regulate the ubiquitination status of TBK-1, and interact with many of the signaling proteins downstream of RIG-I. During SeV infection and TNFα treatment, CYLD levels rapidly

decrease suggesting a possible mechanism that ensures sufficient induction of type I IFN to eliminate viral propagation (Friedman et al., 2008).

Multiple reports have revealed mechanisms, which regulate the functionality of CYLD in different signaling paradigms. Diverse stimuli such as TNFα, LPS, and PMA/Ionomycin give rise to phosphorylation of CYLD. These phosphorylation events are mediated by the IKK complex, and are inhibitory to CYLD functionality. CYLD harbors a cluster of serine residues that can undergo stimulus dependent phosphorylation. Cells expressing compound mutants of CYLD, in which the phosphorylation sites are eliminated, have impaired ligand inducible ubiquitination of CYLD substrates. This is presumably attributed to the inability of the IKK complex to suppress CYLD DUB activity, leading to the deubiquitination reaction dominating over the opposing ubiquitination reaction. In result of impaired ubiquitination of key adaptor proteins, the cells have blunted TNFα-induced JNK activation. In line with this model, mutations mimicking CYLD phosphorylation, abrogates the ability of CYLD to deubiquitinate TRAF2 in an overexpression system (Reiley et al., 2005).

Similarly, IKKε, which is critical for type I interferon production downstream of PRRs and oncogenic in breast cancer, phosphorylates CYLD. This phosphorylation event inhibits CYLD-mediated deubiquitination of TRAF2 and NEMO in overexpression systems. Either CYLD knock-down or ectopic IKKε is sufficient to cause transformation of NIH 3T3 cells. Co-transfection of S418A CYLD but not wild-type CYLD is able to partially suppress IKKε-mediated transformation. The mechanism of transformation upon knock-down of CYLD in 3T3 cells is attributed to NFκB, as transformation can be

blocked via expression of an IκB super repressor (Hutti et al., 2009). Altogether, these data point to an important regulatory mechanism of CYLD function in both physiological and pathophysiological scenarios. Since CYLD tumor suppressive activity can be inhibited by phosphorylation, it is possible that critical phosphatases remove these inhibitory phosphates from CYLD thereby restoring CYLD enzymatic activity. These phosphatases would theoretically be tumor suppressors themselves.

Protease-mediated cleavage of CYLD is yet another example of a regulatory mechanism, which impacts CYLD function. In the context of TNFα signaling, CYLD is cleaved at aspartic acid residue 215 by caspase-8. This leads to proteasomal degradation of the C-terminal fragment of CYLD and suppression of necrosis. Interestingly, cells expressing D215A CYLD, which is resistant to caspase-8 cleavage, no longer require caspase inhibition for necrosis (O'Donnell et al., 2011). This suggests that in contrary to popular belief, the necrosis suppressive function of caspase-8 is primarily through CYLD cleavage. This is difficult to reconcile with the extensive genetic studies, which suggest that RIP1 and RIP3 are the primary targets of caspase-8 mediated necrosis suppression (Kaiser et al., 2011; Oberst et al., 2011).

Multiple studies report that CYLD functions in the adaptive immune system. During T cell development, CYLD functions in TCR-proximal signaling events, which leads to productive double positive (DP) to single positive transition (SP). Mice deficient of CYLD, have a dramatic reduction in the number of single positive thymocytes, and CD4 and CD8 T cells in the spleen. This is attributed to a T cell intrinsic defect. Pertaining to signaling events, CYLD is important for promoting activated LCK

association with Zap70. Indeed, double positive thymocytes from CYLD knock-out mice have impaired phosphorylation of Zap70 and Lat. The authors demonstrate that CYLD deubiquitinates LCK in overexpression studies; however, whether this is responsible for the impaired association between activated LCK and Zap70 in CYLD deficient T cells has not been addressed (Reiley et al., 2006).

In addition to regulating TCR proximal signaling events during T cell development, CYLD is also reported to play a role in regulating T cell activation. Namely, CYLD deficient T cells hyper-proliferate upon *in vitro* stimulation with anti-CD3/CD28. In agreement with dysregulated T cell activation, CYLD knock-out mice develop signs of autoimmunity such as spontaneous inflammation of the colon. Unlike thymocytes, naïve and memory T cells deficient of CYLD showed normal TCR-proximal signaling events; however, they had constitutive activation of the conical NFκB pathway and C-Jun N-terminal Kinase (JNK). Adoptive transfer studies of CYLD-deficient T cells into a $RAG1^{-/-}$ host were able to recapitulate the spontaneous colon inflammation found in the CYLD deficient mice. This demonstrates that the hyper-responsive CYLD-deficient T cells were responsible for pathogenesis (Reiley et al., 2007).

Another report demonstrated that the paracaspase Mucosa Associated Lymphoid Tissue 1 (MALT1) cleaves CYLD during TCR stimulation. MALT1 is a component of the CARMA1-BCL10-MALT1 (CBM) complex, which is required for TCR-driven NFκB and MAP kinase activation. Interestingly, MALT1 cleavage of CYLD is required for JNK activation, as Jurkat cells expressing a cleavage resistant mutant of CYLD (R324A) had impaired TCR-induced JNK activation. Indeed, CYLD is constitutively

expressed in many cells, and in order to bypass its function in negatively regulating JNK activation, it must be inactivated. The requirement of inactivation of negative regulators of T cell activation highlights that the steady-state signaling environment in T cells is not permissive to activation, and therefore ensures that T cells are not aberrantly activated (Staal et al., 2011).

In addition to being required for conventional T cell development, CYLD also plays a role in regulating NKT cell development. In NKT cells CYLD negatively regulates NFκB. Contrary to expectation, hyper-activated NFκB in immature NKT cells ($CD44^{-}NK1.1^{-}$ and $CD44^{+}NK1.1^{-}$) results in a large proportion of the cells succumbing to apoptosis. Interestingly, excess NFκB activation suppresses the up-regulation of IL-7Rα and ICOS, which are required for survival of these cells. The reduction in immature NKT cells in CYLD knock-out mice was T cell intrinsic as clarified by bone marrow chimera experiments. Furthermore, crossing the CYLD knock-out mice to mice expressing a IκBα super repressor, in which the NFκB pathway is blocked, was able to rescue the expression of IL-7Rα and ICOS. This demonstrated that the excess NFκB activation in NKT cells lacking CYLD was indeed responsible for altered expression of IL-7Rα and ICOS. Importantly, the high level of apoptosis was also rescued (Lee et al., 2010).

Reports have also implicated a role for CYLD in B cell homeostasis. There is a splice variant of CYLD, which lacks exon 7 and 8 and occurs naturally. These exons encompass the TRAF2 and NEMO binding domains. The splice variant can be found in many different cell types along with expression of full length CYLD. Transgenic mice overexpressing sCYLD and lacking full length CYLD have enlarged lymph nodes and

spleen attributed to the expansion of mature B cells. This phenotype is indeed B cell intrinsic, as it is recapitulated in mice with conditional expression of sCYLD in B cells. The expansion was not due to enhanced cell proliferation, but rather enhanced survival. B cells from mice expressing sCYLD expressed higher levels of the anti-apoptotic protein Bcl-2, which has been demonstrated as key for B cell survival. Although the evidence for the potential mechanism accounting for the increase Bcl-2 expression level is tenuous, the authors point to an increase in NFκB activation and p38 pathways. Indeed, B cells expressing sCYLD have higher protein levels of p100, IκBα, RelB, which are target genes of NFκB, and they also have increased nuclear localization of Bcl-3, which functions as a co-activator in the non-canonical NFκB pathway (Hovelmeyer et al., 2007). Altogether, unlike the negative regulatory function of CYLD on NFκB activation, the short splice variant activates NFκB. It is possible that the ratio of CYLD splice variant expression in cells can influence their sensitivity to NFκB activating stimuli.

In agreement with the effects of sCYLD in B cells, another report demonstrated that dendritic cells solely expressing sCYLD were hyper-activated both basally and during activation with LPS. This was attributed to enhancement of NFκB activation and Bcl-3 nuclear translocation. The consequence of hyper-activated dendritic cells was enhanced expansion of antigen specific T cells (Srokowski et al., 2009).

Yet another biological context in which CYLD is important is bone homeostasis. CYLD is required to stifle RANKL-induced NFκB activation in pre-osteoclasts. Mice deficient of CYLD, develop osteoporosis due to an overabundance of osteoclasts, which are instrumental in bone resorption. Osteoclast differentiation is contingent upon

RANKL signaling. Indeed pre-osteoclasts from CYLD$^{-/-}$ demonstrate hyper-activation of NFκB. Interestingly, CYLD was found in endogenous complexes with TRAF6, and regulates the ubiquitination status of TRAF6. Furthermore, CYLD and TRAF6 association required the ubiquitin binding protein p62, which also has been demonstrated as a regulator to osteoclastogenesis (Jin et al., 2008).

Current understanding of CYLD in cell death signaling

CYLD is involved in promoting both TNFα-induced apoptosis and necrosis (Fujikura, et al., 2012; Hitomi, et al., 2008). The pro-apoptotic function of CYLD is attributed to its role in promoting the formation of Complex II. It has been shown that TNFα/SMAC mimetic induced Complex II formation is impaired in CYLD knock-down cells, which results in attenuation of apoptosis (Wang et al., 2008). In agreement with CYLD's role in Complex II formation, it is also required for caspase activation during TNFα-induced cell death. Overexpression of CYLD results in enhanced TNFα-induced caspase activation (Fujikura et al., 2012). In a more physiological context, some evidence indicates that the pro-apoptotic function of CYLD is through deubiquitination of RIP1 during the early wave of apoptosis required for productive spermatogenesis. CYLD-mediated apoptosis is critical for this developmental process, as CYLD$^{-/-}$ mice are sterile. Interestingly, this report attributes the pro-apoptotic function of the CYLD-RIP1 signaling axis to the indirect effect of negative regulation of the pro-survival pathway NFκB. It was also demonstrated that CYLD is found in complexes with RIP1, and in CYLD deficient spermatocytes RIP1 is hyperubiquitinated. The purported consequence

of RIP1 hyperubiquitination is enhanced association between RIP1 and NEMO. In accordance with enhanced RIP1/NEMO association, IP kinase assays from CYLD$^{-/-}$ spermatocytes revealed enhanced activation of the IKK complex. Consistent with enhanced IKK activity, enhanced NFκB activation was demonstrated and the concomitant up-regulation of anti-apoptotic NFκB target genes. The stimuli responsible for RIP1 ubiquitination in spermatocytes still must be elucidated (Wright et al., 2007).

The same study demonstrated that in overexpression experiments, CYLD was capable of blocking TNFα-induced RIP1 ubiquitination at time-points during Complex I formation, but it was not ascertained whether this occurred in the TNFR-1 complex (Wright et al., 2007). The current model for the pro-apoptotic mechanism of CYLD was formed based on this data, as well as the aforementioned evidence showing that RIP1 ubiquitination interferes with its engagement with caspase-8 complexes. Altogether, the current model suggests that the pro-apoptotic function of CYLD is attributed to deubiquitination of RIP1 leading to Complex II assembly, caspase activation, and death.

CYLD also has a pro-necrotic function, which is the central topic of this thesis. CYLD-mediated deubiquitination of RIP1 and subsequent transition of RIP1 from Complex I to Complex II has been implicated as its pro-necrotic mechanism (O'Donnell et al., 2011; O'Donnell et al., 2012; Vandenabeele et al., 2010) (Fig.1.4). However, the validity of this model has not been formally demonstrated. One report indicated that CYLD is a target of caspase-8, and the cleavage event suppresses the necrosis program. A cleavage site mutant of CYLD bypasses the requirement for caspase inhibition and results in reduced RIP1 and NEMO association. These complexes are pro-survival and

contingent upon RIP1 ubiquitination. Indeed, the CYLD-mediated disruption of RIP1/NEMO complexes correlated with enhanced RIP1 recruitment to FADD. Furthermore, the reported CYLD-mediated disruption of RIP1/NEMO complexes implies that CYLD exerts its pro-necrotic function by targeting TNFR-1 associated RIP1 (O'Donnell et al., 2011).

Thesis objective

The general aim of my thesis research has been to clarify the biochemical signaling pathway of TNFα-induced necrosis. At the inception of this work, the sub-field of necrosis signaling was just taking off with the discovery of RIP3 as an important regulator of the process, and that RIP1/RIP3 interaction was a required molecular event (Cho et al., 2009; He et al., 2009; Zhang et al., 2009). However, there was still a paucity of data regarding the regulation of RIP1/RIP3 association and their potential downstream targets. Given the inchoate stages of the scientific communities understanding of necrosis signaling, it was an excellent opportunity for discovery. My aim was to reveal new regulators of necrosis, so I screened a cancer gene siRNA library using a necrosis sensitive cell line. This resulted in the independent discovery of CYLD as a positive regulator of necrosis. It also yielded the discovery of FUS1 as a putative positive regulator of necrosis, which is a gene implicated in lung cancer (Deng et al., 2007). The focus of my work then shifted to further characterizing the requirement of CYLD for TNFα-induced cell death in a variety of different cell-lines, as well as its role in other cell death programs. I then ascertained the molecular mechanism accounting for the pro-

necrotic function of CYLD. This ended in the uncovering of an unexpected mechanism of CYLD-mediated necrosis, which illuminated the mechanism of necrosome activation.

Figure 1.4 Current model of CYLD-mediated necrosis

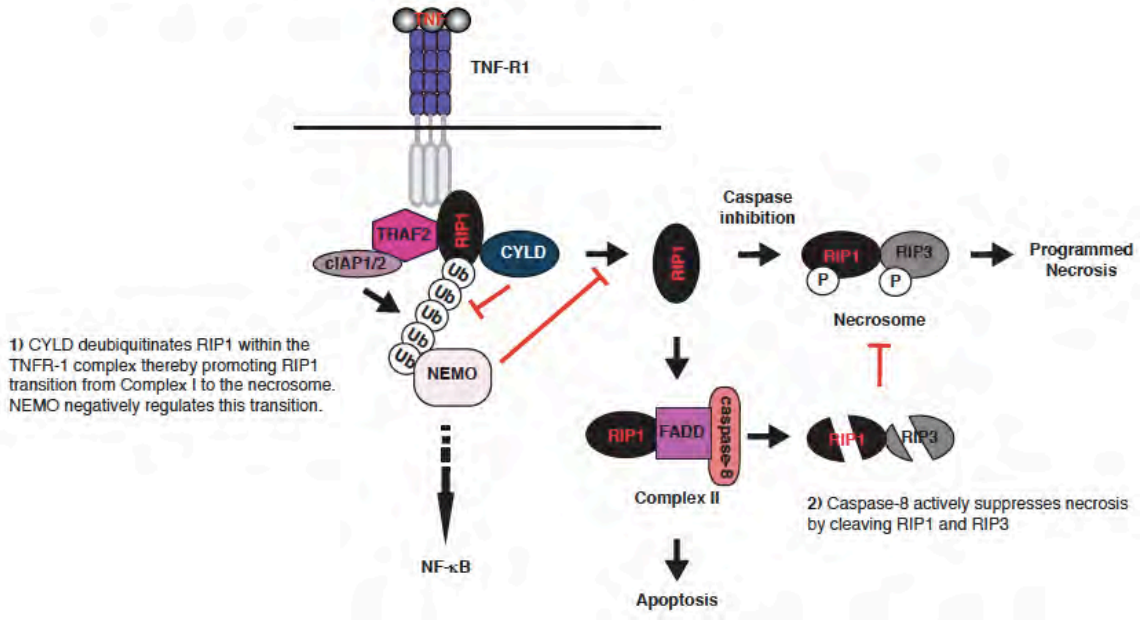

PREFACE TO CHAPTER II

List of author contributions:

David Moquin: conducted all the experiments.

Both David Moquin and Francis Chan designed experiments.

CHAPTER II: Identifying new regulators of programmed necrosis

Introduction

It is now well appreciated that death receptor ligands such as TNFα can give rise to necrotic cell death. Necrosis is a caspase-independent form of programmed cell death. In fact, caspases play a role in actively suppressing the necrosis signaling pathway (Oberst et al., 2011). The details regarding the biochemical signaling pathway leading to necrosis are currently under intense investigation. Receptor interacting protein 1 (RIP1), was the first regulator identified to be required for TNFα-induced necrosis (Holler et. al 2000 Nature). RIP1 is a Serine/Threonine kinase. The function of RIP1 was previously characterized as promoting NFκB, independent of its kinase activity (Kelliher et al., 1998; Lee et al., 2004). RIP1 kinase activity was subsequently shown to be required for its pro-necrotic function (Holler et al., 2000). It was later revealed that RIP3 is also a pro-necrotic protein. The interaction between RIP1 and RIP3 via their RHIMs is a required molecular event for TNFα-induced necrosis (Cho et al., 2009; He et al., 2009; Zhang et al., 2009).

During conditions that are permissive of TNFα-induced cell death, RIP1 dissociates from the receptor complex and forms a cytosolic death inducing signaling complex (DISC) or Complex II. Within this complex caspase-8 is activated and gives rise to a proteolytic cascade involving subsequent activation of executioner caspases and the cleavage of a myriad of cellular substrates leading to apoptosis. It is clear that both RIP1 and RIP3 are cleaved by caspase-8. Therefore, the necrosis pathway is actively suppressed by the apoptosis pathway (Feng et al., 2007; He et al., 2009). During caspase

inhibition, RIP1 and RIP3 are no longer cleaved allowing for the formation of a complex named the necrosome, which is critical for cellular demise via necrosis. The kinase activity of RIP1 is required for association with RIP3. Conversely, the kinase activity of RIP3 is dispensable for interaction with RIP1, but it is still required for necrosis. The requirement for RIP3 kinase activity is due to an auto-phosphorylation event, which is required for recruitment and activation of downstream substrates (Sun et al., 2012). RIP1 and RIP3 undergo auto and trans-phosphorylation events within the necrosome. The hierarchy and number of phosphorylation events still must be clarified (Cho et al., 2009; He et al., 2009; Zhang et al., 2009). Recently, it was demonstrated that Mixed-linage kinase domain like protein (MLKL), PGAM5L, and PGAM5S, are components of the necrosome and substrates of RIP1/RIP kinase activity. MLKL participates in the recruitment of PGAM5S to the necrosome. This is supported by data demonstrating that NSA, the covalent inhibitor of MLKL, blocks MLKL/PGAM5S binding and subsequent necrosis. Downstream of necrosome activation, PGAM5 activates the mitochondrial fission enzyme Drp-1 through dephosphorylation. This leads to mitochondrial fission and death by necrosis (Sun et al., 2012; Wang et al., 2012). It is important to mention that the role of mitochondrial fission in necrosis is still in its infancy, and much work is required to firmly establish its role and mechanism.

In spite of the advancement of the scientific communities knowledge of the necrosis signaling pathway, much work is still required. A number of unanswered questions remain. Firstly, since RIP1 is presumably the apical kinase in this cell death paradigm, mechanistic details regarding the activation of its kinase activity is of great

importance. Secondly, are there additional components of the necrosome? Thirdly, what is the role of the mitochondria in necrosis, and what are the mitochondrial targets either activated or repressed downstream of the necrosome? Given our growing understanding of necrosis being involved in a variety of physiological and pathophysiological situations, clarifying the signaling pathway could potentially create therapeutic targets for many diseases.

This study sought to identify other potential proteins involved in the TNFα-induced necrosis signaling pathway. It is well documented that cancer cells override cell suicide pathways. Chromosomal abnormalities have been demonstrated to lead to increased expression levels of anti-apoptotic proteins such as cIAPs. Therefore, a variety of therapeutic approaches exist to activate cell death pathways in cancer cells (Fulda et al. 2012). It is conceivable that necrosis plays a role in either the initiation, progression, or suppression of cancer. Finding new players in the necrosis signaling pathway can potentially yield new drug targets for the treatment of cancer and beyond. In order to identify potential signaling proteins involved in necrosis, a siRNA cancer gene library was screened. This study independently identified the tumor suppressor CYLD as a regulator of necrosis, as well as the lung cancer tumor suppressor FUS1 as a putative regulator of necrosis.

Results

CYLD and FUS1 are putative regulators of necrosis

In order to identify signaling regulators of necrosis, a cancer gene siRNA library was screened. A Jurkat T cell line deficient of FADD, and stably transfected with TNFR-2 was used in the screen. These cells undergo necrosis with only TNFα treatment and are particularly sensitive to necrosis due to expression of the necrosis enhancing TNFR-2 receptor. Since FADD is required for caspase-8 activation, this cell-line does not require the use of the pan caspase inhibitor zVAD-fmk in order to induce necrosis (Chan et al., 2003). In addition to the experimental siRNA oligos, each plate included both positive and negative controls. Namely, genes that have already been established as dispensable for necrosis and a gene previously established as essential for necrosis were used as controls. Specifically, TR4, GFP, and non-targeting (scrambled) siRNA were used as negative controls in these cell death assays, and RIP1 was used as the positive control. For each gene there were two siRNA oligos in the library. For transfection, the two siRNA oligos targeting the same gene were pooled. This increased the chances of efficient knock-down. For the majority of the genes, both two and three days post-transfection, cells were stimulated to undergo necrosis and then assayed for cell death. Two different doses of TNFα were used for each siRNA oligo. All cells were also treated with the apoptosis inducer, Staurosporine (STS). In addition to being an apoptosis inducer through activation of caspase-3, STS also broadly inhibits kinases (Chae et al., 2000). Thus the death observed using this inducer is most likely independent of kinases. Since necrosis requires kinases to potentiate the pro-necrotic signal, STS-induced death is an appropriate negative control. This control was to ensure that knock-down of genes resulting in protection against TNFα-induced necrosis were not simply conferring

resistance to cell death in general. This was therefore a specificity control for the necrosis signaling program.

A criterion was established in order to determine which genes qualified as putative regulators of necrosis. For each plate of siRNA, the mean and standard deviation of the cell viability for each dose of TNFα was calculated. Any siRNA that conferred protection one standard deviation above the mean was included as a positive hit for a putative regulator of necrosis. There were some instances when the knock-down conferred protection on day three post-transfection, but not two days post-transfection and vice versa. These genes were still included in the list of positive hits. The inclusion of the three-day transfection was to help eliminate the possibility of false negatives. Specifically, a negative hit attributed to a long protein half-life resulting in insufficient knock-down. After the screen was conducted, all of the positive hits (39 genes) were tested again for their ability to confer protection from necrosis and compiled in a table (Table 2.1A-C). There were two genes, which passed the validation round FUS1 and CYLD. An example of one of the graphs for a siRNA plate is included on the next page, and the remaining graphs are compiled in the appendix (Fig. 2.1; Appendix).

Figure 2.1

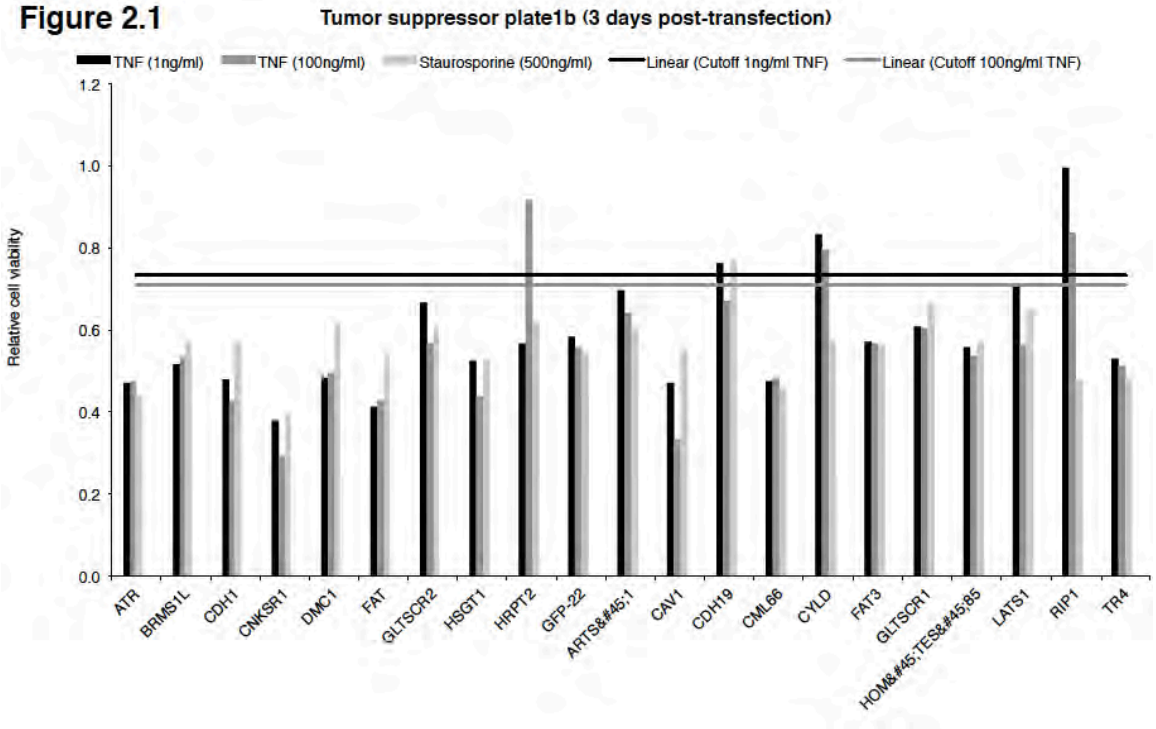
Tumor suppressor plate1b (3 days post-transfection)
TNF (1ng/ml)
TNF (100ng/ml)
Staurosporine (500ng/ml)
Linear (Cutoff 1ng/ml TNF)
Linear (Cutoff 100ng/ml TNF)
Relative cell viability
1.2
1.0
0.8
0.6
0.4
0.2
0.0
ATR
BRMS1L
CDH1
CNKSR1
DMC1
FAT
GLTSCR2
HSGT1
HRPT2
GFP-22
ARTS-1
CAV1
CDH19
CML66
CYLD
FAT3
GLTSCR1
HOM-TES-85
LATS1
RIP1
TR4

Table 2.1A Putative regulators of necrosis from the initial screen

Gene symbol	Name	Alternative name	ID
CCNG2	cyclin G2		901
ATAD2	ATPase family, AAA domain containing 2	ANCCA; PRO2000	29028
CETN2	centrin, EF-hand protein, 2	CALT; CEN2	1069
CHEK1	checkpoint kinase 1	CHK1	1111
CDC20	cell division cycle 20	CDC20A; p55CDC; bA276H19.3	991
FMN2	formin 2		56776
RBBP4	retinoblastoma binding protein 4	NURF55; RBAP48	5928
RAD21	RAD21 homolog (S. pombe)	HR21; MCD1; NXP1; SCC1; CDLS4; hHR21; HRAD21	5885
RACGAP1	Rac GTPase activating protein 1	CYK4; ID-GAP; HsCYK-4; MgcRacGAP	29127
UGCGL1	UDP-glucose glycoprotein glucosyltransferase 1	UGT1; HUGT1; UGCGL1	56886
SNRPA1	small nuclear ribonucleoprotein polypeptide A	Lea1	6627
GADD45A	growth arrest and DNA-damage-inducible, alpha	DDIT1; GADD45	1647

Table 2.1B Putative regulators of necrosis from the initial screen

Gene symbol	Name	Alternative name	ID
LIMK1	LIM domain kinase 1	LIMK; LIMK-1	3984
PCNA	proliferating cell nuclear antigen		5111
MDM2	MDM2 oncogene, E3 ubiquitin protein ligase	HDMX; hdm2; ACTFS	4193
BRCA1	breast cancer 1, early onset	IRIS; PSCP; BRCAI; BRCC1; PNCA4; RNF53; BROVCA1; PPP1R53	672
CHEK2	checkpoint kinase 2	CDS1; CHK2; LFS2; RAD53; hCds1; HuCds1; PP1425	11200
HRASLS3	phospholipase A2, group XVI	AdPLA; HRSL3; HRASLS3; HREV107; HREV107-1; HREV107-3; H-REV107-1	11145
LATS2	LATS, large tumor suppressor, homolog 2 (Drosophila)	KPM	26524
CYLD	cylindromatosis (turban tumor syndrome)	EAC; MFT; SBS; TEM; BRSS; CDMT; MFT1; CYLD1; CYLDI; USPL2	1540
LATS1	LATS, large tumor suppressor, homolog 1 (Drosophila)	wts; WARTS	9113
FUS1	tumor suppressor candidate 2	PAP; TUSC2; PDAP2; C3orf11	11334
TP53BP2	tumor protein p53 binding protein, 2	BBP; 53BP2; ASPP2; P53BP2; PPP1R13A	7159
HOM-TES-103	intermediate filament family orphan 1	IFFO; IFFO1	25900
LZTS2	leucine zipper, putative tumor suppressor 2	LAPSER1; RP11-108L7.8	84445
HIF1A	hypoxia inducible factor 1, alpha subunit (basic helix-loop-helix transcription factor)	HIF1; MOP1; PASD8; HIF-1A; bHLHe78; HIF-1alpha; HIF1-ALPHA	3091
ATM	ataxia telangiectasia mutated	AT1; ATA; ATC; ATD; ATE; ATDC; TEL1; TELO1	472

Table 2.1C Putative regulators of necrosis from the initial screen

Gene symbol	Name	Alternative name	ID
FLT3	fms-related tyrosine kinase 3	FLK2; STK1; CD135; FLK-2	2322
ARF1	ADP-ribosylation factor 1		375
APC	adenomatous polyposis coli	GS; DP2; DP3; BTPS2; DP2.5; PPP1R46	324
IGF1	insulin-like growth factor 1 (somatomedin C)	IGFI; IGF-I; IGF1A	3479
GSK3B	glycogen synthase kinase 3 beta		2932
GPR2	chemokine (C-C motif) receptor 10	CCR10	2826
PARD6A	par-6 partitioning defective 6 homolog alpha (C. elegans)	PAR6; PAR6C; TAX40; PAR-6A; TIP-40; PAR6alpha	50855
MTA3	metastasis associated 1 family, member 3		57504
PIK3CG	phosphatidylinositol-4,5-bisphosphate 3-kinase, catalytic subunit gamma	PI3K; PIK3; PI3CG; PI3Kgamma	5294
TNS	tensin 1	TNS1; MXRA6; MST091; MST122; MST127; MSTP091; MSTP122; MSTP127	7145
WASF2	WAS protein family, member 2	IMD2; SCAR2; WASF4; WAVE2; dJ393P12.2	10163
TGFBR1	transforming growth factor, beta receptor 1	AAT5; ALK5; MSSE; SKR4; ALK-5; LDS1A; LDS2A; TGFR-1; ACVRLK4	7046

Discussion

This study revealed two putative genes involved in TNFα-induced necrosis, FUS1 and CYLD. Previous work demonstrated that FUS1 functions as a tumor suppressor in lung cancer. Chromosomal deletions containing the FUS1 gene are frequently observed in lung cancer cells, which accounts for the loss of FUS1 mRNA and protein expression. Importantly, introduction of exogenous FUS1 into a panel of lung cancer cells was able to induce apoptosis. This was through the activation of the intrinsic mitochondrial apoptosis pathway. It has also been demonstrated that exogenous FUS1 can enhance the chemotherapeutic efficacy of Cisplatin. It appears to enhance the ability of the drug to cause MDM2 protein reduction, p53 protein elevation, and to trigger Apaf-1 dependent cancer cell death (Deng et al. 2008).

Another study provided evidence that FUS1 can negatively regulate the kinase activity of c-Abl. Indeed, a FUS1 peptide that corresponds to a region of the protein deleted in some lung cancer cell lines was able to inhibit c-Abl kinase activity *in vitro*. The FUS1 deletion mutant was unable to regulate c-Abl kinase activity in co-expression studies while the wild-type version could. Importantly, c-Abl tyrosine kinase activation was oncogenic as blocking its activity with an inhibitor was able to block colony formation. Exogenous introduction of FUS1 in a lung cancer cell line devoid of FUS1 and expressing activated c-Abl effectively reduced the level of c-Abl kinase activity. This reveals a target pertinent to the tumor suppressive function of FUS1, as well as kinase inhibition as a mechanism of tumor suppression (Lin et al., 2007).

Some evidence suggests that FUS1 can function as a tumor suppressor in bone and soft tissue sarcomas. Unlike the scenario in lung cancer cells, these sarcomas expressed FUS1 at the mRNA level, but not the protein level. Introduction of exogenous FUS1 was able to induce apoptosis in sarcomas with low levels of protein expression. This supports the notion that FUS1 may function as a tumor suppressor in other types of cancer, but the mechanism of reduced FUS1 protein expression is not attributed to chromosomal deletion in all cancer types. One potential explanation for the deficiency of FUS1 protein expression in bone sarcomas is the expression of an oncogenic E3 ligase, which continuously targets FUS1 protein for proteasomal degradation (Li et al. 2011). Consistent with this hypothesis, it was demonstrated that the tumor suppressive function of FUS1 requires the post-translational modification N-myristoylation. This is possibly explained by the fact that a mutant version FUS1, which cannot be modified with N-myristoylation is susceptible to degradation by the proteasome and has altered subcellular localization (Uno et al. 2004). Another report shows that FUS1 expression may also be blunted by the increased expression of miRNA in cancer cells that target the 3'UTR of FUS1 (Du et al. 2009).

Our study potentially expands upon the know function of FUS1 from promoting the intrinsic mitochondrial apoptosis pathway in cancer cells to being involved in death receptor induced necrosis. Future research must be conducted to confirm that FUS1 is a bona fide promoter of necrosis. It is conceivable that FUS1 only regulates necrosis in specific cell-types; therefore, initial studies should establish whether it is in fact part of the core necrotic machinery. Another important question to address is the molecular

mechanism accounting for the pro-necrotic function of FUS1. Necrosis is an apoptosome independent form of cell death, which excludes the possibility that FUS1 is promoting necrosis through apoptosome formation. Nevertheless, this may in fact provide an important clue as to the subcellular location where FUS1 exerts its pro-necrotic function. Given the paucity of data regarding the mechanism of FUS1-mediated apoptosis, the evidence that does exist provides rationale for investigating the effect of FUS1 on mitochondrial dynamics during necrosis. Furthermore, the requirement of FUS1 to be myristoylated in order to promote apoptosis supports the notion that it requires membrane tethering. One possibility is that FUS1 must be tethered to mitochondrial membranes in order to exert its cell death function and avoid degradation by the proteasome.

One report demonstrates that the necrosome can promote mitochondrial fragmentation through the activation of the mitochondrial fission enzyme Drp-1 (Sun et al, 2012). Given that other reports have implicated Drp-1 mediated mitochondrial fission in the kinetics of necrosis and apoptosis in C. elegans, it is tempting to speculate that FUS1 is involved in mitochondrial fission. Namely, FUS1 may inhibit the fusion machinery or activate the fission machinery (Breckenridge et al., 2008; Jagasia et al., 2005). Since phosphorylation is an important regulatory mechanism of mitochondrial fission during necrosis, FUS1 may regulate kinases that antagonize fission. Interestingly, the phosphatase PGAM5 is required for removal of an inhibitory phosphate group from Drp-1, which activates its GTPase activity and mitochondrial fission function. Since a report indicates that FUS1 can inhibit the kinase activity of c-Abl, it is possible that FUS1 can activate Drp-1 by inhibiting the kinase, which is responsible for phosphorylating

Drp-1 and keeping it inactive. This hypothesis implies that PGAM5 and FUS1 both activate Drp-1, but through different molecular mechanisms. In simplified terms, PGAM5 removes the inhibitory phosphate from Drp-1, and FUS1 might inactivate the kinase that phosphorylates and inhibits Drp-1. The corollary of FUS1 mediated mitochondrial fission would either be the promotion of apoptosis, or alternatively, necrosis when caspases are inactivated. This model implies that in the context of apoptosis the outcome of mitochondrial fission is activation of the apoptosome.

Clearly, the pro-necrotic function of FUS1 needs to be clarified. It will be of value to determine whether its participation in necrosis is cell-type specific or a general requirement for multiple cell types. A cell-type specific scenario of the involvement of FUS1 in necrosis would possibly indicate that it acts in the execution phase of the cell death process. This claim is based on the observation that ROS is not required for all cell-types to undergo necrosis, suggesting that necrosis may engage alternative mechanisms in its execution phase (Zhao et al., 2012). If a general requirement for FUS1 in the necrosis program is observed then this would suggest that it is part of the core necrotic machinery. Once this is delineated, it would be most informative to determine the impact of FUS1 on necrosome formation. If FUS1 has no impact on necrosome formation then it suggests its role is either in promoting necrosome functionality or a downstream event such as mitochondrial dynamics. Given the dearth of knowledge regarding the role of mitochondrial dynamics during necrosis, and the link between FUS1 and the mitochondria, elucidating the molecular mechanism of FUS1-mediated necrosis should be of great interest to the cell death field. The implications of FUS1 as a regulator

of necrosis and a tumor suppressor for lung cancer make this an even more enticing topic of further research. Ultimately, it will be of great interest to determine whether the pro-necrotic function of FUS1 is responsible for its tumor suppressive effects. This may provide rationale for studying the impact of necrosis on lung cancer.

The other gene we identified in this screen was CYLD. The following chapters will focus on the characterization of the requirement of CYLD in programmed necrosis and the molecular mechanism accounting for its pro-necrotic function. During the time when we independently discovered the functional requirement of CYLD for programmed necrosis a model was proposed which explained the molecular mechanism. The prevailing model was that CYLD regulation of RIP1 ubiquitination within the TNFR-1 complex promotes RIP1 transition from the membrane associated pro-survival complex to the cytosolic death mediating complex (Vandenabeele et al., 2010). My research sought to directly test whether this model indeed represented the molecular mechanism accounting for the pro-necrotic function of CYLD. Due to the fact that this gene is covered extensively in other chapters, a detailed discussion will be postponed for the following chapters to avoid unnecessary redundancy.

Materials and Methods

Reagents used

Recombinant human TNF was obtained from Biosource. The siRNA library screened was: Human Cancer siRNA Set V2.0 from Qiagen.

Transfection of siRNA and treatment to undergo necrosis

FADD deficient Jurkat cells stably expressing exogenous TNFR2 (Chan et al., 2003) were transfected with 150 nM of the indicated siRNA using the HiPerfect transfection reagent (Qiagen) and following the manufacture's protocol. Cells were stimulated to undergo necrosis at 48 and 72 hours post-transfection with 10ng/ml recombinant human TNFα for 6-14 hours. For the initial screen, cell viability was determined with CellTiter 96® AQueous One Solution Cell Proliferation Assay (Promega) as per manufacturers instructions. For the validation of positive hits yielded from the initial screen, cells were stained with 10ug/ml propidium iodide (PI) and analyzed via flow cytometry. Any siRNA oligo that resulted in an increase in the percentage of PI negative cells after stimulated to undergo TNFα-induced necrosis passed this round of validation.

PREFACE TO CHAPTER III

This chapter contains material from the following manuscript that is under review for publication:

David M. Moquin, Thomas McQuade, Francis Ka-Ming Chan. **CYLD Deubiquitinates RIP1 in the Necrosome to Facilitate Kinase activation and Programmed Necrosis**

List of author contributions:

Thomas McQuade: Helped with repeating kill assay experiments

David Moquin: Conducted the remaining experiments

Both David Moquin and Francis Chan designed experiments. Some written portions of this chapter were taken from the manuscript co-written by David Moquin and Francis Chan. David Moquin wrote the rest of the chapter.

CHAPTER III: Characterization of the requirement of CYLD in programmed necrosis

Introduction:

Cylindromatosis (CYLD) is an ubiquitin specific protease that is named after an inherited autosomal dominant disease caused by mutations resulting in truncations that abolish its enzymatic activity (Bignell et al., 2000). CYLD is a bona fide tumor suppressor, and it is clear that its tumor suppressive function requires a functional enzymatic domain. It is well documented that CYLD is involved in a diverse set of cellular signaling pathways downstream of many receptors and stimuli regulating cell survival and division. Its functional involvement in these pathways is imparted by its ability to regulate the ubiquitination status and functionality of various signaling proteins that participate in these pathways. More specifically, CYLD is a negative regulator of both the canonical and non-canonical NFκB pathways. Therefore it regulates cell survival, inflammation, and cell cycle progression (Brummelkamp et al., 2003; Kovalenko et al., 2003; Trompouki et al., 2003; Massoumi et al., 2003).

The most compelling evidence accounting for the tumor suppressive function of CYLD is its ability to negatively regulate the non-canonical NFκB pathway in keratinocytes. When keratinocytes are exposed to UV or the chemical mutagen 12-O-tetradecanoylphorbol-13 acetate (TPA), CYLD translocates to the perinuclear region from the cytoplasm. In this subcellular location, CYLD deubiquitinates Bcl-3, which prevents its nuclear translocation and activation of cyclin D1 transcription and concomitant cell cycle progression. Bcl-3 functions as a co-activator of the NFκB family members p50 and p52. In fact, p50 and p52 only contain a DNA binding domain so when they homodimerize they mediate transcriptional silencing. However, when these

proteins heterodimerize with Bcl-3 they are endowed with the ability to mediate transcriptional activation. This is due to the fact that Bcl-3 provides the necessary transactivation domain which p50 and p52 lack. The importance of this CYLD-mediated signaling event is highlighted by the fact that CYLD knock-out mice are more prone to developing skin tumors akin to patients with cylindromatosis (Massoumi et al., 2006).

The tumor suppressive role of CYLD in cancer extends beyond the skin. CYLD expression levels are reduced in a myriad of cancer types such as multiple myeloma, lung cancer, T cell acute lymphoblastic leukemia (T-ALL), hepatocellular carcinoma, and colon carcinoma (Annunziata et al., 2007; Espinosa et al., 2010; Hellerbrand et al. 2007; Keats et al. 2007; Zong et al., 2007). The mechanism behind reduced CYLD expression in T-ALL is Notch-induced Hes1 expression. Hes1 transcriptionally silences CYLD resulting in sustained NFκB activation (Espinosa et al., 2010). As with skin cancer, the broad tumor suppressive role of CYLD is attributed to negative regulation of NFκB. By negatively regulating NFκB, CYLD controls the expression level of anti-apoptotic proteins and thereby indirectly influences cell death (Brummelkamp et al., 2003). However, the data from our lab and others indicates that CYLD has a direct role in promoting death receptor induced cell death (Fujikura et al., 2012; O'Donnell et al., 2011; Wang et al., 2008). It is reasonable to postulate that the tumor suppressive function of CYLD in any of the number of types of cancer it's implicated in, is not limited to negative regulation of NFκB. The tumor suppressive function of CYLD may in part be due to its role in directly promoting death receptor mediated cell death.

The direct role of CYLD in promoting cell death is a more recent advancement in the understanding of how it influences cell fate. CYLD is involved in both death receptor induced apoptosis and necrosis signaling pathways (Fujikura et al., 2012; O'Donnell et al., 2011). As discussed in the previous chapter, our group independently discovered CYLD as a regulator of necrosis via screening a human cancer gene siRNA library. Another group also recently identified CYLD through screening a mouse genome wide siRNA library (Hitomi et al., 2008). As for its apoptotic function, one report shows that siRNA targeting CYLD confers protection from TNFα/SMAC mimetic induced apoptosis in a human pancreatic carcinoma cell line PANC-1. In addition to CYLD knock-down conferring protection from apoptosis, it also caused impaired RIP1 recruitment to Caspase-8. The influence of CYLD on this molecular event was used to describe its pro-apoptotic function (Wang et al., 2008). Consistently, another group also demonstrated that CYLD mediates Caspase-8 activation. Overexpression of CYLD resulted in an enhancement of TNFα driven Caspase-8 activation in HeLa cells. Additionally, CYLD knock-down resulted in an impairment in TNFα driven Caspase-8 activation. The pro-apoptotic function of CYLD was attributed to its role in promoting the formation of the apoptotic DISC. This study also demonstrated that CYLD was required for TNFα/SMAC mimetic driven Caspase-8 activation (Fujikura et al., 2012).

The functional requirement for CYLD in apoptosis is at odds with another recent report, which showed that CYLD is a target of Caspase-8. In this study, CYLD knock-out MEFs ectopically expressing a Caspase-8 cleavage resistant CYLD underwent necrosis in the absence of Caspase-8 inhibition. This group therefore linked Caspase-8

mediated suppression of necrosis with its ability to target CYLD for cleavage. Cleavage of CYLD results in the proteasome mediated degradation of the C-terminal fragment containing the domain responsible for its enzymatic activity (O'Donnell et al., 2011). One potential model that is consistent with the available data is that CYLD drives Caspase-8 activation and then Caspase-8 activation cleaves and inactivates CYLD in order to prevent necrosis. The timing of CYLD inactivation suggests that the pro-necrotic function of CYLD is post-necrosome formation, which does not agree with the current model. This concept will be discussed at length in the discussion section.

In this chapter we sought to further characterize the functional role of CYLD in programmed necrosis. A variety of different cell systems were used in order to thoroughly interrogate the pro-death function of CYLD. We show that CYLD is involved in both TNFα-driven apoptosis and necrosis. However, CYLD is not essential for both forms of cell death as indicated by a substantial amount of residual cell death that occurs in CYLD knock-out MEFs. The residual necrosis is RIP1 kinase dependent, which was previously defined as a pro-necrotic enzymatic activity as it promotes necrosome formation (Cho et al., 2009; Degterev et al., 2005; He et al., 2009). The requirement for RIP1 kinase activity therefore implies that the residual necrosis in the absence of CYLD still requires signal transduction through the necrosome. Since the current model suggests CYLD is an essential upstream regulator of necrosome formation, our data provides rationale for reevaluating the molecular mechanism of CYLD during necrosis.

Results

CYLD promotes but is not essential for TNFα-induced programmed necrosis

Assembly of the RIP1-RIP3 "necrosome" is a key event in programmed necrosis (Cho et al., 2003). The current model predicts that RIP1 in the TNFR-1 complex has to be de-ubiquitinated before it can engage RIP3 to form the necrosome. RIP1 is a known substrate of CYLD and this molecular event has been implicated as a consequential attribute of the necrosis signaling pathway (O'Donnell et al., 2011). In order to further validate the screen results, transfection of two different CYLD targeting siRNA oligos were tested for their ability to confer protection from TNFα-induced programmed necrosis in FADD-deficient Jurkat cells (Fig. 3.1A). Contrary to the expectation that CYLD is an essential member of the necrosis pathway (Vanlangenakker et al., 2011), we consistently observed weaker protection by siRNA against CYLD compared with siRNAs against RIP1 or RIP3 (Fig. 3.1A). Knock-down of A20, another deubiquitinase that regulates RIP1 ubiquitination resulted in enhanced necrosis (Wertz et al., 2004). This is consistent with the notion that CYLD and A20 are not functionally redundant. This is also intuitive considering that A20 serves as an ubiquitin editing enzyme by first removing K63-linked polyubiquitin chains from RIP1 and then tagging RIP1 with K48-linked polyubiquitin chains resulting in proteasomal degradation. Since RIP1 is required for TNFα-induced necrosis, A20 should in fact function as a negative regulator through facilitating RIP1 degradation. Our data supports this model, by showing that A20 does indeed function as a negative regulator of necrosis. Similarly, HT-29 cells with stable

knock-down (kd) of CYLD (Fig. 3.1B) or L929 cells transfected with siRNA against CYLD also exhibited residual TNFα-induced necrosis (Fig. 3.1C-D).

The residual cell death was not due to insufficient inhibition of CYLD expression, since $CYLD^{-/-}$ mouse embryonic fibroblasts (MEFs) also exhibited reduced but residual TNFα-induced programmed necrosis compared to $CYLD^{+/+}$ MEFs (Fig. 3.2A). $CYLD^{-/-}$ MEFs also displayed moderate resistance to apoptosis induced by TNFα and cycloheximide (CHX) (Fig. 3.2C-D). Interestingly, the onset of cell death in $CYLD^{-/-}$ MEFs was kinetically impaired. Although, death still occurred in the absence of CYLD, the magnitude of death did not reach levels observed in cells expressing CYLD (Fig. 3.2B). This may explain why some studies report CYLD as essential for necrosis because they looked at time-points prior to the onset of death in cells with reduced CYLD expression.

CYLD is dispensable in other cell death pathways

We next wanted to determine whether the involvement of CYLD in cell death was specific to the TNFR-1 signaling pathway. To address this question we compared the cell death responses of $CYLD^{+/+}$ and $CYLD^{-/-}$ MEFs sensitized to die via TRAIL, FasL or staurosporine (Fig 3.3A-C). No difference in cell death was observed in $CYLD^{-/-}$ MEFs treated with these stimuli, as compared to wild-type MEFs. This data indicates that CYLD specifically functions as a pro-death regulator downstream of TNFR-1 and not TRAIL, Fas, or the intrinsic mitochondrial apoptosis pathway. This does not preclude the possibility that CYLD plays a role in cell death triggered by TLRs.

MEFs can be sensitized to undergo TNFα-induced necrosis through a variety of different treatment regimens. We were interested in ascertaining whether alternative ways of necrosis sensitization would impact the residual necrosis observed in the absence of CYLD. We therefore compared the death responses of $CYLD^{+/+}$ and $CYLD^{-/-}$ MEFs to cells sensitized with either TNFα/zVAD/CHX, or TNFα/zVAD/LBW242. Cell death sensitization by zVAD/LBW242 was of greater magnitude in the presence or absence of CYLD than zVAD/CHX (Fig. 3.4A). Note that the same doses of TNFα were used for both types of sensitization. The reduced requirement for CYLD-mediated necrosis in SMAC mimetic treated cells is presumably due to the effect SMAC mimetic has on RIP1 ubiquitination. Namely, SMAC mimetic reduces the levels of cIAP1/2, which are the E3 ligases responsible for ubiquitinating RIP1 within the TNFR-1 complex (Varfolomeev et al., 2008). Therefore, elimination of cIAPs reduces RIP1 ubiquitination and should theoretically absolve the requirement of CYLD in TNFα-induced necrosis. Interestingly, the CYLD-independent necrosis is observed predominately in the more potent treatment regimens and is much less pronounced in cells just treated with TNFα/zVAD (Fig 3.4B). Strikingly, the residual necrosis in $CYLD^{-/-}$ MEFs was completely inhibited by the RIP1 kinase inhibitor necrostatin-1 (Fig. 3.4C). Hence, CYLD is not essential for RIP1-dependent necrosis. Rather, it plays an auxiliary role to promote efficient TNFα-induced programmed necrosis.

Hydrogen peroxide is another inducer of programmed necrosis. One report demonstrates that hydrogen peroxide triggered necrosis is independent of the RIP1/RIP3/MLKL necrosome, but dependent on the mitochondrial phosphatases

PGAM5S/L, which are downstream substrates of the necrosome (Xiaodong Wang 2012 Cell). Since our data suggests that CYLD is not essential for necrosome formation, as the current model predicts, we wanted to see whether CYLD functions downstream of hydrogen peroxide induced necrosis, which presumably activates the necrotic machinery downstream of the necrosome. In order to address this question we compared the cell death responses of $CYLD^{+/+}$ and $CYLD^{-/-}$ MEFs to hydrogen peroxide induced necrosis. Our data indicates that CYLD is dispensable for hydrogen peroxide induced necrosis (Fig. 3.5A). This reveals that CYLD does not function downstream of ROS production during necrosis. Additionally, we show that CYLD positively regulates ROS production as demonstrated by the use of the ROS indicator H_2DCFDA. Consistent with residual necrosis in the $CYLD^{-/-}$ MEFs, ROS production is only partially reduced as compared to $CYLD^{+/+}$ MEFs (Fig. 3.5B). This data supports the notion that CYLD acts upstream of ROS production during necrosis.

Figure 3.1

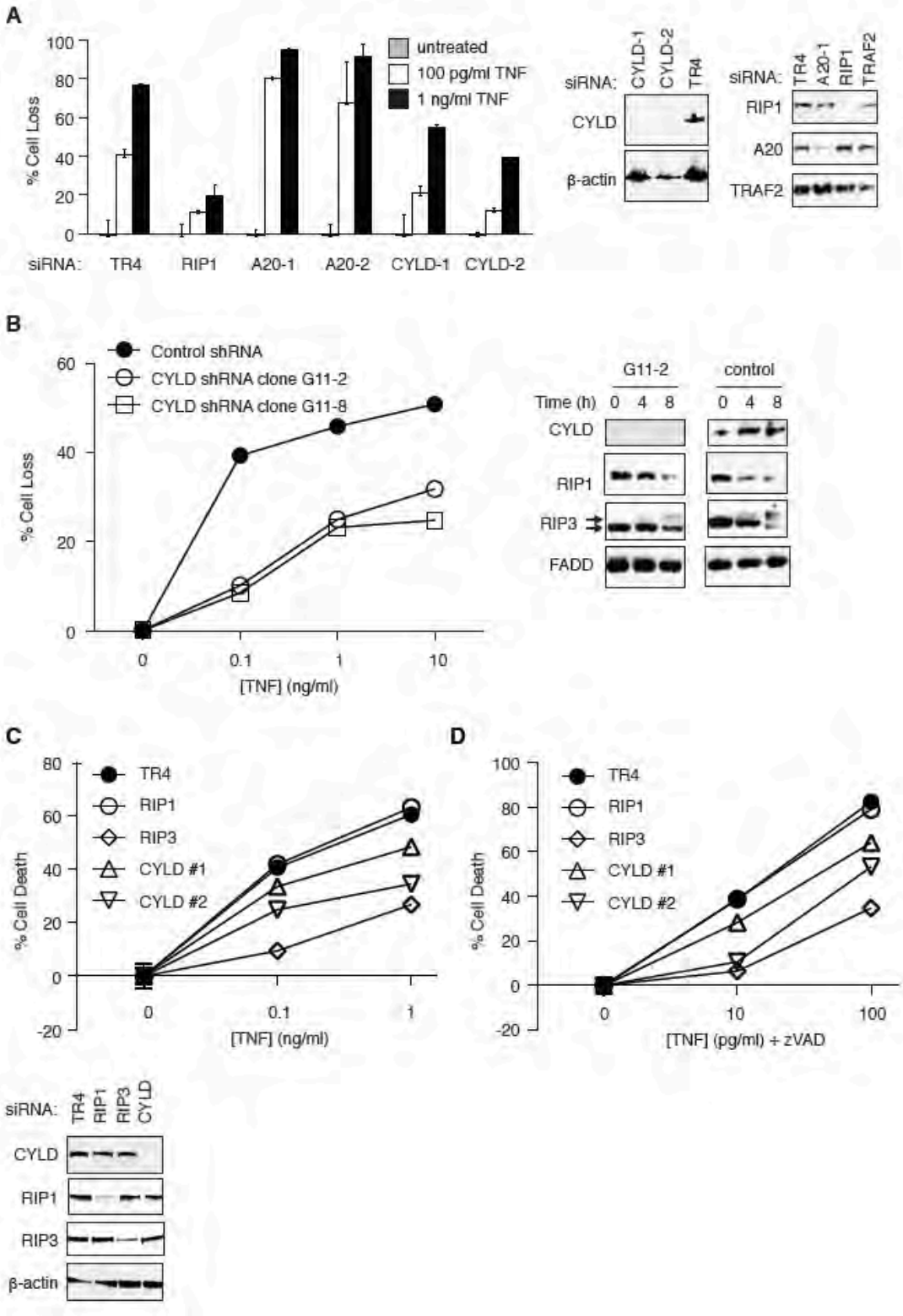
A
% Cell Loss
untreated
100 pg/ml TNF
1 ng/ml TNF
siRNA: TR4 RIP1 A20-1 A20-2 CYLD-1 CYLD-2
siRNA: CYLD-1 CYLD-2 TR4
CYLD
β-actin
siRNA: TR4 A20-1 RIP1 TRAF2
RIP1
A20
TRAF2
B
Control shRNA
CYLD shRNA clone G11-2
CYLD shRNA clone G11-8
% Cell Loss
[TNF] (ng/ml)
G11-2
control
Time (h) 0 4 8 0 4 8
CYLD
RIP1
RIP3
FADD
C
TR4
RIP1
RIP3
CYLD #1
CYLD #2
% Cell Death
[TNF] (ng/ml)
siRNA: TR4 RIP1 RIP3 CYLD
CYLD
RIP1
RIP3
β-actin
D
TR4
RIP1
RIP3
CYLD #1
CYLD #2
% Cell Death
[TNF] (pg/ml) + zVAD

Figure 3.1 Partial protection against TNFα-induced necrosis by CYLD siRNAs. **(A)** CYLD promotes programmed necrosis and A20 negatively regulates it. FADD-deficient Jurkat cells were transiently transfected with the indicated siRNAs. Forty-eight hours post-transfection, the cells were treated with TNFα to induce necrosis. Percentage cell loss was determined by staining with propidium iodide (PI) and flow cytometry. The right panels are Western blots showing the efficiency of gene silencing. **(B)** HT-29 cells were stably transfected with either non-specific shRNA (control) or CYLD targeting shRNA (clones: G11-2 and G11-8). Cells were treated with TNFα, LBW242 and zVAD-fmk. Cell viability was determined by MTS assay (Promega). The right panels are Western blots that validate reduction in protein expression of CYLD in the selected clones. **(C-D)** L929 cells were transfected with the indicated siRNAs. Necrosis was induced with (C) TNFα or (D) TNFα and zVAD-fmk. Cell viability was determined by MTS assay. The panel below shows reduction in protein expression of the indicated siRNA transfected cells.

Figure 3.2

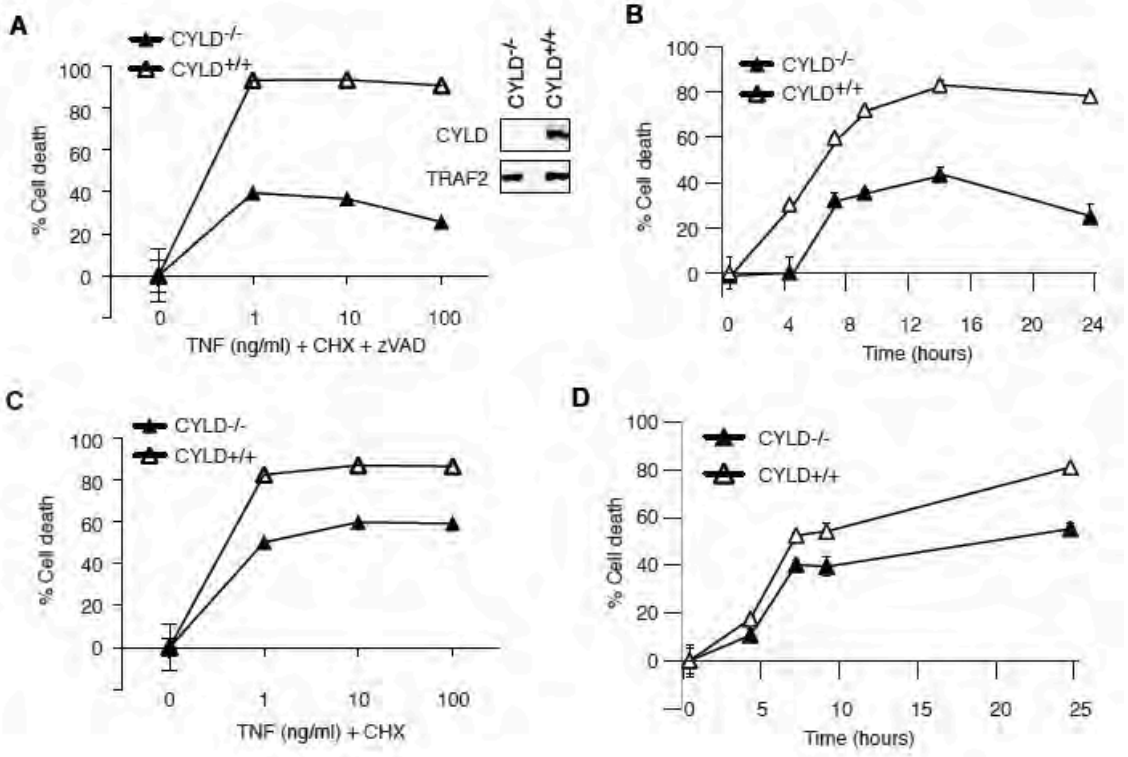
A
CYLD-/-
CYLD+/+
% Cell death
TNF (ng/ml) + CHX + zVAD
CYLD-/-
CYLD+/+
CYLD
TRAF2
B
CYLD-/-
CYLD+/+
% Cell death
Time (hours)
C
CYLD-/-
CYLD+/+
% Cell death
TNF (ng/ml) + CHX
D
CYLD-/-
CYLD+/+
% Cell death
Time (hours)

Figure 3.2 Residual TNFα-induced necrosis and apoptosis in CYLD$^{-/-}$ MEFs.

(A) Wild type (CYLD$^{+/+}$) and CYLD$^{-/-}$ MEFs were treated with cycloheximide (CHX), zVAD-fmk and the indicated doses of TNFα for 12-hours. Cell loss was determined by staining with propidium iodide (PI) and analyzed via flow cytometry. The inset shows the absence of CYLD expression in CYLD$^{-/-}$ MEFs. In **(B)**, cells were treated with 10 ng/ml TNFα, CHX and zVAD-fmk and cell death was measured at the indicated time-points following treatment. **(C)** CYLD$^{+/+}$ and CYLD$^{-/-}$ MEFs were treated with TNFα and CHX for 12 hours. Cell death was determined by PI staining and flow cytometry. **(D)** MEFs were treated with 10 ng/ml TNFα and CHX for the indicated times.

Figure 3.3

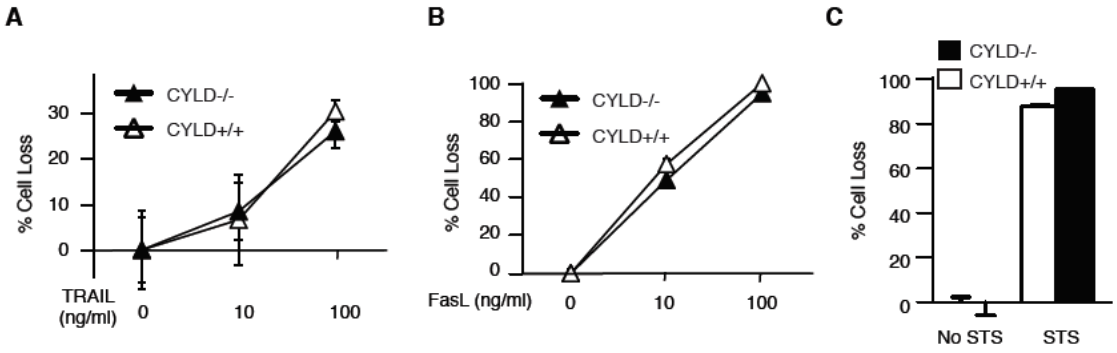
A
% Cell Loss
30
20
10
0
CYLD-/-
CYLD+/+
TRAIL (ng/ml)
0
10
100
B
% Cell Loss
100
80
60
40
20
0
CYLD-/-
CYLD+/+
FasL (ng/ml)
0
10
100
C
% Cell Loss
100
80
60
40
20
0
CYLD-/-
CYLD+/+
No STS
STS

Figure 3.3 CYLD is not involved in other death inducing stimuli in MEFs.

(A-C) Wild type ($CYLD^{+/+}$) and $CYLD^{-/-}$ MEFs were treated with **(A)** TRAIL, **(B)** FasL or **(C)** staurosporine (STS) for 12 hours. Cell death was determined by PI exclusion and flow cytometry.

Figure 3.4

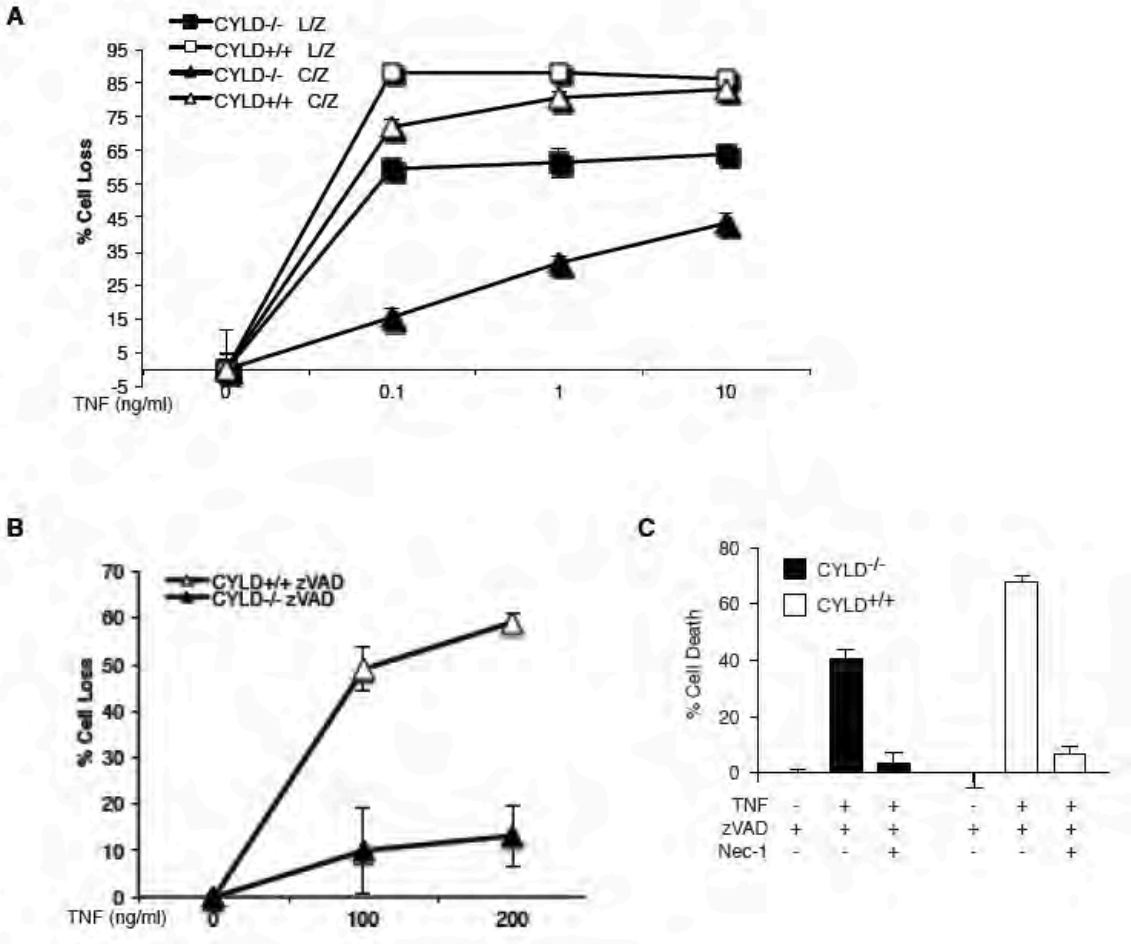
A
CYLD-/- L/Z
CYLD+/+ L/Z
CYLD-/- C/Z
CYLD+/+ C/Z
% Cell Loss
95
85
75
65
55
45
35
25
15
5
-5
TNF (ng/ml)
0
0.1
1
10
B
CYLD+/+ zVAD
CYLD-/- zVAD
% Cell Loss
70
60
50
40
30
20
10
0
TNF (ng/ml)
0
100
200
C
CYLD-/-
CYLD+/+
% Cell Death
80
60
40
20
0
TNF - + + - + +
zVAD + + + + + +
Nec-1 - - + - - +

Figure 3.4 RIP1-dependent necrosis occurs in CYLD$^{-/-}$ MEFs.

(A-B) Wild type (CYLD$^{+/+}$) and CYLD$^{-/-}$ MEFs were treated with either cycloheximide (CHX) or SMAC mimetic (LBW242) in addition to zVAD-fmk **(A)** or zVAD-fmk alone **(B)** and the indicated doses of TNFα for 12 or 24 hours respectively. Cell loss was determined by staining with propidium iodide (PI) and analyzed via flow cytometry. **(C)** Nec-1 inhibited TNFα-induced necrosis in CYLD$^{-/-}$ MEFs.

Figure 3.5

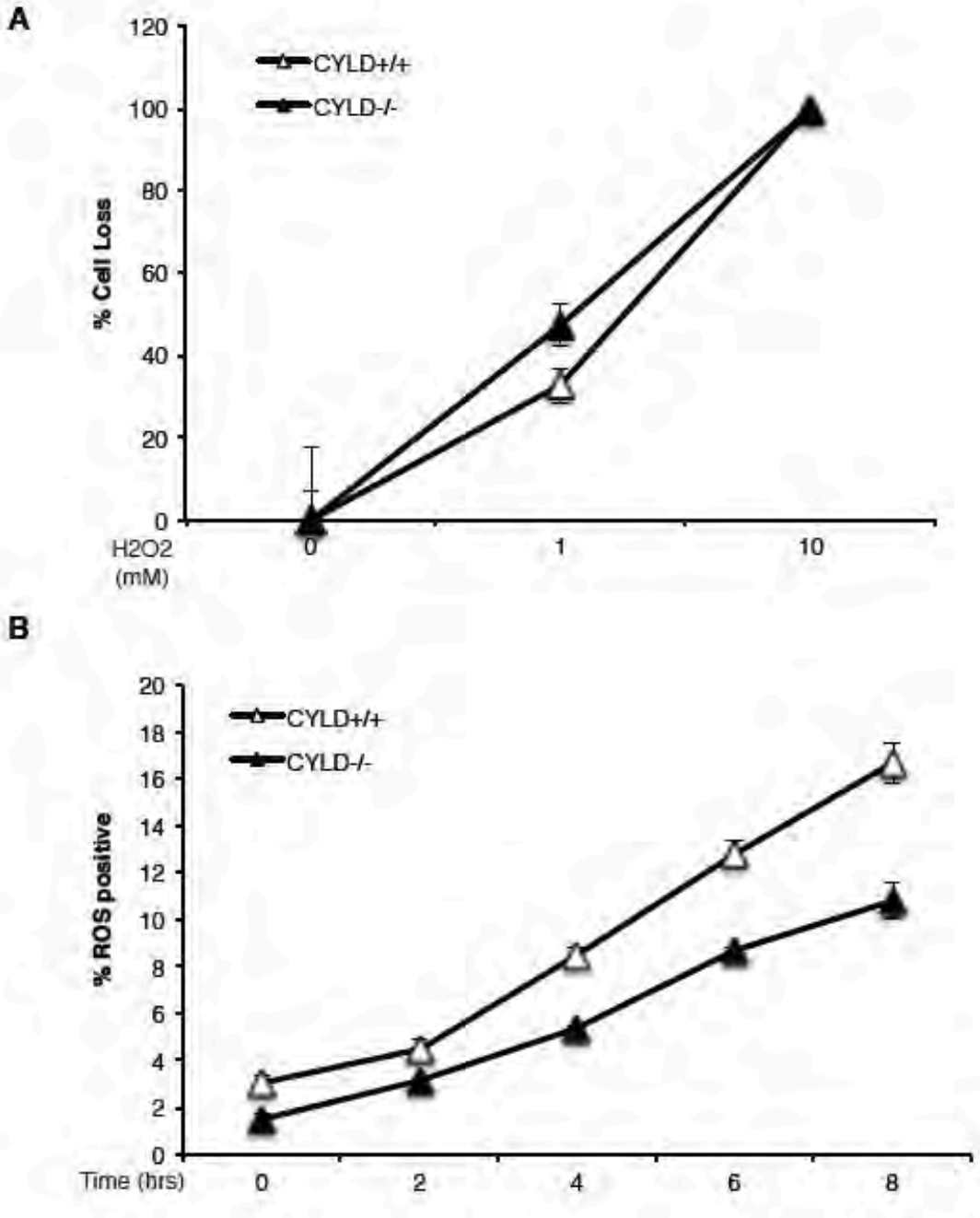
A
120
100
80
60
40
20
0
% Cell Loss
CYLD+/+
CYLD-/-
H2O2
(mM)
0
1
10
B
20
18
16
14
12
10
8
6
4
2
0
% ROS positive
CYLD+/+
CYLD-/-
Time (hrs)
0
2
4
6
8

Figure 3.5 CYLD impacts TNFα-induced ROS production.

(A) Wild type ($CYLD^{+/+}$) and $CYLD^{-/-}$ MEFs were treated with H_2O_2 for 12 hours. Cell death was determined by PI exclusion and flow cytometry. **(B)** MEFs were treated with CHX, zVAD, and TNFα for the indicated time-points. Cellular reactive oxygen species (ROS) were determined by measuring H_2DCFDA fluorescence by flow cytometry.

Discussion

Altogether our data demonstrates that CYLD functions as a positive regulator of both necrosis and apoptosis downstream of TNFR-1, but residual cell death still proceeds in the absence of CYLD. The current model for the pro-necrotic mechanism of CYLD is that it exerts its function upstream of RIP1/RIP3 association, which is a critical molecular event for TNFα-induced necrosis (Cho et al. 2009; Vanlangenakker et al., 2011). Since we report that CYLD is not essential for necrosis this weakens the plausibility of the current model. Furthermore, the CYLD-independent necrosis is still RIP1 kinase dependent. RIP1 kinase activity is essential for RIP1/RIP3 association and TNFα-induced necrosis; therefore, the residual cell death in the absence of CYLD presumably still requires signal transduction through the RIP1/RIP3 necrosome. The RIP1/RIP3 necrosome is upstream of ROS production, which is a cell-type specific effector mechanism of the necrosis program (Cho et al., 2009). Consistent with the kill assay data, we demonstrate that ROS production during TNFα-induced necrosis is attenuated, but not blocked in cells lacking CYLD. Importantly, hydrogen peroxide induced necrosis, which is independent of the RIP1/RIP3 necrosome, was not altered in cells lacking CYLD. This complementary data places the pro-necrotic function of CYLD upstream of ROS production.

The onset of death observed in the $CYLD^{-/-}$ MEFs is kinetically delayed as compared to $CYLD^{+/+}$ MEFs, but the magnitude of cell death remains attenuated even at later time-points. This lends support to the notion that CYLD may regulate both an early and late molecular event required for the onset and magnitude of cell death respectively.

The functional requirement of CYLD in necrosis appears to be more pronounced than apoptosis due to the greater level of protection observed in $CYLD^{-/-}$ MEFs treated to undergo necrosis as compared to apoptosis. One possibility is that CYLD regulates more than one molecular event during necrosis while only one during apoptosis. Since CYLD drives TNFα-induced Caspase-8 activation, and CYLD is a target of Caspase-8 this suggests that the pro-apoptotic function of CYLD is attributed to regulation of a molecular event preceding the formation of the apoptotic DISC (Fujikura et al., 2012; O'Donnell et al., 2011). Consistent with this notion, CYLD has been shown to regulate apoptotic DISC formation (Wang et al., 2008). In the next chapter we demonstrate that CYLD similarly regulates that kinetics of RIP1/RIP3 association as well as other components, which are also found in the apoptotic DISC. The current understanding of the TNFα-induced apoptosis and necrosis pathways is that the two pathways diverge at the point of the cytosolic DISC. All of this information potentially indicates that CYLD mediates an early molecular event that is common to both apoptosis and necrosis. This overlapping mechanism would theoretically precede an additional necrosis specific signaling event. In other words, CYLD would mediate a common molecular event required for apoptosis and necrosis and would mediate a later molecular event that is specific to necrosis. Through simple addition, the comparison between one CYLD-mediated molecular event during apoptosis and two CYLD-mediated molecular events during necrosis may explain the greater requirement for CYLD in necrosis.

The regulation of DISC formation is most likely not through regulation of RIP1 ubiquitination as TNFα/CHX induced necrosis is a RIP1 independent cell death pathway

(Lin et al., 2004). Interestingly, cells deficient of NEMO, are not protected from TNFα-induced apoptosis upon CYLD knock-down. NEMO has also been reported to negatively regulate both apoptosis and necrosis through preventing DISC formation (O'Donnell et al., 2009; O'Donnell et al., 2012). It has also been demonstrated that NEMO is a target of CYLD-mediated de-ubiquitination in overexpression studies (Hutti et al., 2009; Kovalenko et al., 2003). This is potentially an interesting topic of future investigation. If CYLD-mediated NEMO deubiquitination is indeed a common pro-apoptotic and pro-necrotic molecular event, it would suggest that NEMO ubiquitination, like RIP1 ubiquitination is inhibitory to the cell death program. It would be interesting to determine whether mutating the NEMO ubiquitin acceptor site would abrogate its ability to suppress apoptosis and necrosis.

In opposition to previous reports, our data demonstrates that necrosis can proceed independently of CYLD, albeit with a reduced level. A potential explanation for previous reports, which demonstrated that CYLD is essential for necrosis, may be that they only looked at early time-points prior to the onset of cell death in CYLD knock-down cells. Another possibility is that the $CYLD^{-/-}$ MEFs used in our study express a partially compensatory deubiquitinase that is not expressed in the cell-lines used by other groups. However, we also observe consistently weaker protection from necrosis conferred by siRNA knock-down of CYLD as compared to RIP3, in multiple different cell types. Irrespective of the potential explanation for these discrepant results, this is the first report demonstrating that CYLD is not essential for necrosis. This non-essential function does not coincide with the current model.

It is also apparent that CYLD-independent necrosis is less prominent when cells are treated with just TNFα/zVAD. The magnitude of cell death is also less pronounced in the $CYLD^{+/+}$ MEFs. This may be attributed to the fact that specific NFκB target genes might function in actively suppressing necrosis, and are upregulated during TNFα/zVAD treatment. Indeed cFLIP has an anti-necrotic function when heterodimerized with Caspase-8 (Oberst et al., 2011). In this particular case Caspase-8 is inactivated which precludes the possibility that cFLIP is the anti-necrotic factor responsible for the reduced magnitude of TNFα-induced necrosis in MEFs treated with just TNFα/zVAD. A more probable anti-necrotic factor is cIAP2, which has already been demonstrated to negatively regulate TNFα-induced cell death possibly through RIP1 ubiquitination (Varfolomeev et al., 2008).

Nevertheless, this theoretical anti-necrotic protein appears to exert a more potent inhibitory effect on CYLD-independent necrosis. Given that RIP1 kinase activity is required for driving necrosome formation and is still required for CYLD-independent necrosis, it is possible that the reason for the greater inhibitory effect may be due to the fact that it impairs RIP1 kinase activity (Cho et al., 2009). In other words, MEFs devoid of CYLD possibly have impaired RIP1 kinase activation and when they are treated with just TNFα/zVAD a theoretical anti-necrotic factor further attenuates RIP1 kinase activity leading to a more dramatic impairment of CYLD-independent necrosis. Conversely, in cells replete with CYLD, RIP1 kinase activation might be higher than CYLD deficient MEFs, and therefore the upregulation of the theoretical anti-necrotic factor has less of a dramatic effect on necrosis. Future studies should try to identify this anti-necrotic protein.

Materials and Methods

Tissue culture

MEFs and L929 cells were grown in DMEM high sucrose medium supplemented with 10% FCS, 2 mM glutamine, 100 units/ml penicillin, and 100 μg/ml streptomycin. HT-29 and Jurkat cells were grown in McCoy's 5A medium and RPMI1640 media, respectively, supplemented with 10% FCS, 2 mM glutamine, 100 units/ml penicillin, and 100 μg/ml streptomycin. Stable clones of HT-29 cells were generated by transfection using lipofectamine 2000 (Invitrogen) of CYLD-specific and scrambled shRNAs from Thermoscientific/Open Biosystems. Clones were selected by puromycin selection and checked for GFP expression via flow cytometry. GFP^+ clones were tested for reduction of CYLD protein expression and used for subsequent experiments.

Reagents used

Antibodies used in the study were from BD Pharmingen (A20, RIP1, and β-actin), ProSci (RIP3), Santa Cruz Biotechnology (TRAF2 and CYLD) and Invitrogen (CYLD). Antibody against human RIP3 has been described before (Cho et al., 2009). Necrostatin-1 and zVAD-fmk were obtained from Enzo Life Sciences. H_2DCFDA was obtained from Molecular Probes. Recombinant human and mouse TNF were obtained from Biosource/Invitrogen. The Smac mimetic LBW242 was a kind gift of D. Porter (Novartis). Small interference RNAs used in the study are: human A20 (5'-AGUACAAUAGGAAGGCUAAAUAAdTdA-3', 5'-GCAUGAGUACAAGAAAUGGCAGGAA-3'), human CYLD (5'-

CUUAUUUUUAGCAAAGGUUCUACCCUU-3', 5'-
UUGGUUUAUUAUGACUGGAUGAACCUU-3'), mouse CYLD (5'-
GGUUUAGAGAUAAUGAUUGGAAAGA-3', 5'-
AGUGUUGAAAGUACAAUUCUCCUGC-3', 5'-
UGAGUAGAUAGCAGUAAAGUCCUCC-3'), human RIP1 (5'-
UGCAGUCUCUUCAACUUGAdTdT-3', 5'-
UGCUCUUCAUUAUUCAGUUUGCUCCAC-3'), mouse RIP3 (5'-
AAGAUUAACCAUAGCCUUCACCUCCCA-3', 5'-
CCUUCGUUUCCUUUCCUCCUCUCUGUU-3'), human RIP3 (5'-
UAACUUGACGCACGACAUCAGGCUGGA-3', 5'-
GCAGUUGUAUAUGUUAACGAGCGGUCG-3'), human TRAF2 (5'-
GGACCUGGCGAUGGCUGACdTdT), human TR4 (5'-
CCGGAGCUUCCCUCAUUUAdTdT-3'). Mouse RIP1 siRNA sequences have been described (Cho et al., 2009).

Transfection of DNA Plasmids and siRNA

Jurkat cells were transfected with 150 nM of the indicated siRNA. For L929 cells, 20 nM siRNA was used per transfection. All siRNA transfections were performed using the HiPerfect transfection reagent (Qiagen) as per manufacturer's protocols. Forty-eight hours later, cells were stimulated with TNF to induce necrosis.

Cell death assays

Wild type and $CYLD^{-/-}$ MEFs (kind gift from S.C. Sun (Reiley et al., 2006) were treated with 0.5 – 1 μg/ml cycloheximide (CHX) and 20 μM zVAD-fmk where indicated for 1

hour prior to stimulation with the indicated amounts of recombinant mouse TNFα (rmTNF), TRAIL, FasL, staurosporine, or H_2O_2. In some instances, 5 – 10 μM the Smac mimetic LBW242 was used. For FADD and caspase-8 deficient $TNFR2^+$ Jurkat Cells [5], programmed nNecrosis was induced by addition of the indicated amounts of recombinant human TNF (rhTNF). HT-29 cells were treated with 5-10 μM LBW242 and 20 μM zVAD-fmk for 1 hour prior to stimulation with 10 – 100 ng/ml rhTNF. Cell death was determined by flow cytometry with propidium iodide staining or by CellTiter 96® AQueous One Solution Cell Proliferation Assay (Promega).

PREFACE TO CHAPTER IV

This chapter contains material from the following manuscript that is under review for publication:

David M. Moquin, Thomas McQuade, Francis Ka-Ming Chan. **CYLD Deubiquitinates RIP1 in the Necrosome to Facilitate Kinase activation and Programmed Necrosis**

List of author contributions:

Thomas McQuade: Helped with IP and Western Blots

David Moquin: Conducted the remaining experiments

Both David Moquin and Francis Chan designed experiments. Some written portions of this chapter were taken from the manuscript co-written by David Moquin and Francis Chan. David Moquin wrote the rest of the chapter.

CHAPTER IV: The pro-necrotic mechanism of CYLD

Introduction

As revealed from the research of our lab and other groups, the tumor suppressor CYLD has a pro-necrotic function. A model has been established that accounts for the molecular mechanism of CYLD in necrosis. It is believed that CYLD regulates RIP1 ubiquitination within the TNFR1 complex and thus promotes its transition from the pro-survival membrane associated complex to the necrosome (Vandenabeele et al., 2010). This model was based on pieces of indirect evidence provided from other reports. There was already some evidence suggesting that RIP1 is a target of CYLD in certain biological contexts. Namely, during spermatogenesis CYLD was shown to regulate RIP1 ubiquitination and apoptosis; however, the trigger of the signaling pathway was not elucidated. Moreover, it was demonstrated that CYLD is critical for mediating the early wave of spermatocyte cell death, which is important for productive spermatogenesis. This accounts for the fact that CYLD knock-out mice are sterile. The pro-apoptotic function was credited to its effects on the negative regulation of NFκB. In other words, it was suggested that CYLD promoted death by inhibiting a cell survival pathway rather than direct involvement in a cell death signaling pathway. The latter possibility was not formally tested. In further support of RIP1 being a target of CYLD, it was demonstrated that CYLD regulates RIP1 ubiquitination in overexpression experiments (Wright et al., 2007).

CYLD was also demonstrated to mediate deubiquitination of other components of the TNF-R1 signaling complex. This provided additional indirect evidence supporting the notion that CYLD targets RIP1 for deubiquitination within the TNFR1 complex based

on the location. However, all of this data was based on overexpression studies rather than direct evidence for CYLD-mediated regulation within the TNFR-1 complex. In fact, these reports did not demonstrate that CYLD actually gets recruited to the TNFR-1 associated complex (Brummelkamp et al., 2003; Kovalenko et al., 2003; Trompouki et al., 2003).

A number of reports establish that RIP1 ubiquitination promotes its pro-survival function through both NFκB-dependent and NFκB-independent pathways. First, RIP1 ubiquitination is required for the recruitment of the regulatory subunit of the IKK complex NEMO to the TNF-R1 complex. The IKK complex phosphorylates IκBα, which targets it for K48-linked ubiquitination and subsequent proteasomal degradation. This allows for NFκB nuclear translocation, activation of gene transcription, and subsequent expression of anti-apoptotic proteins (Ea et al., 2006). In addition to promoting the recruitment of NEMO to the TNF-R1 complex, RIP1 ubiquitination was shown to prevent RIP1 transition to the cytosolic DISC. Specifically, mutation of the RIP1 ubiquitin acceptor site at lysine residue 377 results in enhanced formation of the TNFα driven DISC (O'Donnell et al., 2007). NEMO also exerts an anti-apoptotic and anti-necrotic function independent of its function to promote NFκB activation. This function is contingent upon binding to ubiquitinated RIP1 (Legarda-Addison et al., 2009; O'Donnell et al., 2012).

Other reports then linked CYLD-mediated RIP1 deubiquitination to enhanced DISC formation. During SMAC mimetic sensitized TNFα-induced apoptosis, CYLD promotes DISC formation as siRNA targeting CYLD impaired DISC formation.

However, this report did not demonstrate that CYLD in fact regulates RIP1 ubiquitination during TNF signaling, and naturally did not show where this potential deubiquitination step takes place. Alternatively, another report has demonstrated a laddering pattern of RIP1 and RIP3 in the necrosome suggesting their ubiquitination. This indicates that ubiquitination of the components of the necrosome may somehow play a role in its functionality (Cho et al., 2009). This also suggests that CYLD may have a function in regulating ubiquitination of components of the necrosome, and thereby promote necrosis.

In addition to RIP1 ubiquitination negatively regulating the formation of the apoptotic DISC and the necrosome, RIP1 kinase activity positively regulates necrosome formation. Pre-treatment of cells with the RIP1 kinase inhibitor Nec-1 is able to block necrosome formation (Cho et al., 2009; He et al., 2009). A few reports provide clues that indicate the potential mechanism of RIP1 kinase activation; however a comprehensive model is still at an inchoate stage. First, overexpression studies of RIP1 in 293T cells revealed many putative RIP1 phosphorylation sites. Some of these phosphorylation events were due to auto-phosphorylation. The auto-phosphorylation site at serine 161 was shown to be important for RIP1 kinase activation. Blocking the phosphorylation of this site by substitution with an alanine resulted in a partial defect in necrosis. Additionally, forced dimerization of wild-type but not kinase inactive RIP1 was able to induce necrosis in the absence of TNFα treatment. This suggests that RIP1 derived from the TNFR-1 receptor complex becomes kinase active through regulation of its oligomeric state. It is conceivable that oligomerization is an important step for auto-phosphorylation and subsequent activation of RIP1 kinase activity (Degterev et al., 2008). Clearly, more

work must be done to define the RIP1 phosphorylation events during necrosis, their functionality, and their influence on other molecular events such as recruitment of components of the necrosome and regulation of RIP1 kinase activity. In addition to necrosis, RIP1 kinase activity is also required for SMAC mimetic sensitized TNFα-induced apoptosis (Degterev et al., 2005).

RIP3 kinase activity is also required for necrosis. Nec-1 can block an auto-phosphorylation event of RIP3 at Serine 199. This supports the notion that necrosome formation activates RIP3 kinase activity. The functional requirement of that particular auto-phosphorylation event for necrosis was not ascertained (He et al., 2009). However, it was recently discovered that RIP3 can be phosphorylated at Serine 227 during necrosis, and it is required for recruitment of another component of the necrosome, MLK-L. This molecular event is consequential for necrosis, as a S227A mutant RIP3 is unable to promote necrosis (Sun et al., 2012). Furthermore, RIP1 and RIP3 were also demonstrated to form amyloid fibrils during necrosis. These amyloid fibrils require intact RIP homotypic interaction motifs (RHIM) of RIP1 and RIP3. Thioflavin T (ThT) and Congo red (CR), which bind to β-amyloid were able to partially inhibit TNFα-induced necrosis. This suggests that the amyloid fibrils are functionally relevant for transducing the pro-necrotic signal. It was demonstrated that the phosphorylated forms of RIP1 and RIP3 were enriched in an NP-40 insoluble SDS-soluble fraction, which is suggestive of the amyloid fraction (Li et al, 2012).

In the previous chapter, evidence was presented that supported the notion that the existing model of CYLD-mediated necrosis is not correct. This chapter covers work that

directly addresses the pro-necrotic mechanism of CYLD. In this section it is demonstrated that CYLD does not regulate the ubiquitination status of RIP1 within the TNF-R1 complex like the current model suggests. Instead, CYLD regulates the ubiquitination status of RIP1 within the NP-40 insoluble necrosome. It is also shown that RIP1 is in fact the primary target of CYLD in the context of TNFα-induced necrosis. Consistent with this finding, CYLD appears to regulate the kinetics of necrosome formation, but at later time-points the complex forms in the absence of CYLD. As demonstrated in the previous chapter, CYLD is not absolutely essential for TNFα-induced necrosis as CYLD knock-out MEFs have residual cell death. Interestingly, necrosome formation catches up to levels observed in wild-type MEFs even though the level of cell death does not. This is most likely attributed to impaired RIP1 kinase activation, as RIP1 kinase dependent RIP3 phopsphorylation is impaired in cells with CYLD knocked down.

Results

CYLD does not control RIP1 ubiquitination within the TNFR-1 complex

Given the current model for CYLD-mediated necrosis, we set out to determine whether this was in fact accurate. As established in the previous chapter, CYLD is not absolutely essential for necrosis. This is not consistent with the model that CYLD is upstream of RIP1. If CYLD was required for RIP1 transition from the TNFR-1 complex to the necrosome, CYLD should be essential for necrosis because RIP1/RIP3 association is an essential molecular event. Nevertheless, we decided to determine whether we could

detect CYLD recruitment to the TNFR1 complex to gather evidence suggesting where it may exert its pro-necrotic function. As previously reported, RIP1 recruited to the TNFR-1 complex was heavily ubiquitinated (Fig. 4.1A). In agreement with the current model, CYLD was also recruited to the TNFR-1 complex in a ligand-dependent manner (Fig. 4.1A, compare lane 1, 3 and 5). However, CYLD did not regulate the ubiquitination status of RIP1 within the TNFR-1 complex. Hyper-ubiquitination of RIP1 within the TNFR1 complex was not observed in $CYLD^{-/-}$ MEFs (Fig. 4.1B, compare lanes 3-6). Polyubiquitinated RIP1 within the TNFR-1 signaling complex is important for assembly and activation of the IKK complex (Ea et al., 2006). Consistent with the normal RIP1 ubiquitination status, IκBα phosphorylation and degradation was normal in $CYLD^{-/-}$ MEFs (Fig. 4.1C). From the previous chapter we concluded that CYLD and A20 are not functionally redundant RIP1 deubiquitinases. Therefore the normal TNFR-1 associated RIP1 ubiquitination in $CYLD^{-/-}$ MEFs was not due to the compensatory effect of another RIP1 deubiquitinase A20, which we also detected within the TNFR-1 complex (Fig. 4.1A, lane 5).

Deubiquitination of RIP1 by CYLD facilitates programmed necrosis

Recently, certain de-ubiquitinases, such as A20, have been shown to regulate cell signaling independent of their enzymatic activity (Skaug et al, 2011). Because RIP1 ubiquitination at the TNFR-1 complex was normal in $CYLD^{-/-}$ cells, we asked if CYLD similarly regulates programmed necrosis independent of its deubiquitinase activity. We found that expression of GFP-tagged wild type CYLD, but not the deubiquitinase

inactive mutant C601S, enhanced TNFα-induced programmed necrosis in CYLD$^{-/-}$ MEFs (Fig. 4.2B). Truncation mutants lacking the carboxyl terminal Ubiquitin Specific Protease (USP) domain also failed to restore programmed necrosis in CYLD$^{-/-}$ MEFs. In contrast, the first and second CAP-Glycine (CG1 and CG2) domains were dispensable for programmed necrosis (Fig. 4.2A and C). A previous report demonstrated that these domains were required for the function of CYLD in negatively regulating histone deacetylase-6 (HDAC6) enzymatic activity during TPA stimulation. Therefore, CYLD promotes an increase in acetylated tubulin in the perinuclear region, which enhances CYLD interaction with Bcl-3. CYLD can then block cell cycle progression through regulating the ubiquitination status of Bcl-3 (Wickstrom et al, 2010). The dispensability of these domains for necrosis demonstrates the differential requirement of CYLD domains for mediating its function in different signaling pathways. It also reduces the likelihood that the pro-necrotic function of CYLD is due to an indirect effect in its function as a cell cycle regulator. The third CAP-Glycine domain is required for the pro-necrotic function of CYLD as the USP alone was not sufficient for enhancing death in the CYLD$^{-/-}$ MEFs. Altogether, both CG3 and the deubiquitinase activity of CYLD are required to promote TNFα-induced programmed necrosis.

Since the deubiquitinase function of CYLD is required for programmed necrosis, and yet RIP1 ubiquitination within the TNFR-1 complex was normal in CYLD$^{-/-}$ cells, we sought to determine if RIP1 is indeed the major substrate of CYLD during programmed necrosis. In order to address this question we took advantage of knowledge regarding a previously characterized TNFα-dependent RIP1 ubiquitination site. We reconstituted a

RIP1 deficient Jurkat cell-line with a RIP1 ubiquitin acceptor site mutant K377R. Importantly, we demonstrated that the RIP1 mutant K377R, which does not undergo TNFα driven RIP1 ubiquitination (Ea et al., 2006; Li et al., 2006), was not ubiquitinated upon TNFα stimulation in the TNFR-1 complex (Fig. 4.3A). We posited that if the primary target of CYLD during TNFα-driven necrosis is indeed ubiquitinated RIP1, then the RIP1 K377R mutant cell-line should not be protected from CYLD knock-down. Consistently, unlike cells expressing wild type RIP1 (Fig. 3.1A), cells that express the K377R mutant were insensitive to CYLD siRNA mediated protection against TNFα-induced necrosis. In contrast, RIP3 siRNA reduced programmed necrosis in these cells (Fig. 4.3B). Hence, we conclude that RIP1 is the major substrate of CYLD in programmed necrosis.

CYLD regulates RIP1 ubiquitination in a spatially and temporally distinct compartment

Since RIP1 is the major substrate of CYLD and yet RIP1 ubiquitination within the TNFR-1 signaling complex was not affected in $CYLD^{-/-}$ cells, we assessed the possibility that CYLD might regulate RIP1 ubiquitination in a different signaling compartment. In order to analyze the total level of RIP1 ubiquitination without other contaminating factors, we boiled the cell extracts in 1% SDS prior to RIP1 immunoprecipitation. Using this method, we detected RIP1 polyubiquitination in a TNFα-dependent manner in both wild type and $CYLD^{-/-}$ cells hours after the dissolution of the TNFR-1 signaling complex. In contrast to RIP1 recruited to the TNFR-1 signaling complex, RIP1 isolated from $CYLD^{-/-}$ cells using this method exhibited higher levels of ubiquitination than wild type

cells at all time points examined (Fig. 4.4A). Moreover, the length of the polyubiquitinated species was longer in the CYLD$^{-/-}$ cells compared with that in wild type cells. Similar results were obtained in HT29 cells with stable expression of shRNA against CYLD (Fig. 4.4B). Hence, RIP1 was indeed hyper-ubiquitinated in CYLD$^{-/-}$ cells.

Ubiquitin-like modifications of RIP1 and RIP3 were previously detected in the late-forming cytosolic necrosome (Cho et al., 2009). This suggests that CYLD might regulate RIP1 ubiquitination within the necrosome instead of the TNFR-1 complex. To confirm that RIP1 was ubiquitinated in the necrosome, we performed sequential immunoprecipitations, first with RIP3, followed by immunoprecipitations with different ubiquitin antibodies. We found that RIP1 within the necrosome was indeed modified by ubiquitination via K48 as well as K63 linkages (Fig. 4.4C). The RIP1-RIP3 necrosome is an amyloid-like structure that is enriched in the NP-40 insoluble fraction (Li et al, 2012). To determine the role of CYLD in necrosome ubiquitination, we performed differential detergent lysis, first with NP-40, followed by extraction of the NP-40 insoluble material with SDS. Despite equal pull-down of RIP1 in wild type and CYLD$^{-/-}$ cells, we found that RIP1 in the NP40-insoluble fraction, but not the NP-40 soluble fractions, was hyper-ubiquitinated in CYLD$^{-/-}$ cells compared with wild type cells (Fig. 4.5D, compare lanes 3-4 and 5-6). These results suggest that CYLD regulates RIP1 ubiquitination in the necrosome.

CYLD controls the kinetics of necrosome formation and activation

We next examined the consequence of this hyper-ubiquitinated form of RIP1 in necrosis signaling. Surprisingly, we found that the assembly of the RIP1-RIP3 necrosome was delayed, but not abolished in the $CYLD^{-/-}$ MEFs (Fig. 4.5A, lanes 5-8). Similar observations were made in CYLD-kd HT-29 cells (Fig. 4.5B-C). Consistent with the requirement of CYLD for TNFα-induced apoptosis (Fig. 3.1), recruitment of RIP1 and FADD to caspase-8 was similarly delayed in CYLD-kd HT29 cells (Fig. 4.6A). Additionally, RIP1 recruitment to FADD was delayed, but at later time-points caught up in CYLD-kd HT29 cells. The recruitment of RIP1 to FADD was contingent upon RIP1 kinase activity in both the control shRNA HT29 cells and CYLD-kd cells (Fig. 4.6B compare lanes 6 and 12 top panel). This supports the findings presented in the previous chapter that the residual cell death in the $CYLD^{-/-}$ MEFs is RIP1 kinase dependent. Altogether, CYLD promotes, but is not essential for assembly of the RIP1-RIP3 necrosome and other components of the necrosome.

Sequential detergent extraction with NP-40 and SDS revealed that RIP1 and especially RIP3 accumulated in this fraction in a TNFα-dependent manner (Fig. 4.7A, bottom panels). Both RIP1 and RIP3 are phosphorylated as they become activated within the necrosome (Cho et al. 2009; He et al., 2009). These phosphorylated species are enriched in the NP-40 insoluble compartment (Li et al., 2012). In agreement with our previous observation, phospho-RIP1 and phospho-RIP3 as indicated by mobility shift were detected in the NP-40 insoluble SDS fraction as early as 2 hours post stimulation in wild type cells (Fig. 4.7A, lane 3). In contrast, appearance of phospho-RIP1 and phospho-RIP3 was not apparent until 4 hours post-stimulation (Fig. 4.7A, lane 6). The

delayed phosphorylation of RIP1 and especially RIP3 was more apparent in CYLD-kd HT29 cells (Fig. 4.7B). Sequential detergent extraction in HT29 cells provided further support for enrichment of phospho-RIP1 and phospho-RIP3 in the SDS fraction, as they were not detectable in the NP-40 soluble fraction. Furthermore, the kinetic delay in the phosphorylated species was pronounced in the CYLD-kd cell extracts (Fig. 4.7C).

The preferential phosphorylation in the SDS fraction suggests that the kinase activity of the necrosome was activated in this compartment. Because SDS inhibited RIP1 and RIP3 kinase activity (unpublished observation), we modified our protocol to determine the kinase activity of the necrosome in the NP-40 insoluble compartment (Fig. 4.8A). We used differential centrifugation to isolate RIP1 complexes from NP-40 insoluble pellets. We confirmed that similar to the differential detergent lysis with NP-40 and SDS (Fig. 4.7A), the insoluble pellet fractions obtained with this method exhibited ligand-dependent accumulation of the necrosome components RIP1, RIP3 and CYLD (Fig. 4.8B). Importantly, TNFα-induced and RIP1-associated kinase activity was detected in the insoluble P10 and P25 fractions (Fig. 4.8C, top panel, lanes 5-8 and 9-12). In contrast, despite the higher background activity, no TNFα-induced kinase activity was observed in the soluble S25 fractions (Fig. 4.8C, top panel, lanes 1-4). The induction of kinase activity correlated with recruitment of RIP3 to the complex (Fig. 4.8C, middle panel). Consistent with our previous report, this activity was transient and disappeared by 6 hours post-stimulation (Cho et al., 2009). Moreover, RIP1-associated ubiquitination was strongly induced in the P10 and P25 compartments concomitant to recruitment of CYLD to the RIP1 complex (Fig. 4.8C, bottom panels and Fig. 4.8D). In contrast,

ubiquitination was not induced in the S25 fractions. These results indicate that the assembly and activation of the necrosome is regulated in the NP-40 insoluble compartment.

Ubiquitination hinders RIP1 autophosphorylation

In addition to induction of kinase activity, we observed that RIP1-associated ubiquitination was strongly induced in the NP-40 insoluble compartments (Fig. 4.8C). Paradoxically, the increase in RIP1-associated ubiquitination correlated with the recruitment of CYLD to RIP1 (Fig. 4.8C, bottom panels). Inducible ubiquitination was not detected in the soluble fractions. The E3 ligases cIAP1 and cIAP2 promote RIP1 ubiquitination in the TNFR-1 complex (Bertrand et al., 2008; Mahoney et al., 2008; Vince et al., 2007). Even when Smac mimetic (SM) was used to eliminate cIAP1 and cIAP2 expression, TNFα stimulated the re-expression of cIAP2 (Fig. 4.9A). This is consistent with the fact that cIAP2 is a NF-κB target gene and that Smac mimetic mediated degradation of cIAP2 requires cIAP1 (Darding et al., 2011). In support of this model, binding between RIP1, cIAP1, cIAP2 and TRAF2 was detected in a ligand-dependent manner late during necrosis (Fig. 4.9B). These results suggest that the E3 ligases responsible for RIP1 ubiquitination in the TNFR-1 complex may be responsible for ubiquitination of components of the necrosome. Over-expression of RIP1 in 293T cells revealed that polyubiquitinated RIP1 was not an effective substrate in RIP1 auto-phosphorylation assays (Fig. 9C). Hence, we provide evidence that RIP1 polyubiquitination within the necrosome sterically hinders RIP1 kinase activation.

Phosphorylated CYLD associates with RIP1 during necrosis

Up to this point the work in this chapter has revealed that CYLD regulates the ubiquitination status of RIP1 within the necrosome, and therefore the focus has been on CYLD-mediated regulation of RIP1. We were interested in the possibility that the converse was true, whether RIP1 mediates regulation of CYLD. Interestingly, in addition to constitutive interaction between CYLD and RIP1 in MEFs, stimulus dependent association between a slower migrating CYLD and RIP1 was observed. This slower migrating CYLD was validated as phosphorylated CYLD, as it could be collapsed to normal migration by treatment with phosphatase (Fig4.10, upper panel, compare lanes 3 and 4). This phosphorylation of CYLD was dependent on RIP1 kinase activity because Nec-1 abolished the slower migrating CYLD (Fig4.10 upper panel, compare lanes 3 and 5).

We next wanted to determine whether this CYLD phosphorylation event was at Serine 418, a previously identified site that negatively regulates CYLD-mediated deubiquitination of TRAF2 and NEMO in overexpression studies. This phosphorylation event can be mediated by the kinase IKKε, which is oncogenic. Inactivation of CYLD deubiquitination of its targets by IKKε is one mechanism in which it promotes transformation. Inactivation of CYLD results in hyperactivation of NFκB (Hutti et al., 2009). Similarly, during TNFα stimulation a cluster of serine residues are phosphorylated, one of which being Serine 418. These phosphorylation events are mediated by the conventional IKK complex, and impair CYLD-mediated deubiquitination of TRAF2. Exogenous expression of a compound mutant of CYLD

with all serine residues substituted with alanine results in impaired TNFα-induced TRAF2 ubiquitination, resulting in impaired NFκB activation (Reiley et al., 2005).

We stably expressed S418A HA-CYLD in CYLD$^{-/-}$ MEFs to address whether this was the site phosphorylated during necrosis. Interestingly, RIP1 associated CYLD phosphorylation still occurred with this phospho-acceptor site mutated (Fig. 4.10B, top panel, compare lanes 1 and 3). CYLD phosphorylation was still observed when the cells were treated with CHX/zVAD, albeit with reduced amounts (Fig. 4.10B, top panel, compare lanes 3 and 4). This is consistent with a previous report demonstrating enhanced DISC formation in cells sensitized to TNFα induced death with SMAC mimetic as compared to CHX (Wang et al., 2008). It also demonstrates that phosphorylation of CYLD during necrosis is not specific to SMAC mimetic sensitization. Altogether, this suggests that S418 is not the sole phosphorylation site, but does not exclude the possibility that CYLD gets phosphorylated at multiple amino acid residues during necrosis. Since RIP1 kinase activity is pro-necrotic, and CYLD phosphorylation during necrosis is RIP1-dependent this suggests the possibility that the phosphorylation event may actually enhance the pro-necrotic function of CYLD.

CYLD interaction with RIP1 is indirect

Up to this point the data presented has indicated that CYLD interacts with RIP1 both constitutively in some cell-lines and in a TNFα-dependent manner during necrosis. In order to further define the nature of this interaction and potential interaction with other components of the necrosome, we utilized two different overexpression systems. Co-

expression of CYLD and RIP3 in 293T cells did not reveal interaction, whereas RIP3 and RIP1 interaction was observed using the same system (Fig4.11A compare lanes 4 and 5). This indicates that CYLD does directly interact with a component of the necrosome. Furthermore, it is unclear whether CYLD can be found in RIP3 complexes during necrosis, but our data indicates that CYLD interacts with RIP1 during time-points when the necrosome is present. Similar to lack of interaction between CYLD and RIP3, co-expression of CYLD and RIP1 in 293T cells did not reveal interaction. Consistent with previous reports, CYLD interaction with TRAF2 was observed using the same system (Fig. 4.11B compare lanes 4 and 5)(Kovalenko et al., 2003). In agreement with the results observed in the 293T system, recombinant baculovirus derived CYLD and RIP1 did not interact when the crude lysates from separately transduced SF9 cells were mixed and subjected to an *in vitro* binding assay. Importantly, RIP3 was co-immunoprecipitated with RIP1 using this same method. This ensured that the lack of interaction between RIP1 and CYLD wasn't attributed to experimental conditions (Fig. 4.11C compare lanes 5 and 6). Additionally, recombinant baculovirus derived CYLD and RIP3 did not interact (Fig.4.11D compare lanes 5 and 6). In summary, CYLD interaction with RIP1 is indirect as suggested by two different overexpression systems. This is in agreement with one report that showed RIP1 and CYLD interaction during TNFα-induced apoptosis required the adaptor protein CLIPR-59 (Fujikura et al., 2012).

Figure 4.1

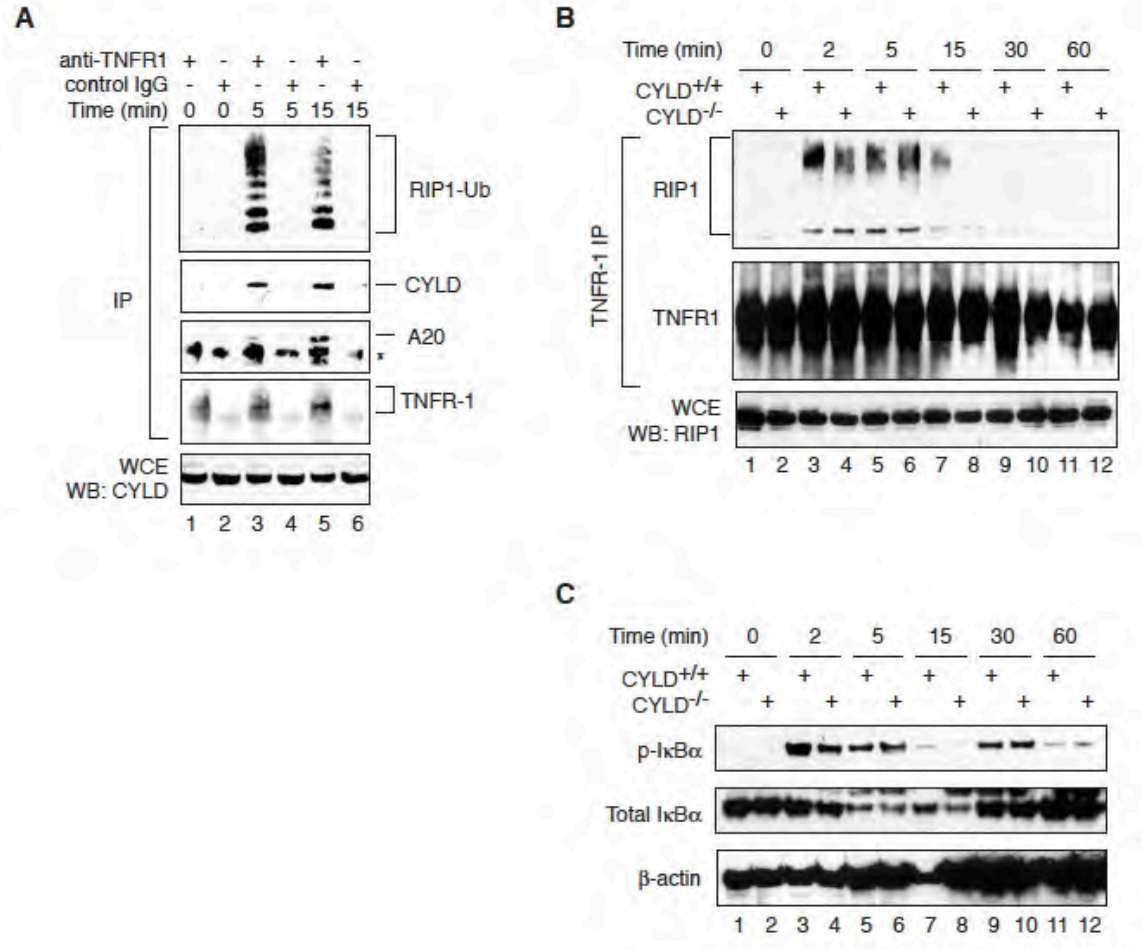
A
anti-TNFR1 + - + - + -
control IgG - + - + - +
Time (min) 0 0 5 5 15 15
RIP1-Ub
IP
CYLD
A20
TNFR-1
WCE
WB: CYLD
1 2 3 4 5 6
B
Time (min) 0 2 5 15 30 60
CYLD+/+ + + + + + +
CYLD-/- + + + + + +
RIP1
TNFR-1 IP
TNFR1
WCE
WB: RIP1
1 2 3 4 5 6 7 8 9 10 11 12
C
Time (min) 0 2 5 15 30 60
CYLD+/+ + + + + + +
CYLD-/- + + + + + +
p-IκBα
Total IκBα
β-actin
1 2 3 4 5 6 7 8 9 10 11 12

Figure 4.1 CYLD does not regulate RIP1 ubiquitination within the TNFR-1 complex.

(A) Recruitment of CYLD and A20 to the TNFR-1 complex. The TNFR1 complex was purified by immunoprecipitation (IP). The recruitment of RIP1, CYLD and A20 was assessed via Western Blot. Control IPs with isotype-matched IgG were included to show the specificity of binding to TNFR-1. **(B)** $CYLD^{+/+}$ and $CYLD^{-/-}$ MEFs were treated with TNFα for the indicated times. The TNFR-1 complex was immuneprecipitated, and recruitment of polyubiquitinated RIP1 was determined by Western blot. **(C)** IκBα phosphorylation and degradation was normal in $CYLD^{-/-}$ MEFs.

Figure 4.2

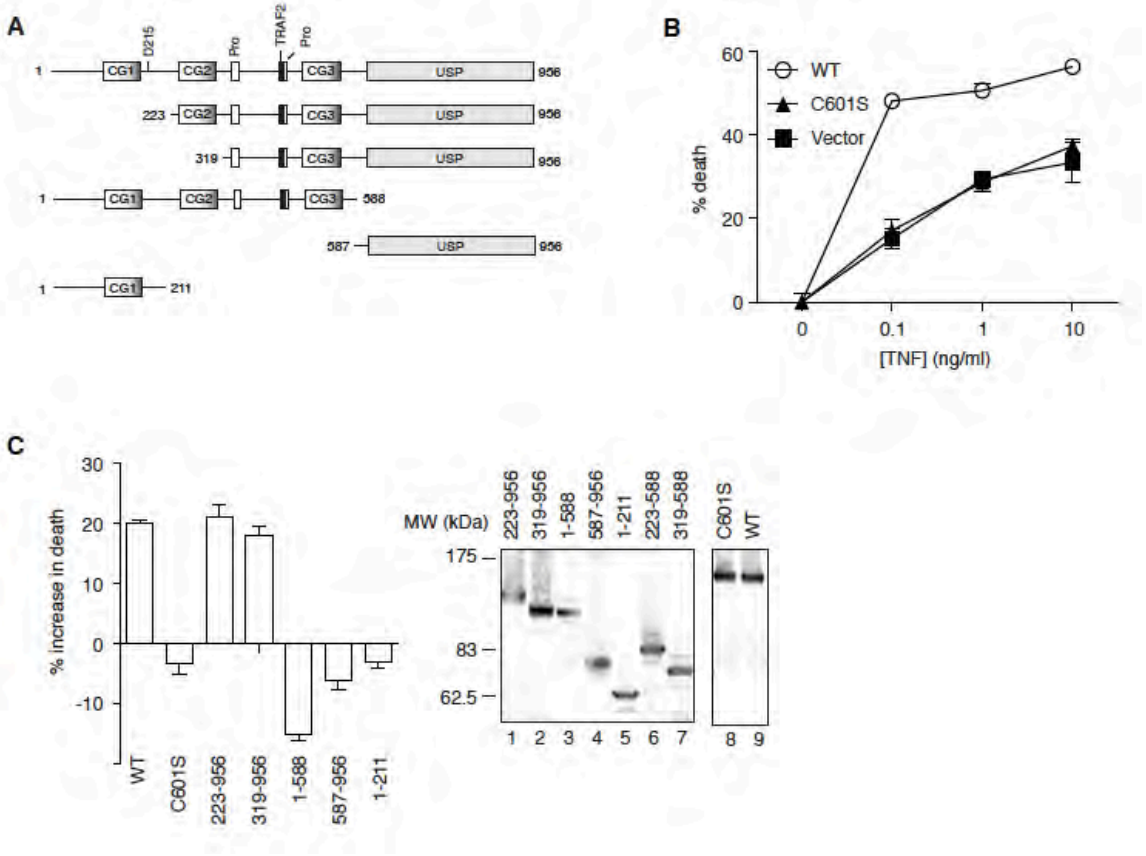
A
0215
Pro
TRAF2
Pro
1
CG1
CG2
CG3
USP
956
223
319
588
587
211
B
WT
C601S
Vector
% death
[TNF] (ng/ml)
C
% increase in death
WT
C601S
223-956
319-956
1-588
587-956
1-211
MW (kDa)
175
83
62.5
1 2 3 4 5 6 7 8 9

Figure 4.2 CYLD deubiquitinase activity and CG3 are required for TNFα-induced necrosis. (A) Schematic diagram of wild-type CYLD and deletion mutants used in the experiments. **(B-C)** $CYLD^{-/-}$ MEFs were transiently transfected with the indicated GFP-tagged CYLD mutants. Necrosis was induced with TNFα, CHX and zVAD-fmk. Cell death was determined in the GFP^{+} population by PI staining and flow cytometry. The panel to the right of (C) is a Western blot showing the GFP-tagged CYLD mutants were expressed at similar levels and of the correct size.

Figure 4.3

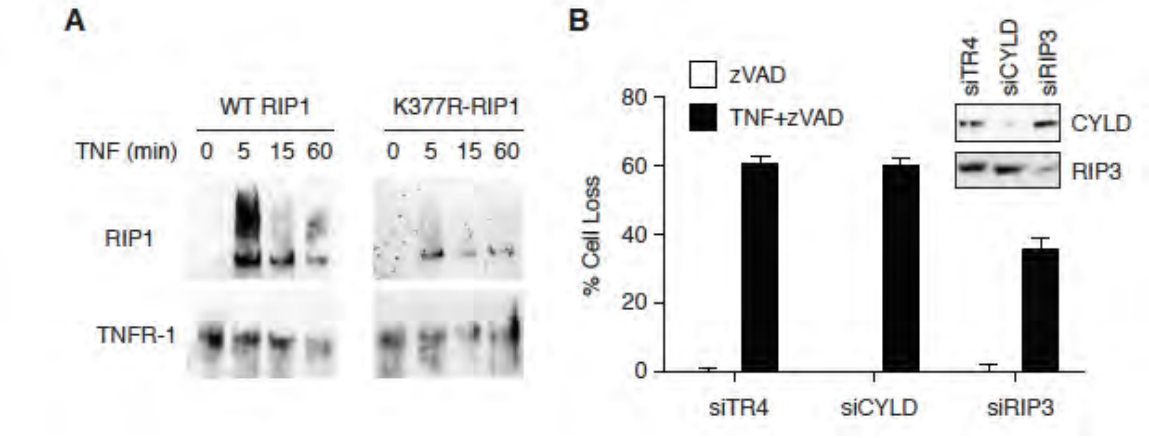
A
WT RIP1
K377R-RIP1
TNF (min) 0 5 15 60 0 5 15 60
RIP1
TNFR-1
B
zVAD
TNF+zVAD
% Cell Loss
80
60
40
20
0
siTR4
siCYLD
siRIP3
siTR4
siCYLD
siRIP3
CYLD
RIP3

Figure 4.3 Poly-ubiquitinated RIP1 is the major substrate for CYLD in TNFα-induced necrosis.

(A) K377R RIP1 is recruited to the TNFR-1 complex and ubiquitination is impaired. WT TNFR2^{+} Jurkat cells or RIP1 deficient TNFR2^{+} Jurkat cells reconstituted with K377R GFP-RIP1 were treated with rhTNFα for the indicated time-points. Complex I was isolated via TNFR-1 immunoprecipitation. The ubiquitination status of RIP1 within Complex I was assessed via Western blot. (B) K377R RIP1 mutant bypasses the requirement for CYLD in necrosis. RIP1 deficient TNFR2^{+} Jurkat cells reconstituted with K377R GFP-RIP1 were transfected with the indicated siRNA oligos and treated with rhTNFα. % cell loss was determined via PI exclusion and flow cytometry. The inset shows reduction in protein expression of CYLD and RIP3 in siRNA transfected cells by Western blot.

Figure 4.4

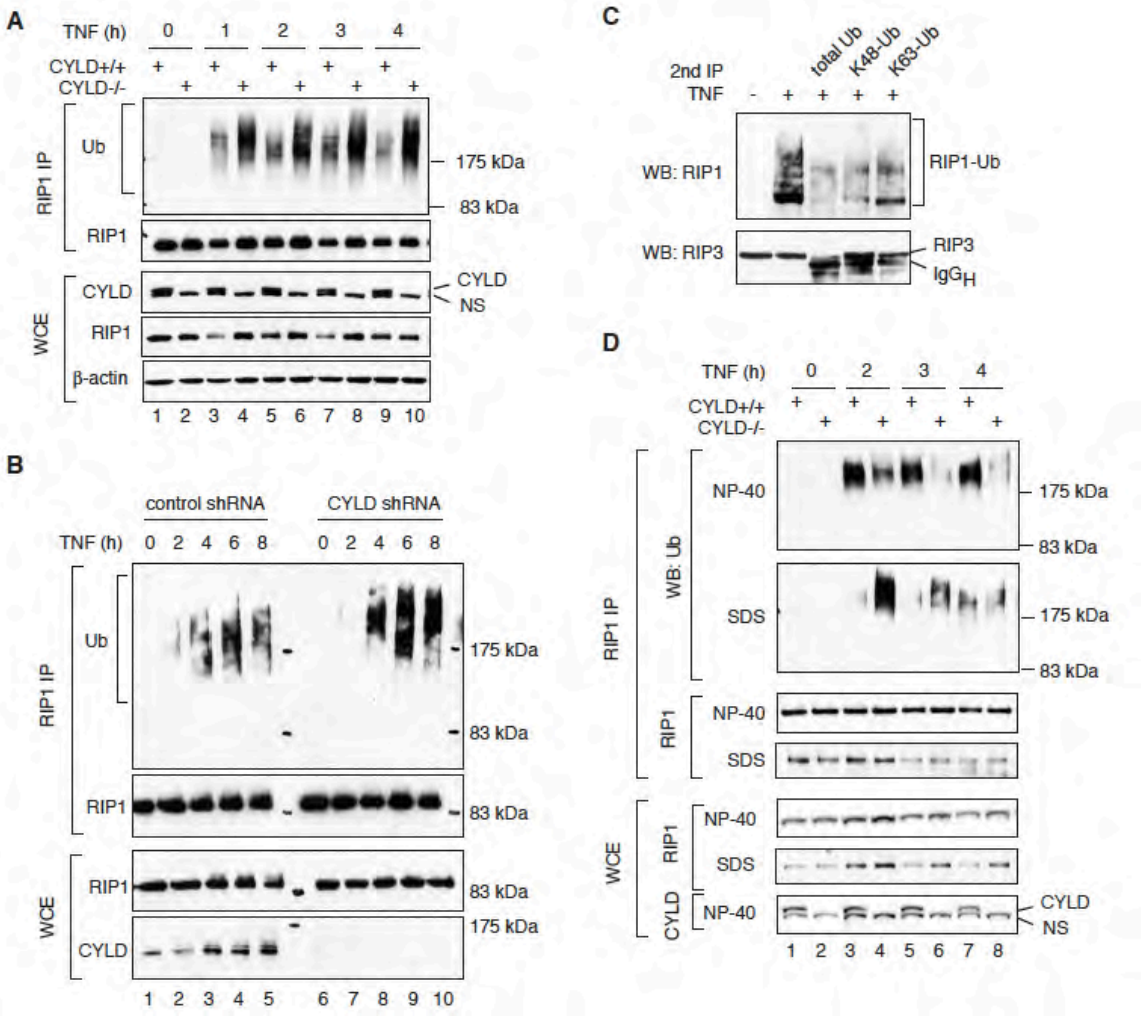
A
TNF (h) 0 1 2 3 4
CYLD+/+ + + + + +
CYLD-/- + + + + +
RIP1 IP
Ub
RIP1
175 kDa
83 kDa
WCE
CYLD
RIP1
β-actin
CYLD
NS
1 2 3 4 5 6 7 8 9 10
B
control shRNA
CYLD shRNA
TNF (h) 0 2 4 6 8 0 2 4 6 8
RIP1 IP
Ub
RIP1
175 kDa
83 kDa
WCE
RIP1
CYLD
83 kDa
175 kDa
1 2 3 4 5 6 7 8 9 10
C
2nd IP
TNF
total Ub
K48-Ub
K63-Ub
- + + + +
WB: RIP1
RIP1-Ub
WB: RIP3
RIP3
IgG_H
D
TNF (h) 0 2 3 4
CYLD+/+ + + + +
CYLD-/- + + + +
RIP1 IP
WB: Ub
NP-40
SDS
175 kDa
83 kDa
RIP1
NP-40
SDS
WCE
RIP1
NP-40
SDS
CYLD
NP-40
CYLD
NS
1 2 3 4 5 6 7 8

Figure 4.4 CYLD regulates the ubiquitination status of RIP1 in the necrosome. **(A-B)** CYLD regulates RIP1 ubiquitination during necrosome formation. $CYLD^{+/+}$ and $CYLD^{-/-}$ MEFs or **(B)** control and CYLD-kd HT-29 cells were treated with TNFα, the SMAC mimetic LBW242, and zVAD-fmk for the indicated time-points. A denaturing RIP1 IP was conducted in 1% SDS as described in the methods. The level of RIP1 ubiquitination was examined by Western blot. NS: non-specific band. **(C)** Necrosome-associated RIP1 contains ubiquitin chains of different linkage types. Cells were treated with TNFα and zVAD-fmk for 3 hours or left untreated. RIP3 immune complexes were denatured in urea, followed by immunoprecipitation with the indicated antibodies against ubiquitin. The ubiquitination of RIP1 within the necrosome was determined by Western blot. **(D)** Selective accumulation of poly-ubiquitinated proteins in RIP1 complexes in the NP-40 insoluble compartment. WT MEFs or $CYLD^{-/-}$ MEFs were treated to undergo necrosis with TNFα, zVAD-fmk, and CHX for the indicated times. Cells were lysed in NP-40 lysis buffer and insoluble material was solubilized with SDS. RIP1 was immunoprecipitated from both fractions followed by Western blot with the indicated antibodies.

Figure 4.5

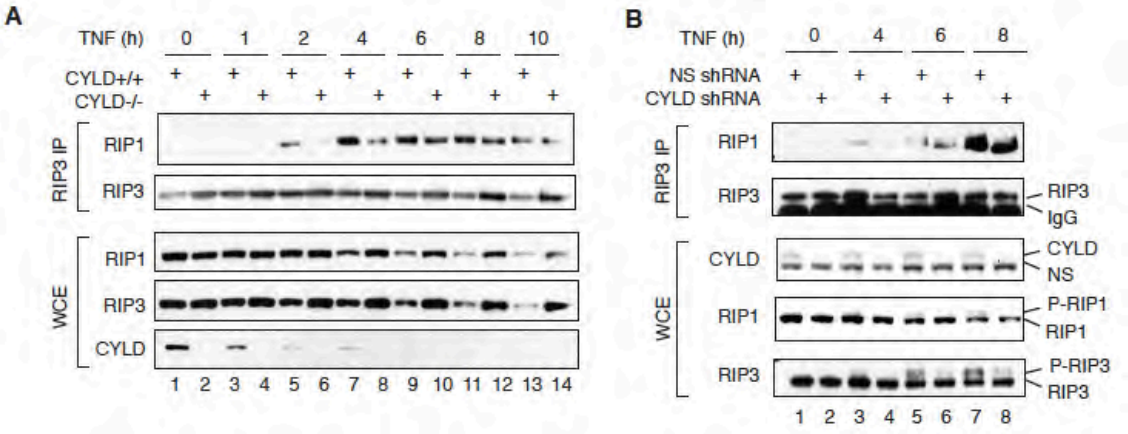
A
TNF (h)
0
1
2
4
6
8
10
CYLD+/+
CYLD-/-
RIP3 IP
RIP1
RIP3
WCE
RIP1
RIP3
CYLD
1 2 3 4 5 6 7 8 9 10 11 12 13 14
B
TNF (h)
0
4
6
8
NS shRNA
CYLD shRNA
RIP3 IP
RIP1
RIP3
RIP3
IgG
WCE
CYLD
CYLD
NS
RIP1
P-RIP1
RIP1
RIP3
P-RIP3
RIP3
1 2 3 4 5 6 7 8

Figure 4.5 CYLD regulates the kinetics of RIP1-RIP3 necrosome assembly.

(A) WT or CYLD$^{-/-}$ MEFs were treated with TNFα, LBW242 and zVAD-fmk for the indicated times. RIP3 complexes were immunoprecipitated and recruitment of RIP1 was determined by Western blot. **(B)** HT-29 cells expressing non-specific shRNA (NS) or CYLD shRNA were treated with TNFα, LBW242 and zVAD-fmk. RIP1 recruitment to RIP3 was determined by Western blot.

Figure 4.6

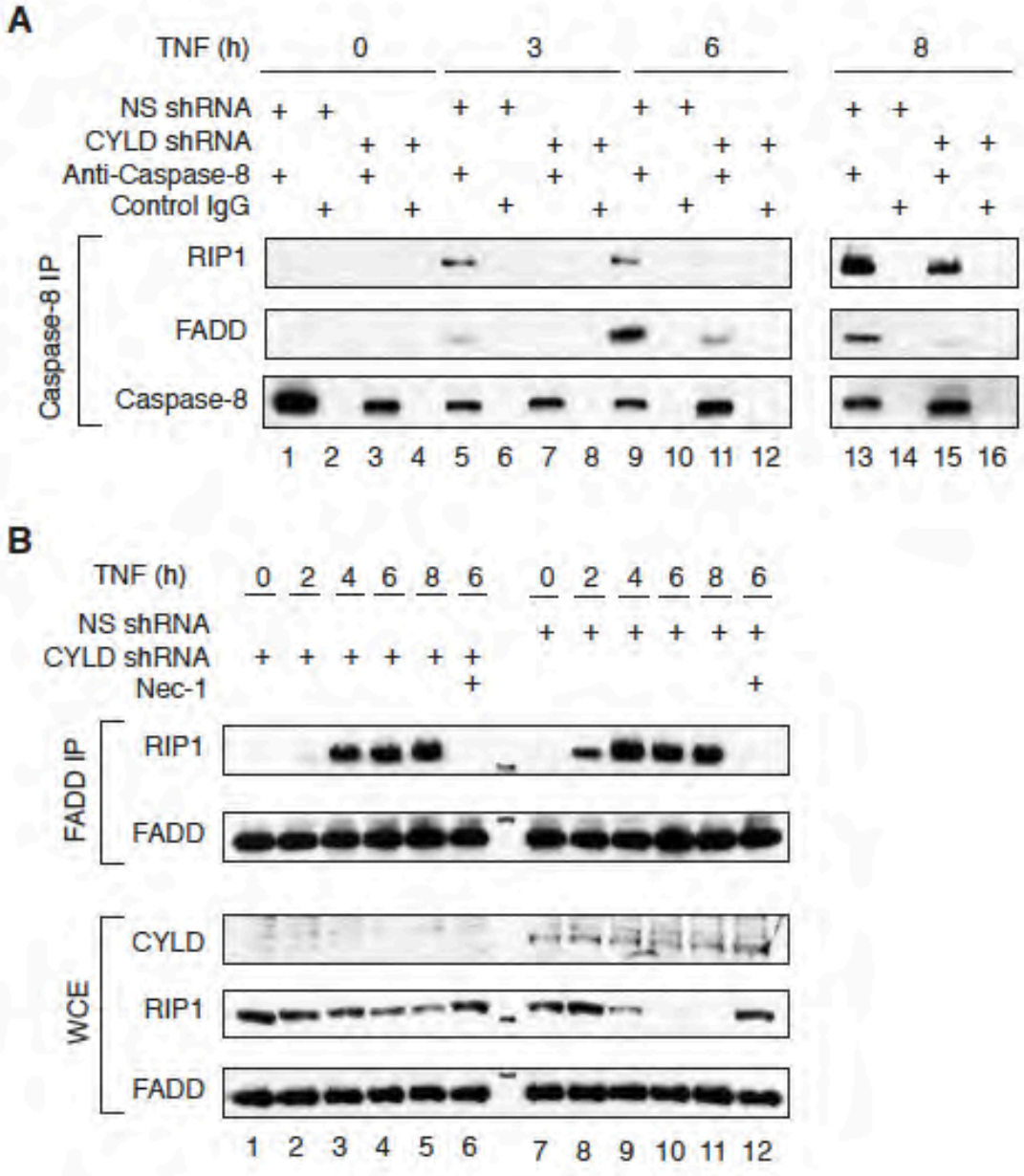
A
TNF (h)
0
3
6
8
NS shRNA
CYLD shRNA
Anti-Caspase-8
Control IgG
Caspase-8 IP
RIP1
FADD
Caspase-8
1 2 3 4 5 6 7 8 9 10 11 12 13 14 15 16
B
TNF (h)
0 2 4 6 8 6 0 2 4 6 8 6
NS shRNA
CYLD shRNA
Nec-1
FADD IP
RIP1
FADD
WCE
CYLD
RIP1
FADD
1 2 3 4 5 6 7 8 9 10 11 12

Figure 4.6 CYLD regulates the kinetics of assembly for multiple components of the necrosome.

(A) HT-29 cells were treated with TNFα, LBW242 and zVAD-fmk. Caspase-8 complexes were isolated via immunoprecipitation. The recruitment of RIP1 and FADD to Caspase-8 was determined by Western blot. **(B)** HT-29 cells were treated with TNFα, LBW242 and zVAD-fmk. Where indicated, cells were also pre-treated with Nec-1. FADD complexes were immunoprecipitated. The recruitment of RIP1 to FADD was determined by Western blot.

Figure 4.7

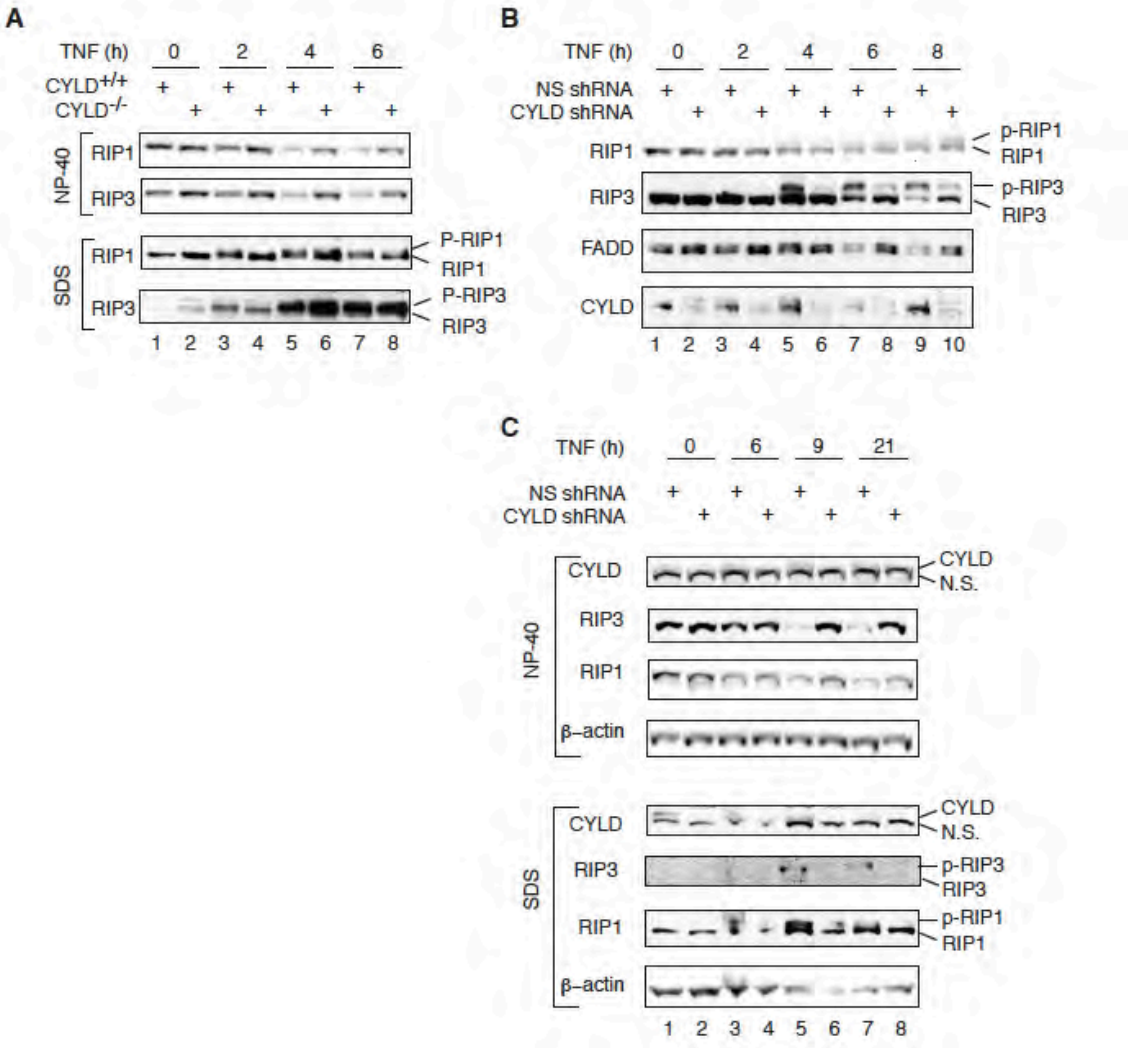
A
TNF (h) 0 2 4 6
CYLD+/+ + + + +
CYLD-/- + + + +
NP-40
RIP1
RIP3
SDS
RIP1
RIP3
P-RIP1
RIP1
P-RIP3
RIP3
1 2 3 4 5 6 7 8
B
TNF (h) 0 2 4 6 8
NS shRNA + + + + +
CYLD shRNA + + + + +
RIP1
RIP3
FADD
CYLD
p-RIP1
RIP1
p-RIP3
RIP3
1 2 3 4 5 6 7 8 9 10
C
TNF (h) 0 6 9 21
NS shRNA + + + +
CYLD shRNA + + + +
NP-40
CYLD
RIP3
RIP1
β–actin
CYLD
N.S.
SDS
CYLD
RIP3
RIP1
β–actin
CYLD
N.S.
p-RIP3
RIP3
p-RIP1
RIP1
1 2 3 4 5 6 7 8

Figure 4.7 Impaired RIP1 and RIP3 phosphorylation in the absence of CYLD.

(A) MEFs were treated with TNFα, zVAD-fmk and LBW242. Cell lysates were extracted by sequential detergent lysis in NP-40 and SDS as described in methods. RIP1 and RIP3 in each fraction were examined by Western blot. Note that phosphorylated RIP1 and RIP3 (p-RIP1 and p-RIP3) were exclusively detected in the SDS fractions. **(B)** HT-29 cells stably expressing non-specific (NS) shRNA or CYLD shRNA were treated with TNFα, LBW242 and zVAD-fmk for the indicated times. Unmodified and phospho-RIP1 and phospho-RIP3 were analyzed by Western blot. **(C)** Same cells and treatment as in (B). Cell lysates were extracted by sequential detergent lysis in NP-40 and SDS as described in methods. The phosphorylation status of RIP1 and RIP3 was determined by Western blot.

Figure 4.8

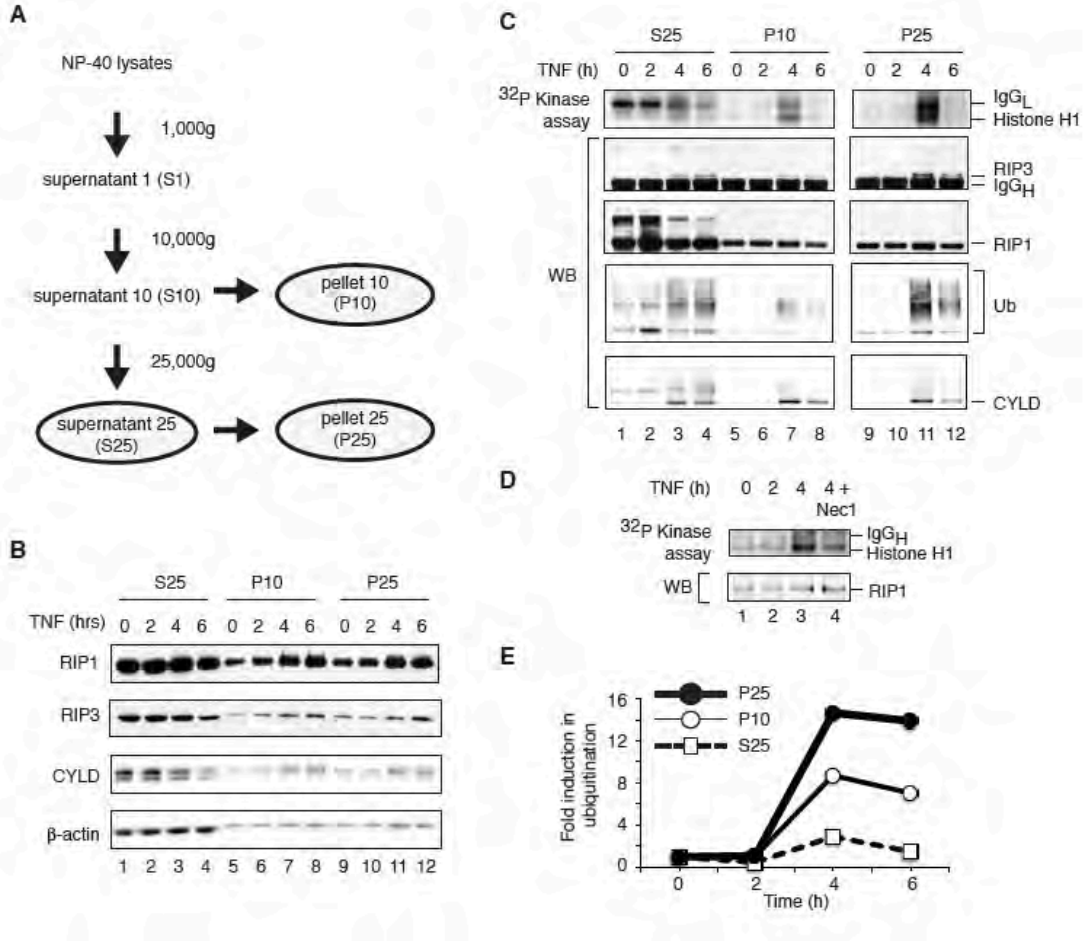
A
NP-40 lysates
1,000g
supernatant 1 (S1)
10,000g
supernatant 10 (S10)
pellet 10 (P10)
25,000g
supernatant 25 (S25)
pellet 25 (P25)
B
S25
P10
P25
TNF (hrs) 0 2 4 6 0 2 4 6 0 2 4 6
RIP1
RIP3
CYLD
β-actin
1 2 3 4 5 6 7 8 9 10 11 12
C
S25
P10
P25
TNF (h) 0 2 4 6 0 2 4 6 0 2 4 6
32P Kinase assay
IgGL
Histone H1
RIP3
IgGH
RIP1
WB
Ub
CYLD
1 2 3 4 5 6 7 8 9 10 11 12
D
TNF (h) 0 2 4 4 + Nec1
32P Kinase assay
IgGH
Histone H1
WB
RIP1
1 2 3 4
E
Fold induction in ubiquitination
16
12
8
4
0
P25
P10
S25
0 2 4 6
Time (h)

Figure 4.8 Induction of RIP1 associated kinase activity in the NP-40 insoluble compartment.

(A) Schematic flowchart showing the procedures by which the different NP-40 soluble and insoluble fractions were obtained. **(B)** Accumulation of necrosis signaling proteins in the NP-40 insoluble fractions. FADD deficient Jurkat cells stably transfected with TNFR-2 were treated to undergo necrosis with rhTNFα for the indicated time-points. The indicated fractions were analyzed for levels of RIP1, RIP3 and CYLD via Western blot. β-actin was used as an internal control. **(C)** The kinase activity of the necrosome is selectively activated in the NP-40 insoluble fractions. Cell lysates were subjected to differential centrifugation as described in (A). RIP1 complexes were obtained via IP and subjected to *in vitro* kinase assays using histone H1 as the substrate. RIP1 ubiquitination and recruitment of RIP3 and CYLD were determined by Western blot (lower panels). **(D)** Induction of kinase activity in the NP-40 insoluble fraction is partially dependent on RIP1 kinase activity. The P10 fractions were prepared, and RIP1 complexes were isolated. Where indicated, 30 μM of Nec-1 was added to the *in vitro* kinase assay. **(E)** Densitometry quantification of RIP1 ubiquitination in the different fractions in (C**)**.

Figure 4.9

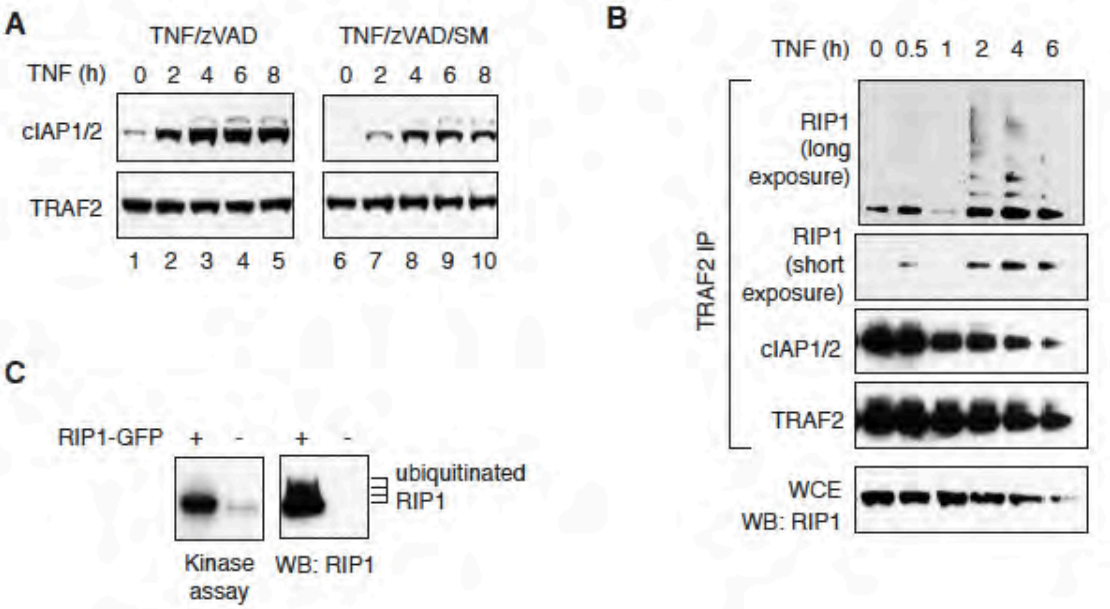
A
TNF/zVAD
TNF/zVAD/SM
TNF (h) 0 2 4 6 8 0 2 4 6 8
cIAP1/2
TRAF2
1 2 3 4 5 6 7 8 9 10
B
TNF (h) 0 0.5 1 2 4 6
RIP1 (long exposure)
RIP1 (short exposure)
cIAP1/2
TRAF2
TRAF2 IP
WCE
WB: RIP1
C
RIP1-GFP + - + -
ubiquitinated RIP1
Kinase assay
WB: RIP1

Figure 4.9 Poly-ubiquitinated RIP1 is a poor substrate for autophosphorylation. **(A)** TNFα induced expression of cIAP2. Wild type MEFs were stimulated with TNFα, zVAD-fmk and SM as indicated. Expression of cIAP1 and cIAP2 was analyzed via Western blot using a pan-cIAP antibody. **(B)** Cellular IAPs associate with polyubiquitinated RIP1 during necrosis induction. TRAF2 complexes were purified from TNFα, CHX, and zVAD-fmk treated cells. Western blot shows that polyubiquitinated RIP1 at 2, 4 and 6 hours post-stimulation were present with the cIAP1/2-TRAF2 complex. **(C)** Polyubiquitinated RIP1 is refractory to autophosphorylation. HEK293T cells were transfected with GFP tagged RIP1. RIP1 was immunoprecipitated with antibody against GFP. The immune complex was tested for autophosphorylation in *in vitro* kinase assay (left). The Western blot on the right panel shows unmodified and ubiquitinated RIP1 species. Note that the ubiquitinated species were not phosphorylated in the kinase assay.

Figure 4.10

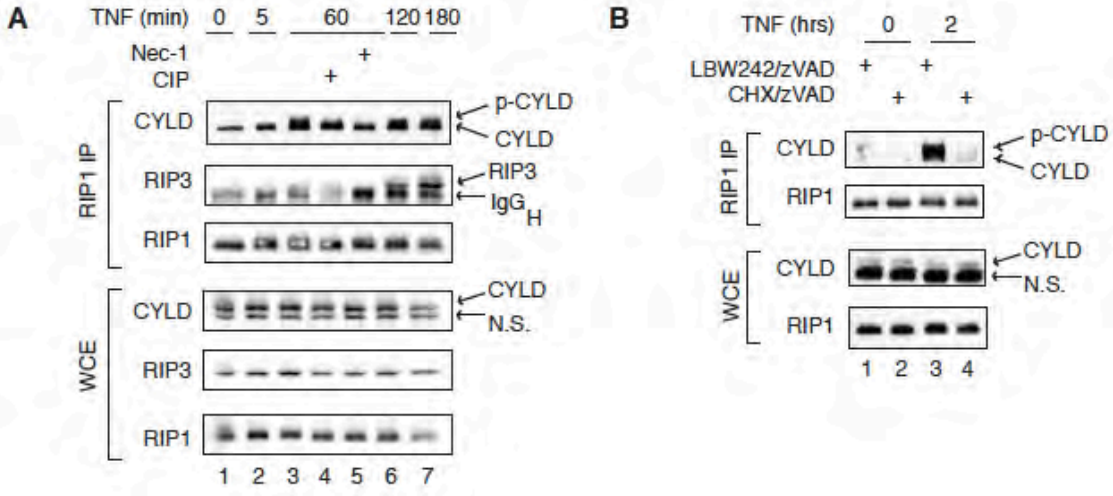
A
TNF (min) 0 5 60 120 180
Nec-1 +
CIP +
RIP1 IP
CYLD
RIP3
RIP1
p-CYLD
CYLD
RIP3
IgG H
WCE
CYLD
RIP3
RIP1
CYLD
N.S.
1 2 3 4 5 6 7
B
TNF (hrs) 0 2
LBW242/zVAD + +
CHX/zVAD + +
RIP1 IP
CYLD
RIP1
p-CYLD
CYLD
WCE
CYLD
RIP1
CYLD
N.S.
1 2 3 4

Figure 4.10 RIP1 kinase dependent phosphorylation of CYLD during TNFα-induced necrosis.

(A) Wild-type MEFs were treated with TNFα, LBW242 and zVAD-fmk. Where indicated, cells were pre-treated with Nec-1 or the immune complexes were treated with phosphatase. RIP1 complexes were isolated by IP. The recruitment of CYLD to RIP1 was determined by Western blot. **(B)** $CYLD^{-/-}$ MEFs stably expressing S418A HA-CYLD were pre-treated with zVAD-fmk and either LBW242 or CHX, and then stimulated with TNFα for the indicated time. RIP1 complexes were isolated by IP. The recruitment of CYLD to RIP1 was determined by Western blot.

Figure 4.11

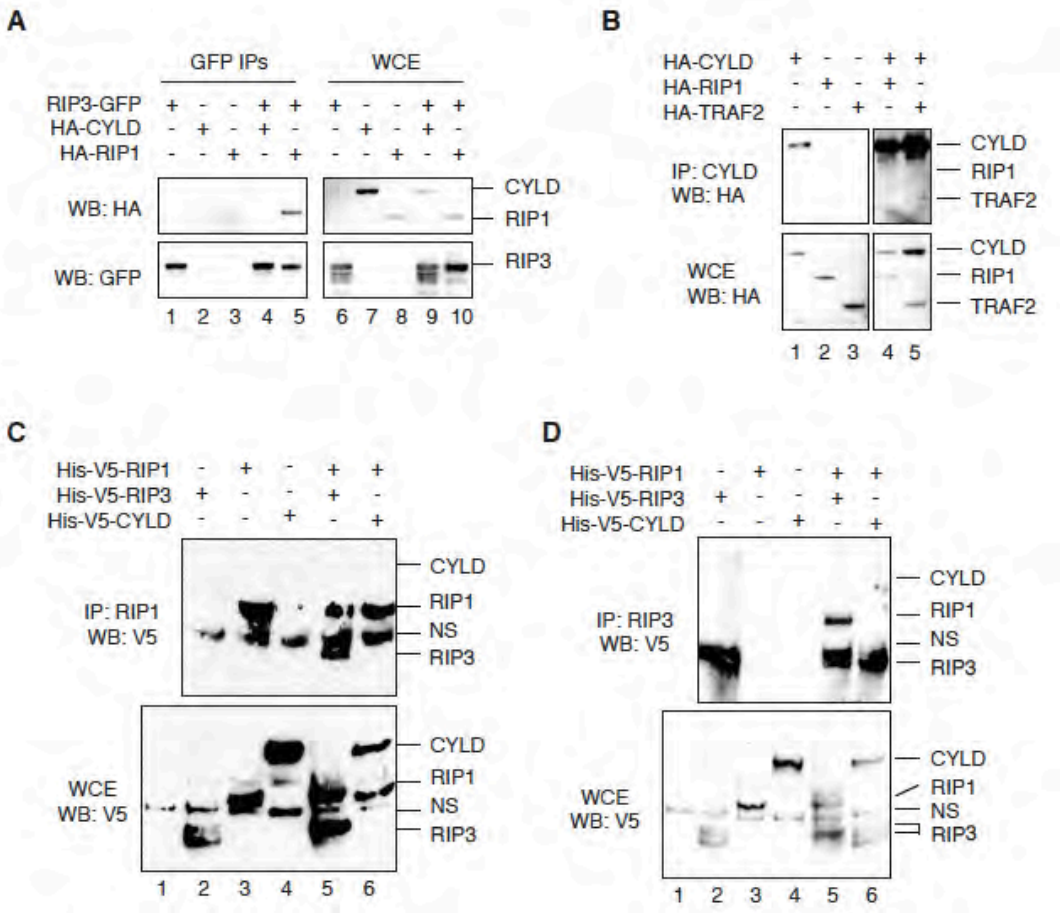
A
GFP IPs
WCE
RIP3-GFP + - - + + + - - + +
HA-CYLD - + - + - - + - + -
HA-RIP1 - - + - + - - + - +
WB: HA
WB: GFP
CYLD
RIP1
RIP3
1 2 3 4 5 6 7 8 9 10
B
HA-CYLD + - - + +
HA-RIP1 - + - + -
HA-TRAF2 - - + - +
IP: CYLD
WB: HA
WCE
WB: HA
CYLD
RIP1
TRAF2
1 2 3 4 5
C
His-V5-RIP1 - + - + +
His-V5-RIP3 + - - + -
His-V5-CYLD - - + - +
IP: RIP1
WB: V5
WCE
WB: V5
CYLD
RIP1
NS
RIP3
1 2 3 4 5 6
D
His-V5-RIP1 - + - + +
His-V5-RIP3 + - - + -
His-V5-CYLD - - + - +
IP: RIP3
WB: V5
WCE
WB: V5
CYLD
RIP1
NS
RIP3
1 2 3 4 5 6

Figure 4.11 CYLD does not directly bind to RIP1 or RIP3.

(A) 293T cells were transfected with the plasmids encoding the indicated genes. RIP3 was immunoprecipitated and association with either CYLD or RIP1 was determined by Western blot. **(B)** Similar to (A) but instead CYLD was immunoprecipitated and association with RIP1 or TRAF2 was determined by Western blot. **(C)** SF9 cells were transduced separately with the indicated recombinant baculovirus. Lysates from transductions were mixed as shown, RIP1 was immunoprecipiated, and association with CYLD and RIP3 was determined through Western blot. **(D)** Same as in (C) but RIP3 was immunoprecipitated.

Discussion

Protein ubiquitination plays key roles in cell death and innate immune signaling pathways (O'Donnell et al., 2011). Polyubiquitinated RIP1 in the TNFR-1 complex was shown to prevent RIP1 association with caspase-8 resulting in inhibition of apoptosis (O'Donnell et al., 2007). SMAC mimetic treatment causes cIAP1/2 degradation, the E3 ligases for RIP1. This sensitizes cells to TNFα-induced apoptosis. CYLD was shown to be required for the formation of the DISC in this cell death context, which was presumed to be CYLD-mediated deubiquitination of residual ubiquitinated RIP1 within the TNFR-1 complex (Wang et al., 2008). A similar role for polyubiquitinated RIP1 has been proposed to inhibit necrosome formation (O'Donnell et al., 2011; O'Donnell et al., 2012). Hence, CYLD was thought to promote necrosis by de-ubiquitination of RIP1 in the TNFR-1 membrane complex. In contrast to this prevailing model, we show that RIP1 ubiquitination in the TNFR-1 complex was unaffected in $CYLD^{-/-}$ cells. Moreover, the RIP1-RIP3 necrosome was formed, albeit with delayed kinetics, in $CYLD^{-/-}$ or CYLD-kd cells. CYLD was recruited to the necrosome in a TNFα-dependent manner. However, this interaction is likely to be indirect, as expression of CYLD in 293T cells or in baculovirus did not reveal a strong interaction between CYLD and RIP1. Adaptors such as the recently reported CLIPR-59 may mediate the interaction between RIP1 and CYLD (Fujikura et al., 2012).

In contrast to RIP1 ubiquitination in the TNFR-1 complex, RIP1 ubiquitination in the necrosome was indeed increased in the absence of CYLD. In particular, the necrosome isolated from the NP-40 insoluble fraction showed strong induction of ubiquitination in response to TNFα, suggesting that CYLD may instead regulate RIP1 ubiquitination in this compartment. This model is consistent with the recent discovery that caspase-8 mediated cleavage of CYLD limits TNFα-induced programmed necrosis, since caspase-8 is present in the necrosome, but not the TNFR-1 complex (O'Donnell et al., 2011). Because CYLD is not essential for necrosome assembly, but rather facilitates its activation, our results also explain why genetic inactivation or siRNA silencing of CYLD was not as effective as inactivating RIP1 or RIP3 in blocking programmed necrosis in cells or in $FADD^{-/-}$ or $caspase\text{-}8^{-/-}$ mice (Bonnet et al., 2011; Welz et al., 2011).

A consequence of increased RIP1 ubiquitination in $CYLD^{-/-}$ cells is impaired RIP1 and RIP3 phosphorylation and activation. The polyubiquitin chains on RIP1 may sterically prevent autophosphorylation of RIP1 or limit access of an upstream RIP1 activating kinase. Alternatively, it may sterically restrict RHIM-mediated amyloid complex assembly, which facilitates kinase activation (Li et al., 2012). Regardless of the mechanism, it is surprising that CYLD deficiency led to a substantial reduction in necrosis and yet necrosome assembly was only marginally affected. The precise reason for this difference is unknown at present. However, it is noteworthy that the levels of RIP1, RIP3 and CYLD in the NP-40 fractions decreased as programmed necrosis ensued (Fig. 4.7A). While some of the loss could be attributed to relocation of these factors to

the NP-40 insoluble fractions, direct lysis with SDS buffer revealed that protein degradation might also contribute to their loss (Fig. 4.7B). This necrosis-induced degradation of signaling regulators was impaired in $CYLD^{-/-}$ cells.

Another fascinating prospect offered by the data presented in this chapter is the reciprocal regulation between CYLD and RIP1 during necrosis. The data strongly supports the notion that polyubiquitinated RIP1 is a target of CYLD, and is suggestive of CYLD being a RIP1 substrate. Although, CYLD phosphorylation is RIP1 kinase dependent, whether CYLD is directly phosphorylated by RIP1 has not been formally demonstrated. The kinetics of RIP1-associated CYLD phosphorylation is consistent with our understanding that RIP1 kinase activation occurs post-TNFR-1 complex dissolution (Cho et al., 2009). Ascertaining whether this phosphorylation event is consequential for the necrosis program is of critical importance.

Given that RIP1 kinase activity is required for necrosis, the most straightforward possibility is that CYLD phosphorylation is pro-necrotic. This is in contrast to IKKγ(NEMO)-dependent phosphorylation of CYLD, which inhibits its function. In addition to NEMO inhibiting CYLD, it has been shown to negatively regulate TNFα-induced necrosis (Reiley et al., 2005; O'Donnell et al., 2012). Future studies should investigate the possibility that NEMO exerts its anti-necrotic function through inactivation of CYLD. Interestingly, RIP1-mediated phosphorylation of associated CYLD does not occur at early time-points during TNFR-1 complex formation (Fig4.10A, top panel, compare lanes 2 and 3). This was the time when the inhibitory phosphorylation of CYLD by the IKK complex was previously observed. The CYLD

phosphorylation event occurs prior and during necrosome formation (Fig4.10A, top two panels, compare lanes 3,6, and 7). This provides the basis for a potentially interesting mode of CYLD regulation during TNFα signaling. Perhaps, early during necrosis signaling phosphatases remove inhibitory phosphates from CYLD, which is followed by RIP1 kinase dependent addition of activating phosphates on CYLD. Since this study establishes CYLD-mediated RIP1 deubiquitination as a molecular event consequential for necrosis, it is also tempting to speculate the existence of a positive feedback regulatory mechanism where RIP1 activates CYLD and CYLD deubiquitinates RIP1 resulting in further RIP1 activation.

However, it is plausible that CYLD phosphorylation is anti-necrotic and serves as a regulatory mechanism to suppress aberrant necrosis. If the latter scenario is correct, it would be suitable to dub RIP1 an "ambivalent kinase" because it mediates both pro-necrotic and anti-necrotic phosphorylation events. This may suggest that additional factors dictate the targets RIP1 phosphorylates and the overall decision of which opposing cellular outcome predominates, survival or death. Namely, these additional factors could be in the form of intervening pro-survival pathways, or supportive pro-death pathways. The potential junction between the necrosis pathway and other pathways may allow the cell to integrate additional information such as its metabolic status before making the decision to commit suicide. It is also possible that CYLD activates RIP1 and then RIP1 phosphorylates and inactivates CYLD. This could serve as a regulatory mechanism to ensure that CYLD does not deubiquitinate other components of the necrosome, which may require ubiquitination for transducing the necrotic signal.

In this report we show that in spite of CYLD recruitment to the TNFR1 complex, it does not regulate RIP1 ubiquitination within this compartment. This may be attributed to the fact that the IKK complex is activated within the TNFR1 complex, and the IKK complex negatively regulates CYLD-mediated deubiquination of target proteins (Reiley et al., 2005). It is unclear whether the TNFR1 complex associated CYLD transitions into the necrosome and is ultimately responsible for deubiquitinating RIP1. Alternatively, CYLD may be recruited to the necrosome independent of a "rite of passage" through the TNFR1 associated complex.

The USP domain is necessary, but not sufficient for the pro-necrotic function of CYLD. We show that a portion of CYLD harboring the third Cap Glycine domain and a TRA2 interaction motif, in addition to an enzymatically active USP, is sufficient for the pro-necrotic function of CYLD. Naturally, further deletion analysis would be needed to determine how much of this portion of CYLD is functionally relevant (Fig. 4.2A). It is of value to note that the third Cap Glycine domain of CYLD is required for binding to NEMO (Kovalenko et al., 2003). In order, TRAF2 contains an N-terminal RING domain followed by a stretch of Zinc fingers, and the TRAF-N and TRAF-C subdomains. The TRAF-N subdomain is required for binding to RIP1, and both the TRAF-N and TRAF-C subdomains are required for binding to CYLD (Takeuchi et al., 1996; Kovalenko et al., 2003). Since our data indicates that CYLD does not bind directly to RIP1, it is tempting to speculate that CYLD is brought into contact with RIP1 through a mutual association with TRAF2. Consistent with this notion, we demonstrate ligand dependent association between TRAF2 and RIP1 during necrosis (Fig 4.9B). A previous report revealed that

expression of a dominant negative TRAF2 causes enhanced TNFα-induced necrosis. The authors explained this phenotype by impaired RIP1 ubiquitination in cells expressing the dominant negative TRAF2. The mutant TRAF2 used in this study was a deletion mutant lacking its RING domain (O'Donnell et al., 2012). Importantly, the RING domain of TRAF2 is not required for its interaction with CYLD or RIP1 (Kovalenko et al., 2003; Takeuchi et al., 1996). This suggests that the enhanced necrosis caused by dominant negative TRAF2 may not be due solely to lack of anti-necrotic RIP1 ubiquitination via TRAF2 E3 ligase activity, but rather through the retained binding of RIP1/TRAF2/CYLD complex, which promotes RIP1 deubiquitination.

Materials and Methods

Reagents used

Antibodies used in the study were from BD Pharmingen (A20, cIAP1/2, FADD, RIP1, β-actin and TNFR-1), Cell Signaling (p-IκBα and total IκBα), Millipore EMD (K48 and K63-specific ubiquitin antibodies), ProSci (RIP3), Santa Cruz Biotechnology (caspase 8, TRAF2, CYLD) and Invitrogen (CYLD and total ubiquitin antibody). Antibody against human RIP3 has been described before [16]. Necrostatin-1 and zVAD-fmk were obtained from Enzo Life Sciences. Recombinant human and mouse TNF were obtained from Biosource/Invitrogen. The Smac mimetic LBW242 was a kind gift of D. Porter (Novartis). Small interference RNAs used in the study are: human CYLD (5'-CUUAUUUUUAGCAAAGGUUCUACCCUU-3', 5'-UUGGUUUAUUAUGACUGGAUGAACCUU-3'), human RIP3 (5'-

UAACUUGACGCACGACAUCAGGCUGGA-3', 5'-GCAGUUGUAUAUGUUAACGAGCGGUCG-3'), human TR4 (5'-CCGGAGCUUCCCUCAUUUAdTdT-3').

Tissue culture

MEFs were grown in DMEM high sucrose medium supplemented with 10% FCS, 2 mM glutamine, 100 units/ml penicillin, and 100 μg/ml streptomycin. HT-29 and Jurkat cells were grown in McCoy's 5A medium and RPMI1640 media, respectively, supplemented with 10% FCS, 2 mM glutamine, 100 units/ml penicillin, and 100 μg/ml streptomycin. SF9 cells were maintained in serum free Sf-900 II SFM supplemented with 100 units/ml penicillin, and 100 μg/ml streptomycin. Stable clones of HT-29 cells were generated by transfection using lipofectamine 2000 (Invitrogen) of CYLD-specific and scrambled shRNAs from Thermoscientific/Open Biosystems. Clones were selected by puromycin selection and checked for GFP expression via flow cytometry. GFP^+ clones were tested for reduction of CYLD protein expression and used for subsequent experiments.

Cell death assays

For FADD and caspase-8 deficient $TNFR2^+$ Jurkat Cells (Chan et al., 2003), programmed nNecrosis was induced by addition of the indicated amounts of recombinant human TNF (rhTNF). Cell death was determined by flow cytometry with propidium iodide staining or by CellTiter 96® AQueous One Solution Cell Proliferation Assay (Promega).

Transfection of DNA Plasmids and siRNA

Jurkat cells were transfected with 150 nM of the indicated siRNA. All siRNA transfections were performed using the HiPerfect transfection reagent (Qiagen) as per manufacturer's protocols. Forty-eight hours later, cells were stimulated with TNFα to induce necrosis.

For DNA plasmid transfection into MEFs, 2.5 x 10^5 cells per well of 12-well plate were plated the day before transfection. Transfection was performed using the Lipofectamine LTX transfection reagent (Invitrogen) as per manufacturer's protocol. CYLD deletion mutants were generated by PCR amplification and cloning into pEGFP-C1 vector. Integrity of the mutant clones was confirmed by sequencing.

For 293T cells, three hours prior to transfection cells were plated at 3 x 10^5 cells/well of 12-well plate. Cells were subsequently transfected with 1 μg/well (12-well plate) of the indicated plasmid DNA using the Fugene6 or Fugene HD transfection reagent (Roche) as per manufacturer's protocol.

Recombinant Baculovirus generation and Transduction

Recombinant baculovirus encoding either hRIP1, hRIP3, hCYLD were generated using the BaculoDirect™ Baculovirus Expression System as per manufactures protocol. Transduction of SF9 cells was conducted as per manufactures protocol.

Immmunoprecipitations and Western Blots

For immunoprecipitations in MEFs, six million cells on two 10 cm tissue culture dishes were used per sample. For HT-29 cells, one plate of cells was used per sample. For Jurkat cells, 100 – 150 million cells were used. Cells were harvested and lysed in either Complex II lysis buffer (150 mM NaCl, 20 mM Tris-Cl [pH 7.5], 1% NP-40, 1 mM EDTA, 3 mM NaF, 1 mM βb-glycerophosphate, 1 mM sodium orthovanadate) or RIPA lysis buffer (150 mM sodium chloride, 1% NP-40, 0.5% sodium deoxycholate, 0.1% SDS, and 50 mM Tris pH 8.0) supplemented with 5 μM iodoacetamide, 2 μM *N*-ethylmaleimide, 1X *Complete* protease inhibitors (Roche) and Phosphatase inhibitor cocktail I (Sigma). For denaturing IPs, cells were lysed in 1% SDS, 50 mM TrisCl pH7.4, 5 mM EDTA, 10 mM DTT, 15 U/ml DNase I supplemented with Complete protease inhibitors (Roche), and phosphatase inhibitor cocktail II (Sigma). After clearance with Sepharose 6B beads, lysates were mixed with specific immunoprecipitation antibodies as indicated for 4 hours to overnight at 4^{o}C. Immune complexes were then washed, boiled, and resolved on a 4-12% Bis-Tris NuPAGE gel (Invitrogen). For sequential IP, the washed immune complex was resuspended in RIPA buffer supplemented with 6 M urea. After rotation at room temperature for 30 minutes, lysates were diluted 10-fold in RIPA buffer without urea and incubated with different ubiquitin antibodies.

For differential centrifugation, cell lysates were centrifuged at 1,000g for 10 minutes. The resulting supernatants were centrifuged at 10,000g for 10 minutes. The resulting pellet was washed in 1 ml lysis buffer and centrifuged at 10,000g for an additional 10 minutes yielding the P10 fraction. The supernatant following first spin at 10,000g was

transferred to a new tube and spun at 25,000g. The resulting supernatant and pellets were the S25 and P25 fractions.

In vitro kinase assays

The IP complexes were incubated for 30 minutes at 30°C in kinase reaction buffer (20 mM HEPES [pH 7.5], 2 mM DTT, 1 mM NaF, 1 mM Na_3VO_4, 20 mM β-glycerophosphate, 20 mM $MgCl_2$, 20 mM $MnCl_2$, 1 mM EDTA, and 200 – 400 μM ATP) supplemented with 10 μCi [^{32}P] γ-ATP and 5 μM Histone H1. Reactions were quenched by boiling in sample loading buffer. Phosphorylation of Histone H1 was visualized by autoradiography.

PREFACE TO CHAPTER V

The conclusions in this chapter are primarily based on findings in the following manuscript that is under review for publication:

David M. Moquin, Thomas McQuade, Francis Ka-Ming Chan. **CYLD Deubiquitinates RIP1 in the Necrosome to Facilitate Kinase activation and Programmed Necrosis**

CHAPTER V: Discussion

Overview

The work presented in this thesis documents the independent finding of the functional involvement of CYLD in TNFα induced necrosis. It was originally believed that CYLD was an essential component of the TNFα induced necrosis signaling pathway (Vanlangenakker et al., 2011). The work here demonstrates that CYLD is not essential for TNFα induced necrosis, as attenuated necrosis proceeds in the absence of CYLD. The CYLD-independent necrosis is RIP1 kinase dependent supporting the notion that the pathway is still transduced through the necrosome. Furthermore, CYLD controls the kinetics of necrosis, as indicated by a delay in the onset of necrosis in CYLD deficient MEFs. This delay in necrosis is congruent with the biochemical data. Namely, RIP1/RIP3 necrosome formation is kinetically delayed in cells deficient of CYLD. Interestingly, although necrosis is attenuated in CYLD deficient MEFs, the RIP1/RIP3 necrosome eventually catches up to levels observed in cells expressing CYLD. We demonstrate that RIP1 is indeed the primary target of CYLD in the context of necrosis. In opposition to the previous model proposed for the pro-necrotic mechanism of CYLD, it does not regulate the ubiquitination status of RIP1 within the TNFR-1 complex. Instead, CYLD is recruited to RIP1 complexes during necrosome formation, and regulates the ubiquitination status of RIP1 within an NP-40 insoluble fraction. The corollary of this is activation of the necrosome as demonstrated by the reduced phosphorylation status of RIP1 and RIP3 in CYLD deficient cells. Consistently, we provide evidence that unmodified RIP1 is a better substrate for auto-phosphorylation than

polyubiquitinated RIP1. Altogether, this thesis independently reveals the pro-necrotic function of CYLD and provides a new model for the molecular mechanism governing this function (Fig 5.1).

The involvement of CYLD in TNFα-induced cell death

Previous studies suggested that CYLD is an essential player in the TNFα-induced signaling pathway (Vanlangenakker et al., 2011). Our studies indicate that necrosis proceeds in the absence of CYLD, but is kinetically impaired and has a decreased magnitude. The discrepancy between the results can potentially be answered by the fact that our data shows a kinetic delay in the onset of necrosis in CYLD deficient MEFs. Previous groups may have used time-points when CYLD-independent necrosis had not yet commenced and thus reported that CYLD was essential for necrosis. Genetic evidence supports the notion that CYLD is not essential for necrosis. Specifically, conditional deletion of FADD in epidermal keratinocytes results in RIP3 dependent programmed necrosis resulting in inflammatory skin lesions. Crossing these mice with RIP3 knock-out mice was sufficient for rescuing the phenotype while crossing to CYLD knock-out mice resulted in only a partial rescue. Therefore, *in vivo* evidence suggests that CYLD is not essential for necrosis, which is in agreement with our findings (Bonnet et al., 2011).

The non-essential function of CYLD in TNFα-induced necrosis raises questions regarding the validity of the current model that is used to describe the mechanism behind its pro-necrotic function. The current model places CYLD upstream of necrosome

formation. Both RIP1 and RIP3 are essential for TNFα-induced necrosis, and require their RHIM domains in order to associate and transduce the necrotic signal (Holler et al., 2001; Cho et al., 2009). The fact that necrosis can occur independently of CYLD suggests that its purported role as a driver of necrosome formation is moot (Fig 1.1). In other words, if CYLD was required for RIP1/RIP3 association this would predict that it should also be an essential component of the necrosis signaling pathway since RIP1/RIP3 association is a critical molecular event. Supporting this notion, RIP1 kinase activity is still required for CYLD-independent TNFα-induced necrosis. Hence, RIP1 kinase activity must still be activated in the absence of CYLD. This data provided us with important clues that the presumed model accounting for the pro-necrotic function of CYLD was incorrect. The biochemical data is consistent with these findings.

Interestingly, our studies indicate a greater requirement for CYLD in necrosis than apoptosis. The apoptotic target of CYLD has been proposed to be polyubiquitinated RIP1; however, it is clear the TNFα-induced apoptosis is RIP1 independent when sensitized with CHX (Lin et al., 2004). This makes it unlikely that RIP1 is the target of CYLD during apoptosis. Nevertheless, it has been demonstrated that CYLD promotes TNFα driven caspase activation (Fujikura et al., 2012). In addition to regulating caspase activation, CYLD is a target of caspase-8 cleavage (O'Donnell et al., 2011). This implies that the pro-apoptotic function of CYLD precedes caspase-8 activation since cleavage results in degradation of the C-terminal fragment. CYLD-mediated caspase activation is likely explained by its role in regulating DISC formation (Wang et al., 2008). Similarly our data indicates that CYLD also regulates the kinetics of necrosome formation;

however, in the absence of CYLD it catches up to levels found in cells replete with CYLD. Therefore, the kinetic delay in cell death is congruent with the kinetic delay in necrosome formation. The fact that the level of necrosome formation catches up, but the magnitude of cell death does not, suggests that CYLD mediates two separate molecular events leading to necrosis. One molecular event is early and results in the regulation of the kinetics of necrosome formation, and the other molecular event is later and determines the functionality of the necrosome. For apoptosis the data indicates that the only molecular event CYLD mediates is prior to DISC formation where caspase-8 is activated. Altogether, the greater requirement for CYLD in necrosis may reflect the fact that it is mediating two molecular events, one early and one later, while CYLD may only mediate an early pro-apoptotic molecular event.

What is the potential early molecular event CYLD regulates? Since CYLD regulates both the kinetics of apoptotic DISC formation and necrosome formation, it is tempting to speculate that the early molecular event it mediates is the same for apoptosis and necrosis. Our current knowledge of the TNFα cell death pathway suggests that the divergence point between apoptosis and necrosis occurs at the DISC. This predicts that the preceding steps in the pathway are similar. Corroborating this hypothesis, our study shows that CYLD deficiency not only leads to a delay in RIP1/RIP3 association, but also delayed association between FADD/RIP, caspase-8/RIP1, and caspase-8/FADD, which are also components of the apoptotic DISC (Micheau et al., 2003). It has not been formally demonstrated whether the deubiqutinase activity of CYLD is required for its pro-apoptotic function. This would perhaps suggest that CYLD regulates the

ubiquitination status of a shared protein/s required for promoting either apoptotic DISC formation or necrosome formation during caspase inhibition.

One intriguing candidate for the target of CYLD during the potential early overlapping pro-apoptotic and pro-necrotic molecular event is polyubiquitinated NEMO. Several lines of evidence suggest that this may be the case. First, NEMO has already been demonstrated to be a target of CYLD in overexpression studies (Kovalenko et al, 2003). Second, NEMO is a negative regulator of both TNFα-induced apoptosis and necrosis (O'Donnell et al, 2009; O'Donnell et al, 2012). Third, CYLD knock-down does not confer protection from TNFα-induced apoptosis in NEMO deficient cells. Fourth, linear ubiquitination of NEMO via LUBAC promotes TNFα-induced NFκB activation and negatively regulates TNFα-induced apoptosis (Tokunaga et al., 2009). Fifth, our study demonstrates that CYLD is recruited to the TNFR-1 complex shortly after TNFα stimulation. Since this is the complex where NEMO binds to polyubiquitinated RIP1 and NEMO itself gets ubiquitinated within this complex, the target and substrate are both temporally and spatially in sync during TNFα signaling. Clearly, more direct evidence is needed to substantiate this potential molecular event. Future studies should evaluate whether CYLD regulates the ubiquitination status of NEMO within the TNFR-1 complex, and address the functional consequences for the pro-apoptotic and pro-necrotic signal. The expectation would be that NEMO ubiquitination regulates the kinetics of apoptotic DISC formation or necrotic DISC formation (Fig. 5.2).

A previous report indicates that the pro-apoptotic function of CYLD is attributed to its role in negatively regulating NFκB (Brummelkamp et al., 2003). However, our

study provides two lines of evidence in opposition to this. First, the use of CHX to sensitize cells to TNFα-induced apoptosis should eliminate the effects of NFκB activation on apoptosis. Second, we did not observe differences in TNFα-induced NFκB activation in CYLD deficient MEFs as compared to wild-type.

Can the early target of CYLD that promotes apoptotic DISC formation and necrosome formation simply be RIP1? The data from our study is not consistent with this model. We demonstrate that CYLD does not regulate the ubiquitination status of RIP1 within the TNFR-1 complex. Instead we demonstrate that CYLD regulates the ubiquitination status of RIP1 within the NP-40 insoluble necrosome. Therefore, our temporal and spatial data regarding CYLD-mediated RIP1 deubiquitination is incongruent with a model in which ubiquitinated RIP1 is the early target of CYLD accounting for its effects on necrosome formation. Additionally, sensitizing cells to apoptosis with TNFα and CHX is RIP1 independent (Li et al., 2004). In our study we show that CYLD is functionally involved in apoptosis induced via this stimuli. This data disqualifies RIP1 as a likely target of CYLD responsible for apoptotic DISC and necrosome formation.

CYLD-mediated regulation of the necrosome

The CYLD regulated molecular event that occurs later and is specific to necrosis is better characterized by the work presented in this thesis. We demonstrate that RIP1 is polyubiquitinated with both K63 and K48 linked chains in the necrosome. Importantly, *in vitro* deubiquitinase activity of CYLD is specific to K63 and linear chains opposed to

K48 chains (Komander et al., 2009). We show that CYLD does not regulate the ubiqutination status of RIP1 within the TNFR-1 complex nor does it regulate RIP1 ubiquitination within the NP-40 soluble fraction at later time-points following dissociation of RIP1 from the TNFR-1 complex. Instead, we show that CYLD regulates the ubiquitination of RIP1 within an NP-40 insoluble fraction following TNFR-1 complex dissociation. Namely, hyperubiquitinated RIP1 is only observed in CYLD deficient MEFs at later time-points in the NP-40 insoluble fraction. This fraction was previously demonstrated to harbor enriched phosphorylated RIP1 and RIP3, which are consequential modifications for the necrosis signaling program (Degterev et al., 2008; Li et al., 2013). The ramification of this deubiquitination event is not regulation of RIP1/RIP3 association, but rather full activation of RIP1 and RIP3 as indicated by phosphorylation.

In addition to revealing that CYLD regulates RIP1 ubiquitination within the NP-40 soluble fraction, we also reveal that induction of RIP1 kinase activity is most pronounced in the equivalent P10/P25 fractions. The equivalence of the NP-40 insoluble fraction and the P10/P25 fractions is supported by the fact that accumulation of components of the necrosome was observed for both these fractions. Importantly, induction of RIP1 ubiquitination is also most pronounced in these fractions, and CYLD can be found in RIP1 complexes from these fractions. Induction of RIP1 ubiquitination is also most pronounced in the P10/P25 fractions. This places CYLD in the same location as its relevant substrate during necrosis. Altogether, this data suggests that CYLD-mediated regulation of RIP1 ubiquitination occurs in the same fraction where

RIP1 kinase activity is induced. This provides a link between CYLD-mediated RIP1 deubiquitination with induction of full RIP1 kinase activation. Preliminary experiments suggest that CYLD regulates the induction of RIP1 kinase activity in the P10/P25 fractions.

It is clear that RIP1/RIP3 association occurs within the NP-40 soluble and S25 fractions. Since RIP1 kinase activity is required for RIP1/RIP3 association, this predicts that RIP1 must be kinase active in the NP-40 soluble or S25 fraction. Interestingly, our data shows that RIP1 is indeed active in the S25 fraction even prior to necrosis signaling, but no distinguishable induction was observed during necrosis. This could possibly be explained by a low signal to noise ratio in the S25 fraction. The pool of activated RIP1 post-stimulation might be too small to observe an increase in RIP1 kinase activity over background. Conversely, in the P10/P25 fractions, kinase active RIP1 may be enriched thereby increasing the signal to noise ratio. The lower background prior to necrosis stimulation may be attributed to a smaller fraction of kinase active RIP1 in the P10/P25 fractions than the S25 fraction prior to stimulation. Future studies should focus on elucidating the stages of RIP1 kinase activation during necrosis. The lower levels of RIP1 phosphorylation observed in the NP-40 soluble fraction are consistent with the lack of observed RIP1 kinase activity in the comparable S25 fraction. Since some evidence suggests that RIP1 kinase activation is promoted by autophosphorylation, it is conceivable that a hierarchy of RIP1 phosphorylation events track with the extent of RIP1 kinase activation throughout the course of necrosis. Early during necrosis, RIP1 autophosphorylation may not be to the extent found when the necrosome has formed.

This could be due to a smaller percentage of RIP1 being autophosphorylated, a fewer number of sites phosphorylated on RIP1, or a combination of the two. Indeed, it has been demonstrated that during necrosis detection of RIP1 phosphorylation only occurs in cells replete with RIP3 (Cho et al., 2009). This suggests a model of RIP1/RIP3 reciprocal kinase activation. It is possible that RIP1/RIP3 formation of amyloid fibrils augments kinase activation and phosphorylation of downstream substrates. We show that CYLD regulates the ubiquitination status of RIP1 within the NP-40 insoluble fraction where RIP1/RIP3 amyloid fibrils are presumably enriched (Li et al., 2012). This potentially indicates that CYLD may regulate amyloid fibril formation, and should be the emphasis of further research.

RIP1 ubiquitination in the necrosome

How does RIP1 ubiquitination within the necrosome interfere with molecular events required for necrosis? We provide evidence that unmodified RIP1 is a better substrate for autophosphorylaton than ubiquitinated RIP1. Previous work found that RIP1 autophosphorylation is required for full activation of its kinase activity (Degterev et al., 2008). Substituition of the RIP1 autophosphorylation site at Serine 161 with an alanine results in a reduction in kinase activity and a partial defect in its ability to promote necrosis. The functional relevance of the other autophosphorylation sites still needs to be clarified. It is tempting to speculate that compound mutations of multiple RIP1 autophosphorylation sites may further impair RIP1 kinase activity and functionality during necrosis. Since our data shows that RIP1 and RIP3 phosphorylation are impaired

in CYLD knock-down HT-29 cells and eventually catches up in MEFs, it is conceivable that RIP1 ubiquitination may block some autophosphorylation sites leading to partial impairment of RIP1 kinase activity. This would explain our results showing a reduction in RIP1/RIP3 phosphorylation in the absence of CYLD. The fact that phosphorylation begins to catch up is consistent with the nonessential function of CYLD in necrosis. Further supporting this model, RIP3 phosphorylation requires RIP1 kinase activity; so impaired RIP1 kinase activity due to hyperubiquitination and a concomitant impairment in autophosphorylation would be expected to result in impaired RIP3 phosphorylation (Cho et al., 2009; He et al., 2009). In agreement with this we provide evidence that RIP3 phosphorylation is indeed impaired in CYLD knock-down cells.

It is feasible that alternative models may explain how hyperubiquitinated RIP1 due to CYLD deficiency results in impaired necrosome functionality. K63-linked polyubiquitin chains act as binding platforms for proteins containing ubiquitin binding domains or proteins that bind to adaptors containing ubiquitin binding domains. Our data indicates that hyperubiquitinated RIP1 within the NP-40 insoluble fraction is inhibitory for necrosis. In this case hyperubiquitinated RIP1 associated with the necrosome may either allow for binding of negative regulators of necrosis, prevent the binding of positive regulators of necrosis, or both. It is presumed that NEMO inhibits TNFα-induced necrosis through binding to polyubiquitinated RIP1 within the TNFR-1 complex (O'Donnell et al., 2012). However, since we demonstrate that RIP1 is decorated with K63-linked polyubiquitin chains within the necrosome, it is possible that NEMO exerts its anti-necrotic function in the necrosome. This would perhaps mean that the

hyperubiquitinated RIP1 found in CYLD deficient cells, results in enhanced recruitment of NEMO to the necrosome. The necrosomes formed in the absence of CYLD would therefore be different in composition due to higher levels of a negative regulator of necrosis. Ultimately, this may stifle necrosome functionality and account for the attenuated magnitude of necrosis in the absence of CYLD. Cells expressing CYLD would theoretically have functionally competent necrosomes due to removal of polyubiquitin chains from RIP1 leading to reduced recruitment of a negative regulator of necrosis.

Similar to NEMO, TAK1 was demonstrated to negatively regulate TNFα-induced necrosis through regulation of necrosome formation (Vanlangenakker et al., 2011). TAK1 binds to polyubiquitinated RIP1 via the ubiquitin binding proteins TAB2/3 (Kanayama et al., 2004). Although TAK1 was demonstrated to regulate necrosome formation it was not addressed whether it could exert its anti-necrotic function directly in the necrosome. Additionally, ABIN-1 (A20 binding and inhibitor of NFκB) is yet another potential candidate for being recruited to the necrosome and negatively regulating its functionality. It was demonstrated to inhibit TNFα-induced cell death through preventing FADD and Caspase-8 association, which is required for apoptosis. ABIN-1 contains a NEMO ubiquitin binding domain (NUB). It was shown that ABIN-1 binds to the apoptotic DISC through a NUB-mediated interaction with polyubiquitinated RIP1. ABIN-1 requires an intact NUB in order to negatively regulate cell death. Whether or not ABIN-1 similarly negatively regulates programmed necrosis has not been

determined, but it is possible that it could also bind to polyubiquitinated RIP1 within the necrosome (Oshima et al., 2009)

CYLD mediated deubiquitination of necrosome associated RIP1 may also promote the recruitment of positive regulators of necrosis. Recently, the mitochondrial phosphatase PGAM5S/L and MLKL were demonstrated to also be components of the necrosome, downstream substrates of RIP1/RIP3, and functionally required for TNFα-induced necrosis (Sun et al., 2011; Wang et al., 2012). It is conceivable that hyperubiquitinated RIP1, due to CYLD deficiency, could result in steric hindrance of the recruitment of these pro-necrotic proteins. Preliminary experiments suggest that during necrosis MLKL recruitment to RIP3 complexes is impaired in cells with CYLD knocked down. For a diagram of additional potential effects of hyperubiquitinated RIP1 refer to Figure 5.3.

In addition to demonstrating that CYLD regulates RIP1 ubiquitination within the necrosome, we also show that CYLD controls the expression level of components of the necrosome at later time-points during necrosis in the NP-40 soluble fraction. Although, our data indicates that some of the loss of expression can be accounted for by transition into the NP-40 insoluble fraction, loss of expression is still observed in cells directly lysed with SDS containing buffer. This suggests that components of the necrosome are degraded. It is unclear whether this degradation has any bearing on the necrosis signaling pathway, but it is attenuated in cells either lacking CYLD or with reduced expression. CYLD may promote the degradation of components of the necrosome either directly or indirectly.

One possibility is that CYLD may promote the degradation of RIP1 through removing K63 polyubiquitin chains, which are non-degrading chains and this may then allow for an associated E3 ligase to target RIP1 with K48 linked polyubiquitin chains, which act as degradation signals. This would be akin to a report that demonstrated a functional interaction between CYLD and the E3 ligase ITCH. In this report they showed that CYLD removes K63-linked polyubiquitin chains from TAK1, and the E3 ligase ITCH then tags TAK1 with K48-linked chains (Ahmed et al., 2011). However, it is difficult to reconcile this model with our finding that CYLD regulates NP-40 insoluble RIP1 ubiquitination. Given this model the expectation would be that in CYLD deficient cells there should be a greater accumulation of RIP1 within the NP-40 insoluble fraction as compared to cells expressing CYLD. This is due to the fact that K63-linked hyper-ubiquitinated RIP1 would be resistant to K48-linked polyubiquitination and degradation. Furthermore, our data indicates that CYLD does not regulate RIP1 ubiquitination within the NP-40 soluble fraction disfavoring the possibility that the impaired degradation in CYLD deficient cells is due to hyperubiquitinated K63-linked polyubiqutinated RIP1. It is also possible that decreased expression of necrosome components could be a consequence of necrosis rather than a cause of necrosis. Future studies should clarify whether the degradation of components of the necrosome influences the pro-necrotic signal.

Implications of CYLD phosphorylation

This thesis also provides evidence of mutual regulation between CYLD and RIP1. In addition to demonstrating CYLD-mediated RIP1 deubiqutination, we also demonstrate RIP1-dependent phosphorylation of CYLD. For the total cellular pool of CYLD, RIP1 kinase dependent phosphorylation was not detectable. We only observed phosphorylated CYLD when it was associated with RIP1 complexes during necrosis. This phosphorylation event was not blocked in CYLD deficient cells reconstituted with S418A CYLD. In overexpression studies, S418 phosphorylation was demonstrated to negatively regulate CYLD-mediated deubiquitination of its targets TRAF2 and NEMO (Hutti et al., 2009). This suggests that RIP1 mediates alternative CYLD phosphorylation events. Supporting this notion, we do not observe phosphorylated CYLD in RIP1 complexes during TNFR-1 complex formation, but we observe it after complex dissolution and during necrosome formation. Since we demonstrate that CYLD deubiquitinase activity is required for its pro-necrotic function, we suggest that this phosphorylation event may enhance the ability of CYLD to deubiquitinate RIP1. Theoretically this may provide a feed-forward mechanism where ubiquitinated RIP1 with weak kinase activity, promotes CYLD phosphorylation resulting in enhanced CYLD-mediated RIP1 deubiquitination. The denouement of this molecular interplay would be enhanced RIP1 autophosphorylation, enhanced kinase activation, and necrosis.

This work provides the inception of several avenues of fascinating research that is contingent upon first determining the functionality of this CYLD phosphorylation event. One avenue of interest is elucidating the mechanism for how phosphorylation of CYLD impacts its ability to deubiquitinate its targets. Several potential mechanisms are

possible. First, CYLD phosphorylation may directly enhance deubiquitinase activity through inducing a conformational change that may enhance active site binding of the transition state. Second, CYLD phosphorylation may alter the orientation between its active site and its substrate resulting in an optimal orientation for processing. Third, it may simply enhance binding with its substrate. Fourth, it may alter the binding of other factors, which influence the ubiquitination reaction. A specific example may be reduced binding of the antagonizing E3 ligase, which ubiquitinates the target protein thus driving the reaction more towards deubiquitination. As mentioned previously, a functional interaction between CYLD and the E3 ligase ITCH, has been reported (Ahmed et al., 2011).

Another potential avenue of interest for future research is determining the role of phosphatases in regulating CYLD activity and necrosis. Since phosphorylation of CYLD is emerging as a recurring theme of regulating the activity of CYLD, there is precedence for investigating potential phosphatases involved in this process. One report indicates that CYLD interacts with the phosphatase PP2A and the mitotic kinase Aurora-B. In this case CYLD promotes PP2A dephosphorylation and inhibition of Aurora-B kinase activity. This was independent of CYLD enzymatic activity (Sun et al., 2010). It is conceivable that PP2A also dephosphorylates CYLD thereby regulating TNFα induced cell death. There is a paucity of data involving the potential role of PP2A in TNFα-induced cell death. However, one report demonstrates that inhibition of PP2A impairs death receptor induced apoptosis (Harmala-Brasken et al., 2003). Naturally, phosphatases that remove inhibitory phosphate groups from CYLD would be predicted to have a pro-

necrotic function, as CYLD enzymatic activity is required in this context. Since the IKK mediated inhibitory phosphorylation of CYLD presumably takes place in the TNFR-1 complex, it is tempting to speculate that this accounts for the lack of CYLD-mediated RIP1 deubiquitination in this compartment (Reiley et al., 2005). Nevertheless, whether this phosphorylation event regulates the ability of CYLD to deubiquitinate RIP1 has not been formally tested. Conversely, phosphatases that remove activating phosphate groups from CYLD would be predicted to have an anti-necrotic function. Furthermore, phosphatase mediated regulation of the necrosis signaling pathway clearly extends beyond regulation of CYLD. Since the TNFα induced necrotic signaling program involves a cascade of phosphorylation events, there are multiple steps along the pathway where phosphatases have the opportunity to impart influence on necrosis.

Figure 5.1 Revised model for CYLD-mediated necrosis

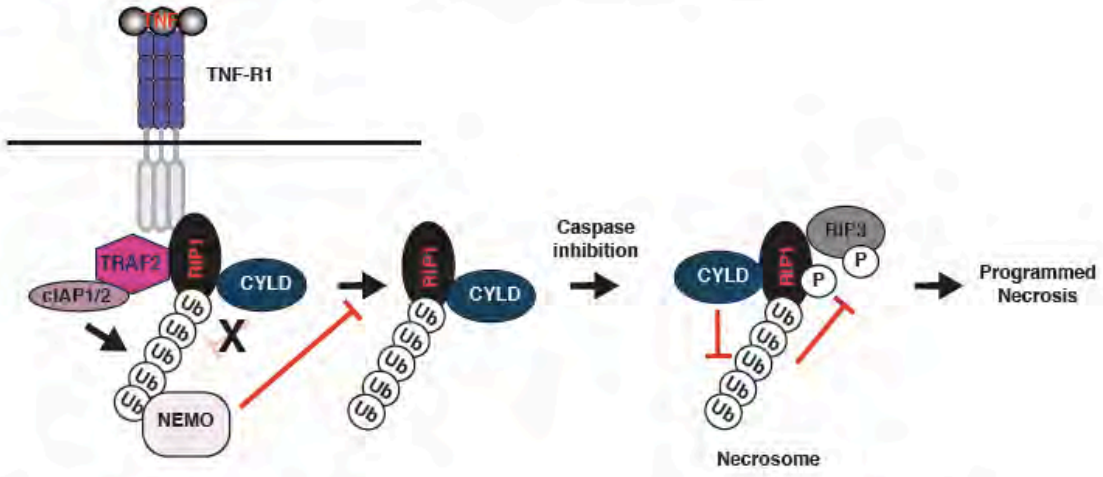

1) CYLD does not deubiquitinate RIP1 within the TNFR-1 complex and thereby promote RIP1 transition from Complex I to the necrosome

2) CYLD deubiquitinates RIP1 within the NP-40 insoluble fraction where the necrosome components are phosphorylated

Figure 5.2 Tentative model for overlapping pro-necrotic and pro-apoptotic function of CYLD

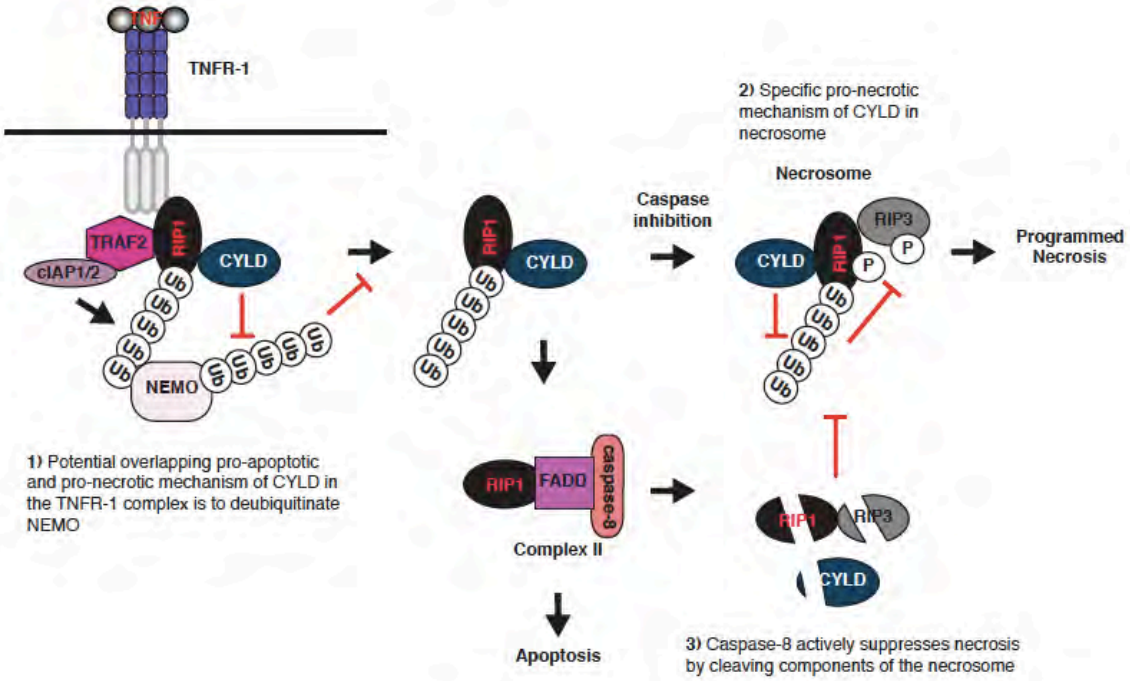

Figure 5.3 Potential impact of hyperubiquitinated RIP1

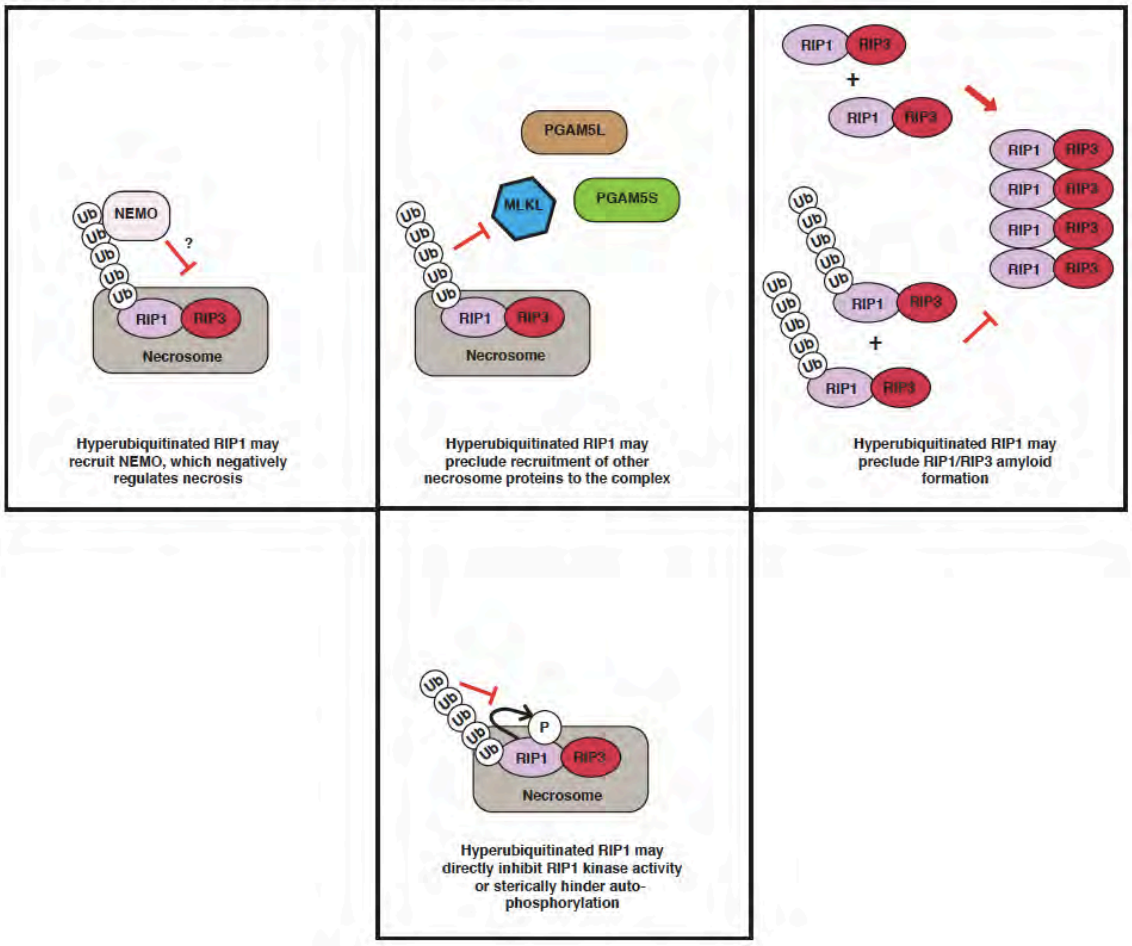

Figure 5.4 Potential effects of CYLD phosphorylation

1) Weak kinase

2) RIP1 phosphorylates CYLD possibly promoting CYLD-mediated RIP1 deubiquitination

3) Unmodified RIP1 is a better substrate for RIP1 autophosphorylation and activation

4A) RIP1 autophosphorylation promotes RIP3 activation and autophosphorylation

4B) In the absence of CYLD hyperubiquitinated RIP1 impairs RIP1 autophosphorylation and subsequent RIP3 kinase activation

Figure 5.5 Potential CYLD phosphorylation mechanism in the context of TNFR-1 signaling

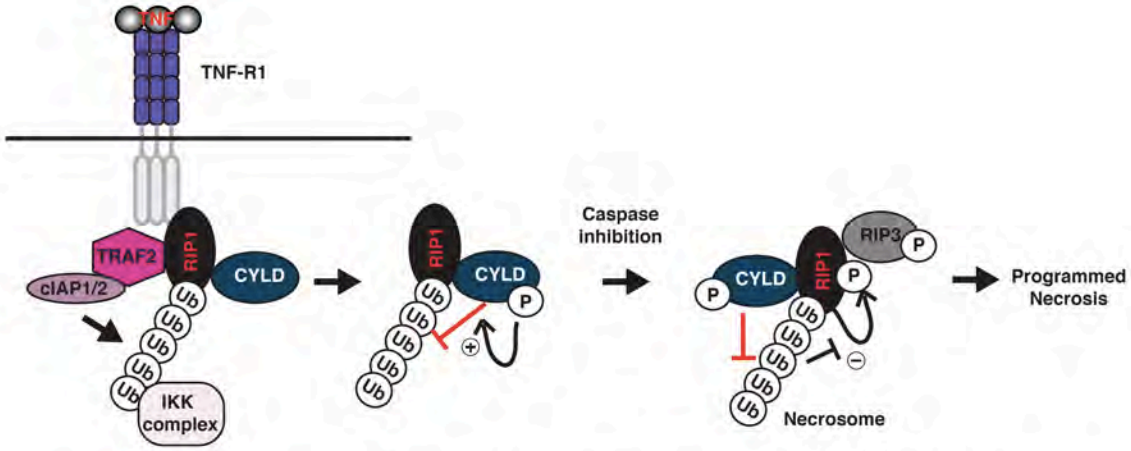

1) RIP1 dissociation from the TNFR-1 complex may liberate sufficient kinase activity to phosphorylate CYLD. Phosphorylation may then enhance its ability to deubiquitinate RIP1.

2) CYLD mediated RIP1 deubiquitination may enhance RIP1 autophosphorylation and subsequent necrosome activation.

PREFACE TO APPENDIX

List of author contributions:

David Moquin: conducted all the experiments.

Both David Moquin and Francis Chan designed experiments.

APPENDIX: Cancer gene siRNA library screen data

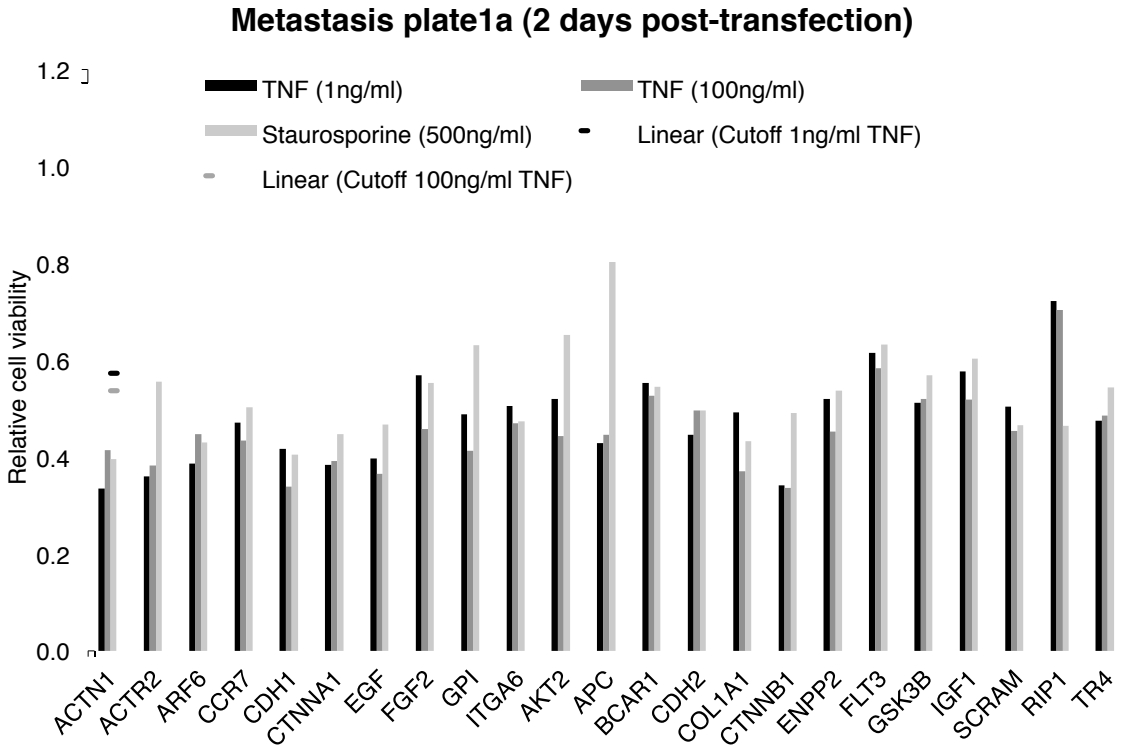
Metastasis plate1a (2 days post-transfection)
TNF (1ng/ml)
TNF (100ng/ml)
Staurosporine (500ng/ml)
Linear (Cutoff 1ng/ml TNF)
Linear (Cutoff 100ng/ml TNF)
Relative cell viability
1.2
1.0
0.8
0.6
0.4
0.2
0.0
ACTN1
ACTR2
ARF6
CCR7
CDH1
CTNNA1
EGF
FGF2
GPI
ITGA6
AKT2
APC
BCAR1
CDH2
COL1A1
CTNNB1
ENPP2
FLT3
GSK3B
IGF1
SCRAM
RIP1
TR4

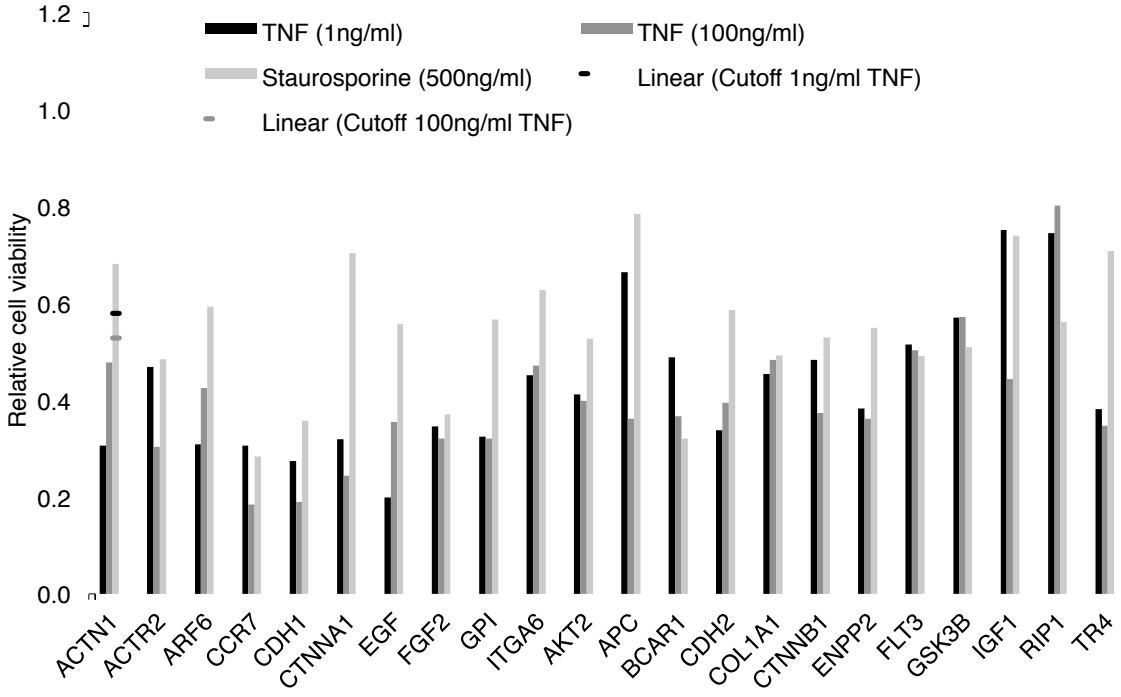
Metastasis plate1a (3 days post-transfection)
TNF (1ng/ml)
TNF (100ng/ml)
Staurosporine (500ng/ml)
Linear (Cutoff 1ng/ml TNF)
Linear (Cutoff 100ng/ml TNF)
Relative cell viability
1.2
1.0
0.8
0.6
0.4
0.2
0.0
ACTN1
ACTR2
ARF6
CCR7
CDH1
CTNNA1
EGF
FGF2
GPI
ITGA6
AKT2
APC
BCAR1
CDH2
COL1A1
CTNNB1
ENPP2
FLT3
GSK3B
IGF1
RIP1
TR4

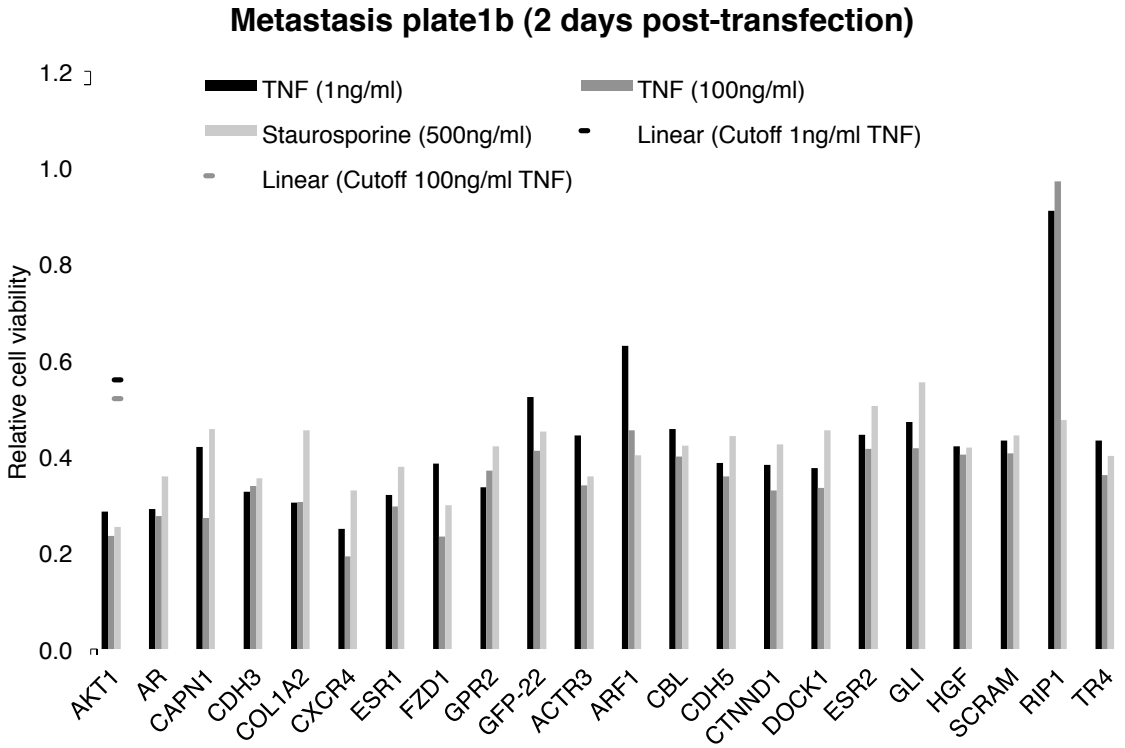
Metastasis plate1b (2 days post-transfection)
TNF (1ng/ml)
TNF (100ng/ml)
Staurosporine (500ng/ml)
Linear (Cutoff 1ng/ml TNF)
Linear (Cutoff 100ng/ml TNF)
Relative cell viability
1.2
1.0
0.8
0.6
0.4
0.2
0.0
AKT1
AR
CAPN1
CDH3
COL1A2
CXCR4
ESR1
FZD1
GPR2
GFP-22
ACTR3
ARF1
CBL
CDH5
CTNND1
DOCK1
ESR2
GLI
HGF
SCRAM
RIP1
TR4

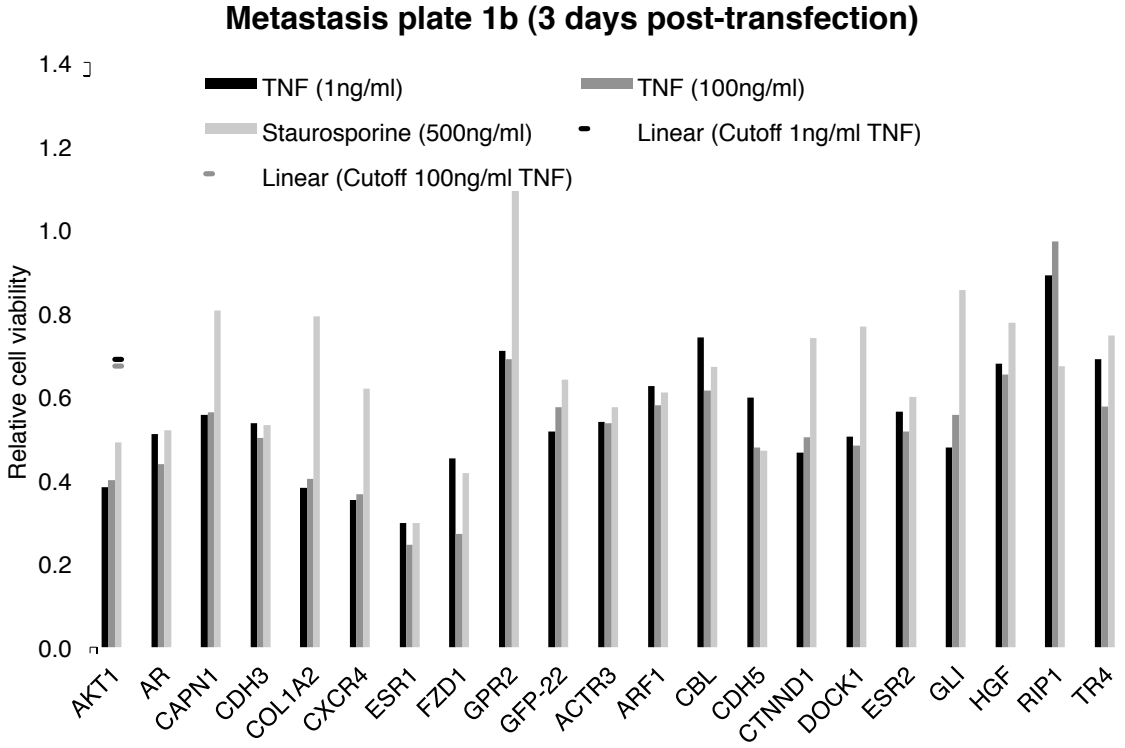
Metastasis plate 1b (3 days post-transfection)
TNF (1ng/ml)
TNF (100ng/ml)
Staurosporine (500ng/ml)
Linear (Cutoff 1ng/ml TNF)
Linear (Cutoff 100ng/ml TNF)
Relative cell viability
1.4
1.2
1.0
0.8
0.6
0.4
0.2
0.0
AKT1
AR
CAPN1
CDH3
COL1A2
CXCR4
ESR1
FZD1
GPR2
GFP-22
ACTR3
ARF1
CBL
CDH5
CTNND1
DOCK1
ESR2
GLI
HGF
RIP1
TR4

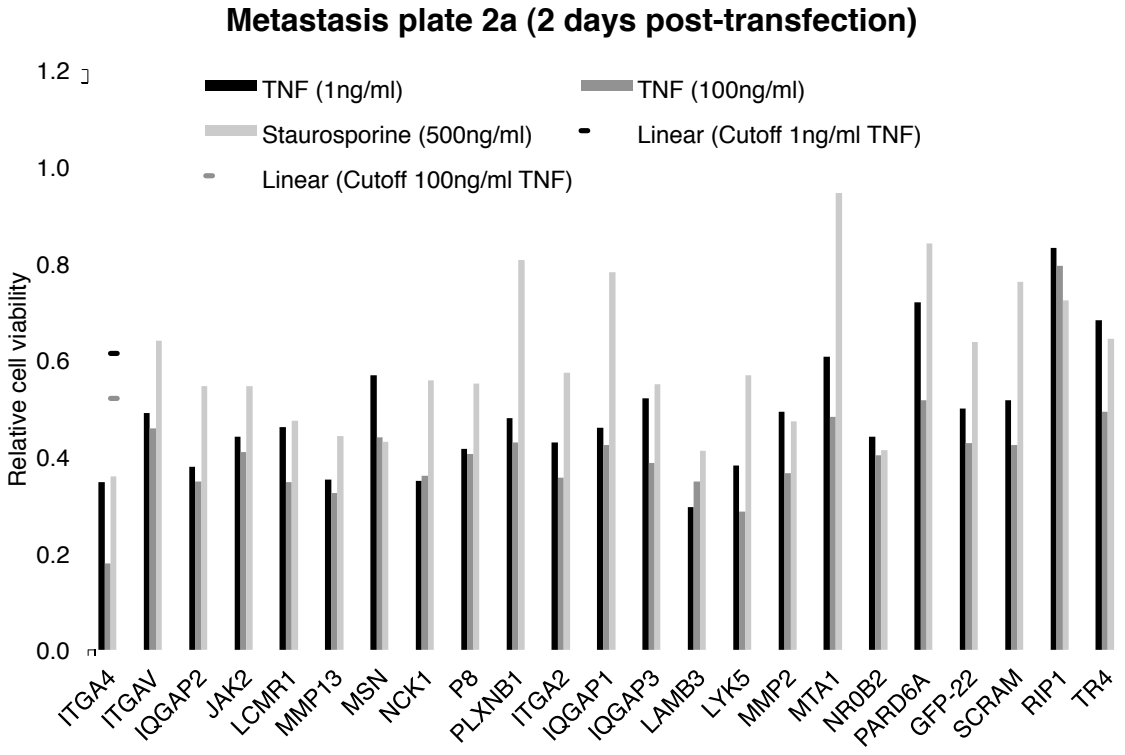
Metastasis plate 2a (2 days post-transfection)
TNF (1ng/ml)
TNF (100ng/ml)
Staurosporine (500ng/ml)
Linear (Cutoff 1ng/ml TNF)
Linear (Cutoff 100ng/ml TNF)
Relative cell viability
1.2
1.0
0.8
0.6
0.4
0.2
0.0
ITGA4
ITGAV
IQGAP2
JAK2
LCMR1
MMP13
MSN
NCK1
P8
PLXNB1
ITGA2
IQGAP1
IQGAP3
LAMB3
LYK5
MMP2
MTA1
NR0B2
PARD6A
GFP-22
SCRAM
RIP1
TR4

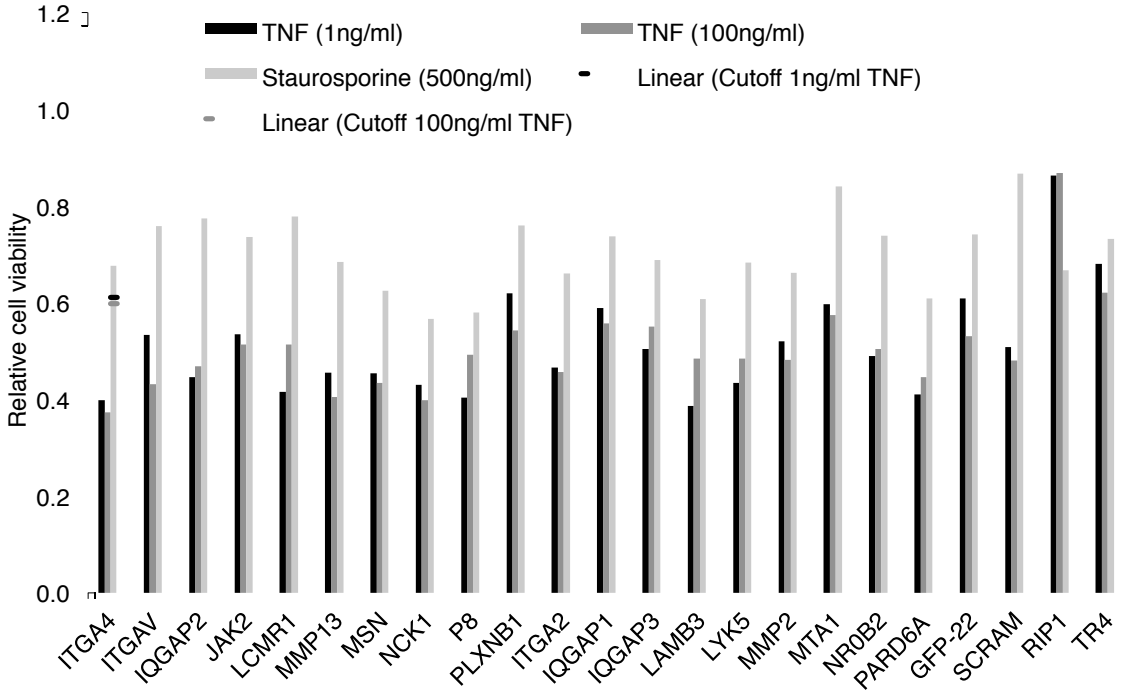
Metastasis plate2a (3 days post-transfection)
TNF (1ng/ml)
TNF (100ng/ml)
Staurosporine (500ng/ml)
Linear (Cutoff 1ng/ml TNF)
Linear (Cutoff 100ng/ml TNF)
Relative cell viability
1.2
1.0
0.8
0.6
0.4
0.2
0.0
ITGA4
ITGAV
IQGAP2
JAK2
LCMR1
MMP13
MSN
NCK1
P8
PLXNB1
ITGA2
IQGAP1
IQGAP3
LAMB3
LYK5
MMP2
MTA1
NR0B2
PARD6A
GFP-22
SCRAM
RIP1
TR4

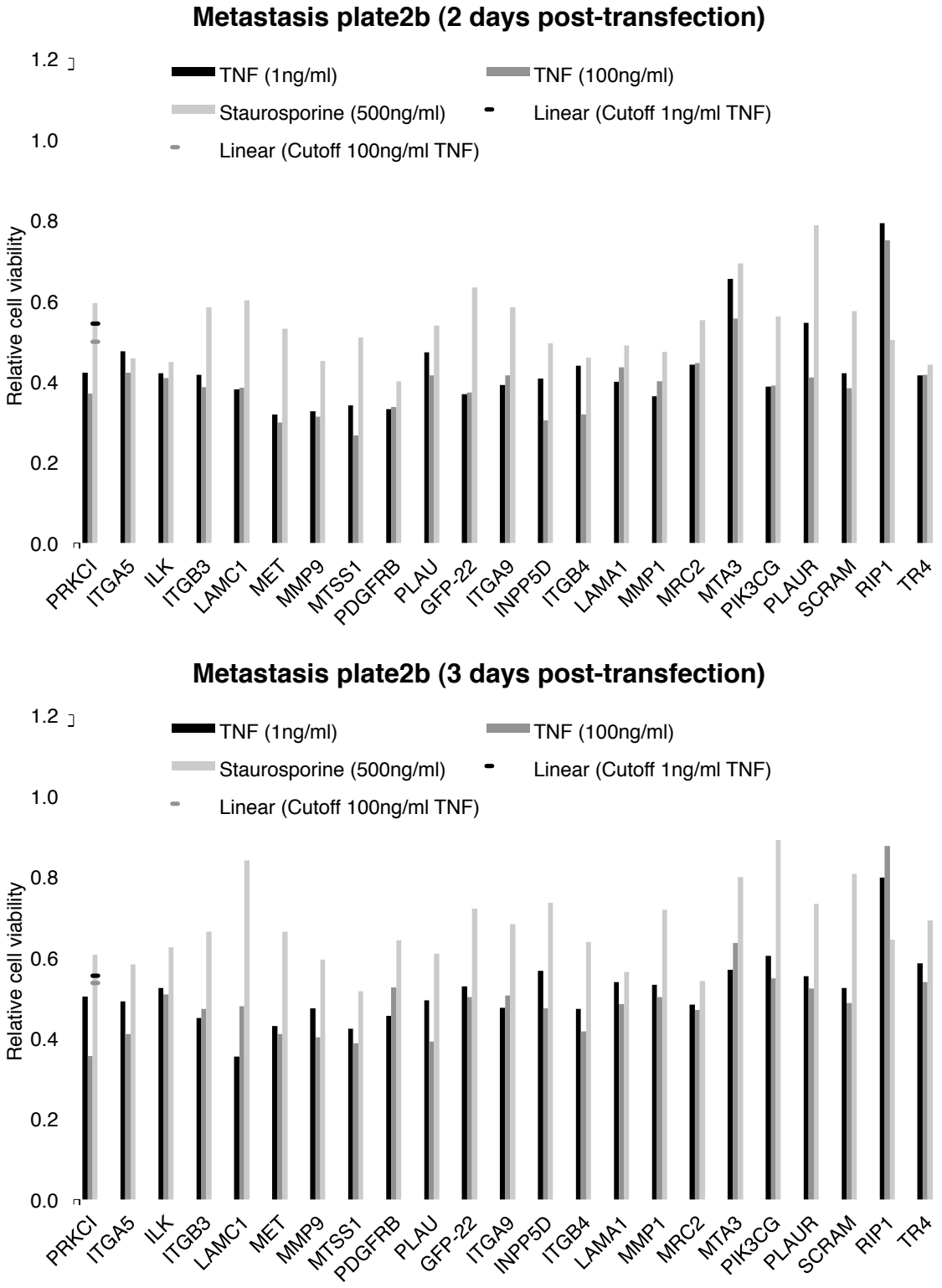
Metastasis plate2b (2 days post-transfection)
TNF (1ng/ml)
TNF (100ng/ml)
Staurosporine (500ng/ml)
Linear (Cutoff 1ng/ml TNF)
Linear (Cutoff 100ng/ml TNF)
Relative cell viability
1.2
1.0
0.8
0.6
0.4
0.2
0.0
PRKCI
ITGA5
ILK
ITGB3
LAMC1
MET
MMP9
MTSS1
PDGFRB
PLAU
GFP-22
ITGA9
INPP5D
ITGB4
LAMA1
MMP1
MRC2
MTA3
PIK3CG
PLAUR
SCRAM
RIP1
TR4
Metastasis plate2b (3 days post-transfection)
TNF (1ng/ml)
TNF (100ng/ml)
Staurosporine (500ng/ml)
Linear (Cutoff 1ng/ml TNF)
Linear (Cutoff 100ng/ml TNF)
Relative cell viability
1.2
1.0
0.8
0.6
0.4
0.2
0.0
PRKCI
ITGA5
ILK
ITGB3
LAMC1
MET
MMP9
MTSS1
PDGFRB
PLAU
GFP-22
ITGA9
INPP5D
ITGB4
LAMA1
MMP1
MRC2
MTA3
PIK3CG
PLAUR
SCRAM
RIP1
TR4

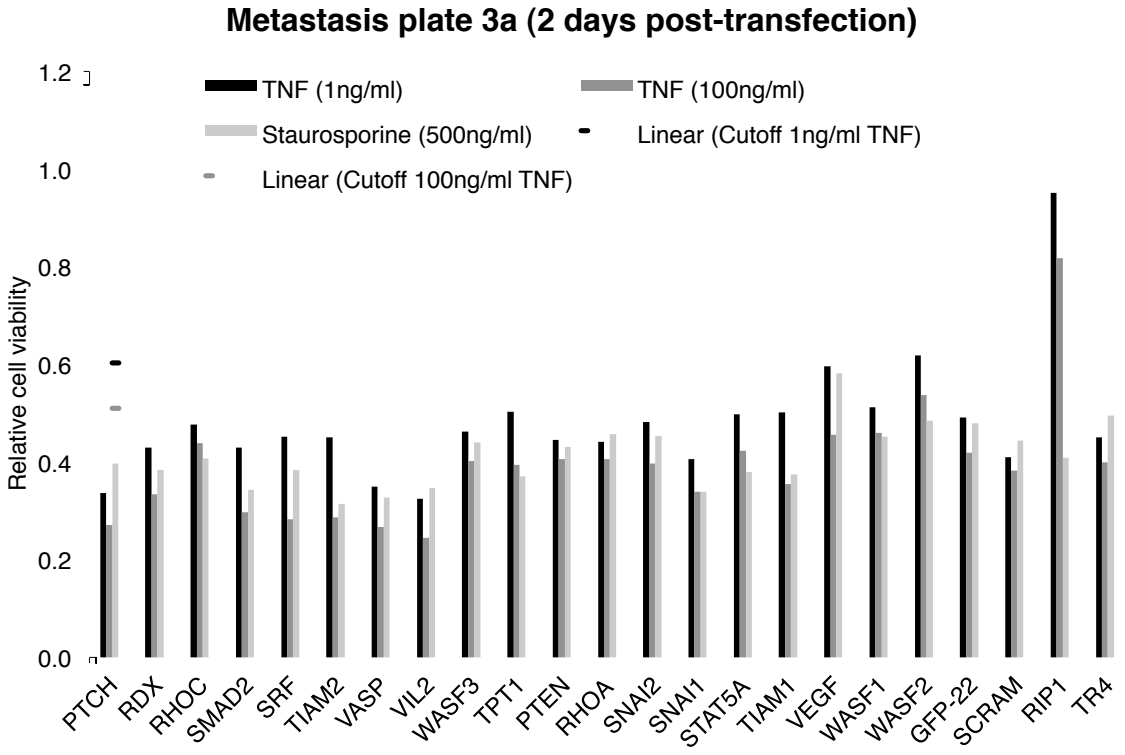
Metastasis plate 3a (2 days post-transfection)
TNF (1ng/ml)
TNF (100ng/ml)
Staurosporine (500ng/ml)
Linear (Cutoff 1ng/ml TNF)
Linear (Cutoff 100ng/ml TNF)
Relative cell viability
1.2
1.0
0.8
0.6
0.4
0.2
0.0
PTCH
RDX
RHOC
SMAD2
SRF
TIAM2
VASP
VIL2
WASF3
TPT1
PTEN
RHOA
SNAI2
SNAI1
STAT5A
TIAM1
VEGF
WASF1
WASF2
GFP-22
SCRAM
RIP1
TR4

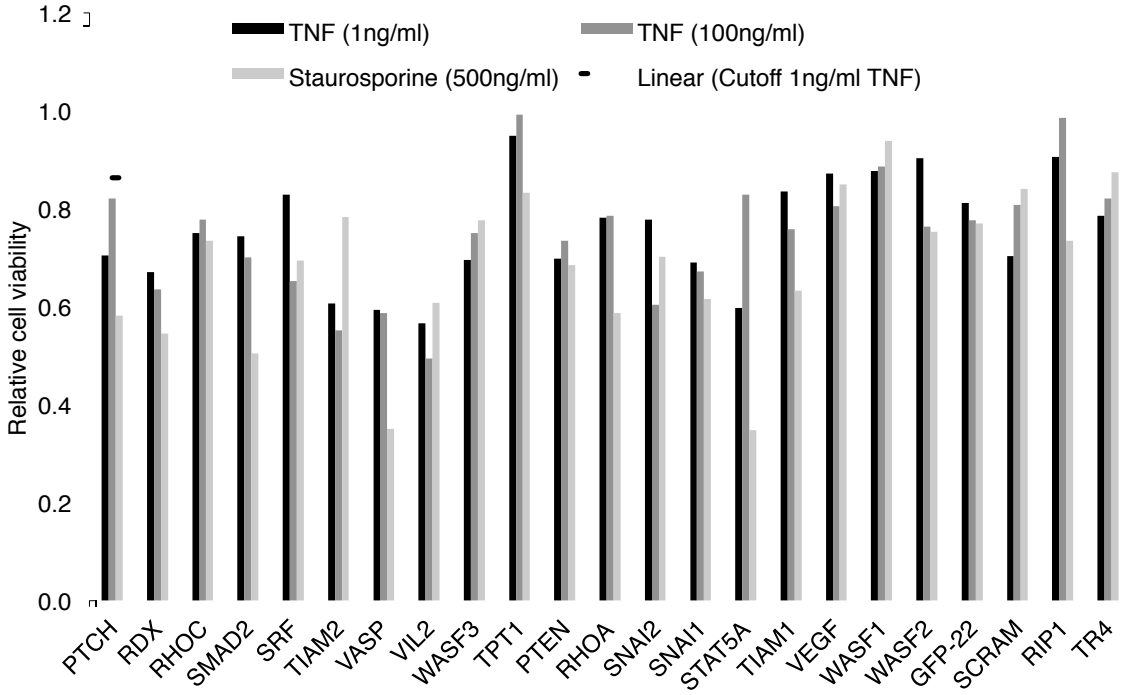
Metastasis plate 3a (3 days post-transfection)
TNF (1ng/ml)
TNF (100ng/ml)
Staurosporine (500ng/ml)
Linear (Cutoff 1ng/ml TNF)
Relative cell viability
1.2
1.0
0.8
0.6
0.4
0.2
0.0
PTCH
RDX
RHOC
SMAD2
SRF
TIAM2
VASP
VIL2
WASF3
TPT1
PTEN
RHOA
SNAI2
SNAI1
STAT5A
TIAM1
VEGF
WASF1
WASF2
GFP-22
SCRAM
RIP1
TR4

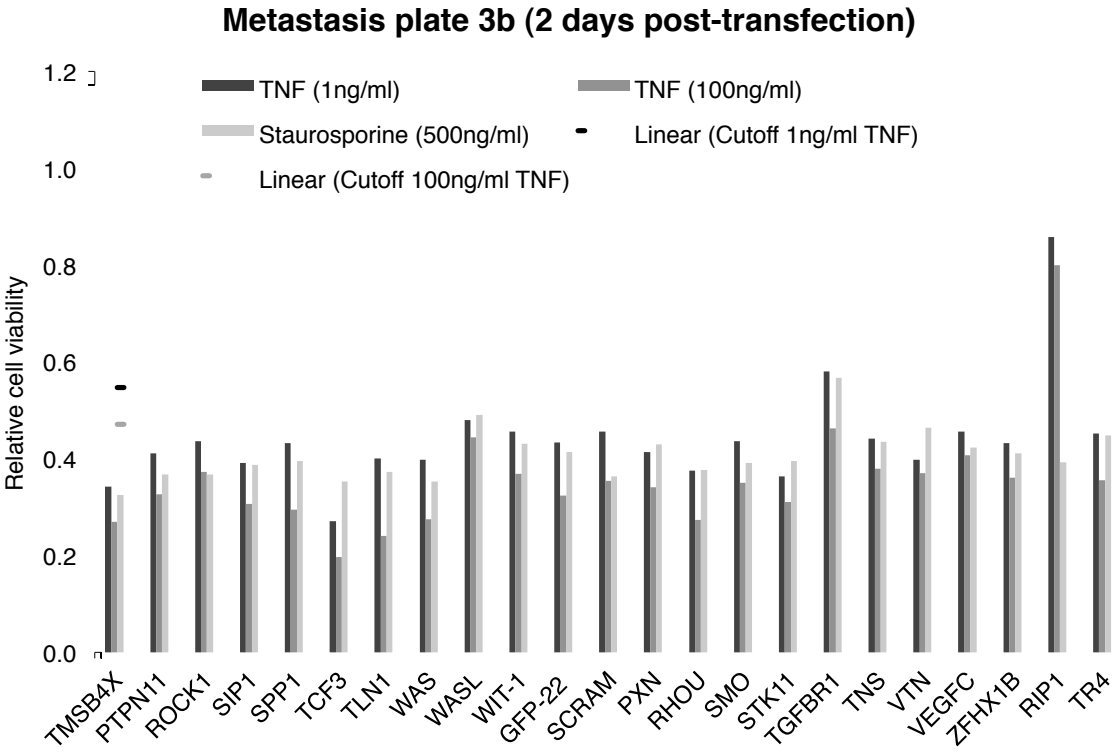
Metastasis plate 3b (2 days post-transfection)
TNF (1ng/ml)
TNF (100ng/ml)
Staurosporine (500ng/ml)
Linear (Cutoff 1ng/ml TNF)
Linear (Cutoff 100ng/ml TNF)
Relative cell viability
1.2
1.0
0.8
0.6
0.4
0.2
0.0
TMSB4X
PTPN11
ROCK1
SIP1
SPP1
TCF3
TLN1
WAS
WASL
WIT-1
GFP-22
SCRAM
PXN
RHOU
SMO
STK11
TGFBR1
TNS
VTN
VEGFC
ZFHX1B
RIP1
TR4

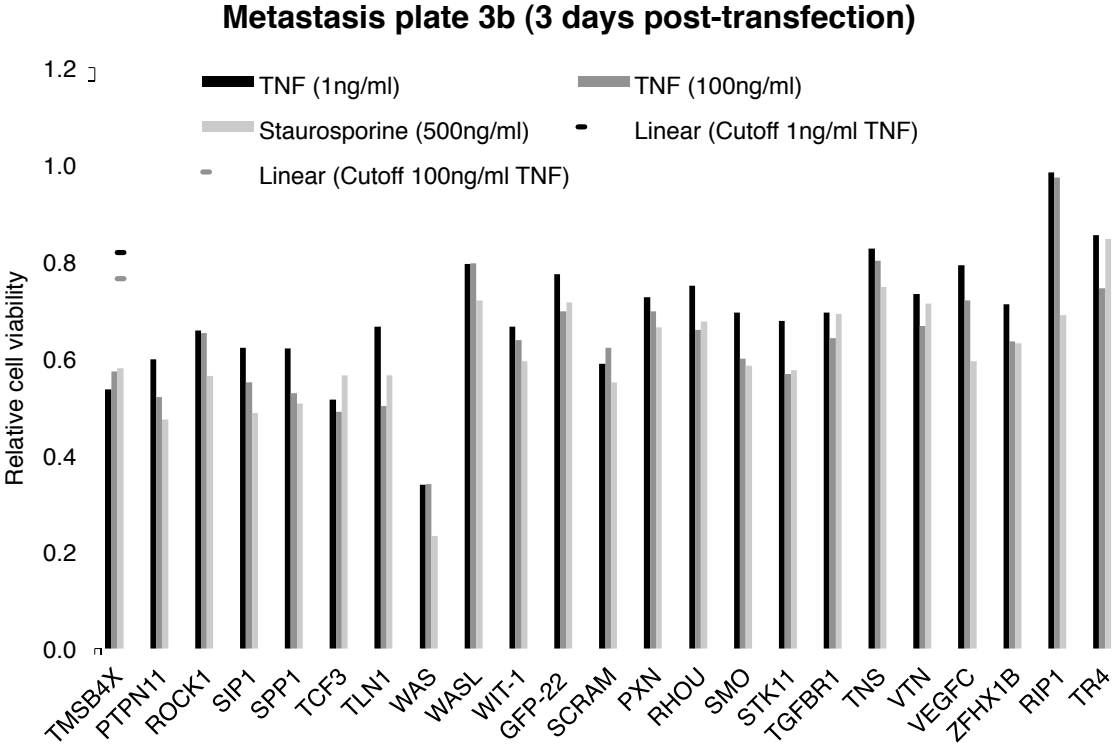
Metastasis plate 3b (3 days post-transfection)
TNF (1ng/ml)
TNF (100ng/ml)
Staurosporine (500ng/ml)
Linear (Cutoff 1ng/ml TNF)
Linear (Cutoff 100ng/ml TNF)
Relative cell viability
1.2
1.0
0.8
0.6
0.4
0.2
0.0
TMSB4X
PTPN11
ROCK1
SIP1
SPP1
TCF3
TLN1
WAS
WASL
WIT-1
GFP-22
SCRAM
PXN
RHOU
SMO
STK11
TGFBR1
TNS
VTN
VEGFC
ZFHX1B
RIP1
TR4

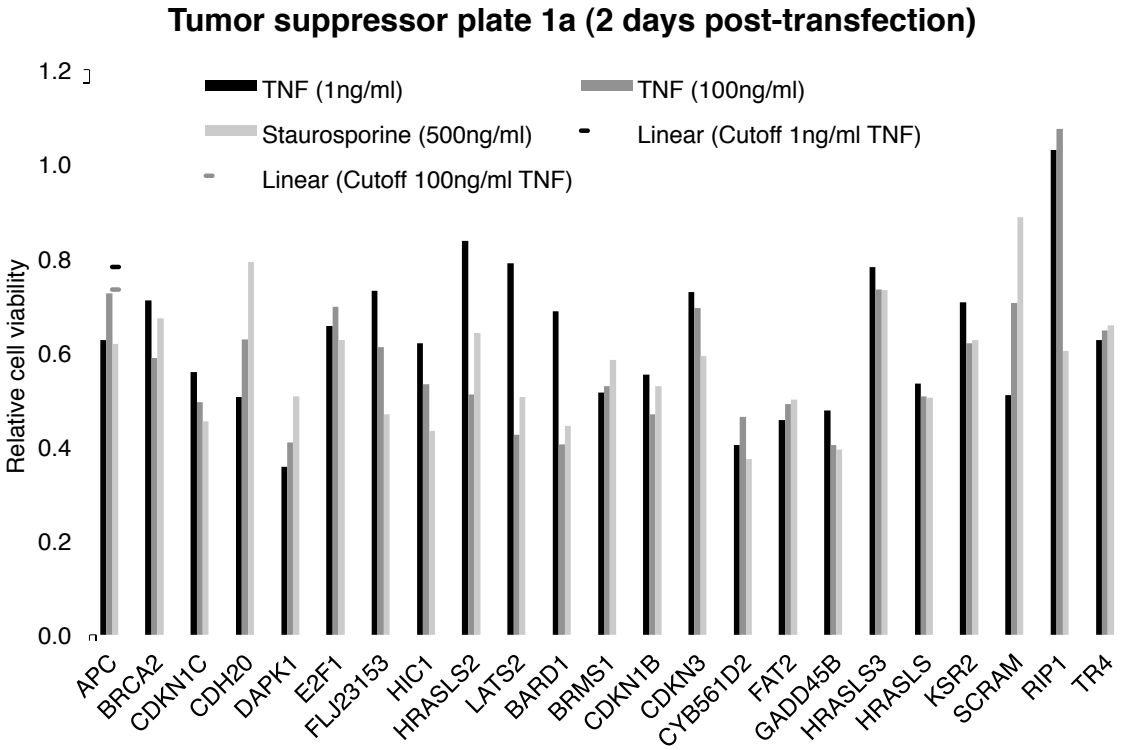
Tumor suppressor plate 1a (2 days post-transfection)
TNF (1ng/ml)
TNF (100ng/ml)
Staurosporine (500ng/ml)
Linear (Cutoff 1ng/ml TNF)
Linear (Cutoff 100ng/ml TNF)
Relative cell viability
1.2
1.0
0.8
0.6
0.4
0.2
0.0
APC
BRCA2
CDKN1C
CDH20
DAPK1
E2F1
FLJ23153
HIC1
HRASLS2
LATS2
BARD1
BRMS1
CDKN1B
CDKN3
CYB561D2
FAT2
GADD45B
HRASLS3
HRASLS
KSR2
SCRAM
RIP1
TR4

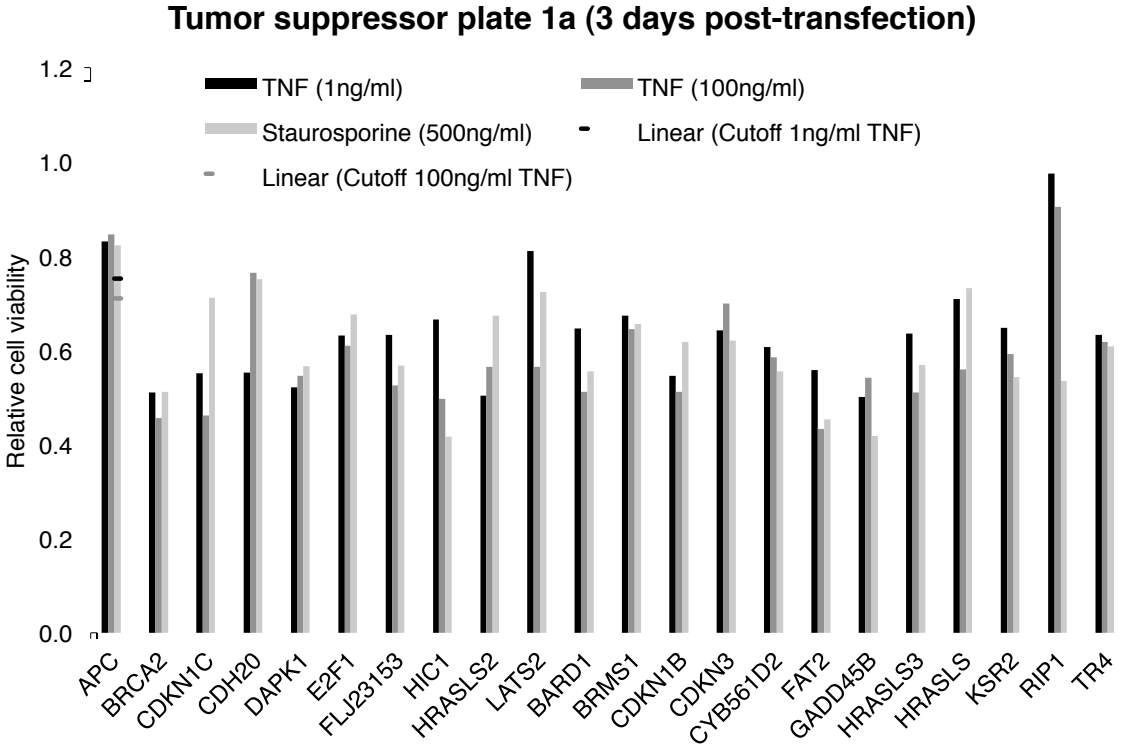
Tumor suppressor plate 1a (3 days post-transfection)
TNF (1ng/ml)
TNF (100ng/ml)
Staurosporine (500ng/ml)
Linear (Cutoff 1ng/ml TNF)
Linear (Cutoff 100ng/ml TNF)
Relative cell viability
1.2
1.0
0.8
0.6
0.4
0.2
0.0
APC
BRCA2
CDKN1C
CDH20
DAPK1
E2F1
FLJ23153
HIC1
HRASLS2
LATS2
BARD1
BRMS1
CDKN1B
CDKN3
CYB561D2
FAT2
GADD45B
HRASLS3
HRASLS
KSR2
RIP1
TR4

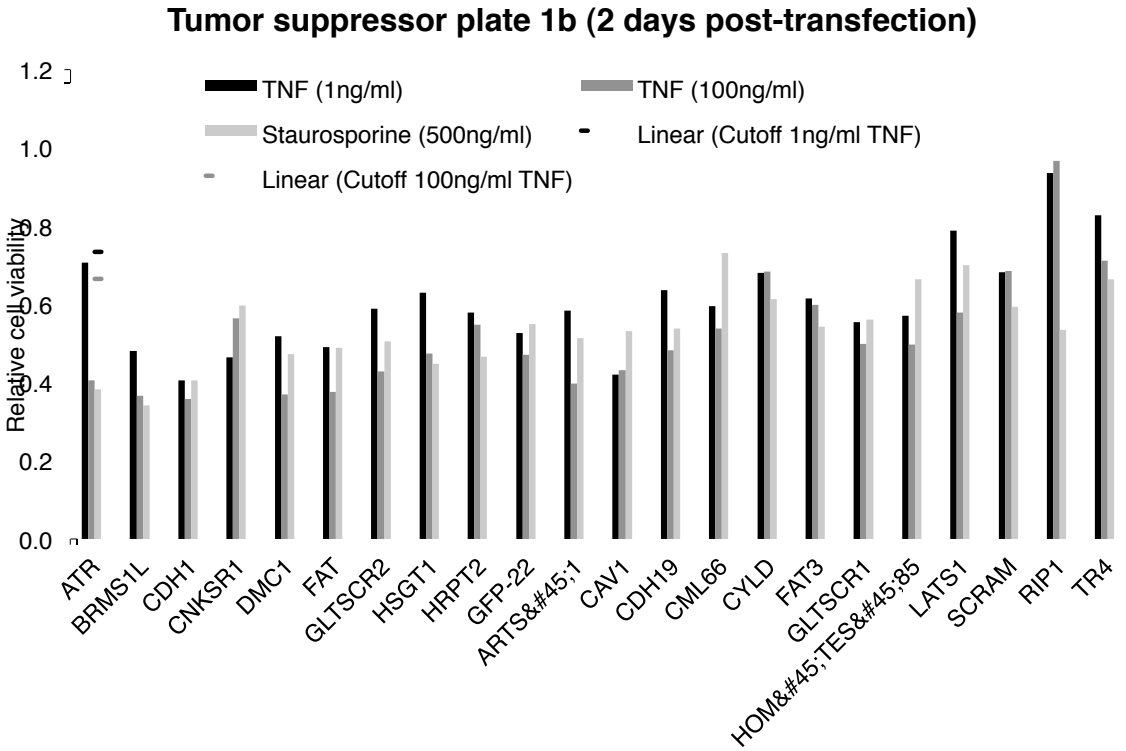
Tumor suppressor plate 1b (2 days post-transfection)
TNF (1ng/ml)
TNF (100ng/ml)
Staurosporine (500ng/ml)
Linear (Cutoff 1ng/ml TNF)
Linear (Cutoff 100ng/ml TNF)
Relative cell viability
1.2
1.0
0.8
0.6
0.4
0.2
0.0
ATR
BRMS1L
CDH1
CNKSR1
DMC1
FAT
GLTSCR2
HSGT1
HRPT2
GFP-22
ARTS-1
CAV1
CDH19
CML66
CYLD
FAT3
GLTSCR1
HOM-TES-85
LATS1
SCRAM
RIP1
TR4

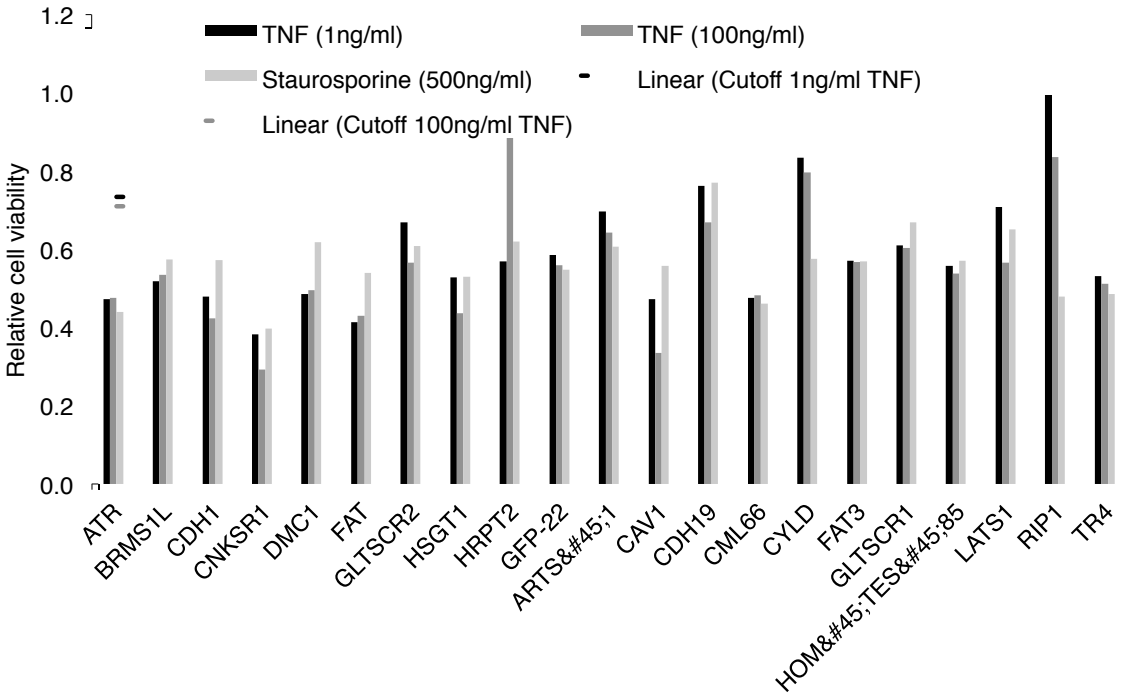
Tumor suppressor plate 1b (3 days post-transfection)
TNF (1ng/ml)
TNF (100ng/ml)
Staurosporine (500ng/ml)
Linear (Cutoff 1ng/ml TNF)
Linear (Cutoff 100ng/ml TNF)
Relative cell viability
1.2
1.0
0.8
0.6
0.4
0.2
0.0
ATR
BRMS1L
CDH1
CNKSR1
DMC1
FAT
GLTSCR2
HSGT1
HRPT2
GFP-22
ARTS-1
CAV1
CDH19
CML66
CYLD
FAT3
GLTSCR1
HOM-TES-85
LATS1
RIP1
TR4

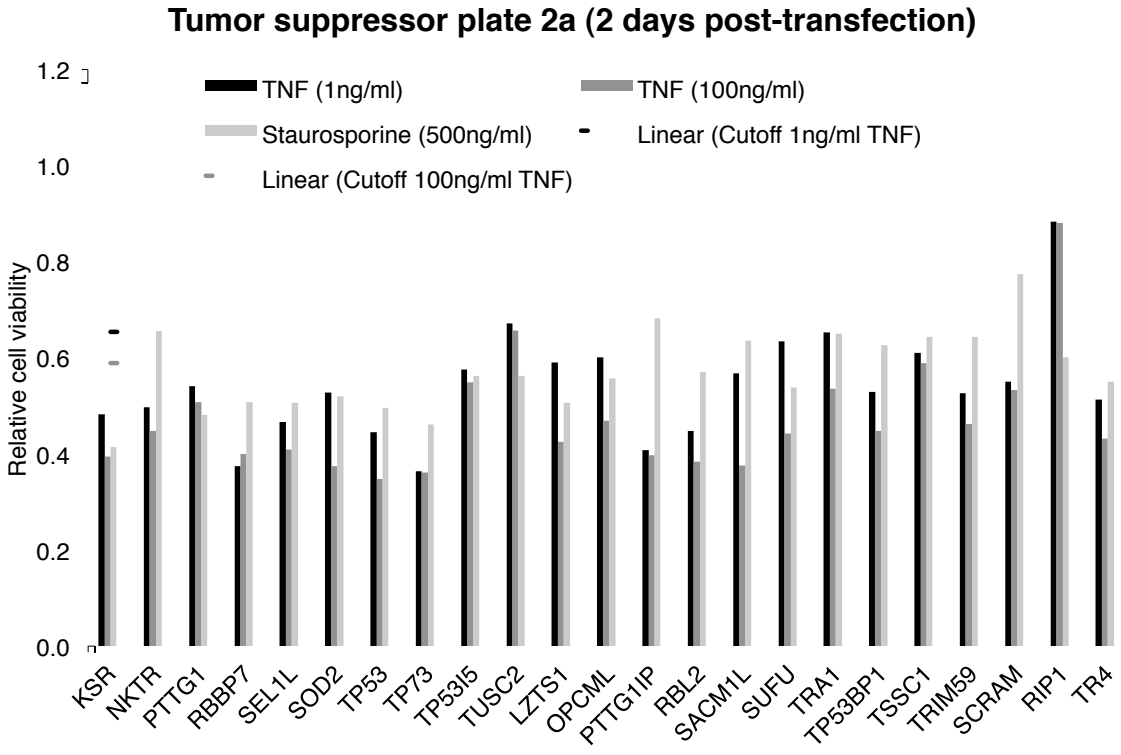
Tumor suppressor plate 2a (2 days post-transfection)
TNF (1ng/ml)
TNF (100ng/ml)
Staurosporine (500ng/ml)
Linear (Cutoff 1ng/ml TNF)
Linear (Cutoff 100ng/ml TNF)
Relative cell viability
1.2
1.0
0.8
0.6
0.4
0.2
0.0
KSR
NKTR
PTTG1
RBBP7
SEL1L
SOD2
TP53
TP73
TP53I5
TUSC2
LZTS1
OPCML
PTTG1IP
RBL2
SACM1L
SUFU
TRA1
TP53BP1
TSSC1
TRIM59
SCRAM
RIP1
TR4

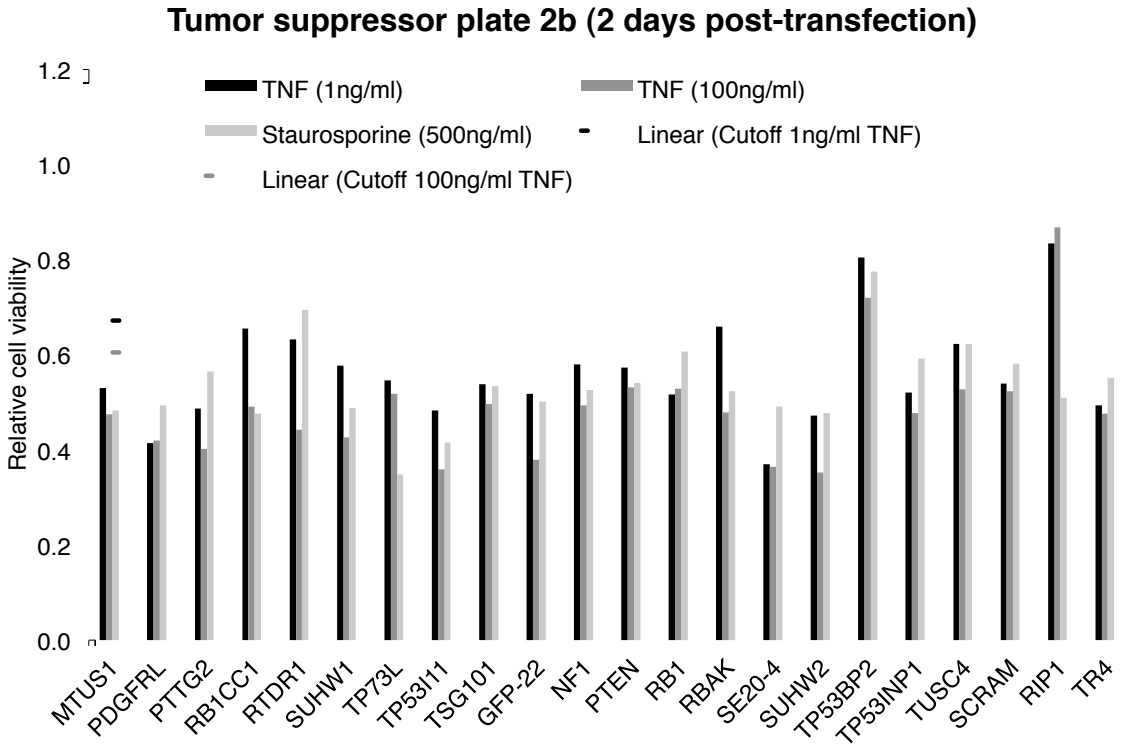
Tumor suppressor plate 2b (2 days post-transfection)
TNF (1ng/ml)
TNF (100ng/ml)
Staurosporine (500ng/ml)
Linear (Cutoff 1ng/ml TNF)
Linear (Cutoff 100ng/ml TNF)
Relative cell viability
1.2
1.0
0.8
0.6
0.4
0.2
0.0
MTUS1
PDGFRL
PTTG2
RB1CC1
RTDR1
SUHW1
TP73L
TP53I11
TSG101
GFP-22
NF1
PTEN
RB1
RBAK
SE20-4
SUHW2
TP53BP2
TP53INP1
TUSC4
SCRAM
RIP1
TR4

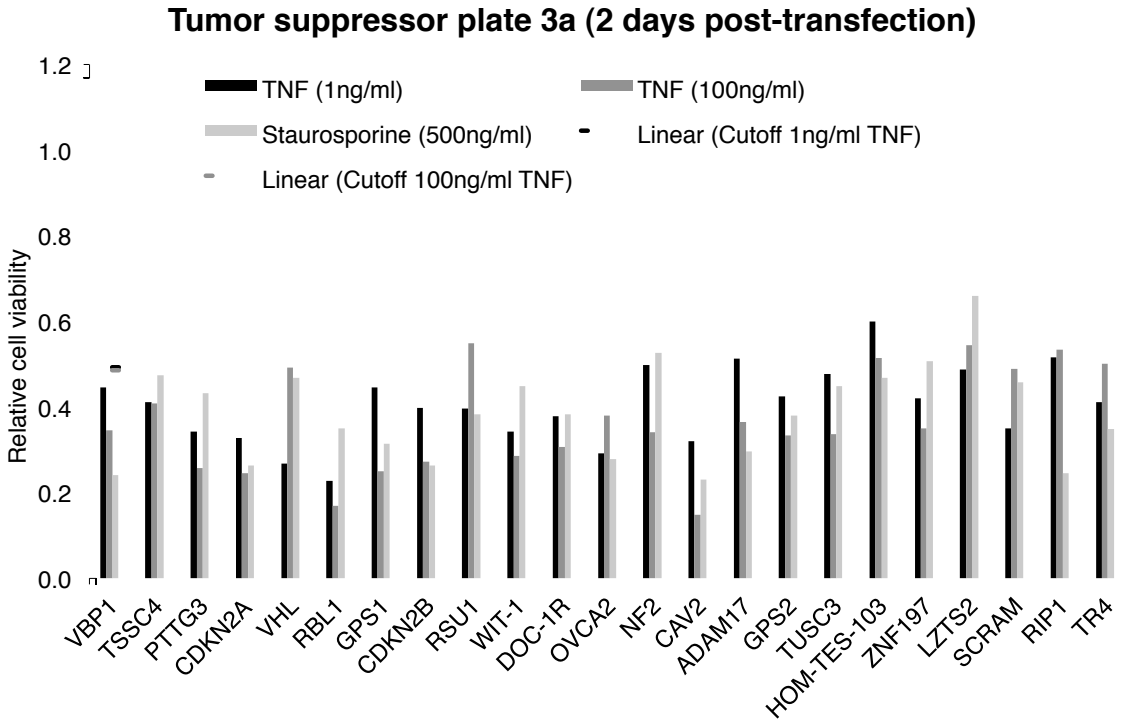
Tumor suppressor plate 3a (2 days post-transfection)
TNF (1ng/ml)
TNF (100ng/ml)
Staurosporine (500ng/ml)
Linear (Cutoff 1ng/ml TNF)
Linear (Cutoff 100ng/ml TNF)
Relative cell viability
1.2
1.0
0.8
0.6
0.4
0.2
0.0
VBP1
TSSC4
PTTG3
CDKN2A
VHL
RBL1
GPS1
CDKN2B
RSU1
WIT-1
DOC-1R
OVCA2
NF2
CAV2
ADAM17
GPS2
TUSC3
HOM-TES-103
ZNF197
LZTS2
SCRAM
RIP1
TR4

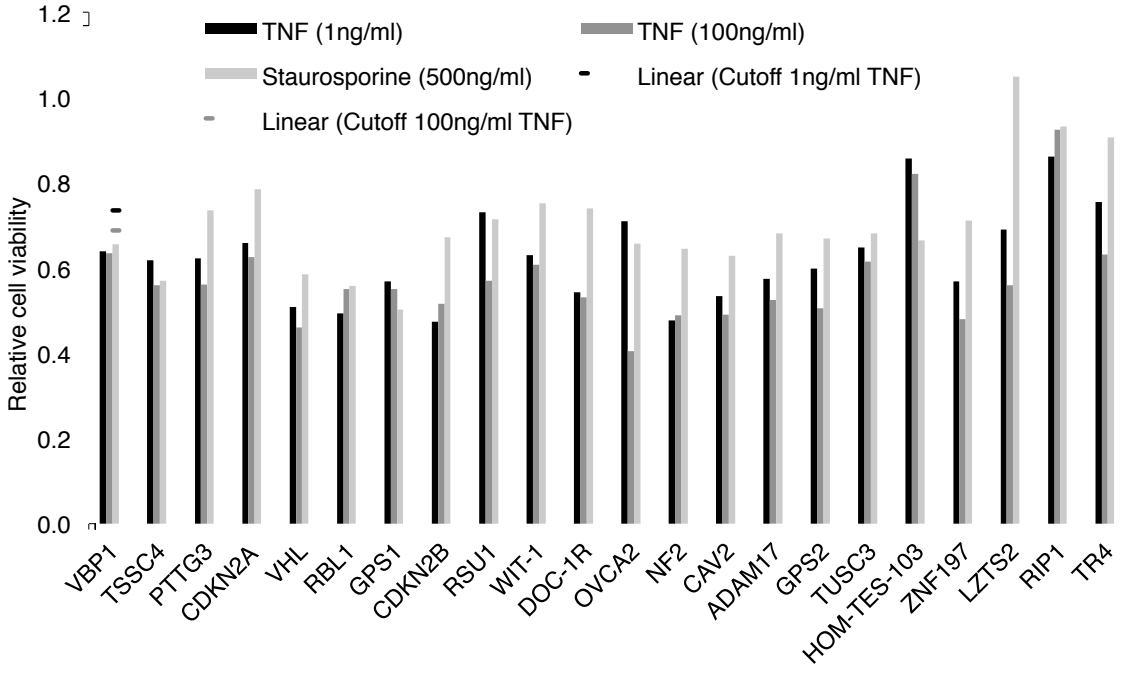
Tumor suppressor plate 3a (3 days post-transfection)
TNF (1ng/ml)
TNF (100ng/ml)
Staurosporine (500ng/ml)
Linear (Cutoff 1ng/ml TNF)
Linear (Cutoff 100ng/ml TNF)
Relative cell viability
1.2
1.0
0.8
0.6
0.4
0.2
0.0
VBP1
TSSC4
PTTG3
CDKN2A
VHL
RBL1
GPS1
CDKN2B
RSU1
WIT-1
DOC-1R
OVCA2
NF2
CAV2
ADAM17
GPS2
TUSC3
HOM-TES-103
ZNF197
LZTS2
RIP1
TR4

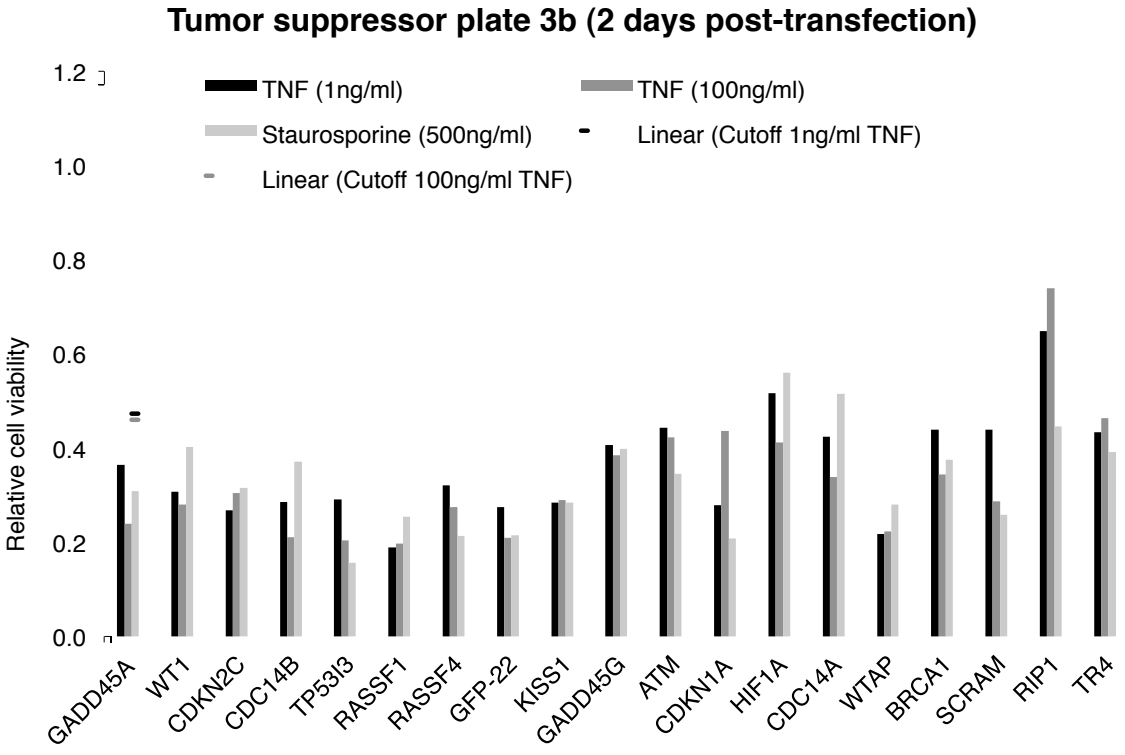
Tumor suppressor plate 3b (2 days post-transfection)
TNF (1ng/ml)
TNF (100ng/ml)
Staurosporine (500ng/ml)
Linear (Cutoff 1ng/ml TNF)
Linear (Cutoff 100ng/ml TNF)
Relative cell viability
1.2
1.0
0.8
0.6
0.4
0.2
0.0
GADD45A
WT1
CDKN2C
CDC14B
TP53I3
RASSF1
RASSF4
GFP-22
KISS1
GADD45G
ATM
CDKN1A
HIF1A
CDC14A
WTAP
BRCA1
SCRAM
RIP1
TR4

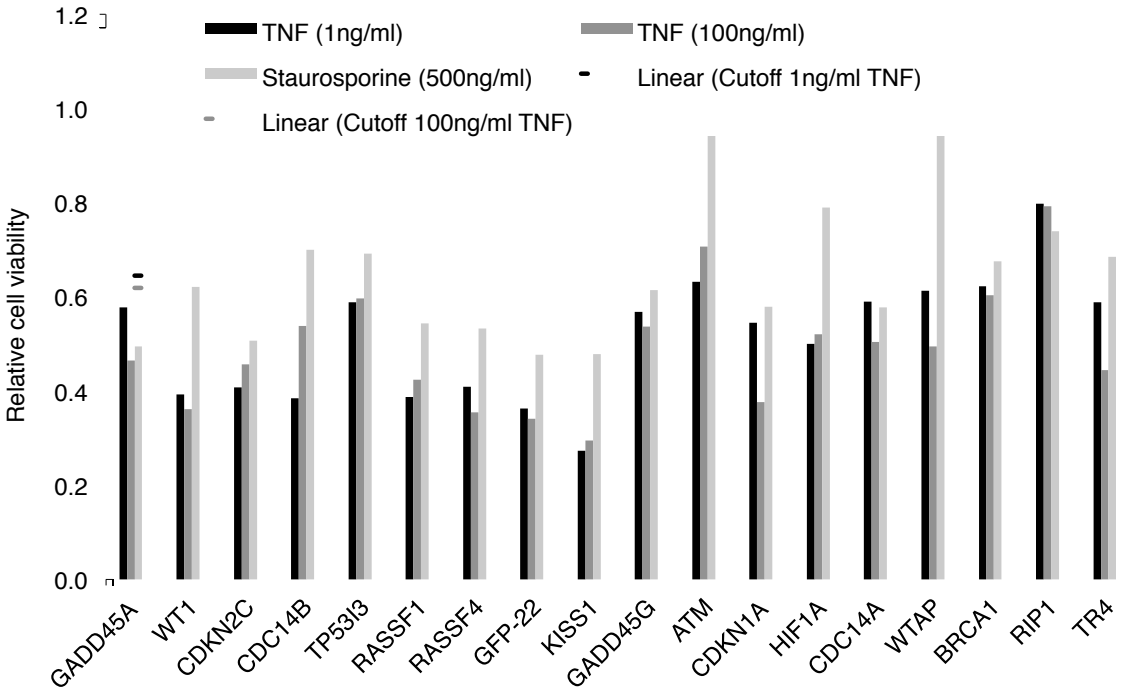
Tumor suppressor plate 3b (3 days post-transfection)
TNF (1ng/ml)
TNF (100ng/ml)
Staurosporine (500ng/ml)
Linear (Cutoff 1ng/ml TNF)
Linear (Cutoff 100ng/ml TNF)
Relative cell viability
1.2
1.0
0.8
0.6
0.4
0.2
0.0
GADD45A
WT1
CDKN2C
CDC14B
TP53I3
RASSF1
RASSF4
GFP-22
KISS1
GADD45G
ATM
CDKN1A
HIF1A
CDC14A
WTAP
BRCA1
RIP1
TR4

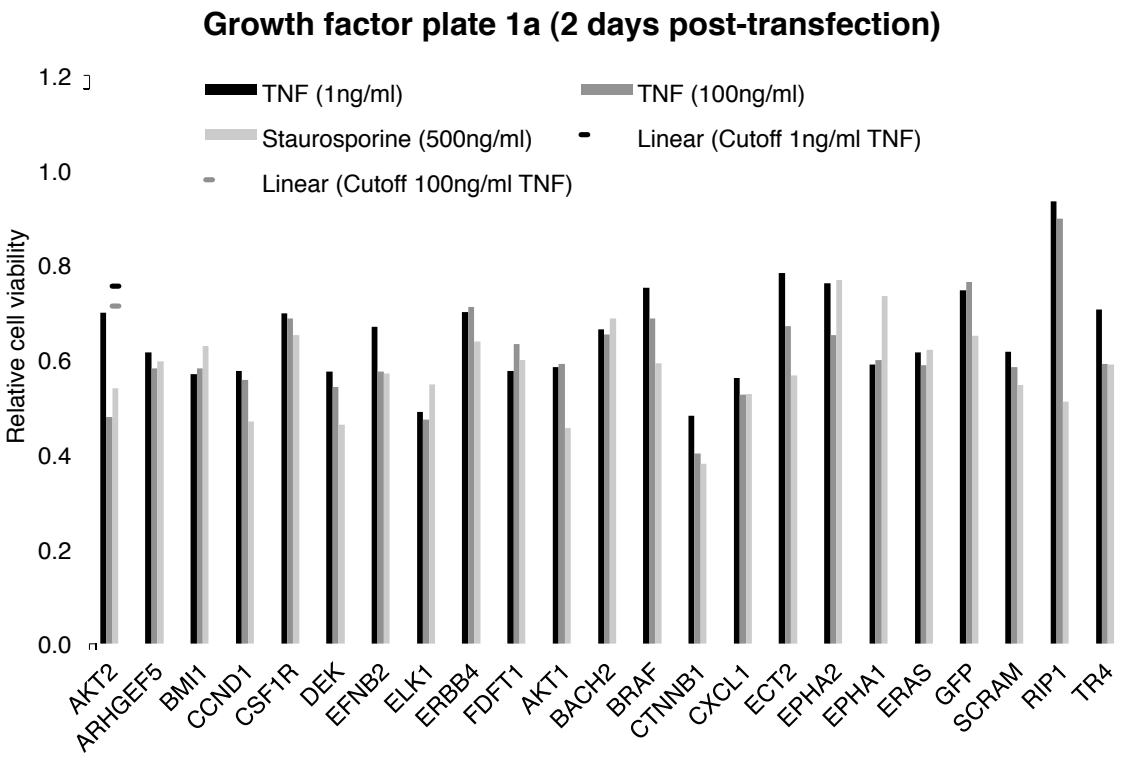
Growth factor plate 1a (2 days post-transfection)
TNF (1ng/ml)
TNF (100ng/ml)
Staurosporine (500ng/ml)
Linear (Cutoff 1ng/ml TNF)
Linear (Cutoff 100ng/ml TNF)
Relative cell viability
1.2
1.0
0.8
0.6
0.4
0.2
0.0
AKT2
ARHGEF5
BMI1
CCND1
CSF1R
DEK
EFNB2
ELK1
ERBB4
FDFT1
AKT1
BACH2
BRAF
CTNNB1
CXCL1
ECT2
EPHA2
EPHA1
ERAS
GFP
SCRAM
RIP1
TR4

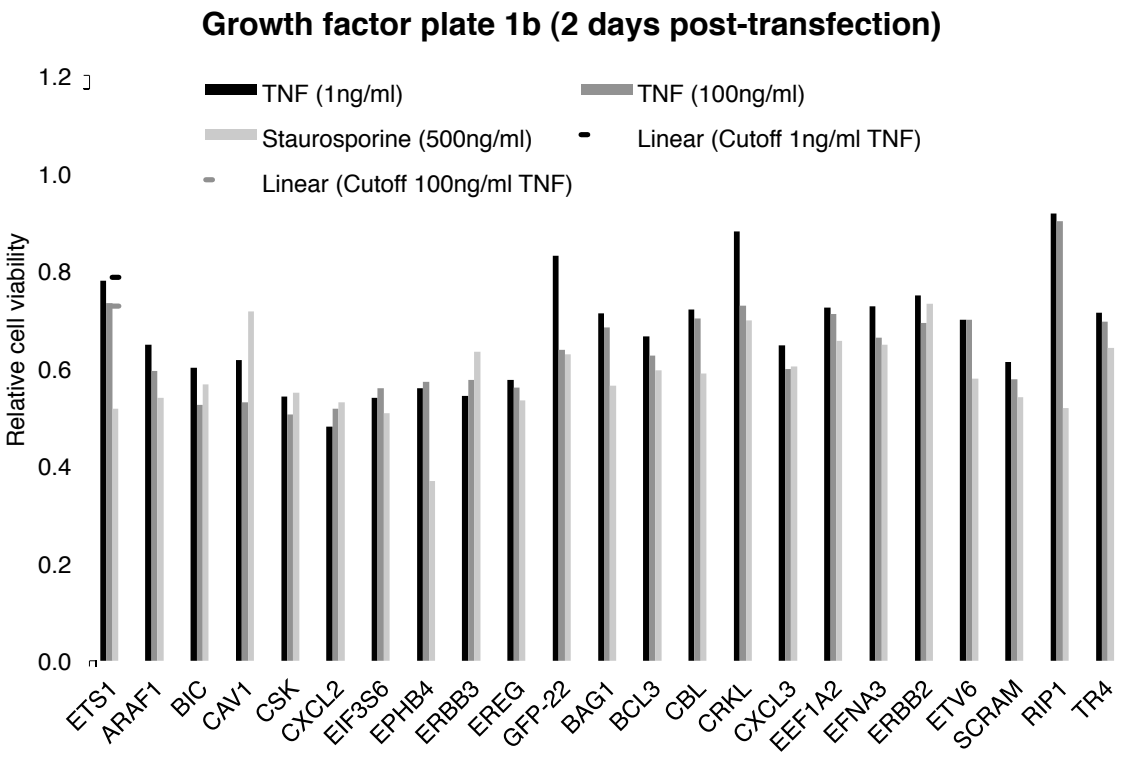
Growth factor plate 1b (2 days post-transfection)
TNF (1ng/ml)
TNF (100ng/ml)
Staurosporine (500ng/ml)
Linear (Cutoff 1ng/ml TNF)
Linear (Cutoff 100ng/ml TNF)
Relative cell viability
1.2
1.0
0.8
0.6
0.4
0.2
0.0
ETS1
ARAF1
BIC
CAV1
CSK
CXCL2
EIF3S6
EPHB4
ERBB3
EREG
GFP-22
BAG1
BCL3
CBL
CRKL
CXCL3
EEF1A2
EFNA3
ERBB2
ETV6
SCRAM
RIP1
TR4

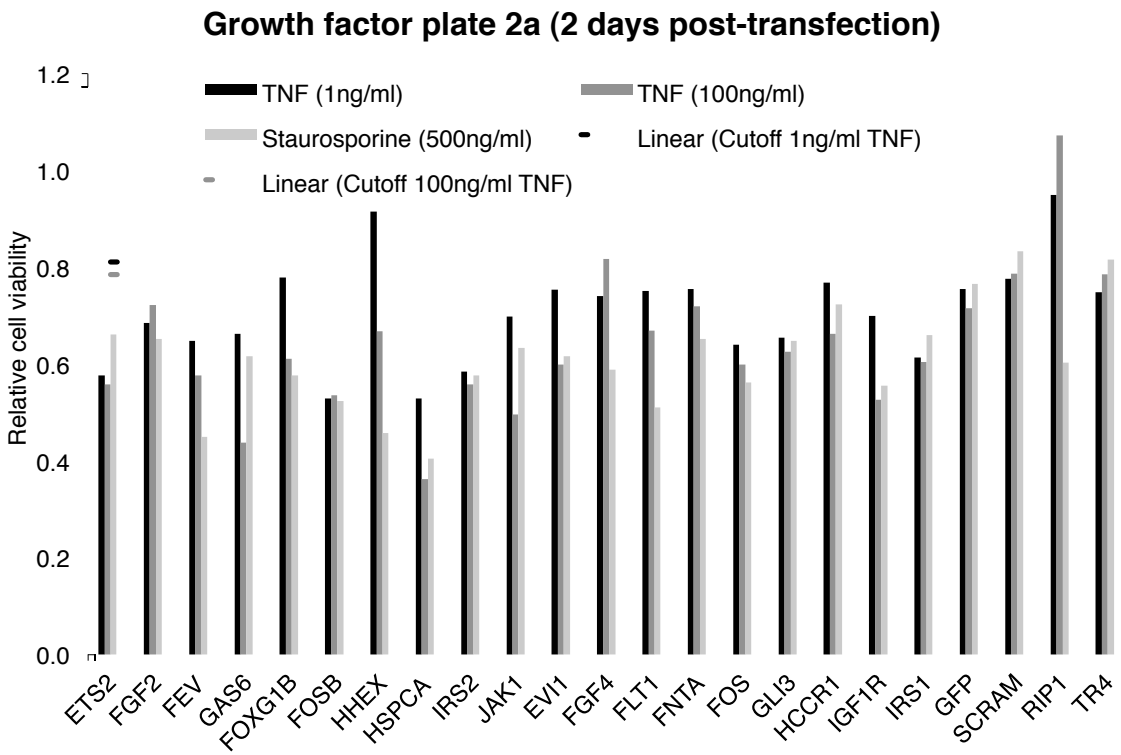
Growth factor plate 2a (2 days post-transfection)
TNF (1ng/ml)
TNF (100ng/ml)
Staurosporine (500ng/ml)
Linear (Cutoff 1ng/ml TNF)
Linear (Cutoff 100ng/ml TNF)
Relative cell viability
1.2
1.0
0.8
0.6
0.4
0.2
0.0
ETS2
FGF2
FEV
GAS6
FOXG1B
FOSB
HHEX
HSPCA
IRS2
JAK1
EVI1
FGF4
FLT1
FNTA
FOS
GLI3
HCCR1
IGF1R
IRS1
GFP
SCRAM
RIP1
TR4

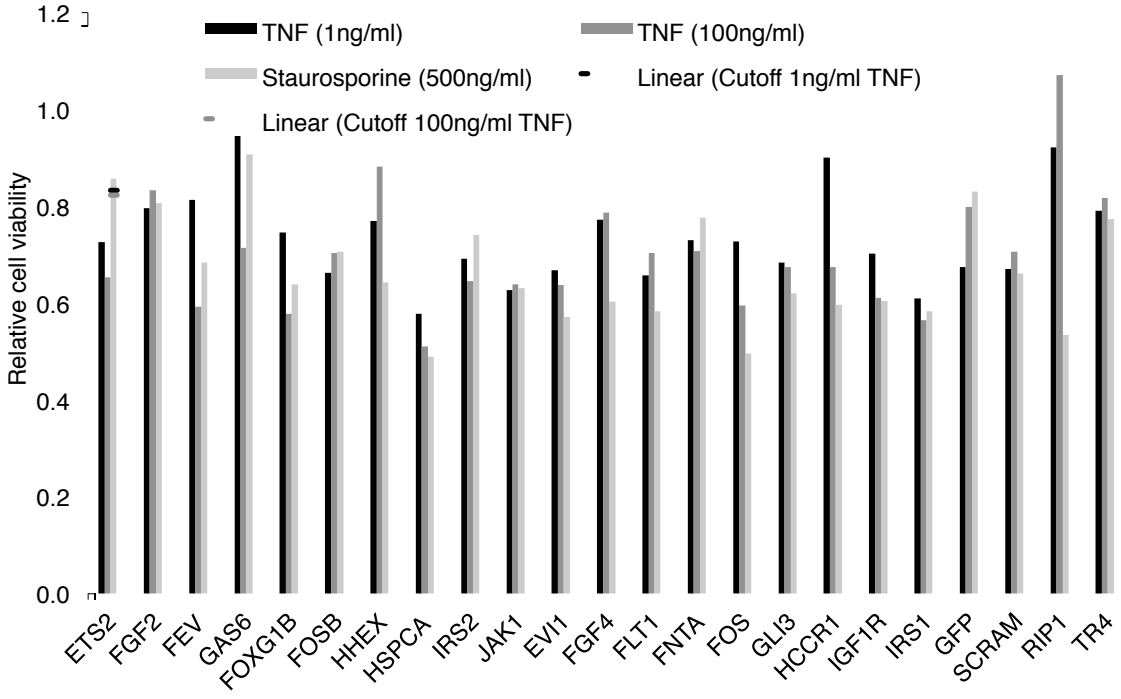
Growth factor plate 2a (3 days post-transfection)
TNF (1ng/ml)
TNF (100ng/ml)
Staurosporine (500ng/ml)
Linear (Cutoff 1ng/ml TNF)
Linear (Cutoff 100ng/ml TNF)
Relative cell viability
1.2
1.0
0.8
0.6
0.4
0.2
0.0
ETS2
FGF2
FEV
GAS6
FOXG1B
FOSB
HHEX
HSPCA
IRS2
JAK1
EVI1
FGF4
FLT1
FNTA
FOS
GLI3
HCCR1
IGF1R
IRS1
GFP
SCRAM
RIP1
TR4

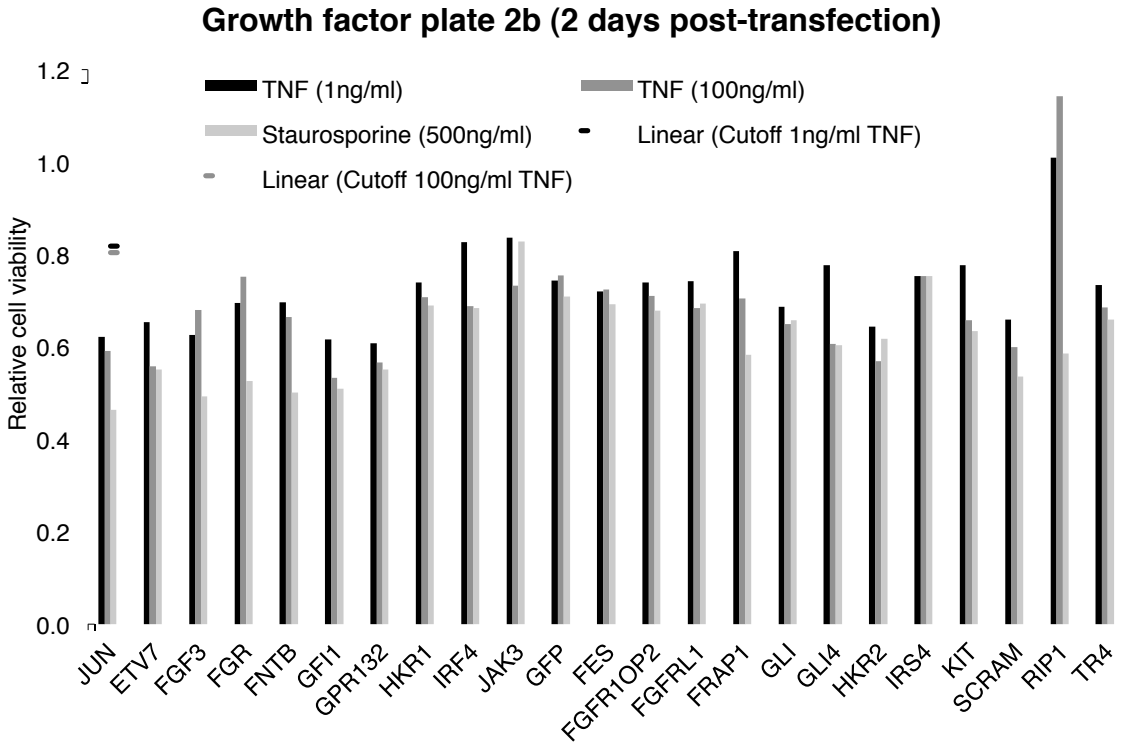
Growth factor plate 2b (2 days post-transfection)
TNF (1ng/ml)
TNF (100ng/ml)
Staurosporine (500ng/ml)
Linear (Cutoff 1ng/ml TNF)
Linear (Cutoff 100ng/ml TNF)
Relative cell viability
1.2
1.0
0.8
0.6
0.4
0.2
0.0
JUN
ETV7
FGF3
FGR
FNTB
GFI1
GPR132
HKR1
IRF4
JAK3
GFP
FES
FGFR1OP2
FGFRL1
FRAP1
GLI
GLI4
HKR2
IRS4
KIT
SCRAM
RIP1
TR4

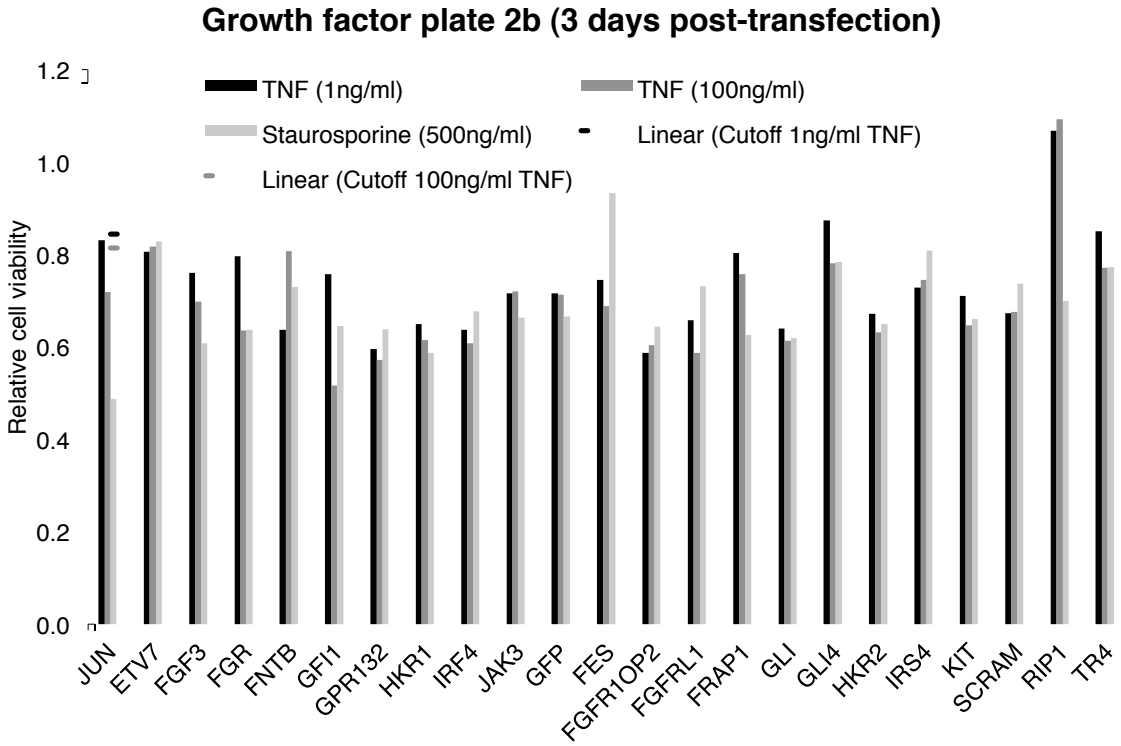
Growth factor plate 2b (3 days post-transfection)
TNF (1ng/ml)
TNF (100ng/ml)
Staurosporine (500ng/ml)
Linear (Cutoff 1ng/ml TNF)
Linear (Cutoff 100ng/ml TNF)
Relative cell viability
1.2
1.0
0.8
0.6
0.4
0.2
0.0
JUN
ETV7
FGF3
FGR
FNTB
GFI1
GPR132
HKR1
IRF4
JAK3
GFP
FES
FGFR1OP2
FGFRL1
FRAP1
GLI
GLI4
HKR2
IRS4
KIT
SCRAM
RIP1
TR4

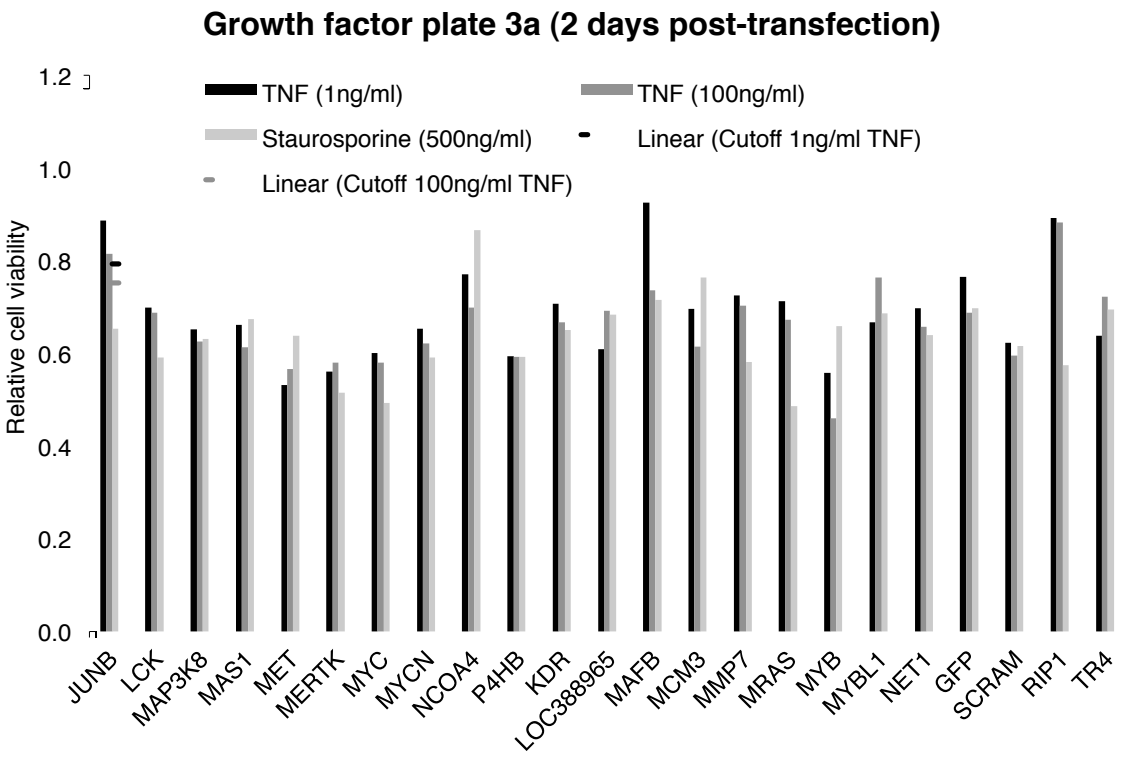
Growth factor plate 3a (2 days post-transfection)
TNF (1ng/ml)
TNF (100ng/ml)
Staurosporine (500ng/ml)
Linear (Cutoff 1ng/ml TNF)
Linear (Cutoff 100ng/ml TNF)
Relative cell viability
1.2
1.0
0.8
0.6
0.4
0.2
0.0
JUNB
LCK
MAP3K8
MAS1
MET
MERTK
MYC
MYCN
NCOA4
P4HB
KDR
LOC388965
MAFB
MCM3
MMP7
MRAS
MYB
MYBL1
NET1
GFP
SCRAM
RIP1
TR4

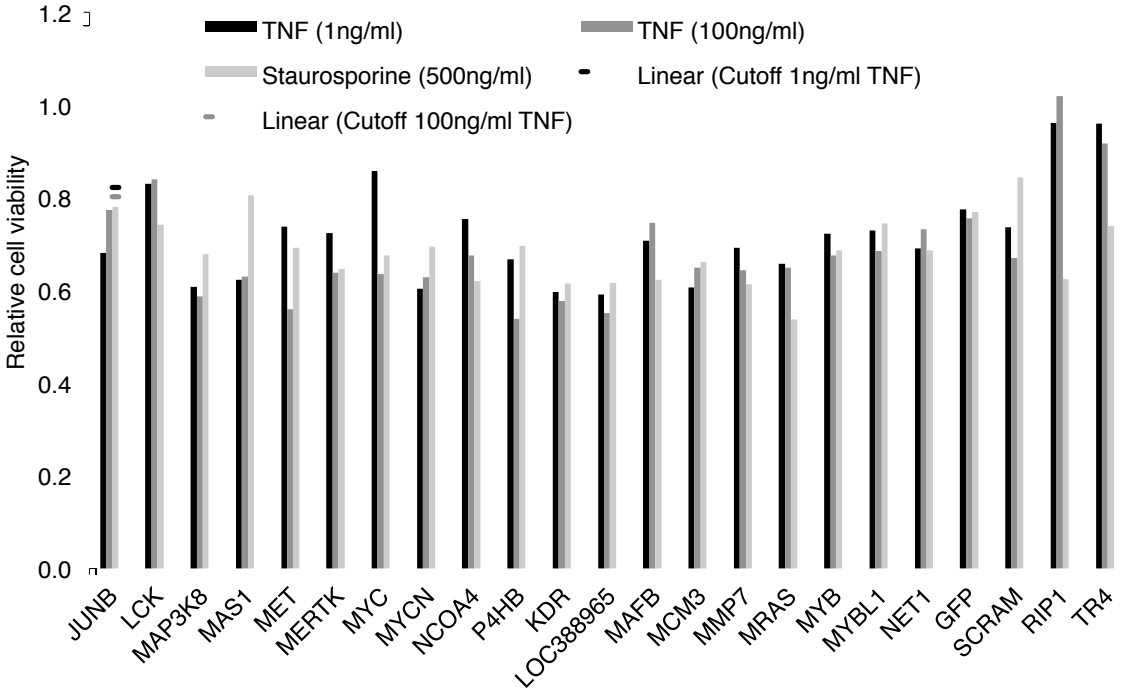
Growth factor plate 3a (3 days post-transfection)
TNF (1ng/ml)
TNF (100ng/ml)
Staurosporine (500ng/ml)
Linear (Cutoff 1ng/ml TNF)
Linear (Cutoff 100ng/ml TNF)
Relative cell viability
1.2
1.0
0.8
0.6
0.4
0.2
0.0
JUNB
LCK
MAP3K8
MAS1
MET
MERTK
MYC
MYCN
NCOA4
P4HB
KDR
LOC388965
MAFB
MCM3
MMP7
MRAS
MYB
MYBL1
NET1
GFP
SCRAM
RIP1
TR4

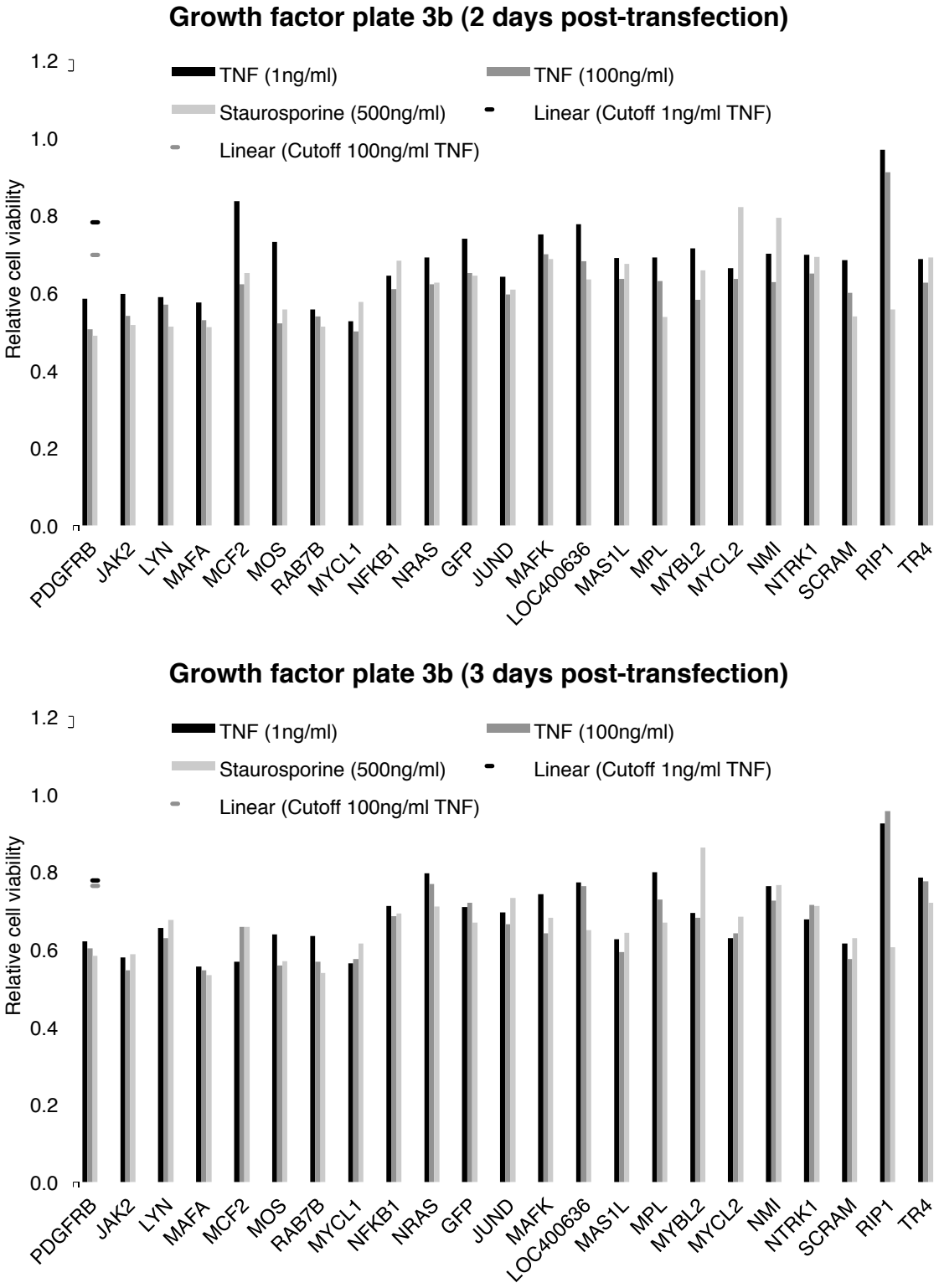
Growth factor plate 3b (2 days post-transfection)
TNF (1ng/ml)
TNF (100ng/ml)
Staurosporine (500ng/ml)
Linear (Cutoff 1ng/ml TNF)
Linear (Cutoff 100ng/ml TNF)
Relative cell viability
1.2
1.0
0.8
0.6
0.4
0.2
0.0
PDGFRB
JAK2
LYN
MAFA
MCF2
MOS
RAB7B
MYCL1
NFKB1
NRAS
GFP
JUND
MAFK
LOC400636
MAS1L
MPL
MYBL2
MYCL2
NMI
NTRK1
SCRAM
RIP1
TR4
Growth factor plate 3b (3 days post-transfection)
TNF (1ng/ml)
TNF (100ng/ml)
Staurosporine (500ng/ml)
Linear (Cutoff 1ng/ml TNF)
Linear (Cutoff 100ng/ml TNF)
Relative cell viability
1.2
1.0
0.8
0.6
0.4
0.2
0.0
PDGFRB
JAK2
LYN
MAFA
MCF2
MOS
RAB7B
MYCL1
NFKB1
NRAS
GFP
JUND
MAFK
LOC400636
MAS1L
MPL
MYBL2
MYCL2
NMI
NTRK1
SCRAM
RIP1
TR4

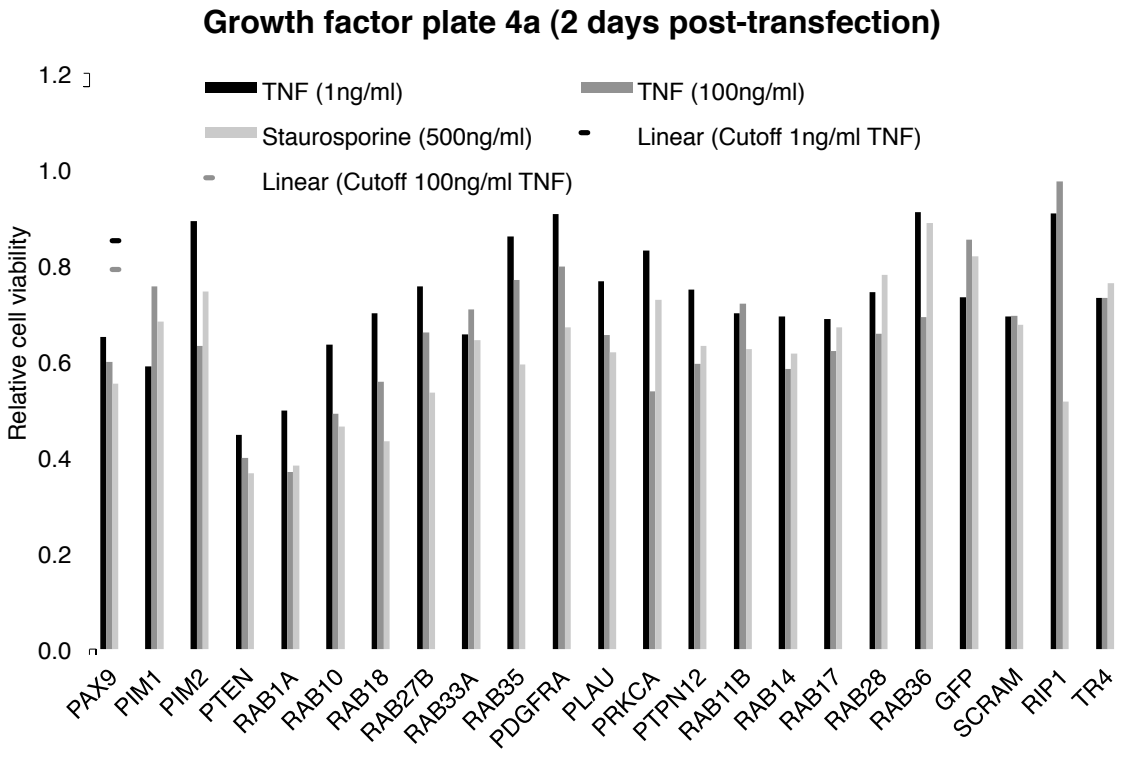
Growth factor plate 4a (2 days post-transfection)
TNF (1ng/ml)
TNF (100ng/ml)
Staurosporine (500ng/ml)
Linear (Cutoff 1ng/ml TNF)
Linear (Cutoff 100ng/ml TNF)
Relative cell viability
1.2
1.0
0.8
0.6
0.4
0.2
0.0
PAX9
PIM1
PIM2
PTEN
RAB1A
RAB10
RAB18
RAB27B
RAB33A
RAB35
PDGFRA
PLAU
PRKCA
PTPN12
RAB11B
RAB14
RAB17
RAB28
RAB36
GFP
SCRAM
RIP1
TR4

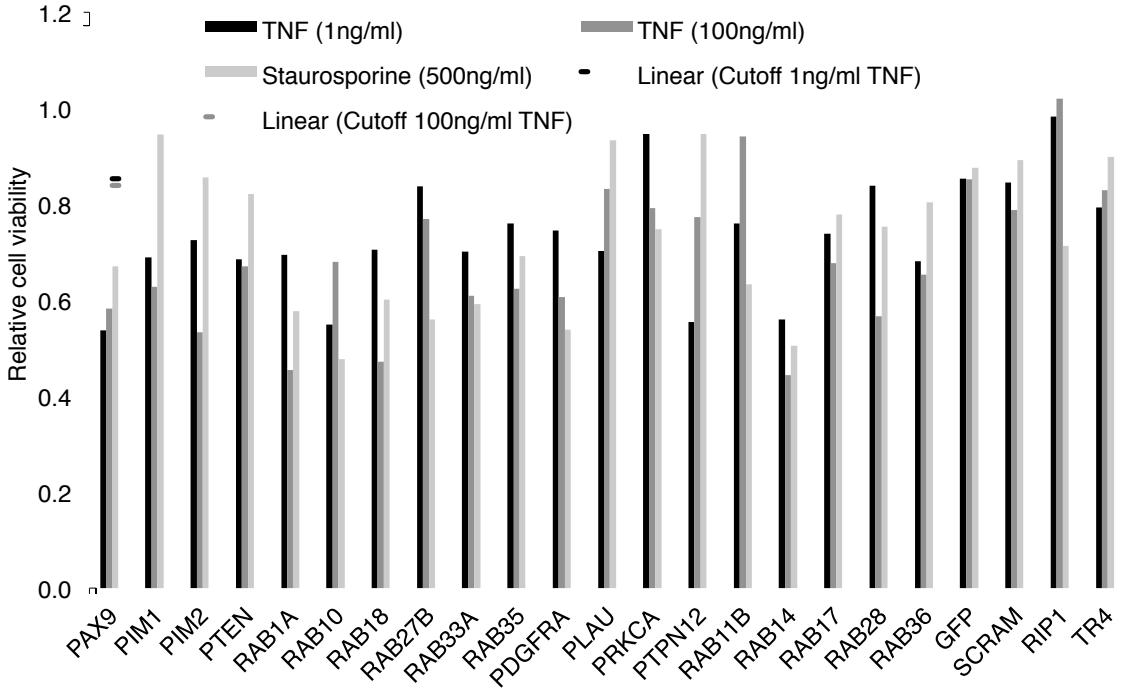
Growth Factor Plate 4a (3 days post-transfection)
TNF (1ng/ml)
TNF (100ng/ml)
Staurosporine (500ng/ml)
Linear (Cutoff 1ng/ml TNF)
Linear (Cutoff 100ng/ml TNF)
Relative cell viability
1.2
1.0
0.8
0.6
0.4
0.2
0.0
PAX9
PIM1
PIM2
PTEN
RAB1A
RAB10
RAB18
RAB27B
RAB33A
RAB35
PDGFRA
PLAU
PRKCA
PTPN12
RAB11B
RAB14
RAB17
RAB28
RAB36
GFP
SCRAM
RIP1
TR4

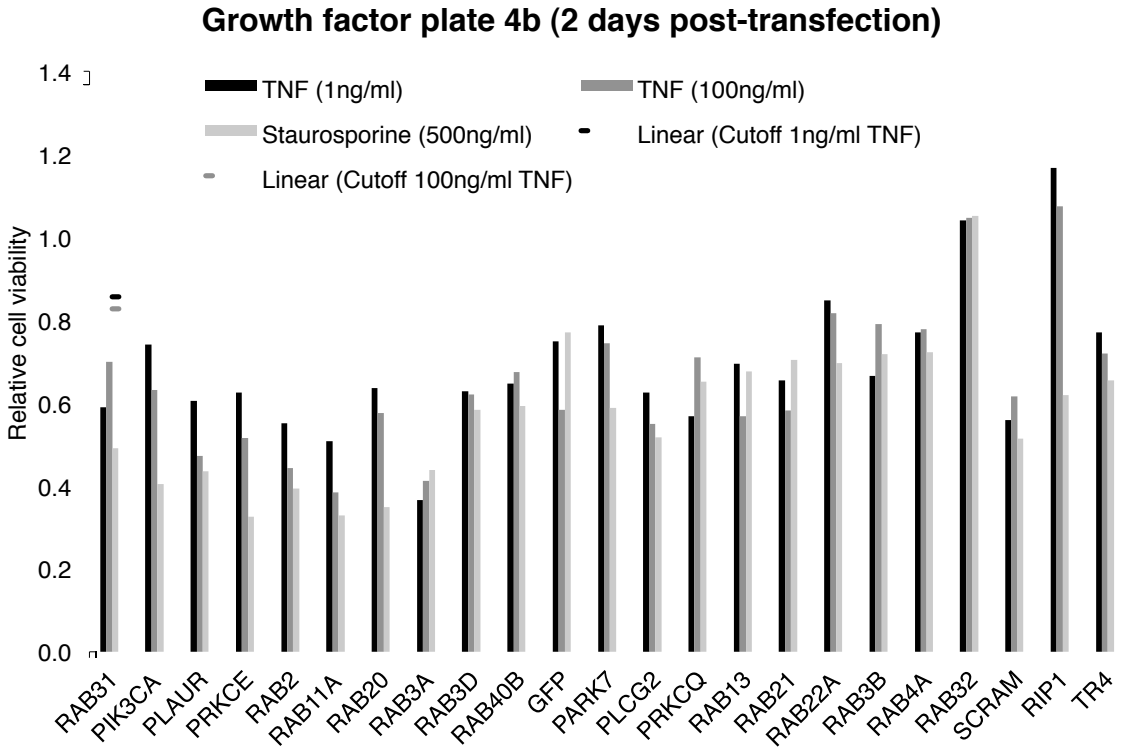
Growth factor plate 4b (2 days post-transfection)
TNF (1ng/ml)
TNF (100ng/ml)
Staurosporine (500ng/ml)
Linear (Cutoff 1ng/ml TNF)
Linear (Cutoff 100ng/ml TNF)
Relative cell viability
1.4
1.2
1.0
0.8
0.6
0.4
0.2
0.0
RAB31
PIK3CA
PLAUR
PRKCE
RAB2
RAB11A
RAB20
RAB3A
RAB3D
RAB40B
GFP
PARK7
PLCG2
PRKCQ
RAB13
RAB21
RAB22A
RAB3B
RAB4A
RAB32
SCRAM
RIP1
TR4

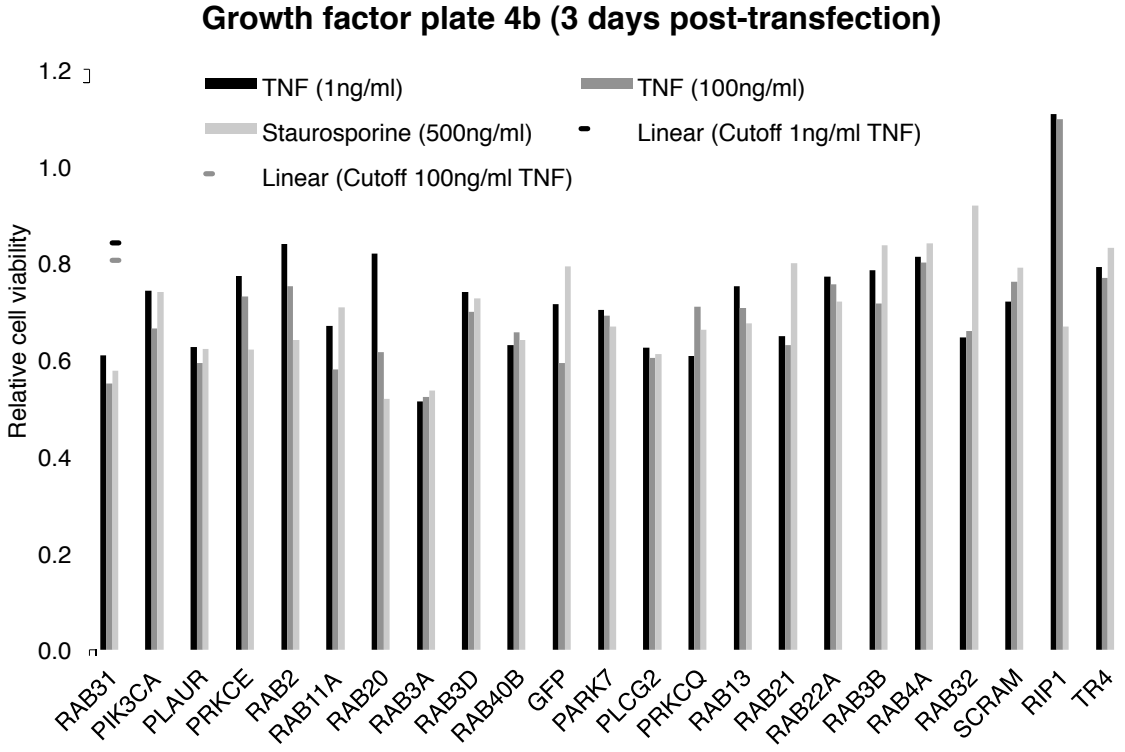
Growth factor plate 4b (3 days post-transfection)
TNF (1ng/ml)
TNF (100ng/ml)
Staurosporine (500ng/ml)
Linear (Cutoff 1ng/ml TNF)
Linear (Cutoff 100ng/ml TNF)
Relative cell viability
1.2
1.0
0.8
0.6
0.4
0.2
0.0
RAB31
PIK3CA
PLAUR
PRKCE
RAB2
RAB11A
RAB20
RAB3A
RAB3D
RAB40B
GFP
PARK7
PLCG2
PRKCQ
RAB13
RAB21
RAB22A
RAB3B
RAB4A
RAB32
SCRAM
RIP1
TR4

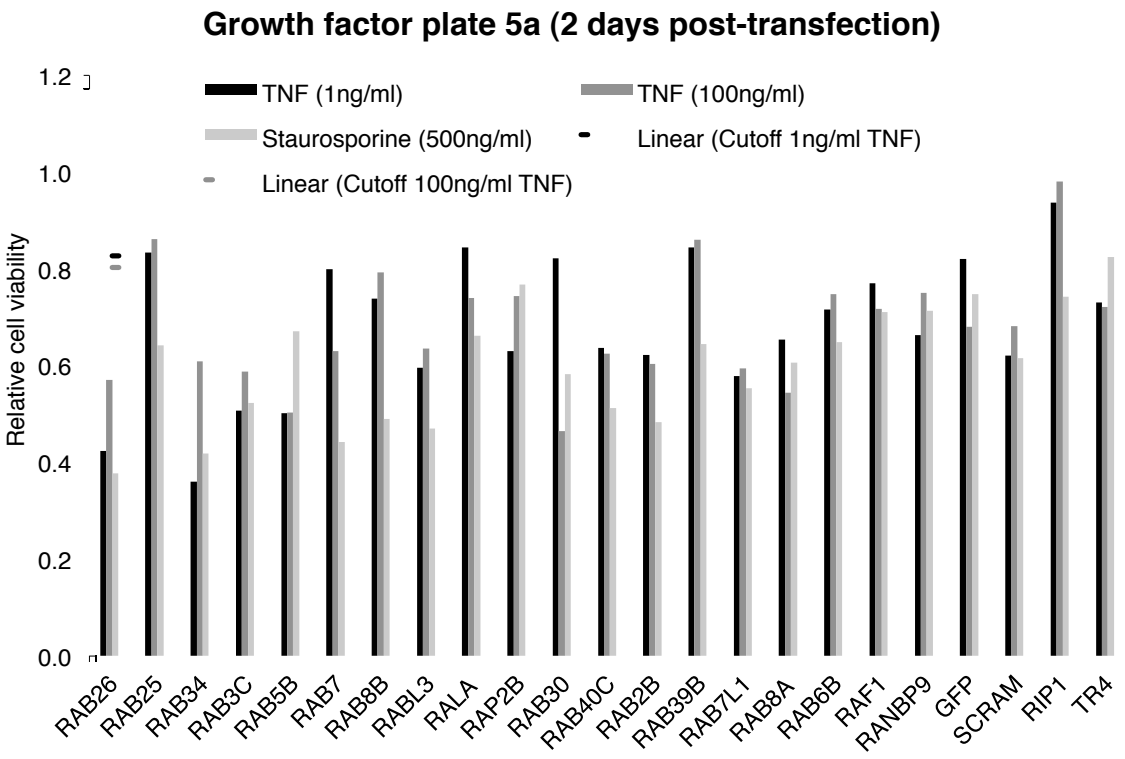
Growth factor plate 5a (2 days post-transfection)
TNF (1ng/ml)
TNF (100ng/ml)
Staurosporine (500ng/ml)
Linear (Cutoff 1ng/ml TNF)
Linear (Cutoff 100ng/ml TNF)
Relative cell viability
1.2
1.0
0.8
0.6
0.4
0.2
0.0
RAB26
RAB25
RAB34
RAB3C
RAB5B
RAB7
RAB8B
RABL3
RALA
RAP2B
RAB30
RAB40C
RAB2B
RAB39B
RAB7L1
RAB8A
RAB6B
RAF1
RANBP9
GFP
SCRAM
RIP1
TR4

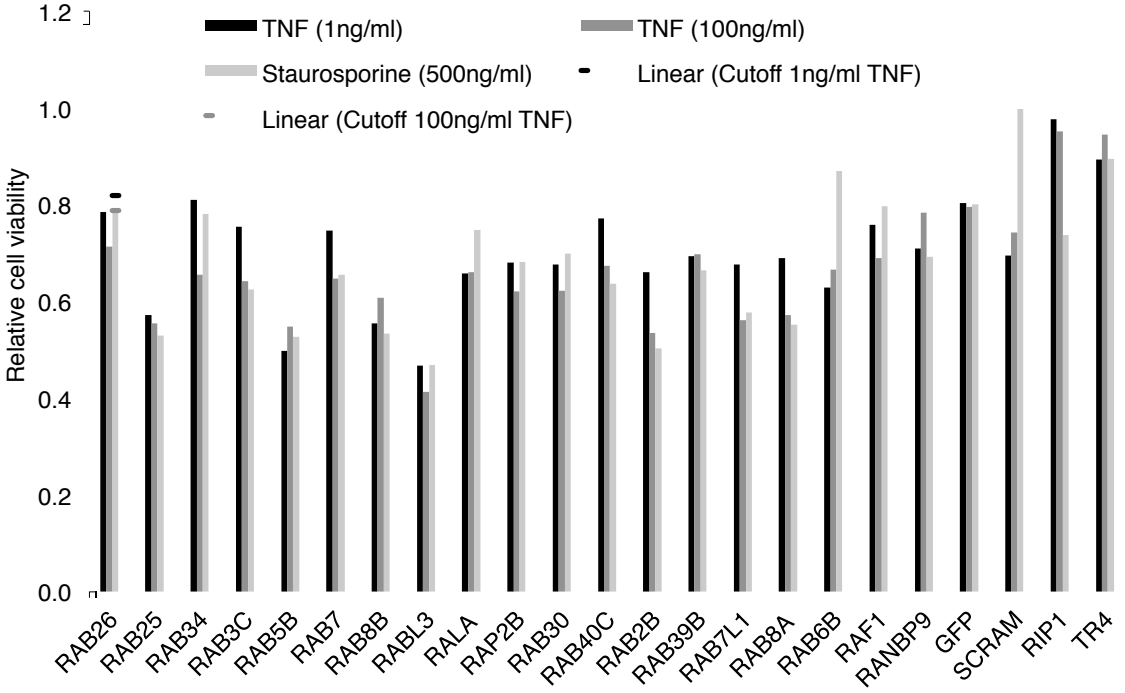
Growth factor plate 5a (3 days post-transfection)
TNF (1ng/ml)
TNF (100ng/ml)
Staurosporine (500ng/ml)
Linear (Cutoff 1ng/ml TNF)
Linear (Cutoff 100ng/ml TNF)
Relative cell viability
1.2
1.0
0.8
0.6
0.4
0.2
0.0
RAB26
RAB25
RAB34
RAB3C
RAB5B
RAB7
RAB8B
RABL3
RALA
RAP2B
RAB30
RAB40C
RAB2B
RAB39B
RAB7L1
RAB8A
RAB6B
RAF1
RANBP9
GFP
SCRAM
RIP1
TR4

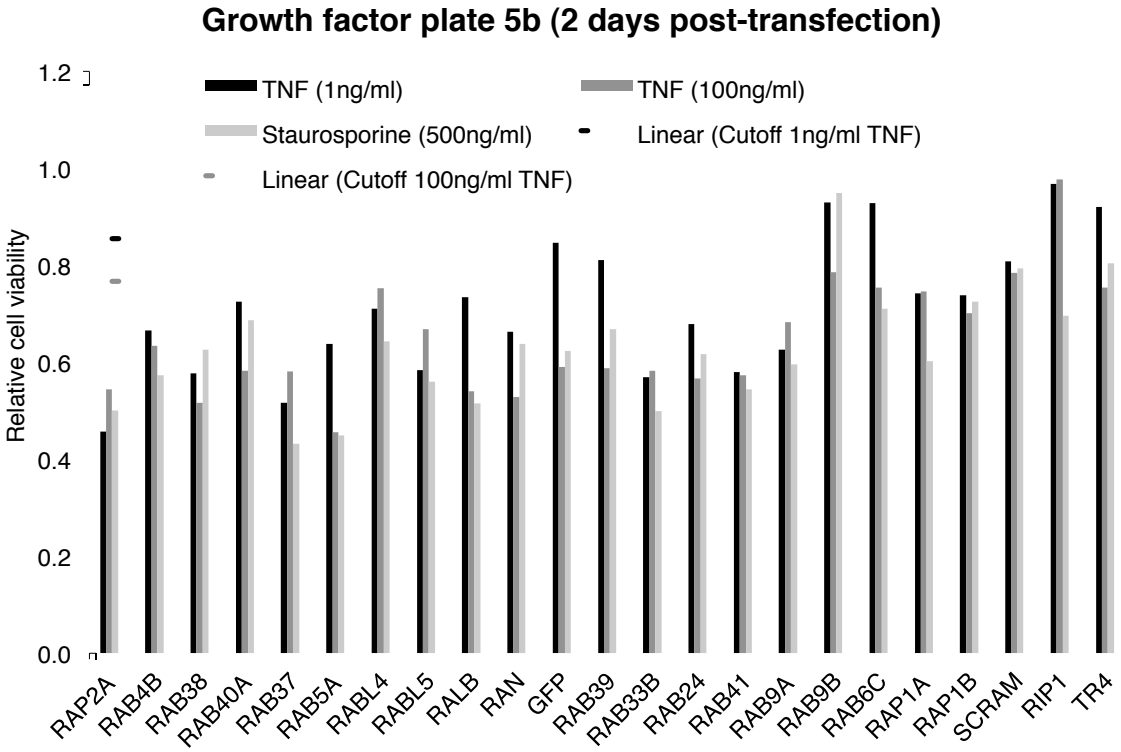
Growth factor plate 5b (2 days post-transfection)
TNF (1ng/ml)
TNF (100ng/ml)
Staurosporine (500ng/ml)
Linear (Cutoff 1ng/ml TNF)
Linear (Cutoff 100ng/ml TNF)
Relative cell viability
1.2
1.0
0.8
0.6
0.4
0.2
0.0
RAP2A
RAB4B
RAB38
RAB40A
RAB37
RAB5A
RABL4
RABL5
RALB
RAN
GFP
RAB39
RAB33B
RAB24
RAB41
RAB9A
RAB9B
RAB6C
RAP1A
RAP1B
SCRAM
RIP1
TR4

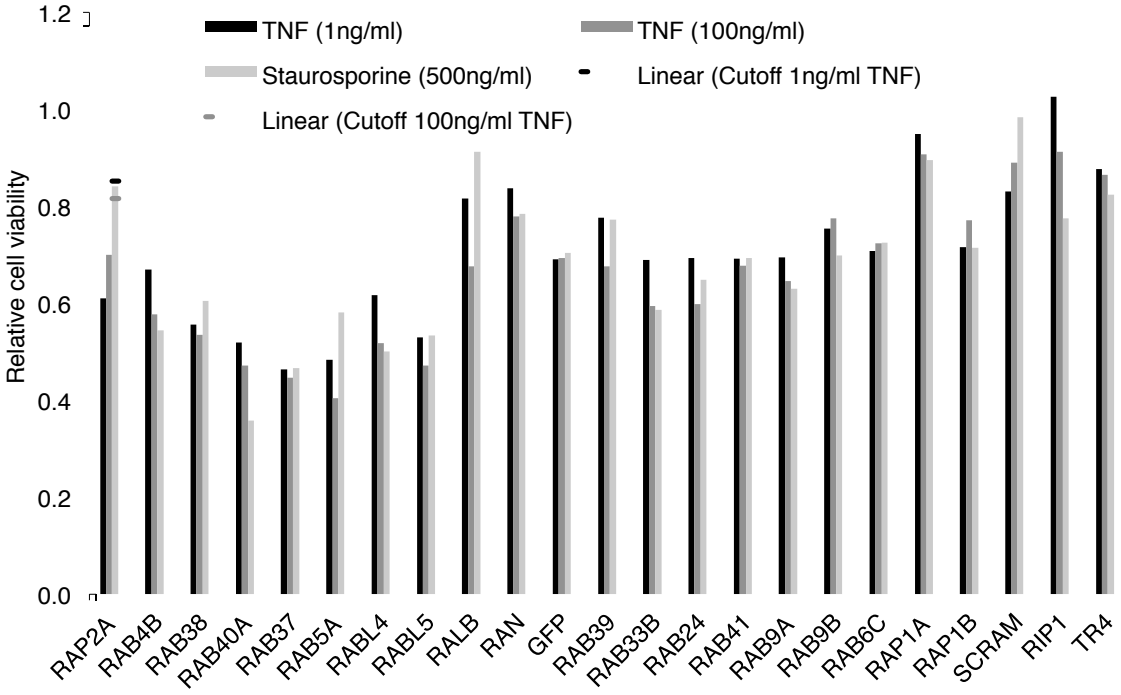
Growth factor plate 5b (3 days post-transfection)
TNF (1ng/ml)
TNF (100ng/ml)
Staurosporine (500ng/ml)
Linear (Cutoff 1ng/ml TNF)
Linear (Cutoff 100ng/ml TNF)
Relative cell viability
1.2
1.0
0.8
0.6
0.4
0.2
0.0
RAP2A
RAB4B
RAB38
RAB40A
RAB37
RAB5A
RABL4
RABL5
RALB
RAN
GFP
RAB39
RAB33B
RAB24
RAB41
RAB9A
RAB9B
RAB6C
RAP1A
RAP1B
SCRAM
RIP1
TR4

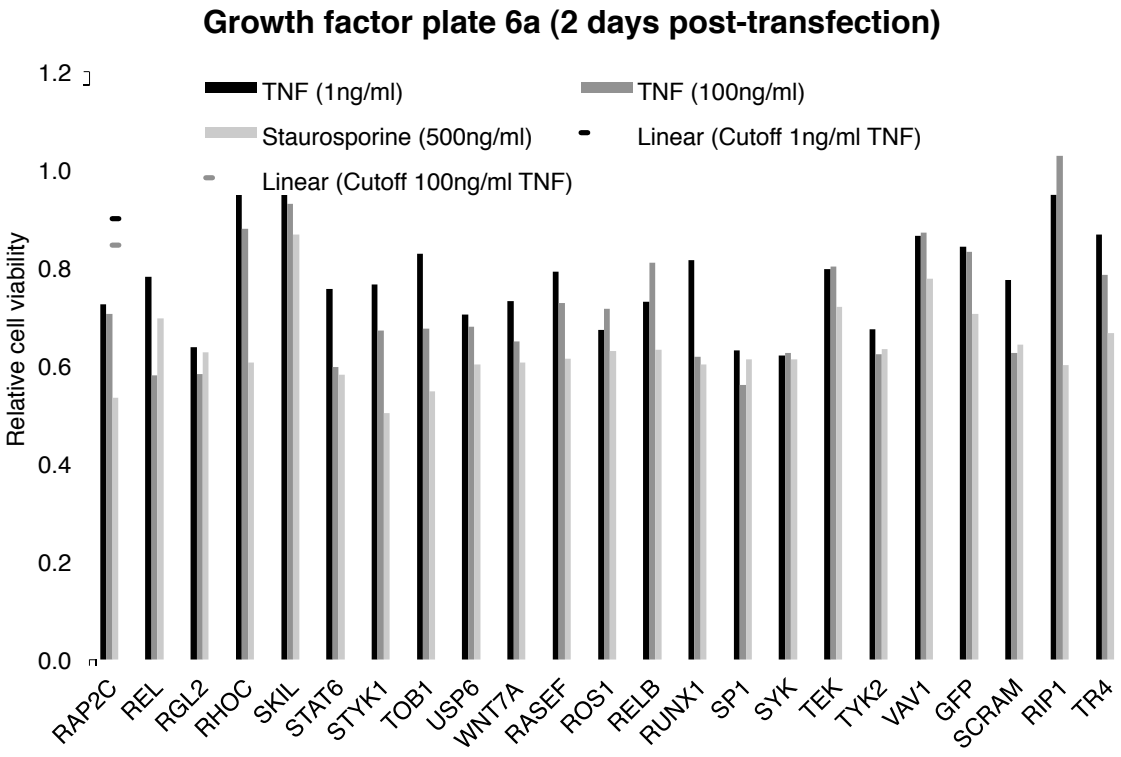
Growth factor plate 6a (2 days post-transfection)
TNF (1ng/ml)
TNF (100ng/ml)
Staurosporine (500ng/ml)
Linear (Cutoff 1ng/ml TNF)
Linear (Cutoff 100ng/ml TNF)
Relative cell viability
1.2
1.0
0.8
0.6
0.4
0.2
0.0
RAP2C
REL
RGL2
RHOC
SKIL
STAT6
STYK1
TOB1
USP6
WNT7A
RASEF
ROS1
RELB
RUNX1
SP1
SYK
TEK
TYK2
VAV1
GFP
SCRAM
RIP1
TR4

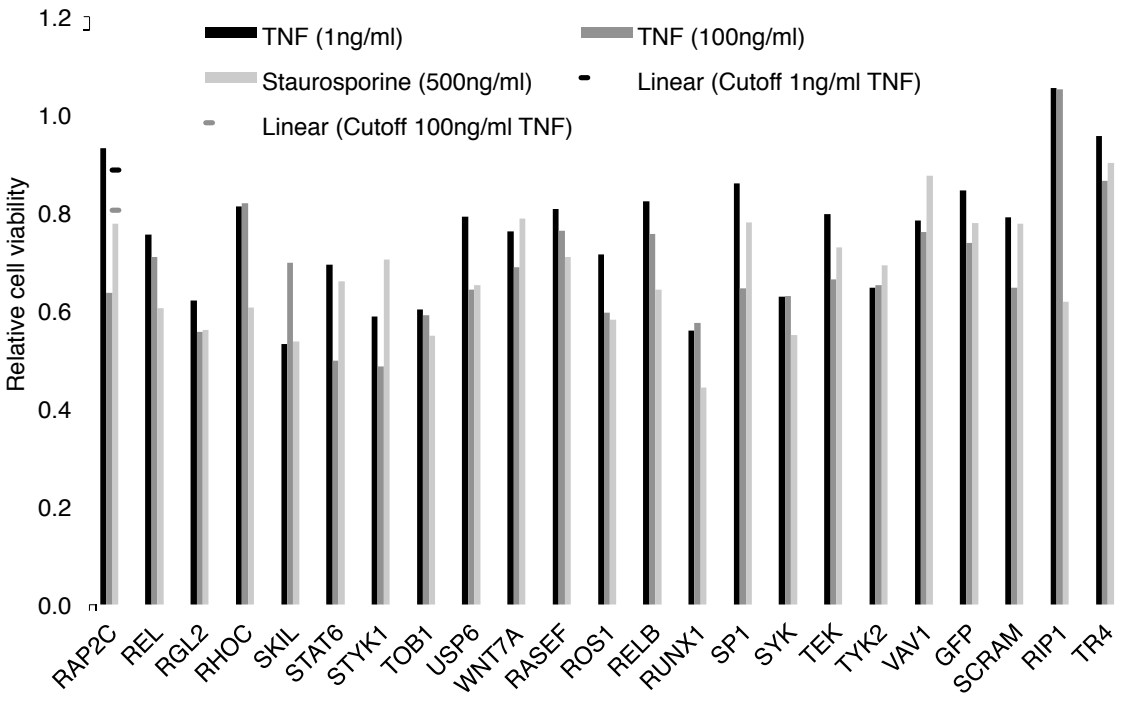
Growth factor plate 6a (3 days post-transfection)
TNF (1ng/ml)
TNF (100ng/ml)
Staurosporine (500ng/ml)
Linear (Cutoff 1ng/ml TNF)
Linear (Cutoff 100ng/ml TNF)
Relative cell viability
1.2
1.0
0.8
0.6
0.4
0.2
0.0
RAP2C
REL
RGL2
RHOC
SKIL
STAT6
STYK1
TOB1
USP6
WNT7A
RASEF
ROS1
RELB
RUNX1
SP1
SYK
TEK
TYK2
VAV1
GFP
SCRAM
RIP1
TR4

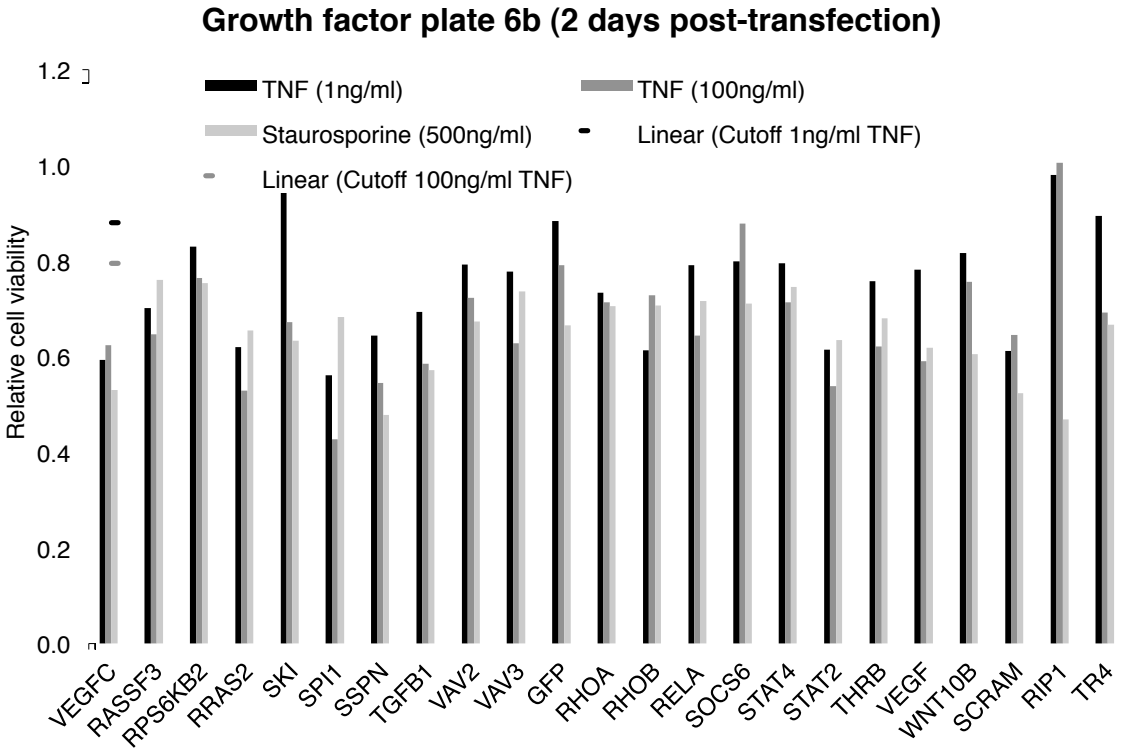
Growth factor plate 6b (2 days post-transfection)
TNF (1ng/ml)
TNF (100ng/ml)
Staurosporine (500ng/ml)
Linear (Cutoff 1ng/ml TNF)
Linear (Cutoff 100ng/ml TNF)
Relative cell viability
1.2
1.0
0.8
0.6
0.4
0.2
0.0
VEGFC
RASSF3
RPS6KB2
RRAS2
SKI
SPI1
SSPN
TGFB1
VAV2
VAV3
GFP
RHOA
RHOB
RELA
SOCS6
STAT4
STAT2
THRB
VEGF
WNT10B
SCRAM
RIP1
TR4

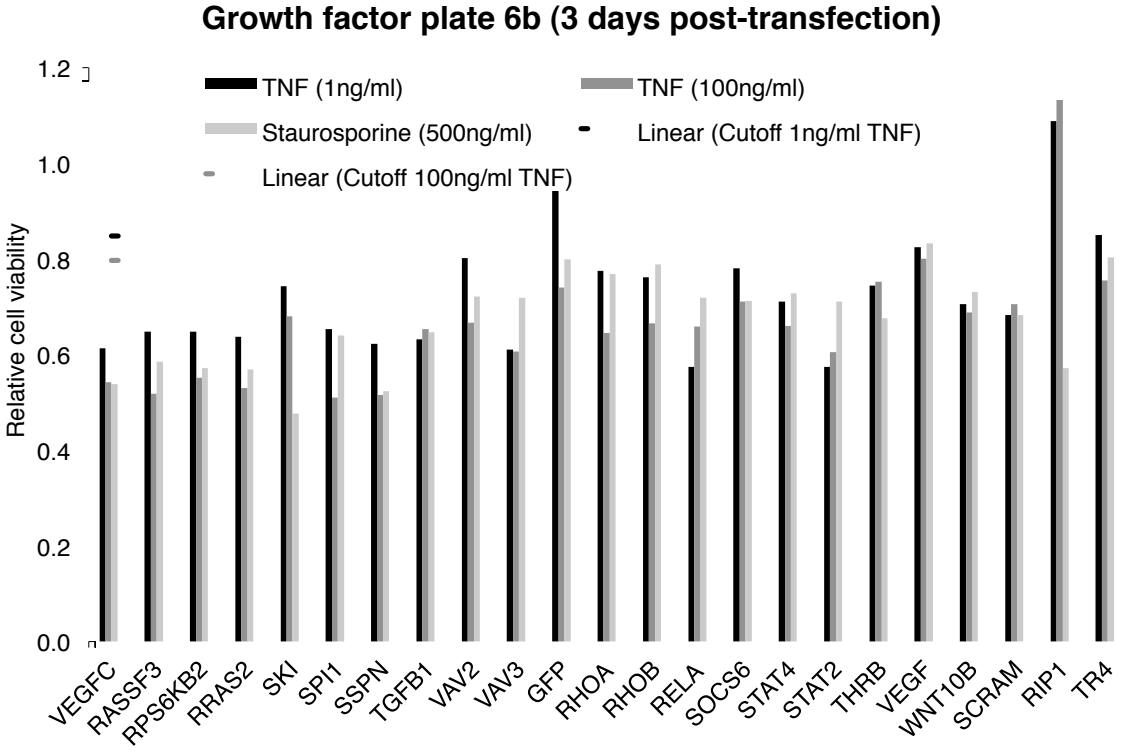
Growth factor plate 6b (3 days post-transfection)
TNF (1ng/ml)
TNF (100ng/ml)
Staurosporine (500ng/ml)
Linear (Cutoff 1ng/ml TNF)
Linear (Cutoff 100ng/ml TNF)
Relative cell viability
1.2
1.0
0.8
0.6
0.4
0.2
0.0
VEGFC
RASSF3
RPS6KB2
RRAS2
SKI
SPI1
SSPN
TGFB1
VAV2
VAV3
GFP
RHOA
RHOB
RELA
SOCS6
STAT4
STAT2
THRB
VEGF
WNT10B
SCRAM
RIP1
TR4

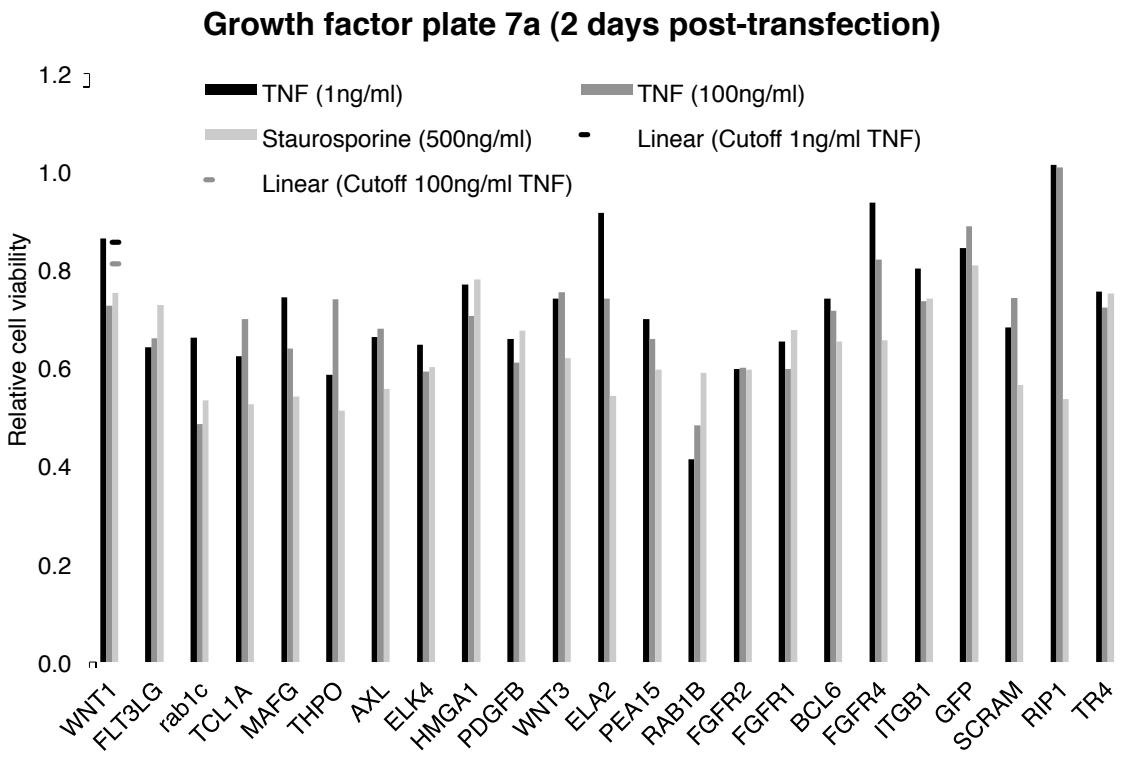
Growth factor plate 7a (2 days post-transfection)
TNF (1ng/ml)
TNF (100ng/ml)
Staurosporine (500ng/ml)
Linear (Cutoff 1ng/ml TNF)
Linear (Cutoff 100ng/ml TNF)
Relative cell viability
1.2
1.0
0.8
0.6
0.4
0.2
0.0
WNT1
FLT3LG
rab1c
TCL1A
MAFG
THPO
AXL
ELK4
HMGA1
PDGFB
WNT3
ELA2
PEA15
RAB1B
FGFR2
FGFR1
BCL6
FGFR4
ITGB1
GFP
SCRAM
RIP1
TR4

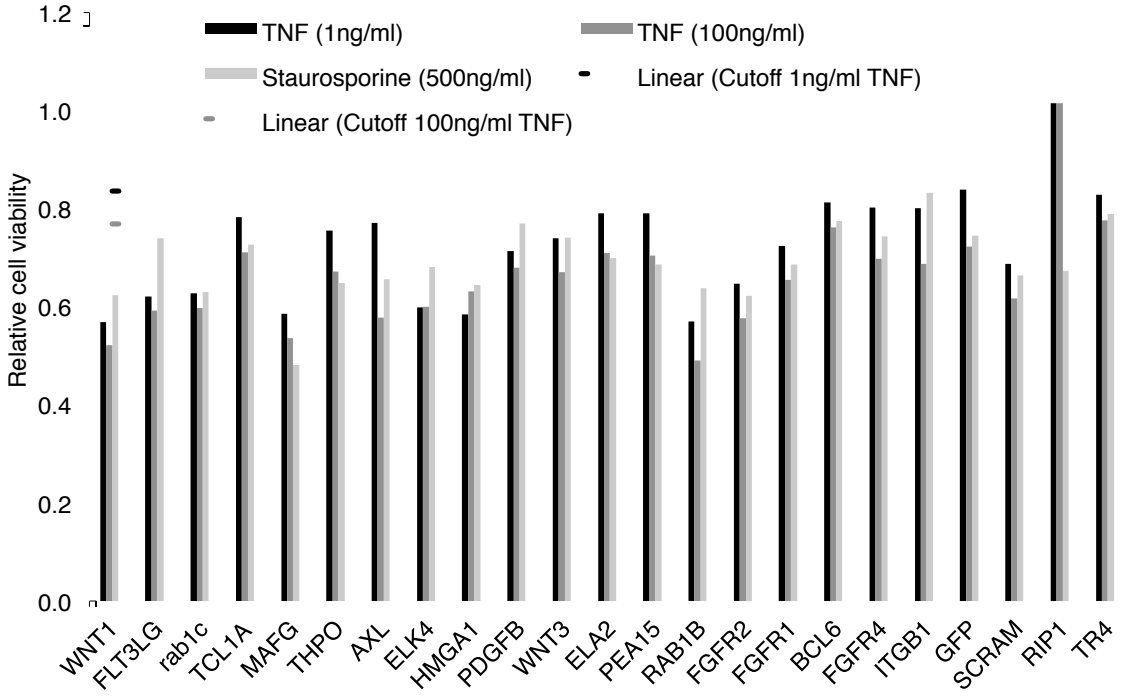
Growth factor plate 7a (3 days post-transfection)
TNF (1ng/ml)
TNF (100ng/ml)
Staurosporine (500ng/ml)
Linear (Cutoff 1ng/ml TNF)
Linear (Cutoff 100ng/ml TNF)
Relative cell viability
1.2
1.0
0.8
0.6
0.4
0.2
0.0
WNT1
FLT3LG
rab1c
TCL1A
MAFG
THPO
AXL
ELK4
HMGA1
PDGFB
WNT3
ELA2
PEA15
RAB1B
FGFR2
FGFR1
BCL6
FGFR4
ITGB1
GFP
SCRAM
RIP1
TR4

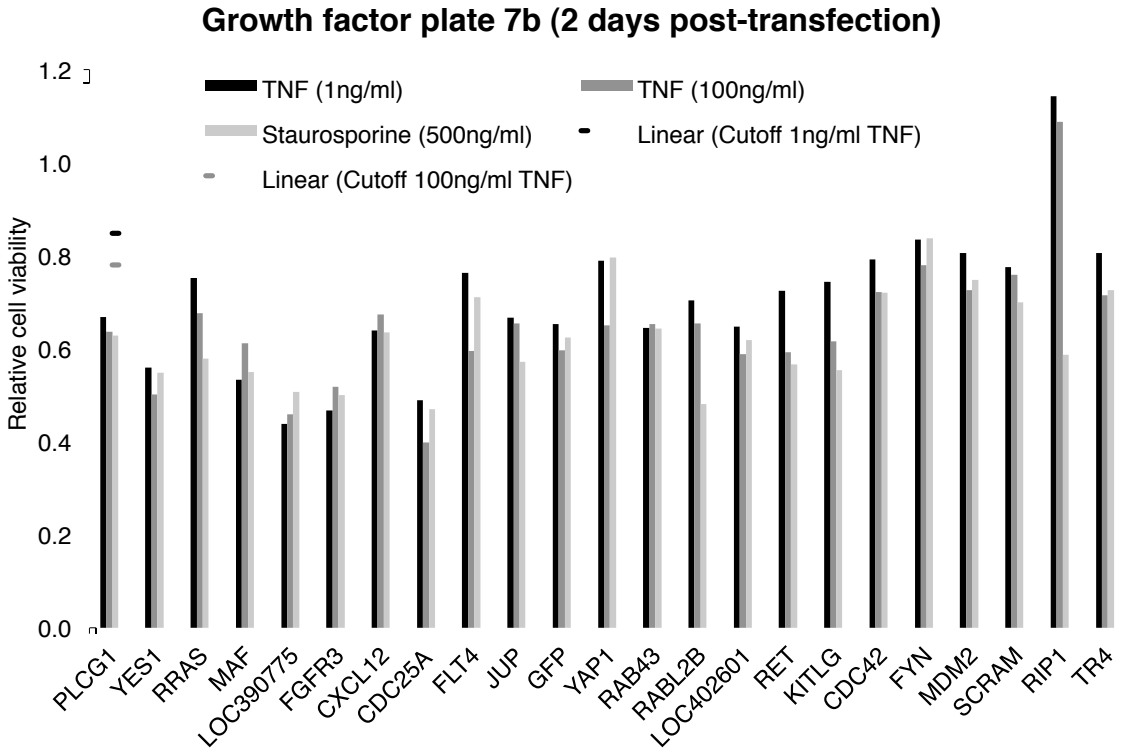
Growth factor plate 7b (2 days post-transfection)
TNF (1ng/ml)
TNF (100ng/ml)
Staurosporine (500ng/ml)
Linear (Cutoff 1ng/ml TNF)
Linear (Cutoff 100ng/ml TNF)
Relative cell viability
1.2
1.0
0.8
0.6
0.4
0.2
0.0
PLCG1
YES1
RRAS
MAF
LOC390775
FGFR3
CXCL12
CDC25A
FLT4
JUP
GFP
YAP1
RAB43
RABL2B
LOC402601
RET
KITLG
CDC42
FYN
MDM2
SCRAM
RIP1
TR4

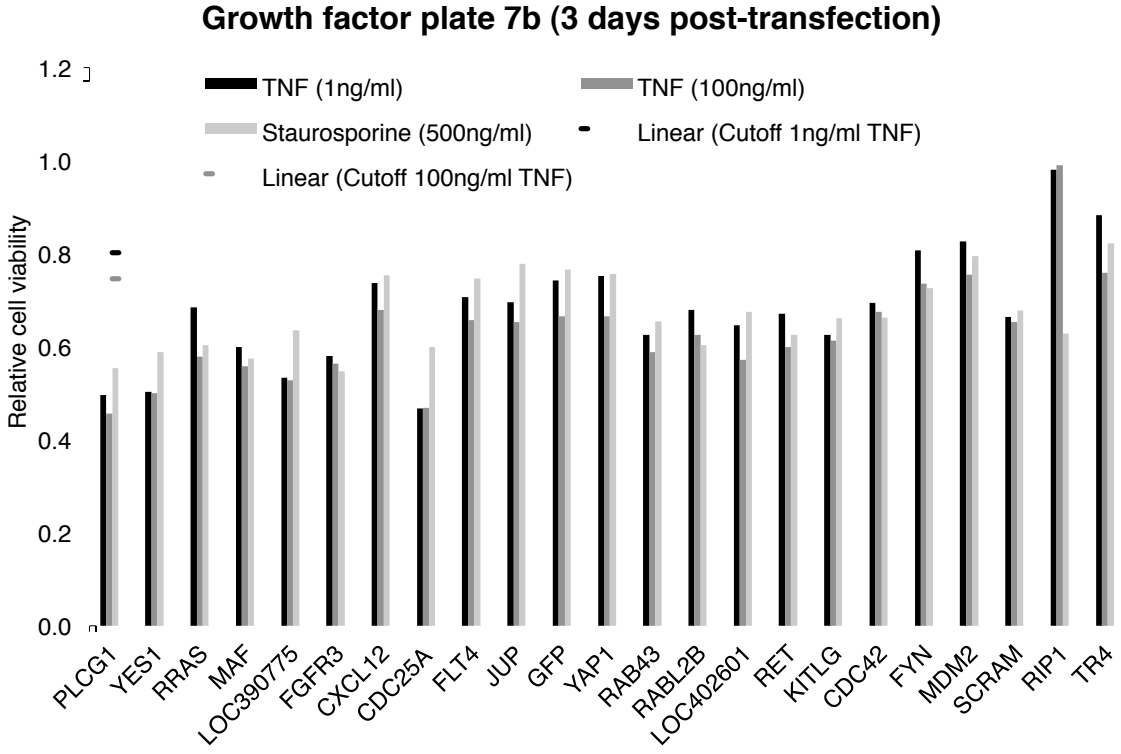
Growth factor plate 7b (3 days post-transfection)
TNF (1ng/ml)
TNF (100ng/ml)
Staurosporine (500ng/ml)
Linear (Cutoff 1ng/ml TNF)
Linear (Cutoff 100ng/ml TNF)
Relative cell viability
1.2
1.0
0.8
0.6
0.4
0.2
0.0
PLCG1
YES1
RRAS
MAF
LOC390775
FGFR3
CXCL12
CDC25A
FLT4
JUP
GFP
YAP1
RAB43
RABL2B
LOC402601
RET
KITLG
CDC42
FYN
MDM2
SCRAM
RIP1
TR4

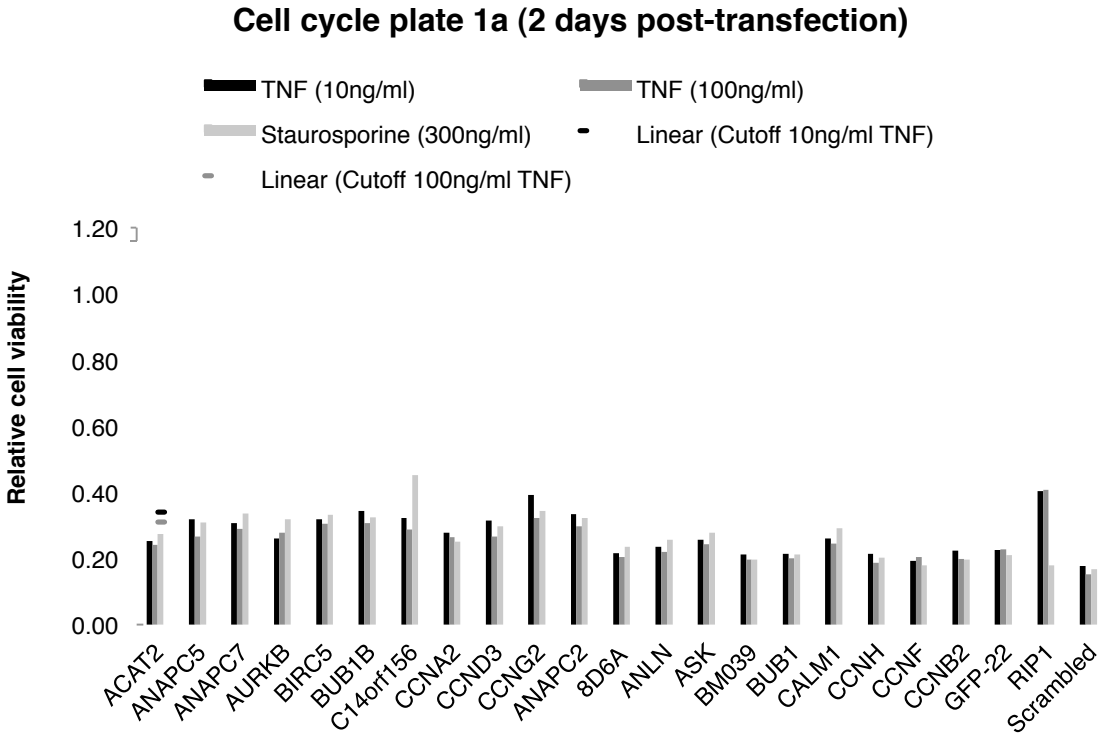
Cell cycle plate 1a (2 days post-transfection)
TNF (10ng/ml)
TNF (100ng/ml)
Staurosporine (300ng/ml)
Linear (Cutoff 10ng/ml TNF)
Linear (Cutoff 100ng/ml TNF)
Relative cell viability
1.20
1.00
0.80
0.60
0.40
0.20
0.00
ACAT2
ANAPC5
ANAPC7
AURKB
BIRC5
BUB1B
C14orf156
CCNA2
CCND3
CCNG2
ANAPC2
8D6A
ANLN
ASK
BM039
BUB1
CALM1
CCNH
CCNF
CCNB2
GFP-22
RIP1
Scrambled

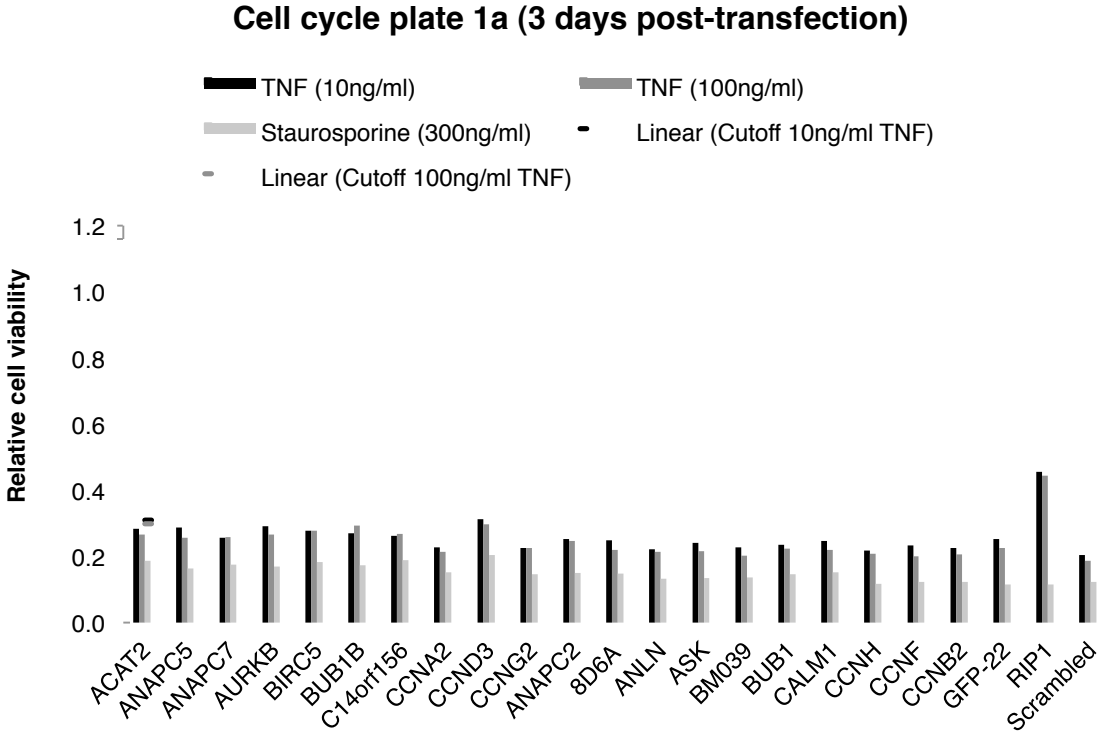
Cell cycle plate 1a (3 days post-transfection)
TNF (10ng/ml)
TNF (100ng/ml)
Staurosporine (300ng/ml)
Linear (Cutoff 10ng/ml TNF)
Linear (Cutoff 100ng/ml TNF)
Relative cell viability
1.2
1.0
0.8
0.6
0.4
0.2
0.0
ACAT2
ANAPC5
ANAPC7
AURKB
BIRC5
BUB1B
C14orf156
CCNA2
CCND3
CCNG2
ANAPC2
8D6A
ANLN
ASK
BM039
BUB1
CALM1
CCNH
CCNF
CCNB2
GFP-22
RIP1
Scrambled

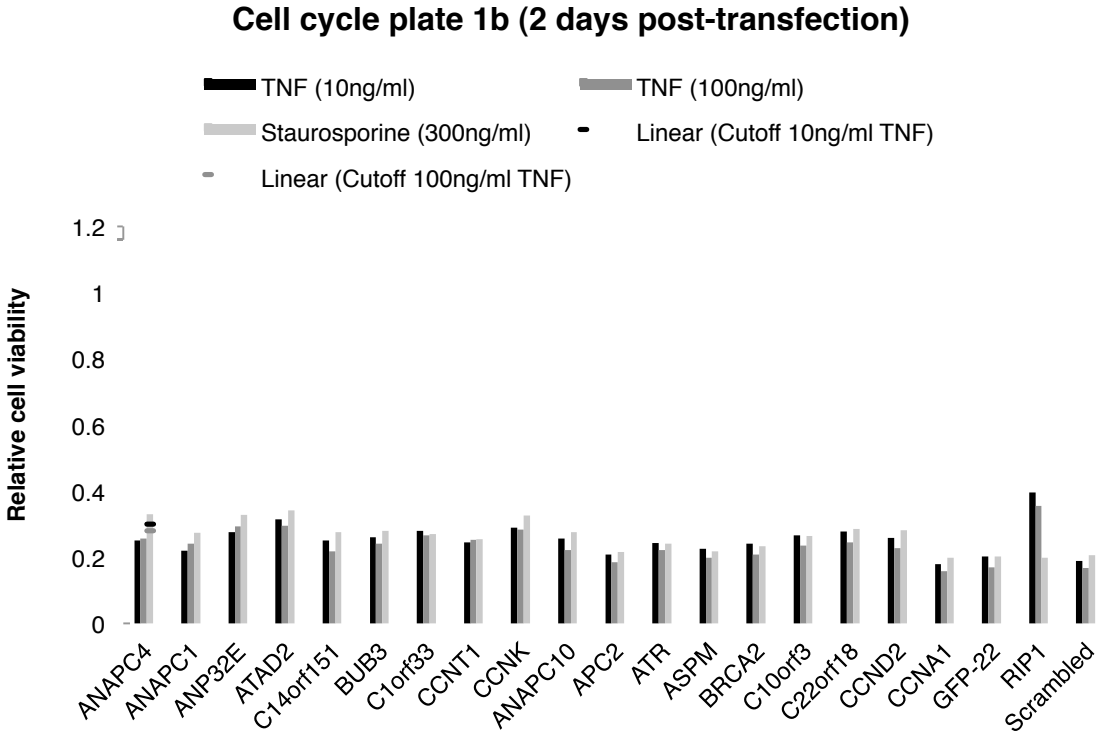
Cell cycle plate 1b (2 days post-transfection)
TNF (10ng/ml)
TNF (100ng/ml)
Staurosporine (300ng/ml)
Linear (Cutoff 10ng/ml TNF)
Linear (Cutoff 100ng/ml TNF)
Relative cell viability
1.2
1
0.8
0.6
0.4
0.2
0
ANAPC4
ANAPC1
ANP32E
ATAD2
C14orf151
BUB3
C1orf33
CCNT1
CCNK
ANAPC10
APC2
ATR
ASPM
BRCA2
C10orf3
C22orf18
CCND2
CCNA1
GFP-22
RIP1
Scrambled

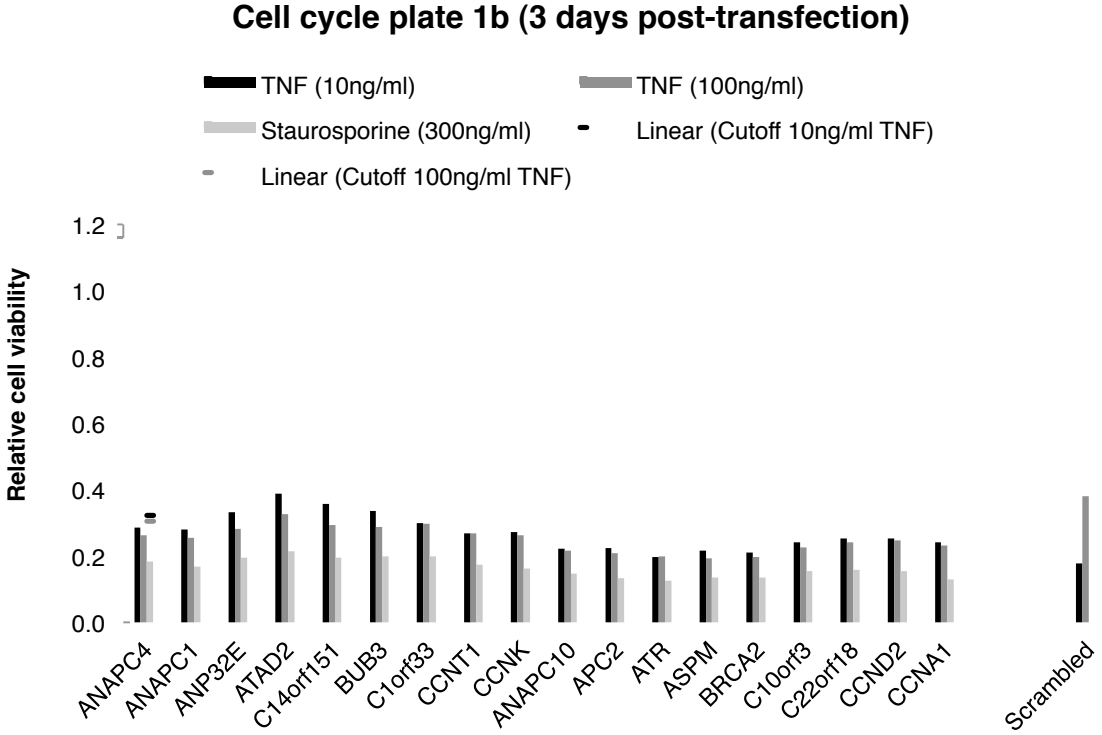
Cell cycle plate 1b (3 days post-transfection)
TNF (10ng/ml)
TNF (100ng/ml)
Staurosporine (300ng/ml)
Linear (Cutoff 10ng/ml TNF)
Linear (Cutoff 100ng/ml TNF)
Relative cell viability
1.2
1.0
0.8
0.6
0.4
0.2
0.0
ANAPC4
ANAPC1
ANP32E
ATAD2
C14orf151
BUB3
C1orf33
CCNT1
CCNK
ANAPC10
APC2
ATR
ASPM
BRCA2
C10orf3
C22orf18
CCND2
CCNA1
Scrambled

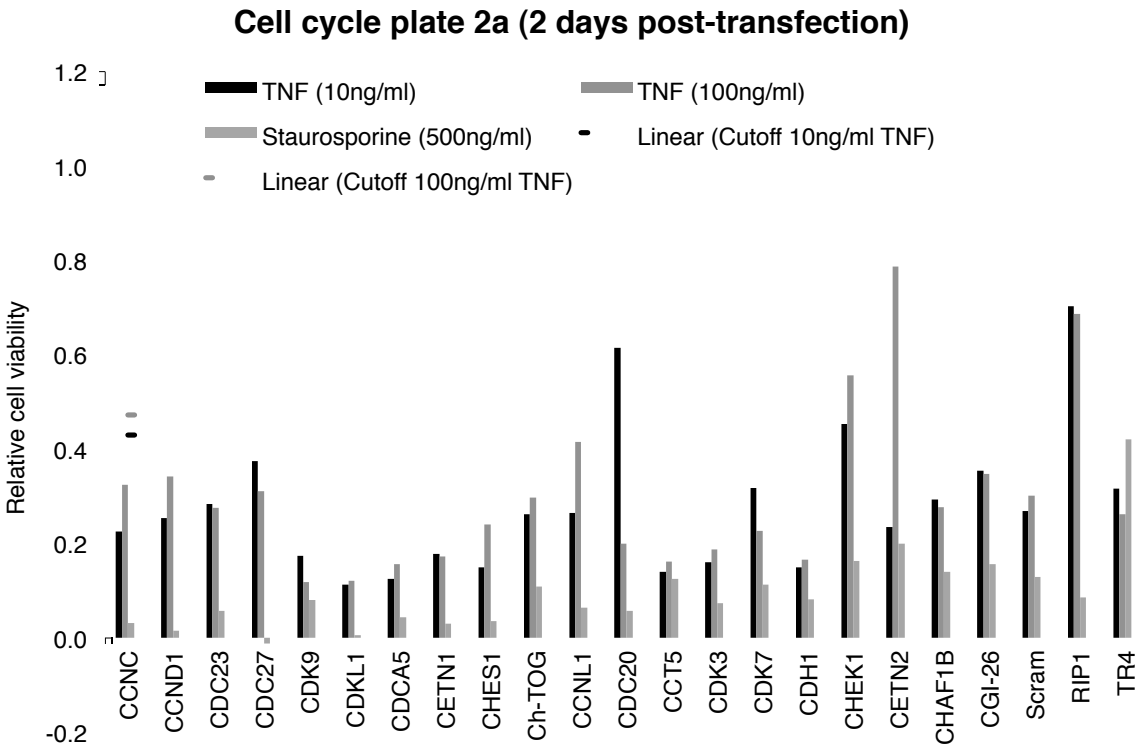
Cell cycle plate 2a (2 days post-transfection)
TNF (10ng/ml)
TNF (100ng/ml)
Staurosporine (500ng/ml)
Linear (Cutoff 10ng/ml TNF)
Linear (Cutoff 100ng/ml TNF)
Relative cell viability
1.2
1.0
0.8
0.6
0.4
0.2
0.0
-0.2
CCNC
CCND1
CDC23
CDC27
CDK9
CDKL1
CDCA5
CETN1
CHES1
Ch-TOG
CCNL1
CDC20
CCT5
CDK3
CDK7
CDH1
CHEK1
CETN2
CHAF1B
CGI-26
Scram
RIP1
TR4

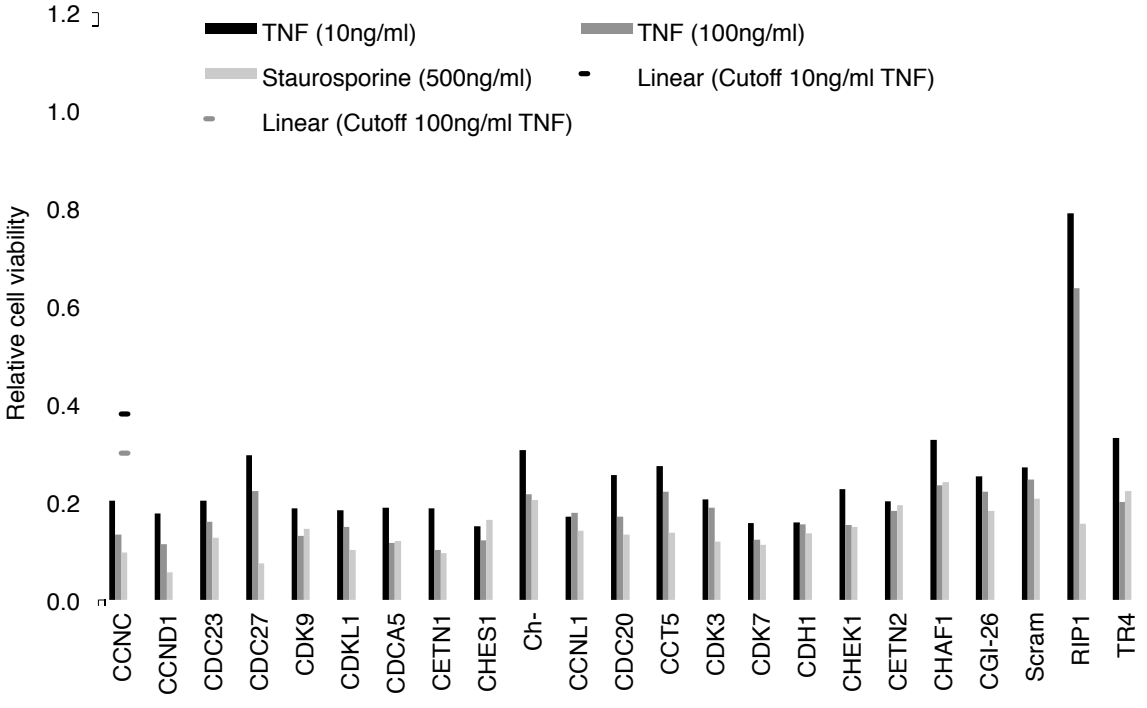
Cell cycle plate 2a (3 days post-transfection)
TNF (10ng/ml)
TNF (100ng/ml)
Staurosporine (500ng/ml)
Linear (Cutoff 10ng/ml TNF)
Linear (Cutoff 100ng/ml TNF)
Relative cell viability
1.2
1.0
0.8
0.6
0.4
0.2
0.0
CCNC
CCND1
CDC23
CDC27
CDK9
CDKL1
CDCA5
CETN1
CHES1
Ch-
CCNL1
CDC20
CCT5
CDK3
CDK7
CDH1
CHEK1
CETN2
CHAF1
CGI-26
Scram
RIP1
TR4

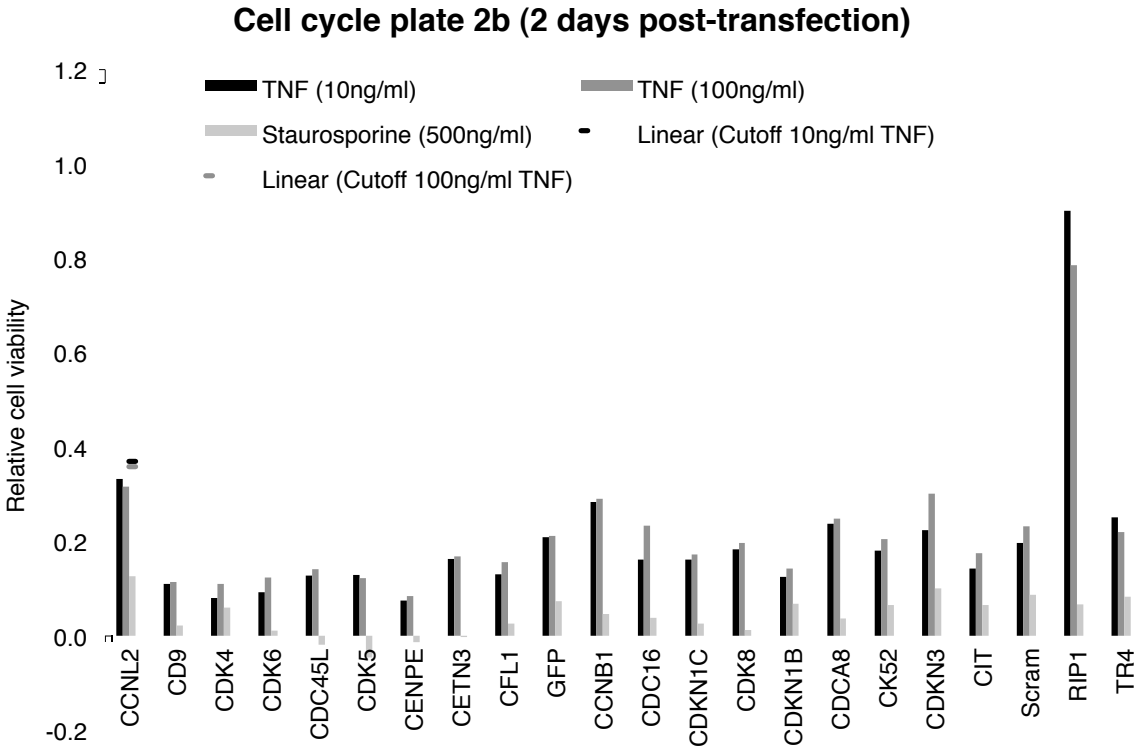
Cell cycle plate 2b (2 days post-transfection)
TNF (10ng/ml)
TNF (100ng/ml)
Staurosporine (500ng/ml)
Linear (Cutoff 10ng/ml TNF)
Linear (Cutoff 100ng/ml TNF)
Relative cell viability
1.2
1.0
0.8
0.6
0.4
0.2
0.0
-0.2
CCNL2
CD9
CDK4
CDK6
CDC45L
CDK5
CENPE
CETN3
CFL1
GFP
CCNB1
CDC16
CDKN1C
CDK8
CDKN1B
CDCA8
CK52
CDKN3
CIT
Scram
RIP1
TR4

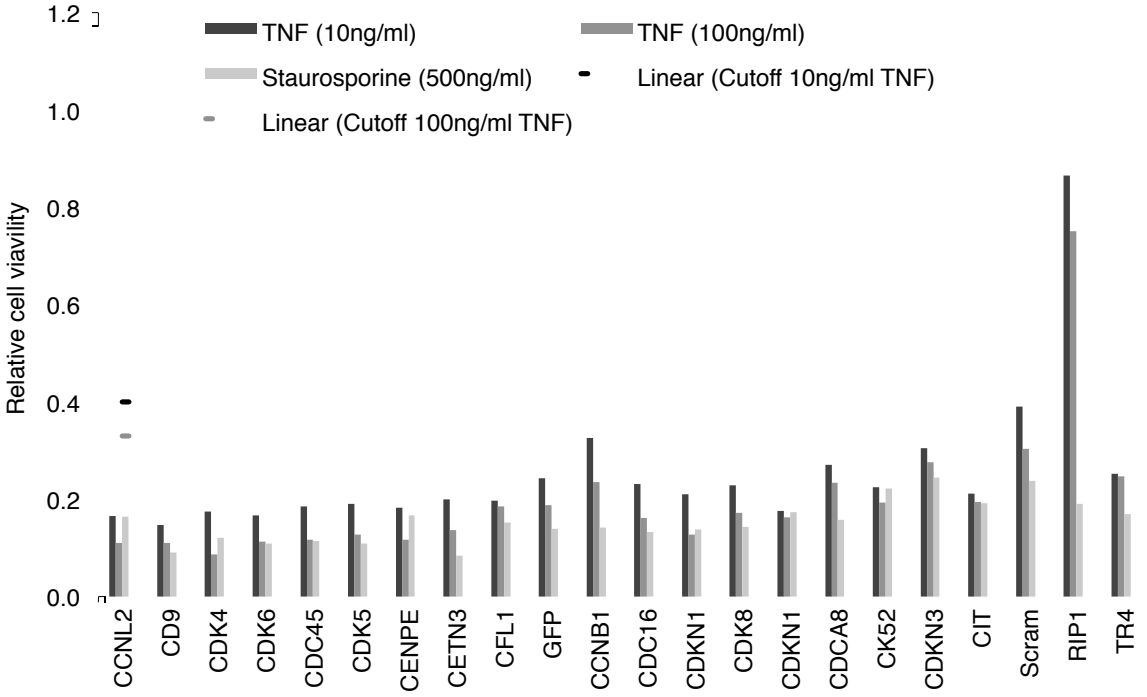
Cell cycle plate 2b (3 days post-transfection)
TNF (10ng/ml)
TNF (100ng/ml)
Staurosporine (500ng/ml)
Linear (Cutoff 10ng/ml TNF)
Linear (Cutoff 100ng/ml TNF)
Relative cell viavility
1.2
1.0
0.8
0.6
0.4
0.2
0.0
CCNL2
CD9
CDK4
CDK6
CDC45
CDK5
CENPE
CETN3
CFL1
GFP
CCNB1
CDC16
CDKN1
CDK8
CDKN1
CDCA8
CK52
CDKN3
CIT
Scram
RIP1
TR4

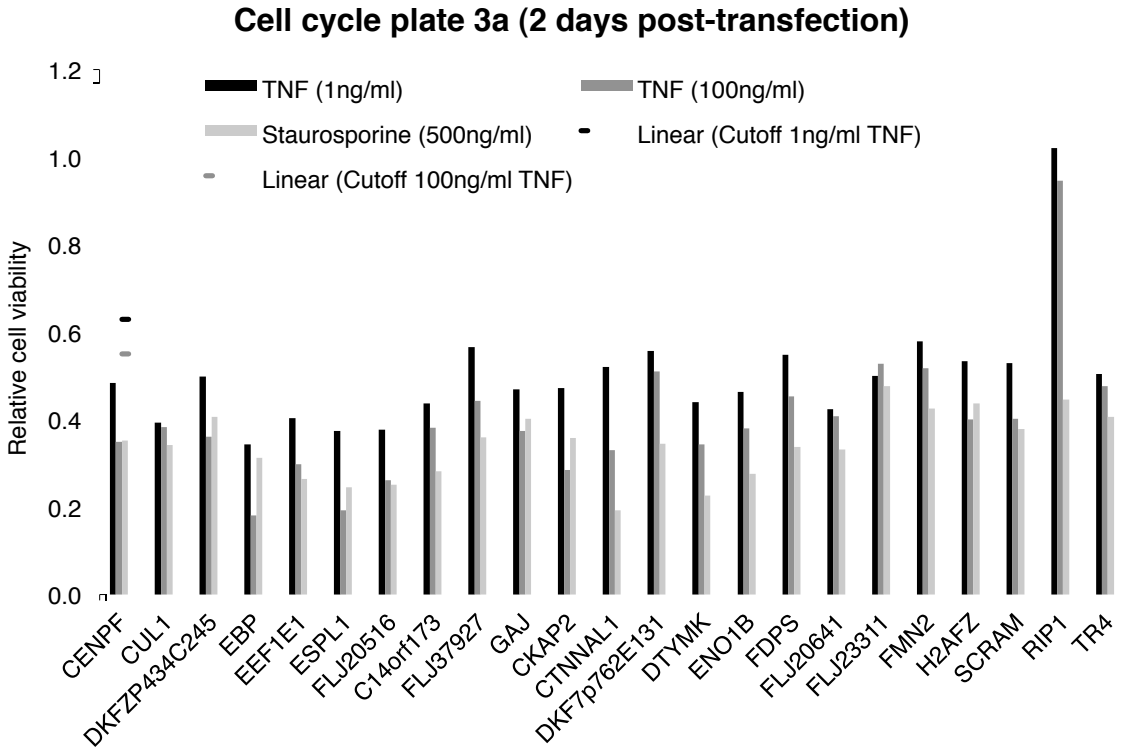
Cell cycle plate 3a (2 days post-transfection)
TNF (1ng/ml)
TNF (100ng/ml)
Staurosporine (500ng/ml)
Linear (Cutoff 1ng/ml TNF)
Linear (Cutoff 100ng/ml TNF)
Relative cell viability
1.2
1.0
0.8
0.6
0.4
0.2
0.0
CENPF
CUL1
DKFZP434C245
EBP
EEF1E1
ESPL1
FLJ20516
C14orf173
FLJ37927
GAJ
CKAP2
CTNNAL1
DKF7p762E131
DTYMK
ENO1B
FDPS
FLJ20641
FLJ23311
FMN2
H2AFZ
SCRAM
RIP1
TR4

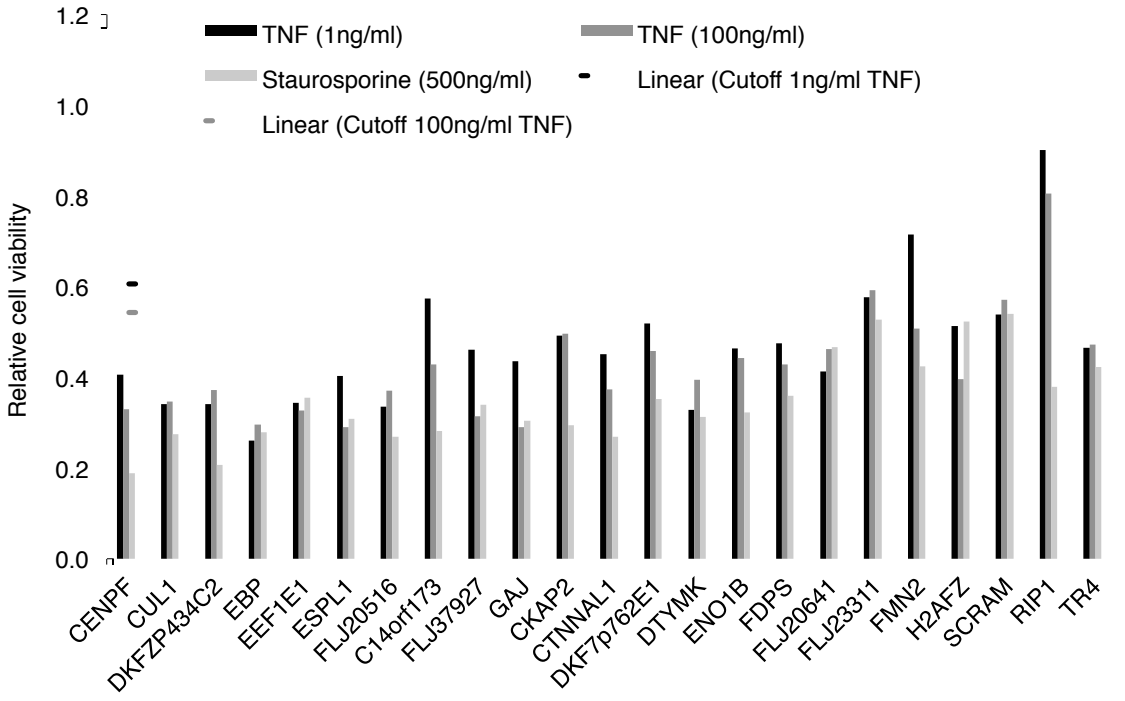
Cell cycle plate 3a (3 days post-transfection)
TNF (1ng/ml)
TNF (100ng/ml)
Staurosporine (500ng/ml)
Linear (Cutoff 1ng/ml TNF)
Linear (Cutoff 100ng/ml TNF)
Relative cell viability
1.2
1.0
0.8
0.6
0.4
0.2
0.0
CENPF
CUL1
DKFZP434C2
EBP
EEF1E1
ESPL1
FLJ20516
C14orf173
FLJ37927
GAJ
CKAP2
CTNNAL1
DKF7p762E1
DTYMK
ENO1B
FDPS
FLJ20641
FLJ23311
FMN2
H2AFZ
SCRAM
RIP1
TR4

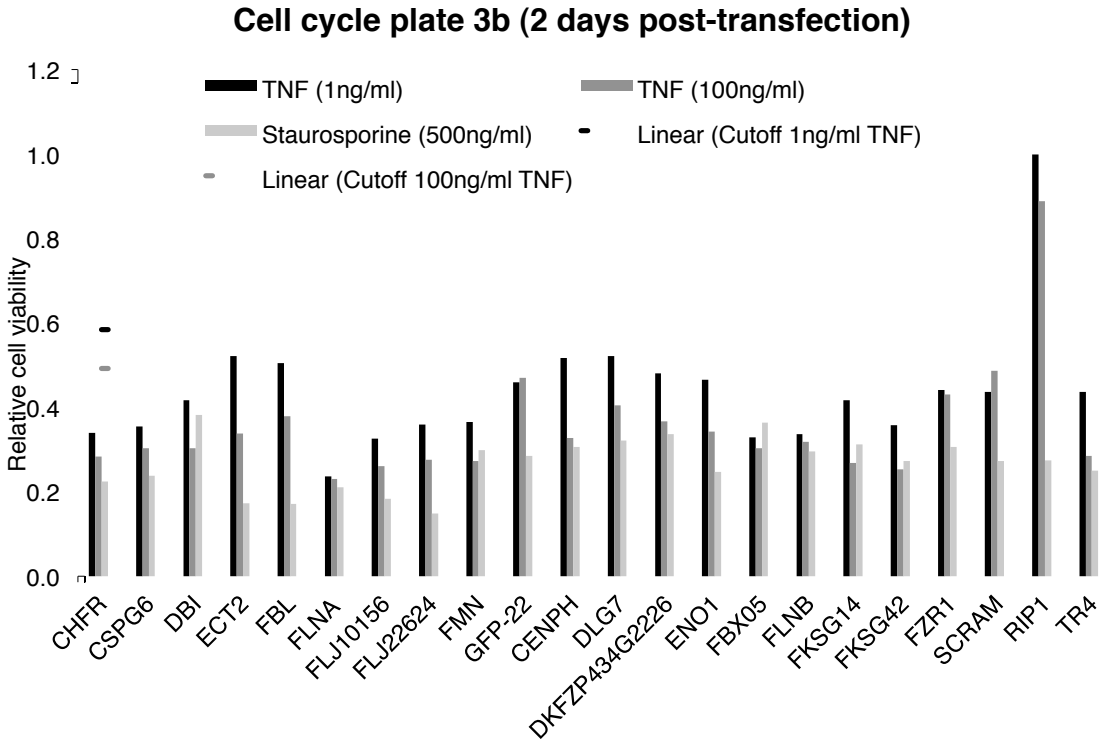
Cell cycle plate 3b (2 days post-transfection)
TNF (1ng/ml)
TNF (100ng/ml)
Staurosporine (500ng/ml)
Linear (Cutoff 1ng/ml TNF)
Linear (Cutoff 100ng/ml TNF)
Relative cell viability
1.2
1.0
0.8
0.6
0.4
0.2
0.0
CHFR
CSPG6
DBI
ECT2
FBL
FLNA
FLJ10156
FLJ22624
FMN
GFP-22
CENPH
DLG7
DKFZP434G2226
ENO1
FBX05
FLNB
FKSG14
FKSG42
FZR1
SCRAM
RIP1
TR4

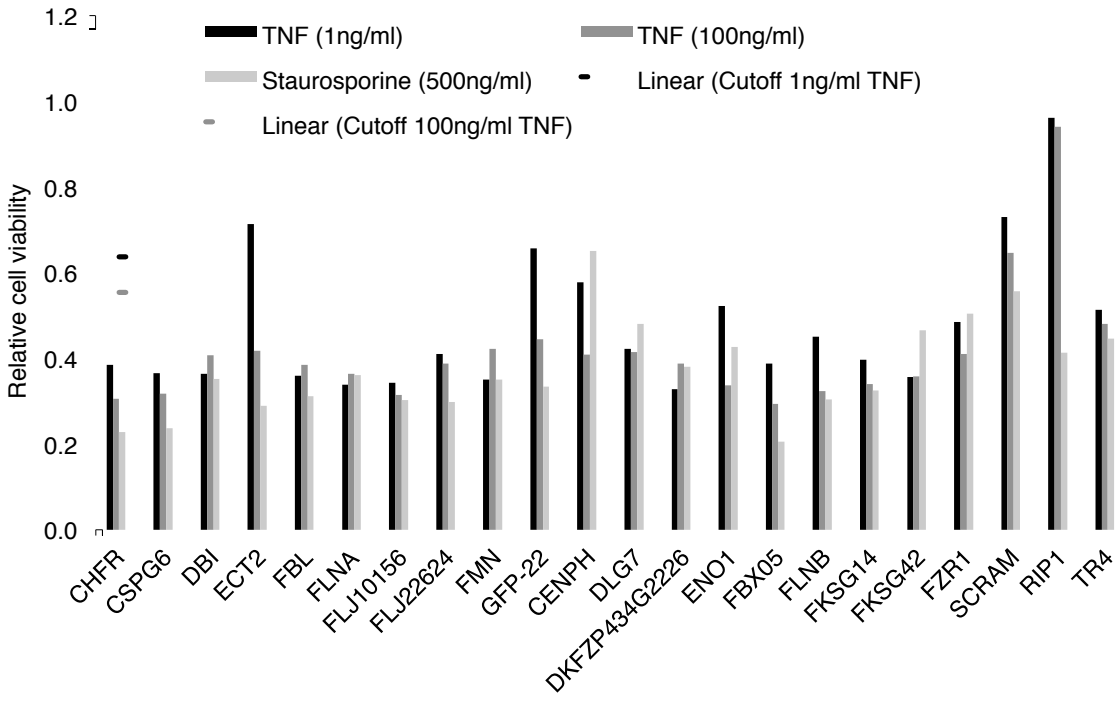
Cell cycle plate 3b (3 days post-transfection)
TNF (1ng/ml)
TNF (100ng/ml)
Staurosporine (500ng/ml)
Linear (Cutoff 1ng/ml TNF)
Linear (Cutoff 100ng/ml TNF)
Relative cell viability
1.2
1.0
0.8
0.6
0.4
0.2
0.0
CHFR
CSPG6
DBI
ECT2
FBL
FLNA
FLJ10156
FLJ22624
FMN
GFP-22
CENPH
DLG7
DKFZP434G2226
ENO1
FBX05
FLNB
FKSG14
FKSG42
FZR1
SCRAM
RIP1
TR4

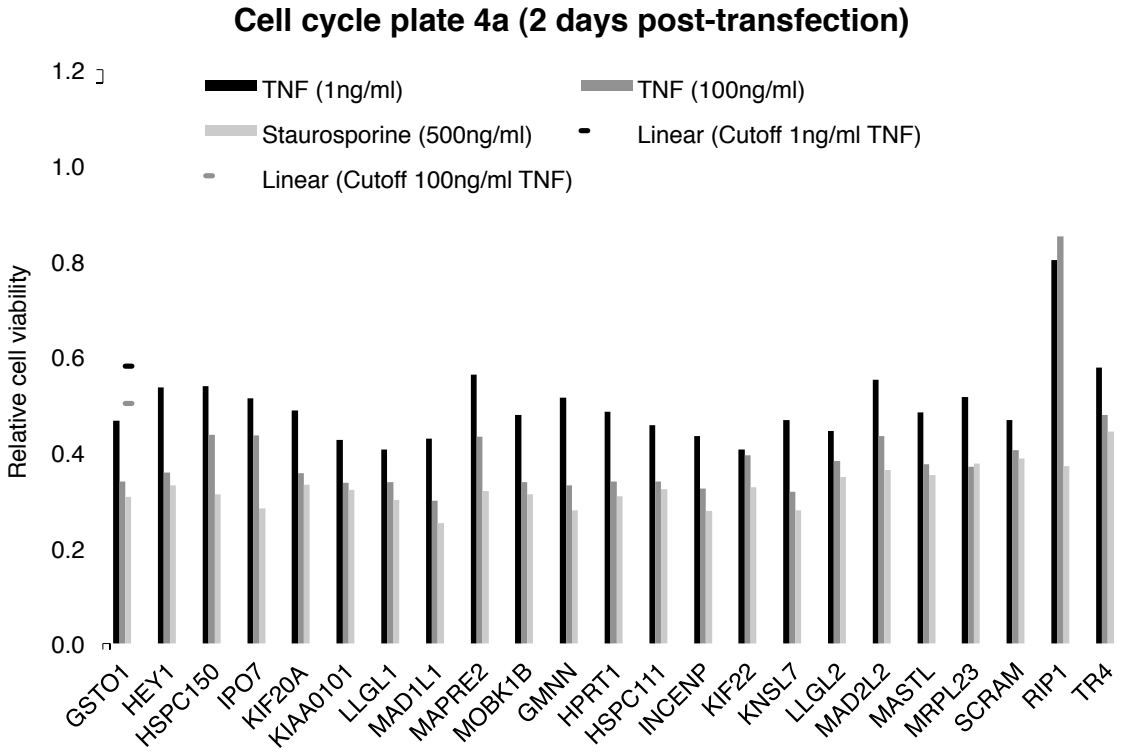
Cell cycle plate 4a (2 days post-transfection)
TNF (1ng/ml)
TNF (100ng/ml)
Staurosporine (500ng/ml)
Linear (Cutoff 1ng/ml TNF)
Linear (Cutoff 100ng/ml TNF)
Relative cell viability
1.2
1.0
0.8
0.6
0.4
0.2
0.0
GSTO1
HEY1
HSPC150
IPO7
KIF20A
KIAA0101
LLGL1
MAD1L1
MAPRE2
MOBK1B
GMNN
HPRT1
HSPC111
INCENP
KIF22
KNSL7
LLGL2
MAD2L2
MASTL
MRPL23
SCRAM
RIP1
TR4

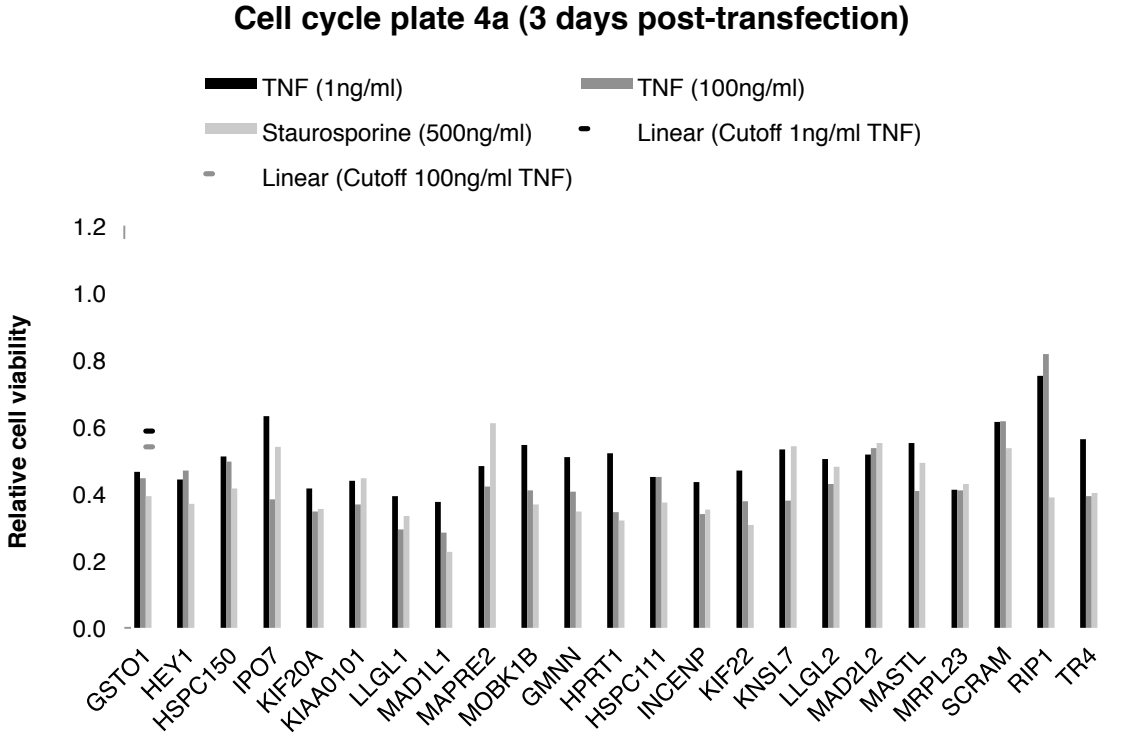
Cell cycle plate 4a (3 days post-transfection)
TNF (1ng/ml)
TNF (100ng/ml)
Staurosporine (500ng/ml)
Linear (Cutoff 1ng/ml TNF)
Linear (Cutoff 100ng/ml TNF)
Relative cell viability
1.2
1.0
0.8
0.6
0.4
0.2
0.0
GSTO1
HEY1
HSPC150
IPO7
KIF20A
KIAA0101
LLGL1
MAD1L1
MAPRE2
MOBK1B
GMNN
HPRT1
HSPC111
INCENP
KIF22
KNSL7
LLGL2
MAD2L2
MASTL
MRPL23
SCRAM
RIP1
TR4

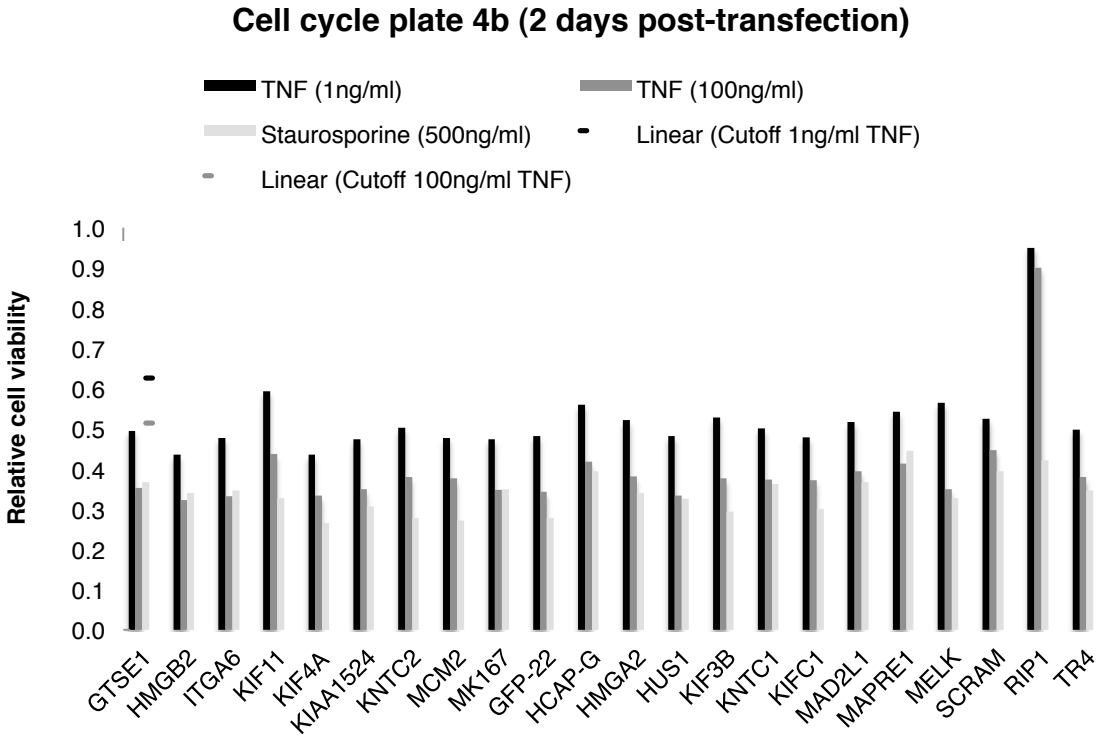
Cell cycle plate 4b (2 days post-transfection)
TNF (1ng/ml)
TNF (100ng/ml)
Staurosporine (500ng/ml)
Linear (Cutoff 1ng/ml TNF)
Linear (Cutoff 100ng/ml TNF)
Relative cell viability
1.0
0.9
0.8
0.7
0.6
0.5
0.4
0.3
0.2
0.1
0.0
GTSE1
HMGB2
ITGA6
KIF11
KIF4A
KIAA1524
KNTC2
MCM2
MK167
GFP-22
HCAP-G
HMGA2
HUS1
KIF3B
KNTC1
KIFC1
MAD2L1
MAPRE1
MELK
SCRAM
RIP1
TR4

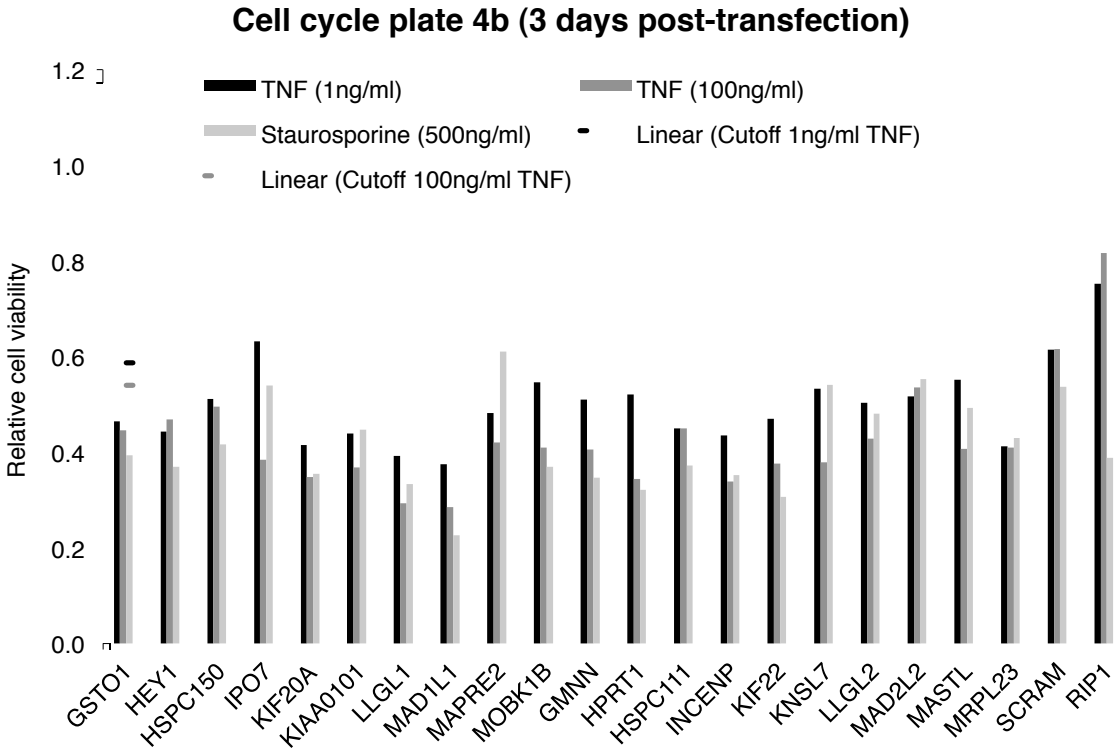
Cell cycle plate 4b (3 days post-transfection)
TNF (1ng/ml)
TNF (100ng/ml)
Staurosporine (500ng/ml)
Linear (Cutoff 1ng/ml TNF)
Linear (Cutoff 100ng/ml TNF)
Relative cell viability
1.2
1.0
0.8
0.6
0.4
0.2
0.0
GSTO1
HEY1
HSPC150
IPO7
KIF20A
KIAA0101
LLGL1
MAD1L1
MAPRE2
MOBK1B
GMNN
HPRT1
HSPC111
INCENP
KIF22
KNSL7
LLGL2
MAD2L2
MASTL
MRPL23
SCRAM
RIP1

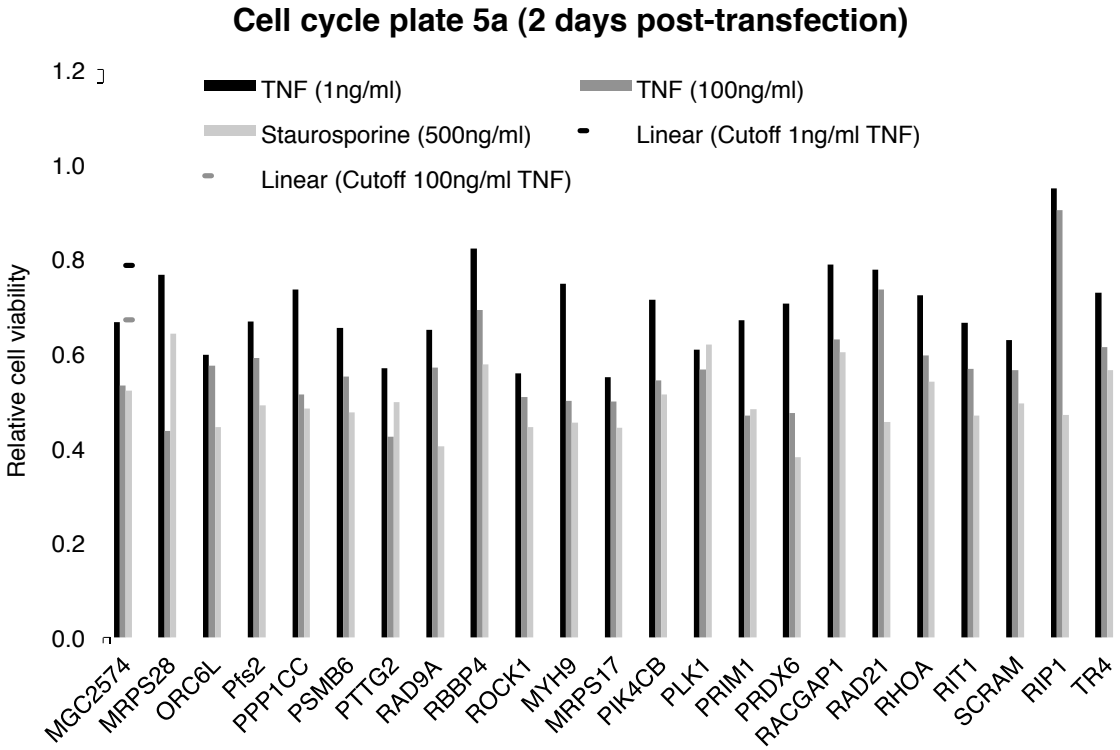
Cell cycle plate 5a (2 days post-transfection)
TNF (1ng/ml)
TNF (100ng/ml)
Staurosporine (500ng/ml)
Linear (Cutoff 1ng/ml TNF)
Linear (Cutoff 100ng/ml TNF)
Relative cell viability
1.2
1.0
0.8
0.6
0.4
0.2
0.0
MGC2574
MRPS28
ORC6L
Pfs2
PPP1CC
PSMB6
PTTG2
RAD9A
RBBP4
ROCK1
MYH9
MRPS17
PIK4CB
PLK1
PRIM1
PRDX6
RACGAP1
RAD21
RHOA
RIT1
SCRAM
RIP1
TR4

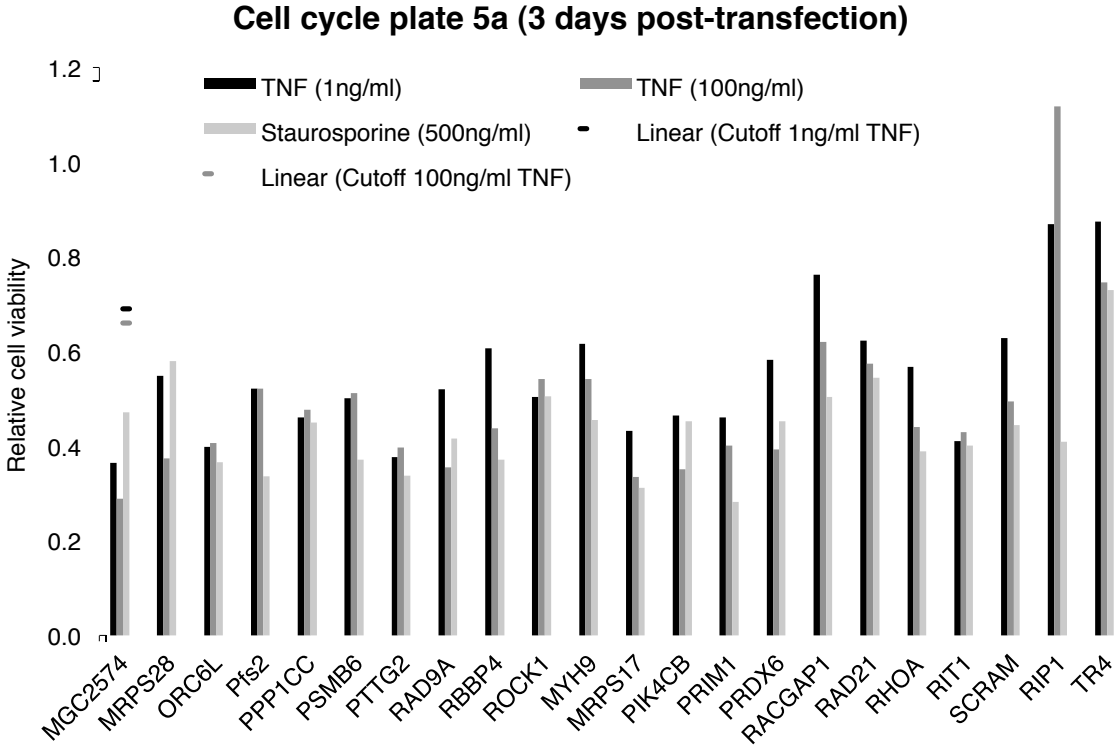
Cell cycle plate 5a (3 days post-transfection)
TNF (1ng/ml)
TNF (100ng/ml)
Staurosporine (500ng/ml)
Linear (Cutoff 1ng/ml TNF)
Linear (Cutoff 100ng/ml TNF)
Relative cell viability
1.2
1.0
0.8
0.6
0.4
0.2
0.0
MGC2574
MRPS28
ORC6L
Pfs2
PPP1CC
PSMB6
PTTG2
RAD9A
RBBP4
ROCK1
MYH9
MRPS17
PIK4CB
PRIM1
PRDX6
RACGAP1
RAD21
RHOA
RIT1
SCRAM
RIP1
TR4

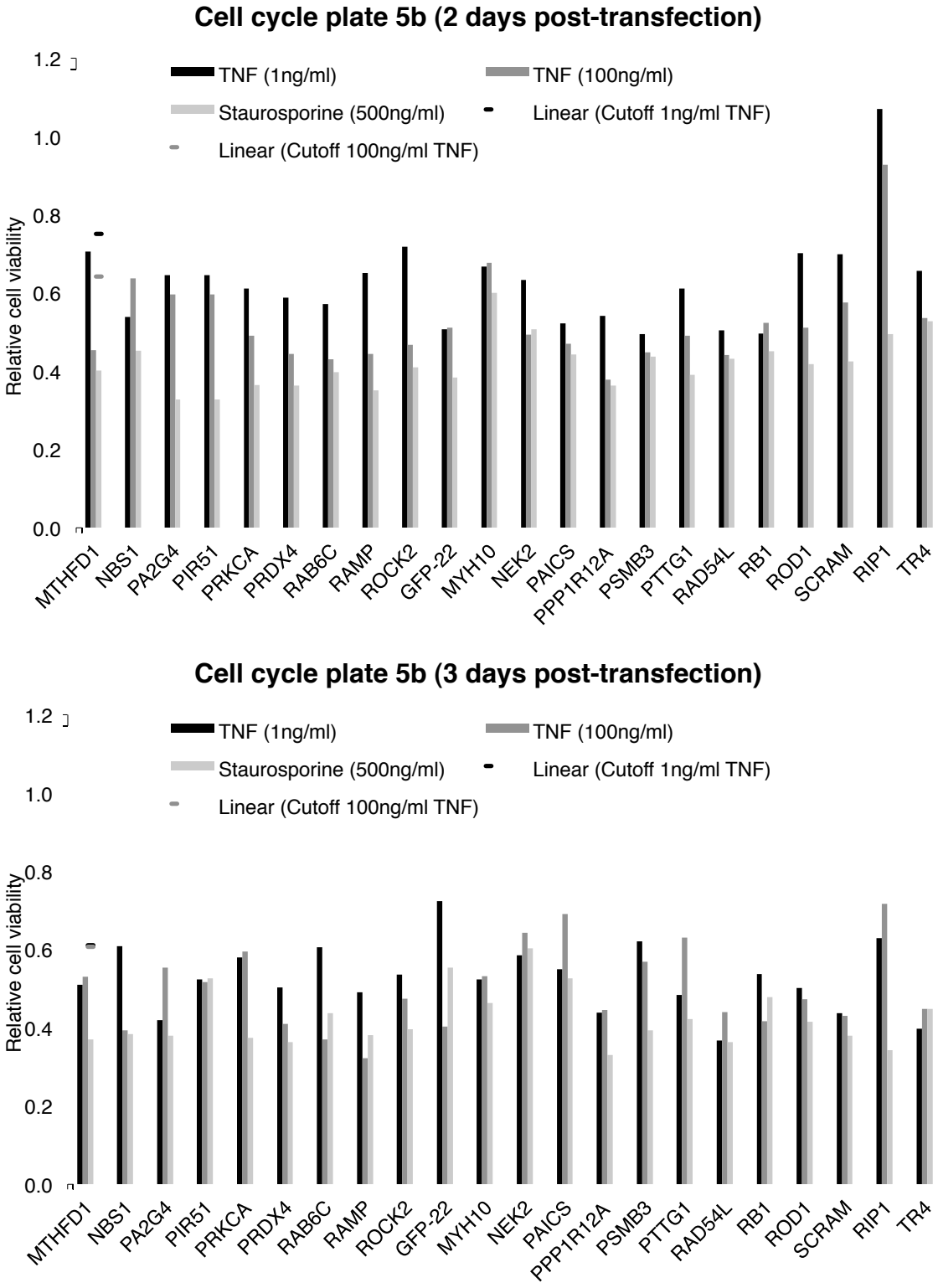
Cell cycle plate 5b (2 days post-transfection)
TNF (1ng/ml)
TNF (100ng/ml)
Staurosporine (500ng/ml)
Linear (Cutoff 1ng/ml TNF)
Linear (Cutoff 100ng/ml TNF)
Relative cell viability
1.2
1.0
0.8
0.6
0.4
0.2
0.0
MTHFD1
NBS1
PA2G4
PIR51
PRKCA
PRDX4
RAB6C
RAMP
ROCK2
GFP-22
MYH10
NEK2
PAICS
PPP1R12A
PSMB3
PTTG1
RAD54L
RB1
ROD1
SCRAM
RIP1
TR4
Cell cycle plate 5b (3 days post-transfection)
TNF (1ng/ml)
TNF (100ng/ml)
Staurosporine (500ng/ml)
Linear (Cutoff 1ng/ml TNF)
Linear (Cutoff 100ng/ml TNF)
Relative cell viability
1.2
1.0
0.8
0.6
0.4
0.2
0.0
MTHFD1
NBS1
PA2G4
PIR51
PRKCA
PRDX4
RAB6C
RAMP
ROCK2
GFP-22
MYH10
NEK2
PAICS
PPP1R12A
PSMB3
PTTG1
RAD54L
RB1
ROD1
SCRAM
RIP1
TR4

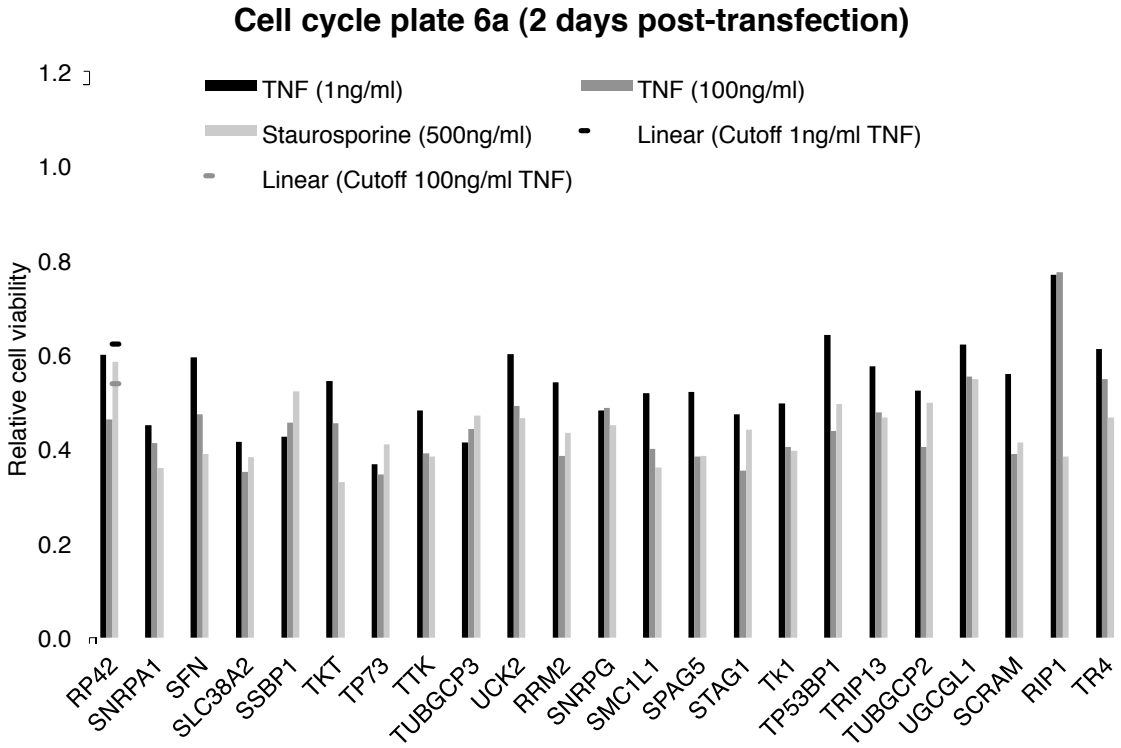
Cell cycle plate 6a (2 days post-transfection)
TNF (1ng/ml)
TNF (100ng/ml)
Staurosporine (500ng/ml)
Linear (Cutoff 1ng/ml TNF)
Linear (Cutoff 100ng/ml TNF)
Relative cell viability
1.2
1.0
0.8
0.6
0.4
0.2
0.0
RP42
SNRPA1
SFN
SLC38A2
SSBP1
TKT
TP73
TTK
TUBGCP3
UCK2
RRM2
SNRPG
SMC1L1
SPAG5
STAG1
Tk1
TP53BP1
TRIP13
TUBGCP2
UGCGL1
SCRAM
RIP1
TR4

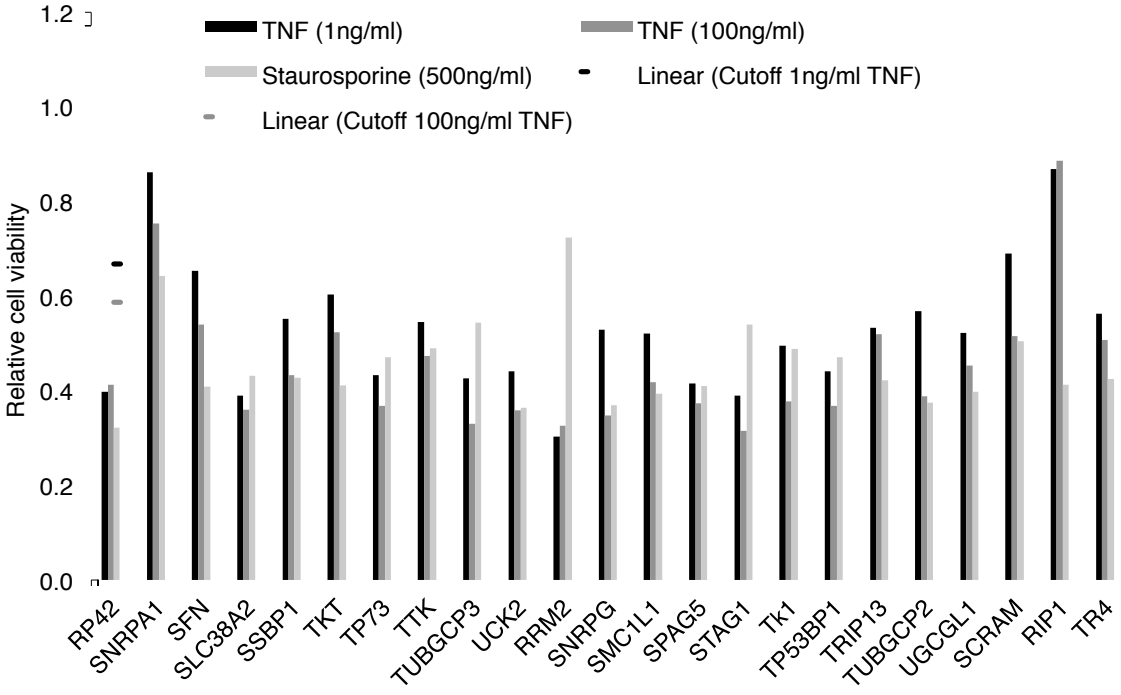
Cell cycle plate 6a (3 days post-transfection)
TNF (1ng/ml)
TNF (100ng/ml)
Staurosporine (500ng/ml)
Linear (Cutoff 1ng/ml TNF)
Linear (Cutoff 100ng/ml TNF)
Relative cell viability
1.2
1.0
0.8
0.6
0.4
0.2
0.0
RP42
SNRPA1
SFN
SLC38A2
SSBP1
TKT
TP73
TTK
TUBGCP3
UCK2
RRM2
SNRPG
SMC1L1
SPAG5
STAG1
Tk1
TP53BP1
TRIP13
TUBGCP2
UGCGL1
SCRAM
RIP1
TR4

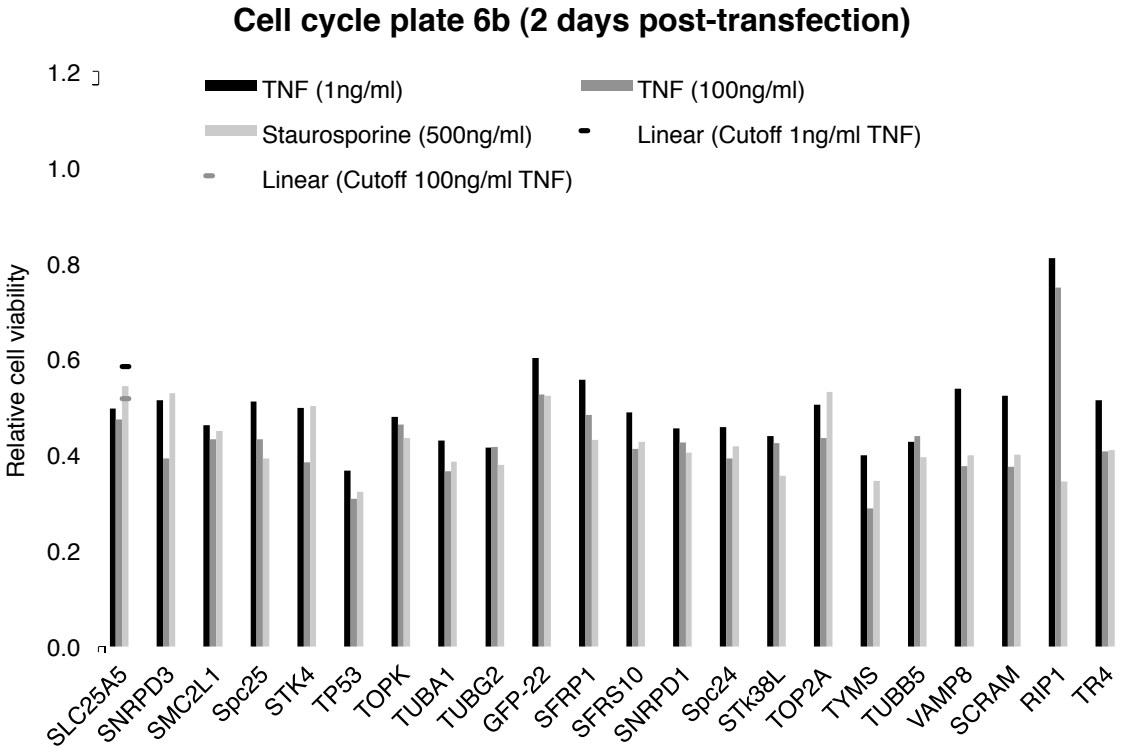
Cell cycle plate 6b (2 days post-transfection)
TNF (1ng/ml)
TNF (100ng/ml)
Staurosporine (500ng/ml)
Linear (Cutoff 1ng/ml TNF)
Linear (Cutoff 100ng/ml TNF)
Relative cell viability
1.2
1.0
0.8
0.6
0.4
0.2
0.0
SLC25A5
SNRPD3
SMC2L1
Spc25
STK4
TP53
TOPK
TUBA1
TUBG2
GFP-22
SFRP1
SFRS10
SNRPD1
Spc24
STK38L
TOP2A
TYMS
TUBB5
VAMP8
SCRAM
RIP1
TR4

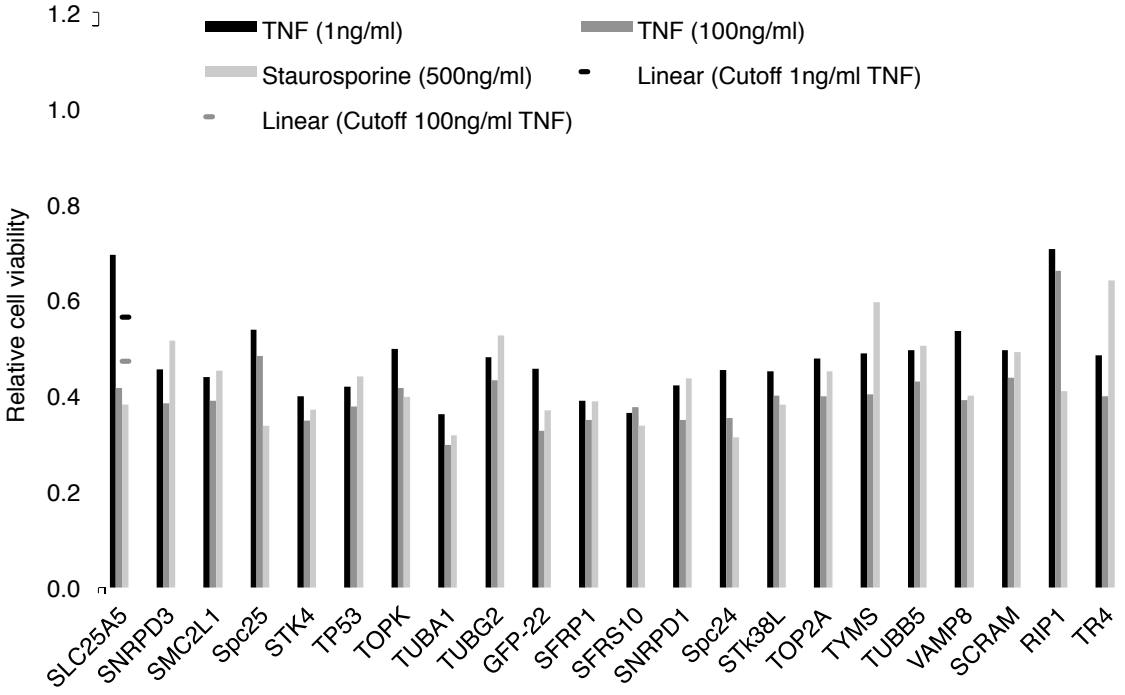
Cell cycle plate 6b (3 days post-transfection)
TNF (1ng/ml)
TNF (100ng/ml)
Staurosporine (500ng/ml)
Linear (Cutoff 1ng/ml TNF)
Linear (Cutoff 100ng/ml TNF)
Relative cell viability
1.2
1.0
0.8
0.6
0.4
0.2
0.0
SLC25A5
SNRPD3
SMC2L1
Spc25
STK4
TP53
TOPK
TUBA1
TUBG2
GFP-22
SFRP1
SFRS10
SNRPD1
Spc24
STK38L
TOP2A
TYMS
TUBB5
VAMP8
SCRAM
RIP1
TR4

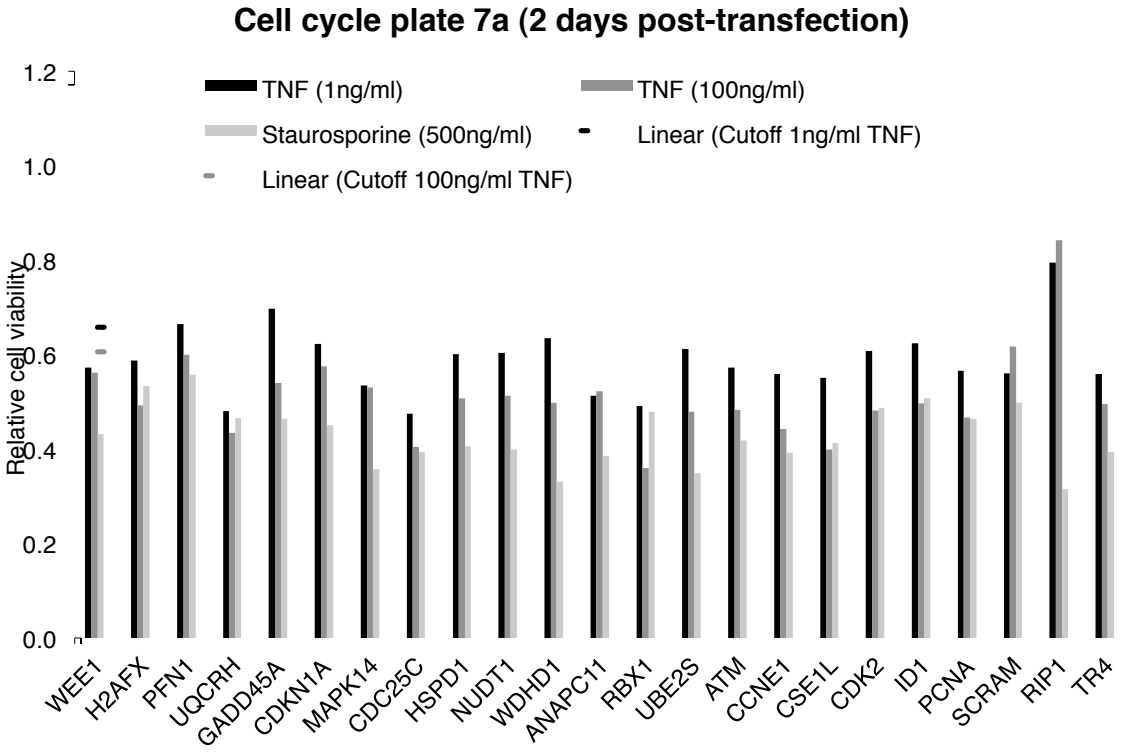
Cell cycle plate 7a (2 days post-transfection)
TNF (1ng/ml)
TNF (100ng/ml)
Staurosporine (500ng/ml)
Linear (Cutoff 1ng/ml TNF)
Linear (Cutoff 100ng/ml TNF)
Relative cell viability
1.2
1.0
0.8
0.6
0.4
0.2
0.0
WEE1
H2AFX
PFN1
UQCRH
GADD45A
CDKN1A
MAPK14
CDC25C
HSPD1
NUDT1
WDHD1
ANAPC11
RBX1
UBE2S
ATM
CCNE1
CSE1L
CDK2
ID1
PCNA
SCRAM
RIP1
TR4

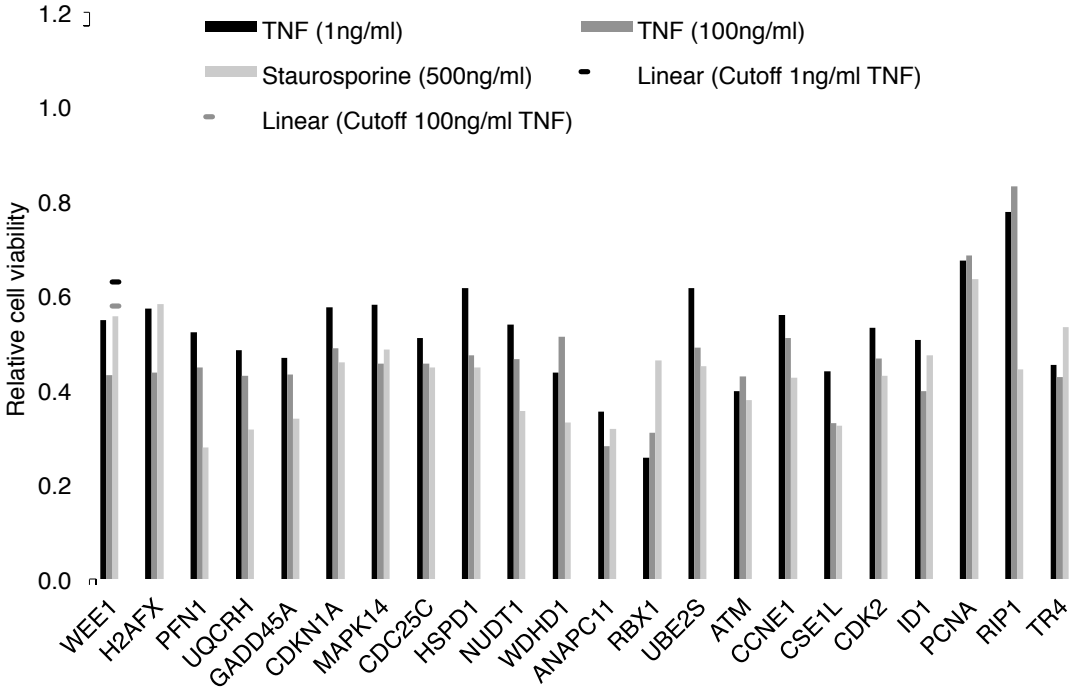
Cell cycle plate 7a (3 days post-transfection)
TNF (1ng/ml)
TNF (100ng/ml)
Staurosporine (500ng/ml)
Linear (Cutoff 1ng/ml TNF)
Linear (Cutoff 100ng/ml TNF)
Relative cell viability
1.2
1.0
0.8
0.6
0.4
0.2
0.0
WEE1
H2AFX
PFN1
UQCRH
GADD45A
CDKN1A
MAPK14
CDC25C
HSPD1
NUDT1
WDHD1
ANAPC11
RBX1
UBE2S
ATM
CCNE1
CSE1L
CDK2
ID1
PCNA
RIP1
TR4

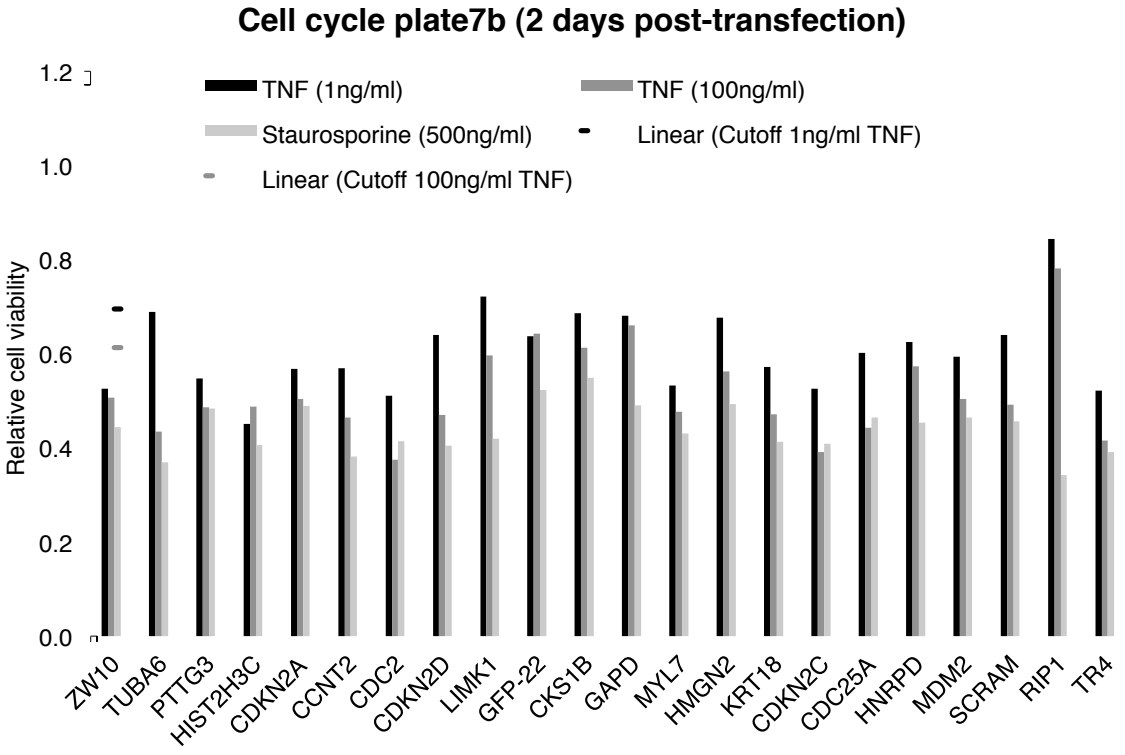
Cell cycle plate7b (2 days post-transfection)
TNF (1ng/ml)
TNF (100ng/ml)
Staurosporine (500ng/ml)
Linear (Cutoff 1ng/ml TNF)
Linear (Cutoff 100ng/ml TNF)
Relative cell viability
1.2
1.0
0.8
0.6
0.4
0.2
0.0
ZW10
TUBA6
PTTG3
HIST2H3C
CDKN2A
CCNT2
CDC2
CDKN2D
LIMK1
GFP-22
CKS1B
GAPD
MYL7
HMGN2
KRT18
CDKN2C
CDC25A
HNRPD
MDM2
SCRAM
RIP1
TR4

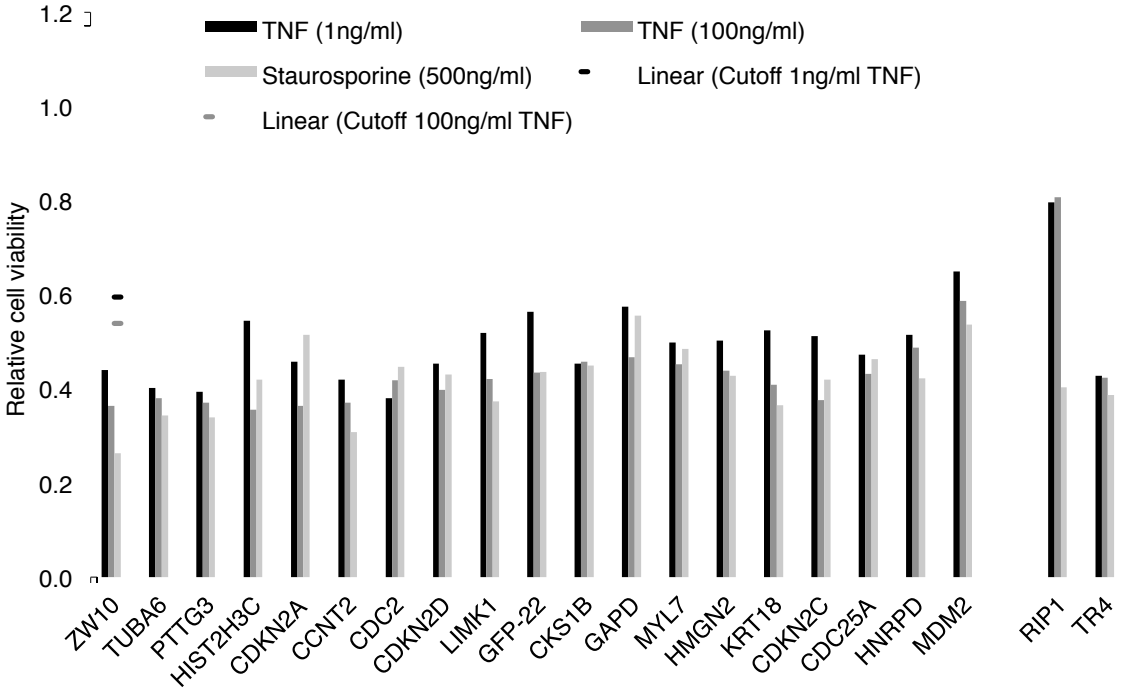
Cell cycle plate 7b (3 days post-transfection)
TNF (1ng/ml)
TNF (100ng/ml)
Staurosporine (500ng/ml)
Linear (Cutoff 1ng/ml TNF)
Linear (Cutoff 100ng/ml TNF)
Relative cell viability
1.2
1.0
0.8
0.6
0.4
0.2
0.0
ZW10
TUBA6
PTTG3
HIST2H3C
CDKN2A
CCNT2
CDC2
CDKN2D
LIMK1
GFP-22
CKS1B
GAPD
MYL7
HMGN2
KRT18
CDKN2C
CDC25A
HNRPD
MDM2
RIP1
TR4

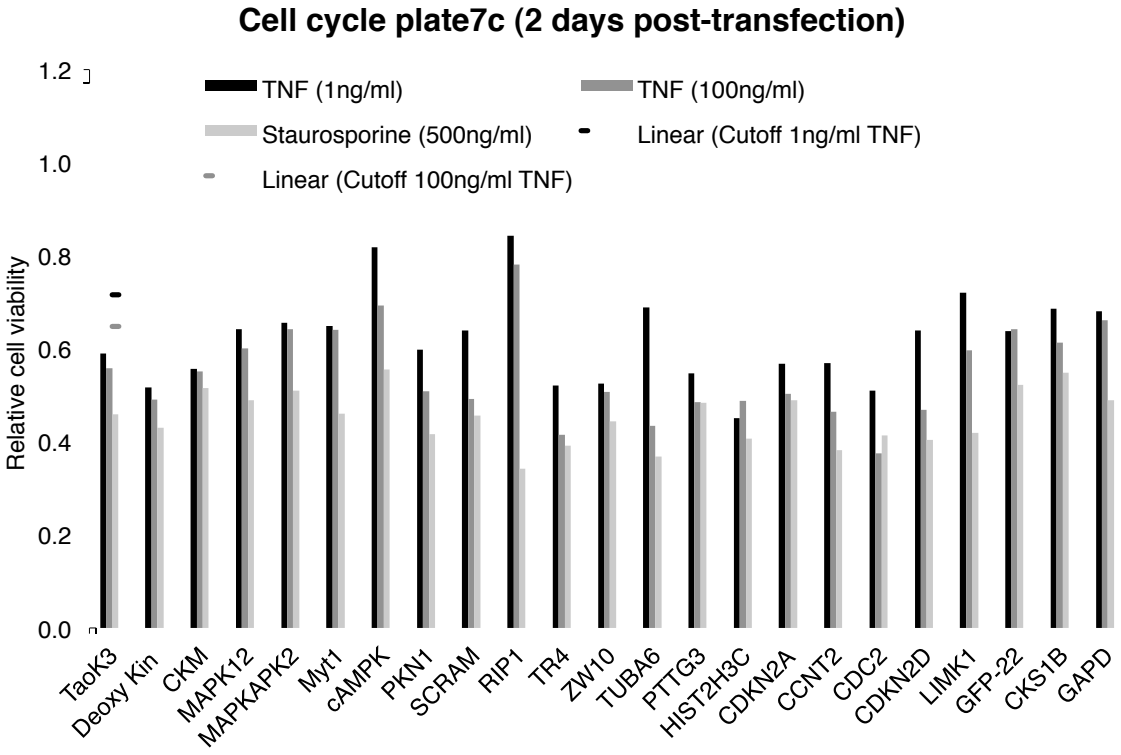
Cell cycle plate7c (2 days post-transfection)
TNF (1ng/ml)
TNF (100ng/ml)
Staurosporine (500ng/ml)
Linear (Cutoff 1ng/ml TNF)
Linear (Cutoff 100ng/ml TNF)
Relative cell viability
1.2
1.0
0.8
0.6
0.4
0.2
0.0
TaoK3
Deoxy Kin
CKM
MAPK12
MAPKAPK2
Myt1
cAMPK
PKN1
SCRAM
RIP1
TR4
ZW10
TUBA6
PTTG3
HIST2H3C
CDKN2A
CCNT2
CDC2
CDKN2D
LIMK1
GFP-22
CKS1B
GAPD

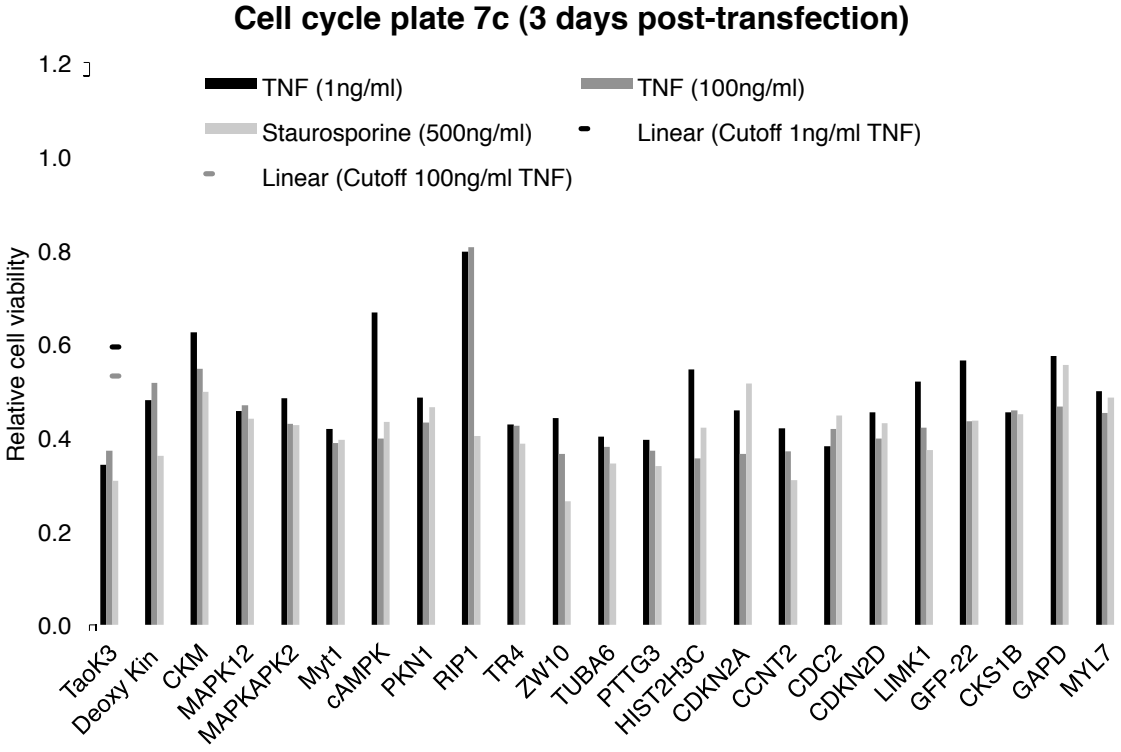
Cell cycle plate 7c (3 days post-transfection)
TNF (1ng/ml)
TNF (100ng/ml)
Staurosporine (500ng/ml)
Linear (Cutoff 1ng/ml TNF)
Linear (Cutoff 100ng/ml TNF)
Relative cell viability
1.2
1.0
0.8
0.6
0.4
0.2
0.0
TaoK3
Deoxy Kin
CKM
MAPK12
MAPKAPK2
Myt1
cAMPK
PKN1
RIP1
TR4
ZW10
TUBA6
PTTG3
HIST2H3C
CDKN2A
CCNT2
CDC2
CDKN2D
LIMK1
GFP-22
CKS1B
GAPD
MYL7

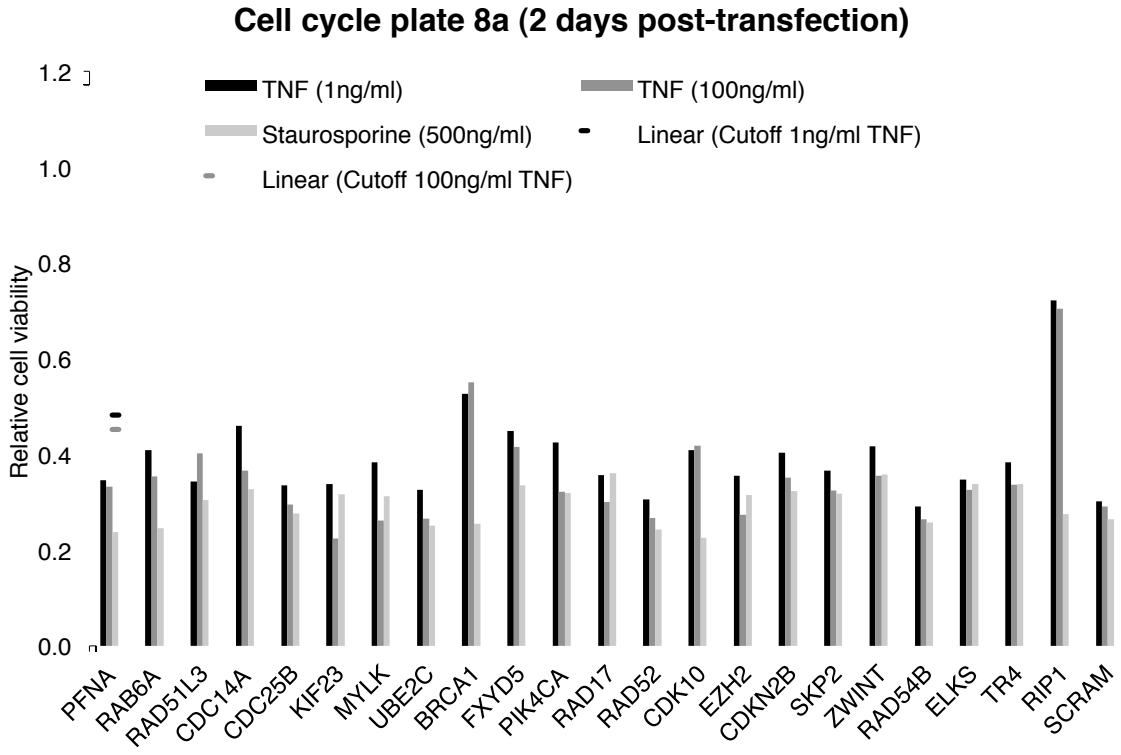
Cell cycle plate 8a (2 days post-transfection)
TNF (1ng/ml)
TNF (100ng/ml)
Staurosporine (500ng/ml)
Linear (Cutoff 1ng/ml TNF)
Linear (Cutoff 100ng/ml TNF)
Relative cell viability
1.2
1.0
0.8
0.6
0.4
0.2
0.0
PFNA
RAB6A
RAD51L3
CDC14A
CDC25B
KIF23
MYLK
UBE2C
BRCA1
FXYD5
PIK4CA
RAD17
RAD52
CDK10
EZH2
CDKN2B
SKP2
ZWINT
RAD54B
ELKS
TR4
RIP1
SCRAM

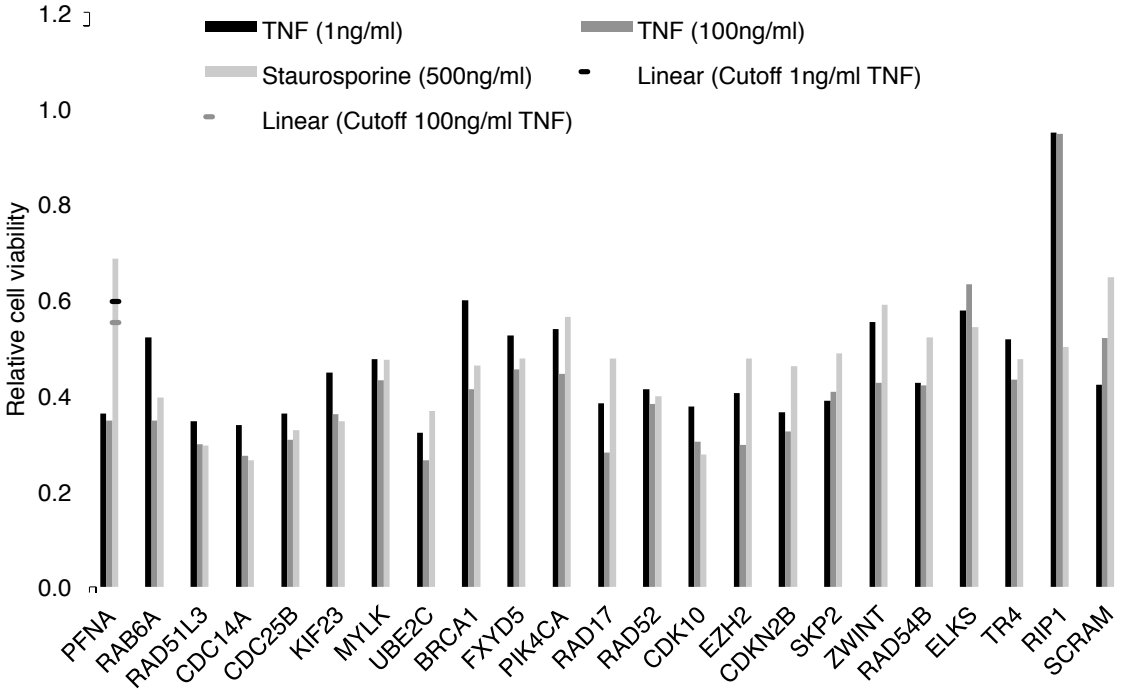
Cell cycle plate 8a (3 days post-transfection)
TNF (1ng/ml)
TNF (100ng/ml)
Staurosporine (500ng/ml)
Linear (Cutoff 1ng/ml TNF)
Linear (Cutoff 100ng/ml TNF)
Relative cell viability
1.2
1.0
0.8
0.6
0.4
0.2
0.0
PFNA
RAB6A
RAD51L3
CDC14A
CDC25B
KIF23
MYLK
UBE2C
BRCA1
FXYD5
PIK4CA
RAD17
RAD52
CDK10
EZH2
CDKN2B
SKP2
ZWINT
RAD54B
ELKS
TR4
RIP1
SCRAM

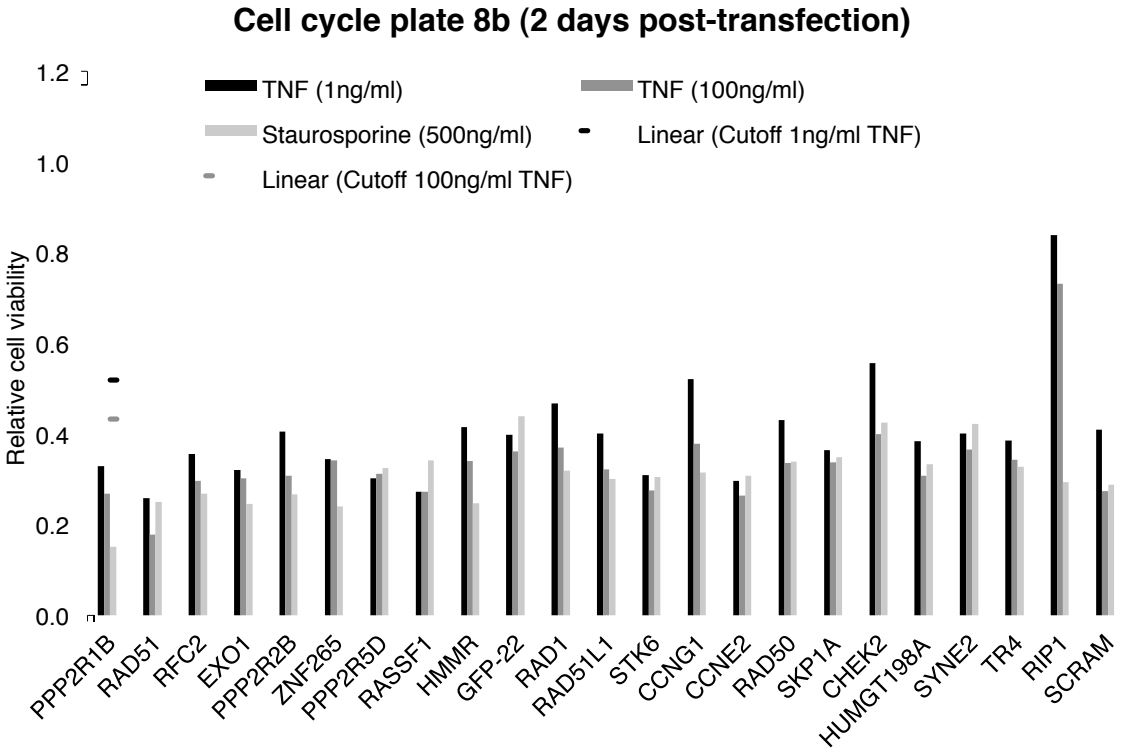
Cell cycle plate 8b (2 days post-transfection)
TNF (1ng/ml)
TNF (100ng/ml)
Staurosporine (500ng/ml)
Linear (Cutoff 1ng/ml TNF)
Linear (Cutoff 100ng/ml TNF)
Relative cell viability
1.2
1.0
0.8
0.6
0.4
0.2
0.0
PPP2R1B
RAD51
RFC2
EXO1
PPP2R2B
ZNF265
PPP2R5D
RASSF1
HMMR
GFP-22
RAD1
RAD51L1
STK6
CCNG1
CCNE2
RAD50
SKP1A
CHEK2
HUMGT198A
SYNE2
TR4
RIP1
SCRAM

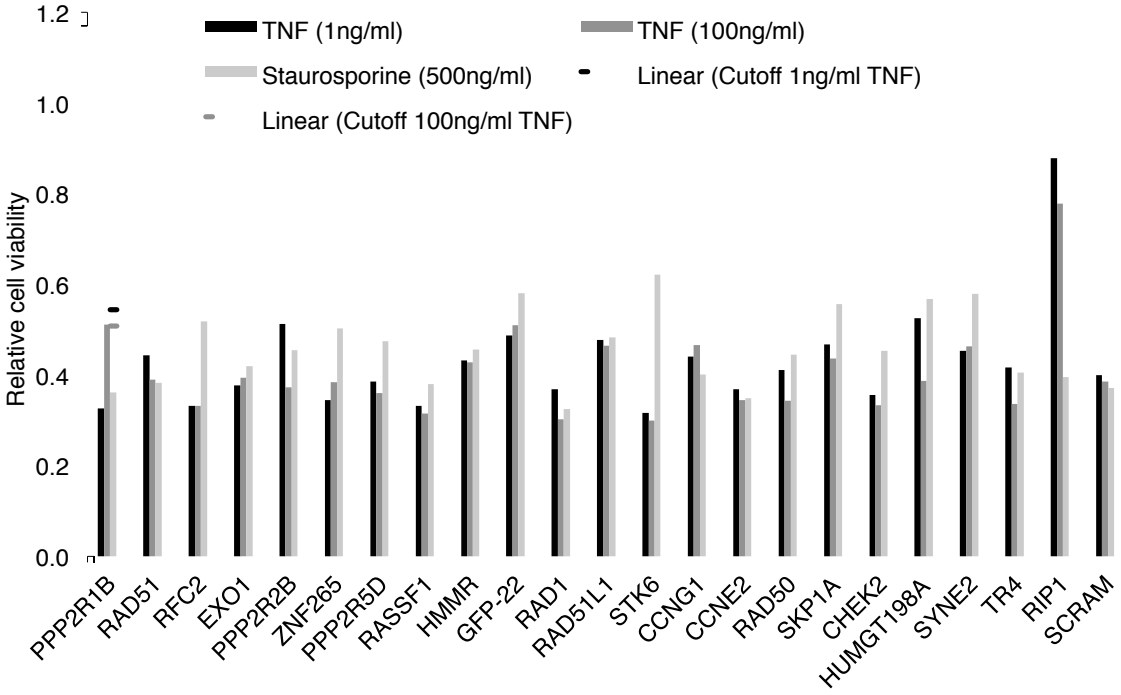
Cell cycle plate 8b (3 days post-transfection)
TNF (1ng/ml)
TNF (100ng/ml)
Staurosporine (500ng/ml)
Linear (Cutoff 1ng/ml TNF)
Linear (Cutoff 100ng/ml TNF)
Relative cell viability
1.2
1.0
0.8
0.6
0.4
0.2
0.0
PPP2R1B
RAD51
RFC2
EXO1
PPP2R2B
ZNF265
PPP2R5D
RASSF1
HMMR
GFP-22
RAD1
RAD51L1
STK6
CCNG1
CCNE2
RAD50
SKP1A
CHEK2
HUMGT198A
SYNE2
TR4
RIP1
SCRAM

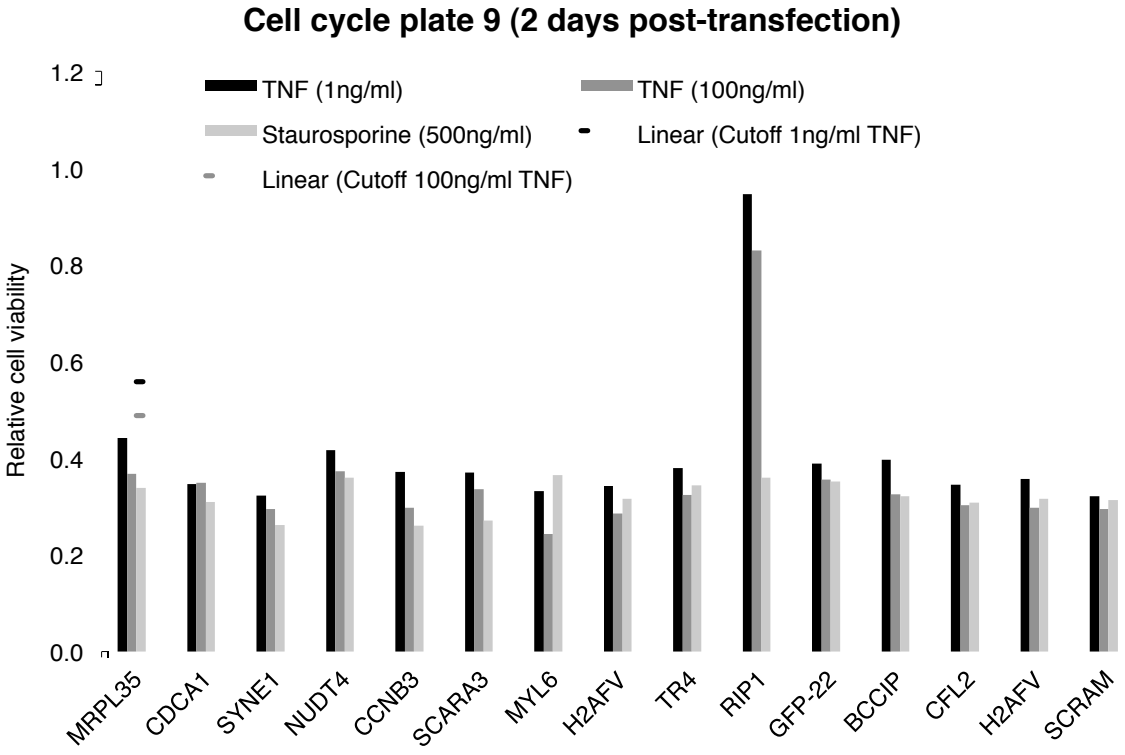
Cell cycle plate 9 (2 days post-transfection)
TNF (1ng/ml)
TNF (100ng/ml)
Staurosporine (500ng/ml)
Linear (Cutoff 1ng/ml TNF)
Linear (Cutoff 100ng/ml TNF)
Relative cell viability
1.2
1.0
0.8
0.6
0.4
0.2
0.0
MRPL35
CDCA1
SYNE1
NUDT4
CCNB3
SCARA3
MYL6
H2AFV
TR4
RIP1
GFP-22
BCCIP
CFL2
H2AFV
SCRAM

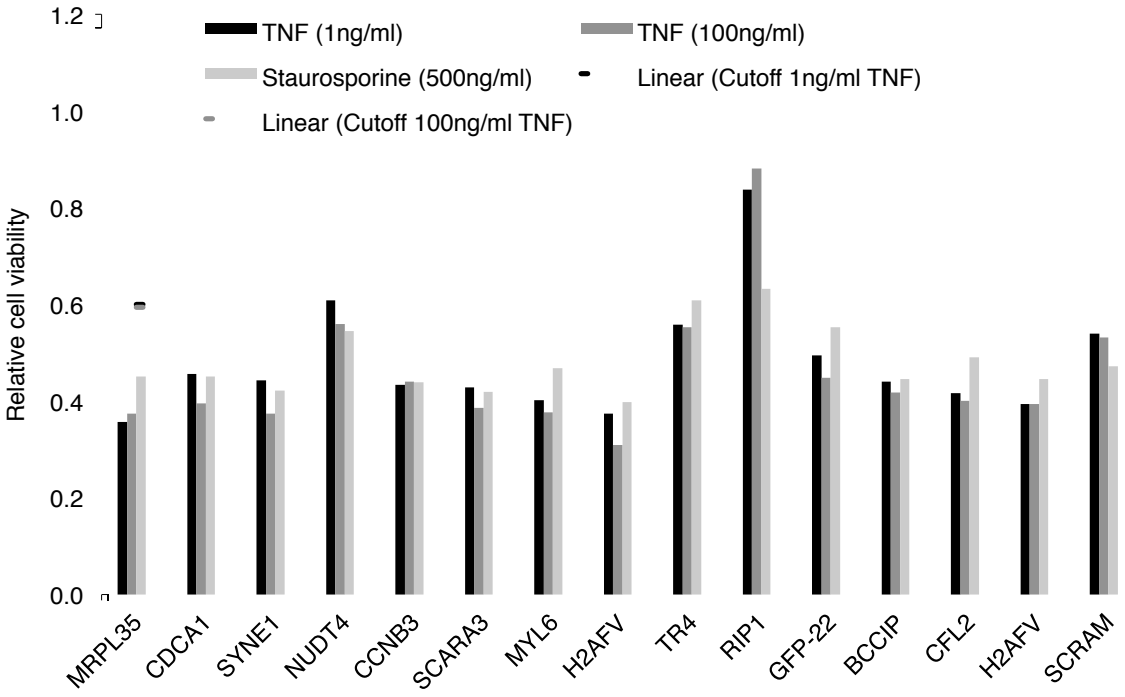
Cell cycle plate 9 (3 days post-transfection)
TNF (1ng/ml)
TNF (100ng/ml)
Staurosporine (500ng/ml)
Linear (Cutoff 1ng/ml TNF)
Linear (Cutoff 100ng/ml TNF)
Relative cell viability
1.2
1.0
0.8
0.6
0.4
0.2
0.0
MRPL35
CDCA1
SYNE1
NUDT4
CCNB3
SCARA3
MYL6
H2AFV
TR4
RIP1
GFP-22
BCCIP
CFL2
H2AFV
SCRAM

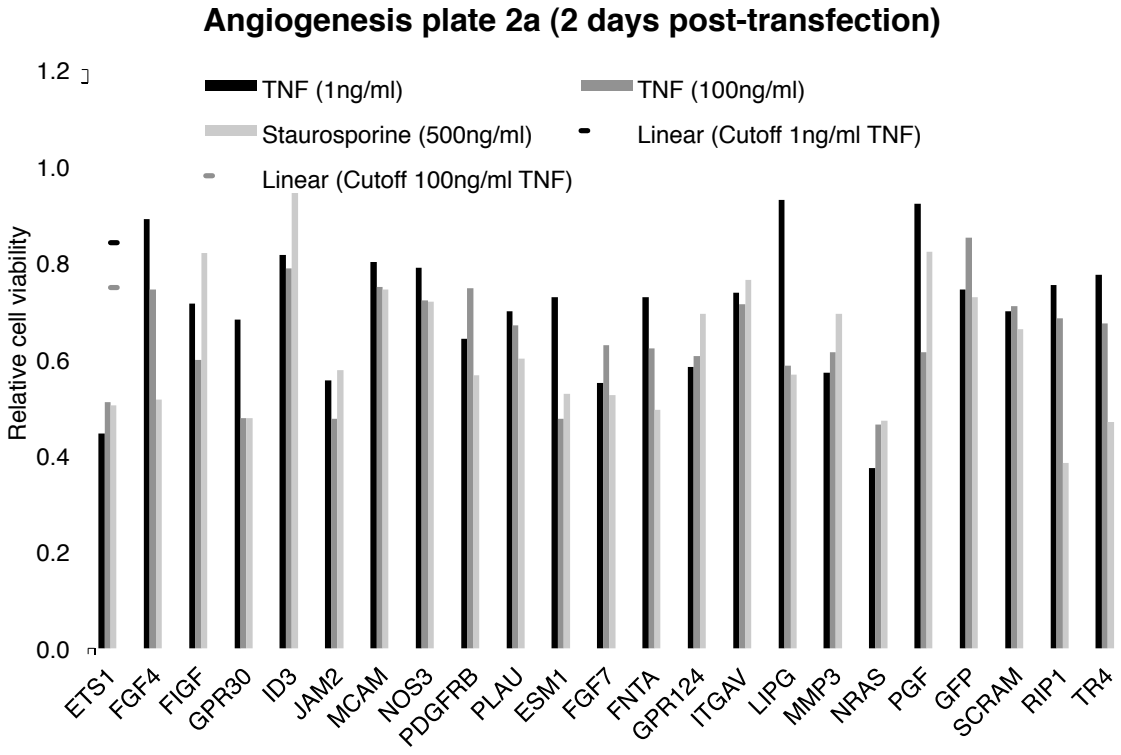
Angiogenesis plate 2a (2 days post-transfection)
TNF (1ng/ml)
TNF (100ng/ml)
Staurosporine (500ng/ml)
Linear (Cutoff 1ng/ml TNF)
Linear (Cutoff 100ng/ml TNF)
Relative cell viability
1.2
1.0
0.8
0.6
0.4
0.2
0.0
ETS1
FGF4
FIGF
GPR30
ID3
JAM2
MCAM
NOS3
PDGFRB
PLAU
ESM1
FGF7
FNTA
GPR124
ITGAV
LIPG
MMP3
NRAS
PGF
GFP
SCRAM
RIP1
TR4

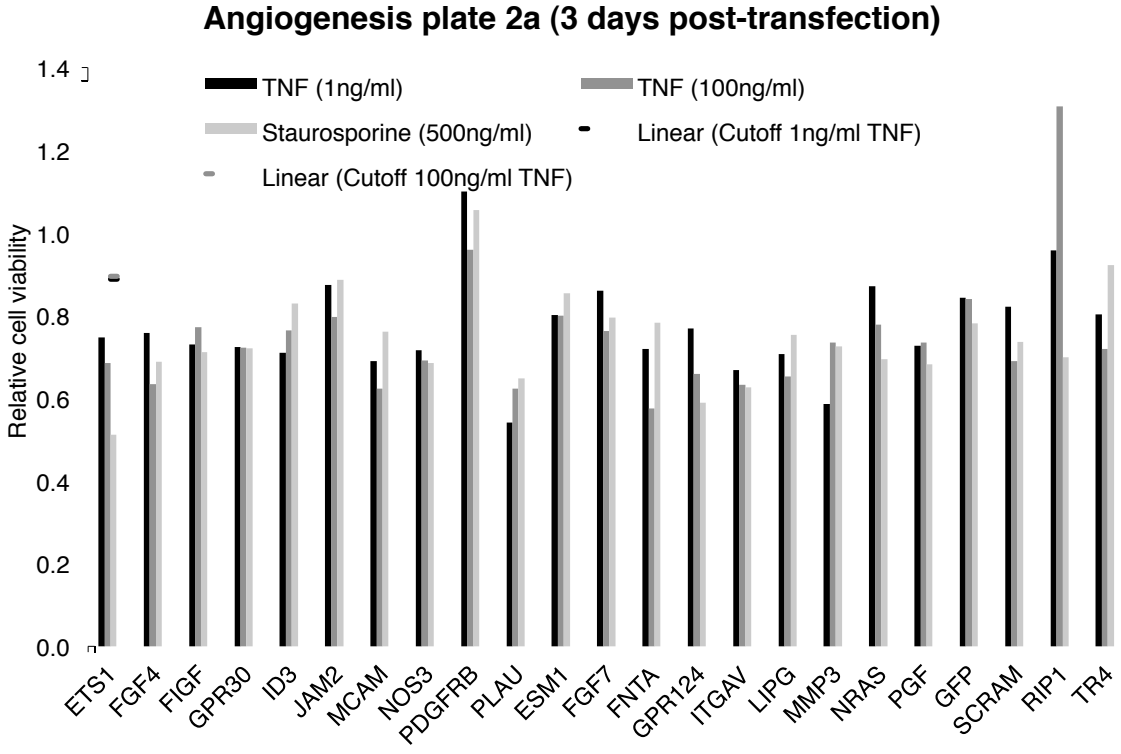
Angiogenesis plate 2a (3 days post-transfection)
TNF (1ng/ml)
TNF (100ng/ml)
Staurosporine (500ng/ml)
Linear (Cutoff 1ng/ml TNF)
Linear (Cutoff 100ng/ml TNF)
Relative cell viability
1.4
1.2
1.0
0.8
0.6
0.4
0.2
0.0
ETS1
FGF4
FIGF
GPR30
ID3
JAM2
MCAM
NOS3
PDGFRB
PLAU
ESM1
FGF7
FNTA
GPR124
ITGAV
LIPG
MMP3
NRAS
PGF
GFP
SCRAM
RIP1
TR4

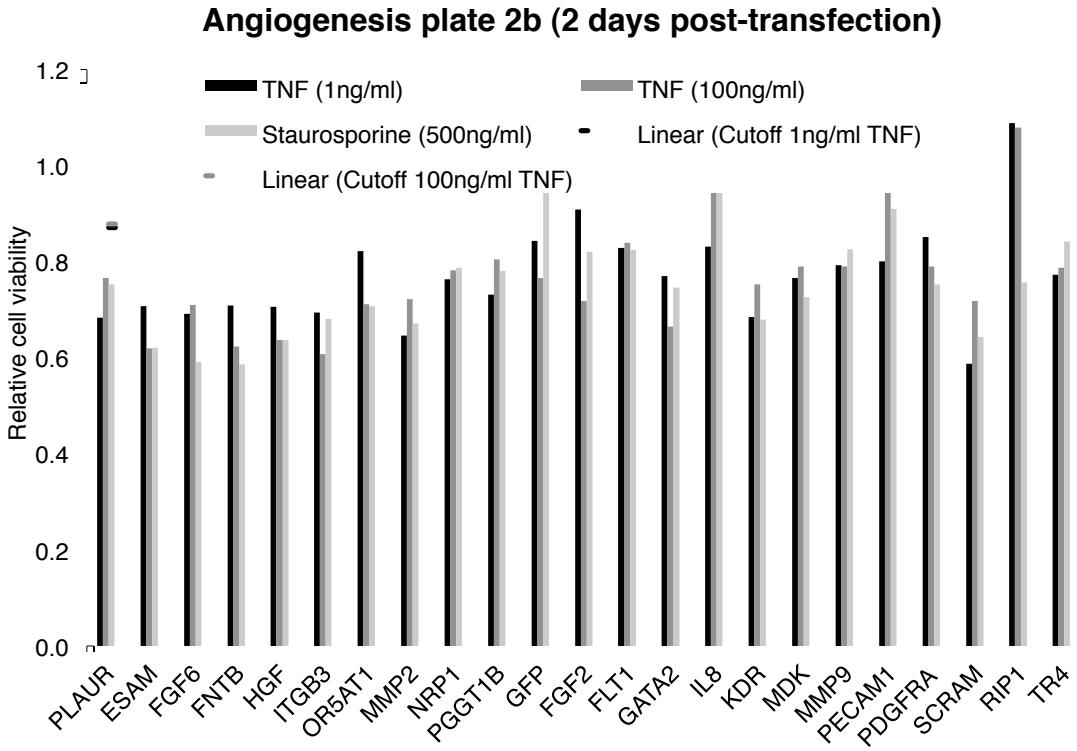
Angiogenesis plate 2b (2 days post-transfection)
TNF (1ng/ml)
TNF (100ng/ml)
Staurosporine (500ng/ml)
Linear (Cutoff 1ng/ml TNF)
Linear (Cutoff 100ng/ml TNF)
Relative cell viability
1.2
1.0
0.8
0.6
0.4
0.2
0.0
PLAUR
ESAM
FGF6
FNTB
HGF
ITGB3
OR5AT1
MMP2
NRP1
PGGT1B
GFP
FGF2
FLT1
GATA2
IL8
KDR
MDK
MMP9
PECAM1
PDGFRA
SCRAM
RIP1
TR4

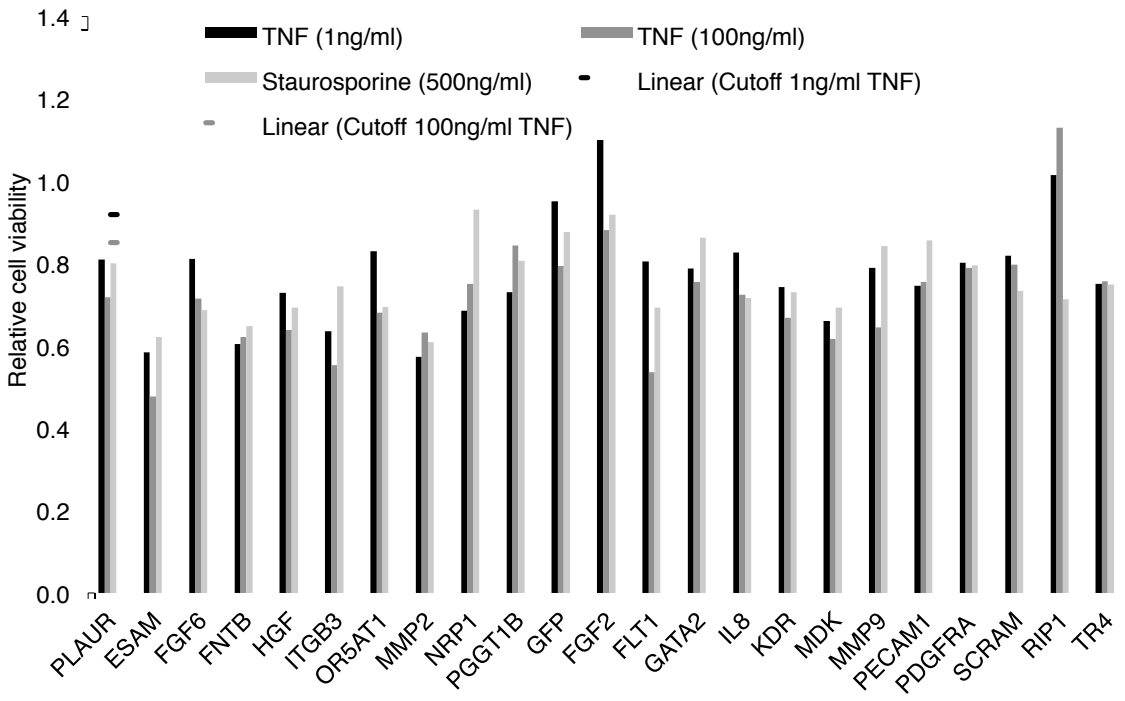
Angiogenesis plate 2b (3 days post-transfection)
TNF (1ng/ml)
TNF (100ng/ml)
Staurosporine (500ng/ml)
Linear (Cutoff 1ng/ml TNF)
Linear (Cutoff 100ng/ml TNF)
Relative cell viability
1.4
1.2
1.0
0.8
0.6
0.4
0.2
0.0
PLAUR
ESAM
FGF6
FNTB
HGF
ITGB3
OR5AT1
MMP2
NRP1
PGGT1B
GFP
FGF2
FLT1
GATA2
IL8
KDR
MDK
MMP9
PECAM1
PDGFRA
SCRAM
RIP1
TR4

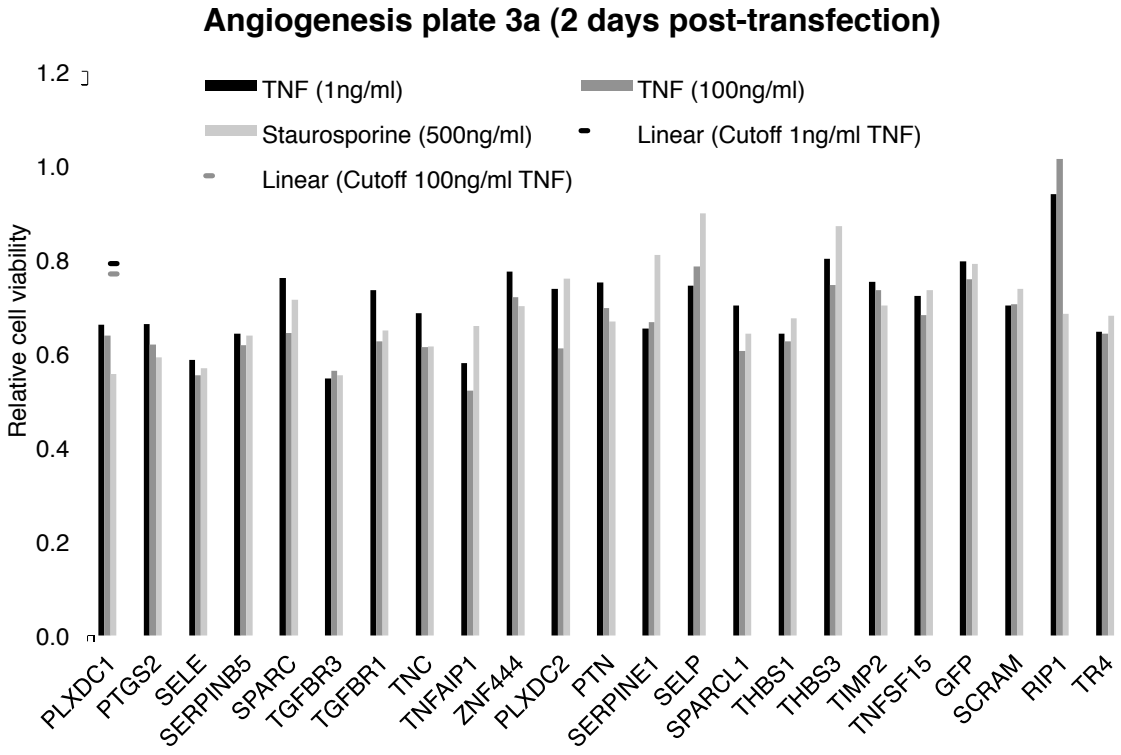
Angiogenesis plate 3a (2 days post-transfection)
TNF (1ng/ml)
TNF (100ng/ml)
Staurosporine (500ng/ml)
Linear (Cutoff 1ng/ml TNF)
Linear (Cutoff 100ng/ml TNF)
Relative cell viability
1.2
1.0
0.8
0.6
0.4
0.2
0.0
PLXDC1
PTGS2
SELE
SERPINB5
SPARC
TGFBR3
TGFBR1
TNC
TNFAIP1
ZNF444
PLXDC2
PTN
SERPINE1
SELP
SPARCL1
THBS1
THBS3
TIMP2
TNFSF15
GFP
SCRAM
RIP1
TR4

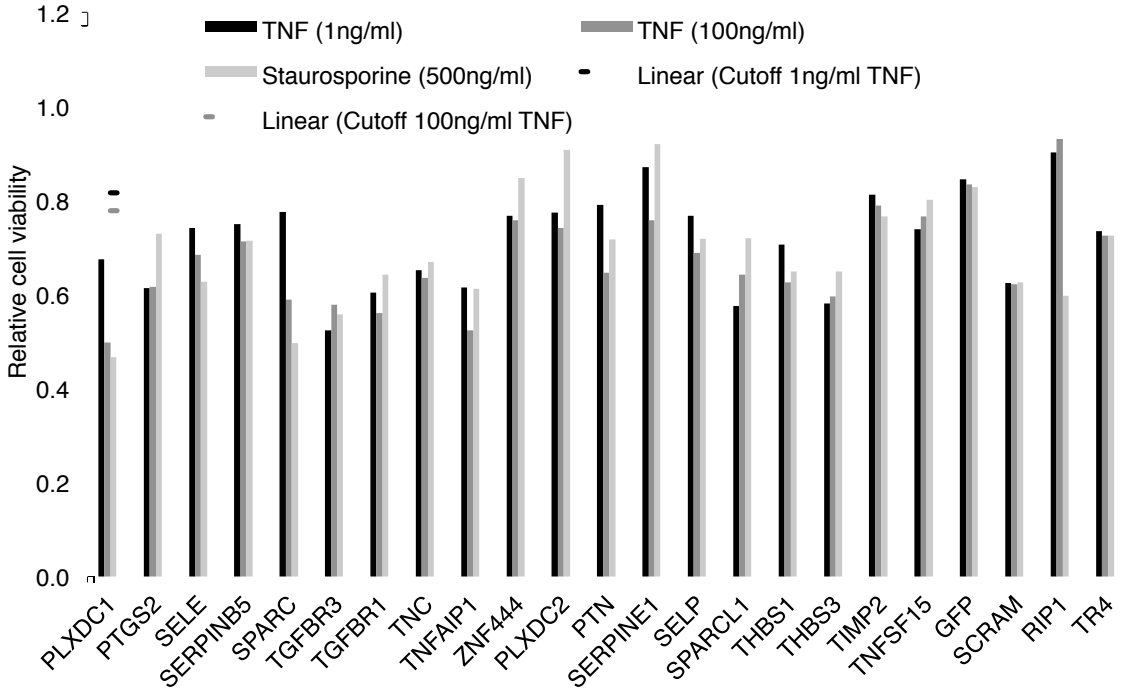
Angiogenesis plate 3a (3 days post-transfection)
TNF (1ng/ml)
TNF (100ng/ml)
Staurosporine (500ng/ml)
Linear (Cutoff 1ng/ml TNF)
Linear (Cutoff 100ng/ml TNF)
Relative cell viability
1.2
1.0
0.8
0.6
0.4
0.2
0.0
PLXDC1
PTGS2
SELE
SERPINB5
SPARC
TGFBR3
TGFBR1
TNC
TNFAIP1
ZNF444
PLXDC2
PTN
SERPINE1
SELP
SPARCL1
THBS1
THBS3
TIMP2
TNFSF15
GFP
SCRAM
RIP1
TR4

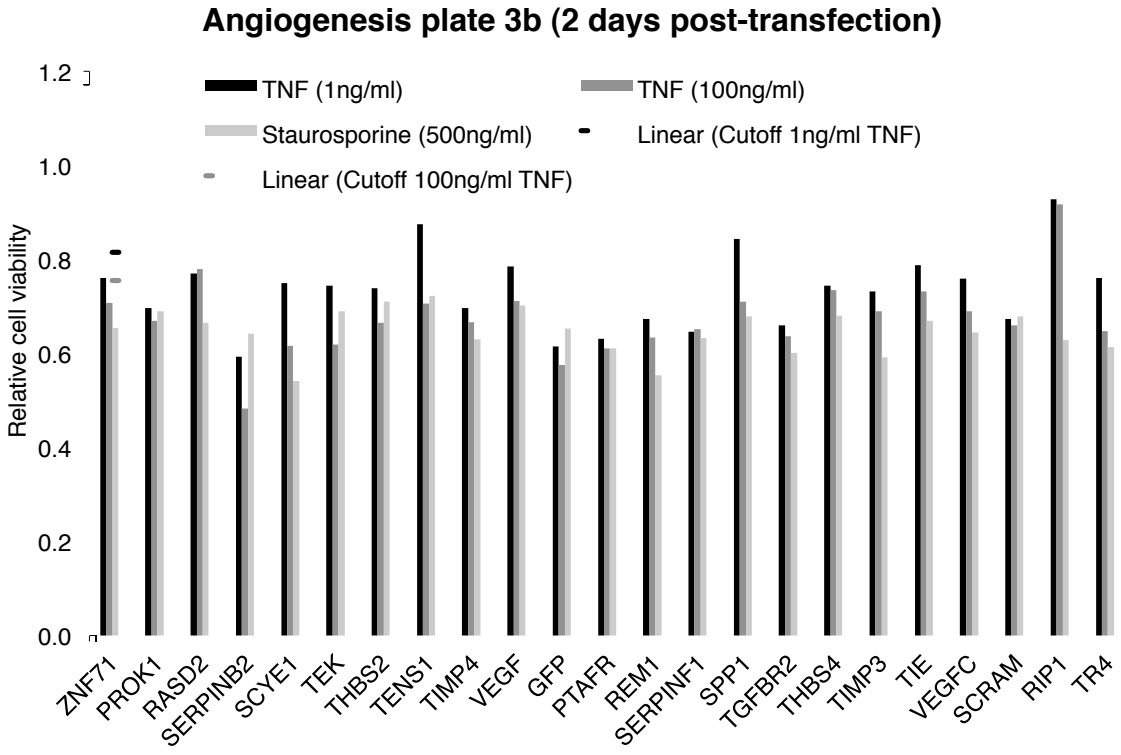
Angiogenesis plate 3b (2 days post-transfection)
TNF (1ng/ml)
TNF (100ng/ml)
Staurosporine (500ng/ml)
Linear (Cutoff 1ng/ml TNF)
Linear (Cutoff 100ng/ml TNF)
Relative cell viability
1.2
1.0
0.8
0.6
0.4
0.2
0.0
ZNF71
PROK1
RASD2
SERPINB2
SCYE1
TEK
THBS2
TENS1
TIMP4
VEGF
GFP
PTAFR
REM1
SERPINF1
SPP1
TGFBR2
THBS4
TIMP3
TIE
VEGFC
SCRAM
RIP1
TR4

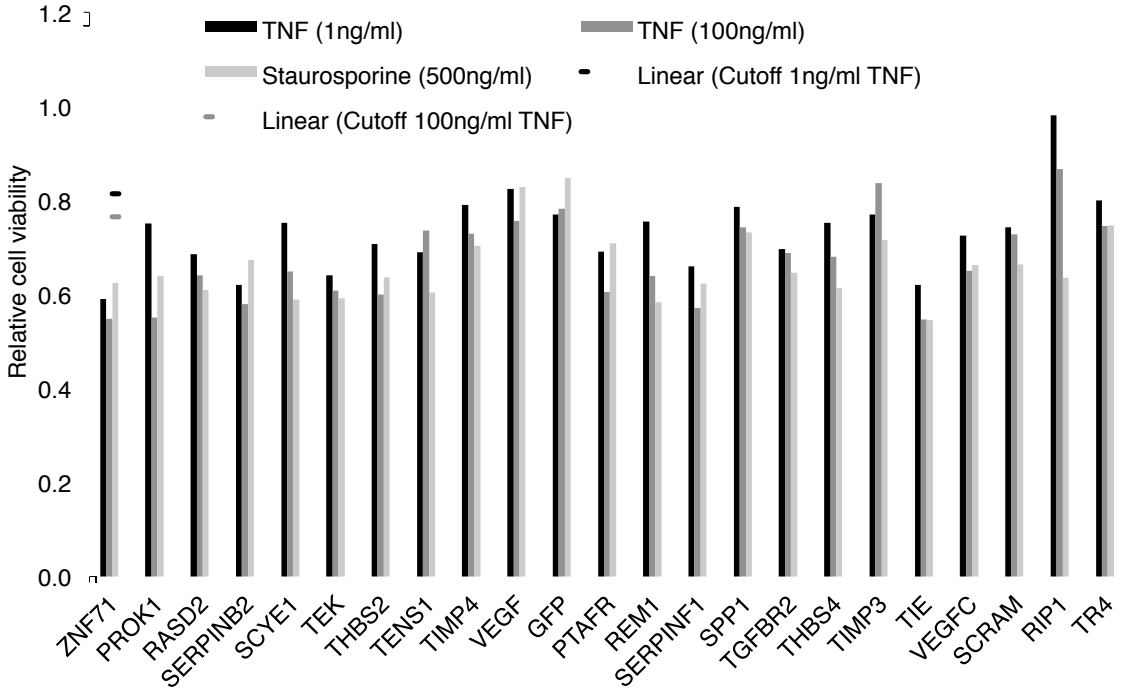
Angiogenesis Plate 3b (3 days post-transfection)
TNF (1ng/ml)
TNF (100ng/ml)
Staurosporine (500ng/ml)
Linear (Cutoff 1ng/ml TNF)
Linear (Cutoff 100ng/ml TNF)
Relative cell viability
1.2
1.0
0.8
0.6
0.4
0.2
0.0
ZNF71
PROK1
RASD2
SERPINB2
SCYE1
TEK
THBS2
TENS1
TIMP4
VEGF
GFP
PTAFR
REM1
SERPINF1
SPP1
TGFBR2
THBS4
TIMP3
TIE
VEGFC
SCRAM
RIP1
TR4

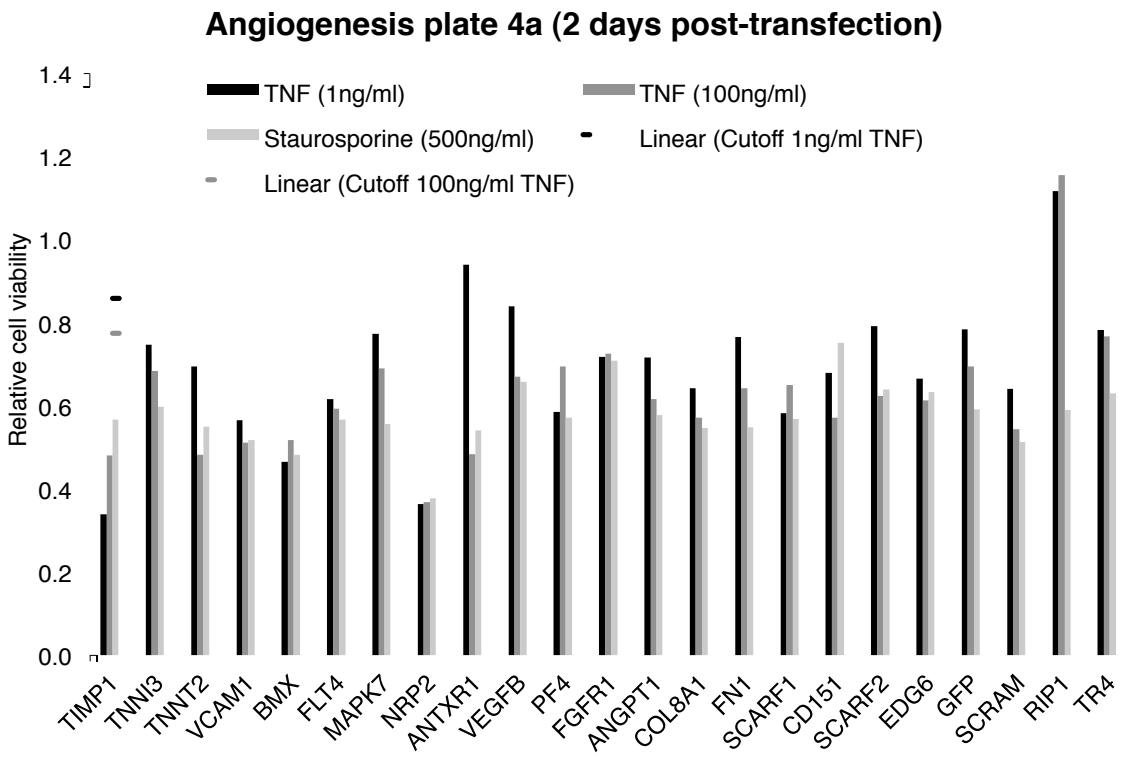
Angiogenesis plate 4a (2 days post-transfection)
TNF (1ng/ml)
TNF (100ng/ml)
Staurosporine (500ng/ml)
Linear (Cutoff 1ng/ml TNF)
Linear (Cutoff 100ng/ml TNF)
Relative cell viability
1.4
1.2
1.0
0.8
0.6
0.4
0.2
0.0
TIMP1
TNNI3
TNNT2
VCAM1
BMX
FLT4
MAPK7
NRP2
ANTXR1
VEGFB
PF4
FGFR1
ANGPT1
COL8A1
FN1
SCARF1
CD151
SCARF2
EDG6
GFP
SCRAM
RIP1
TR4

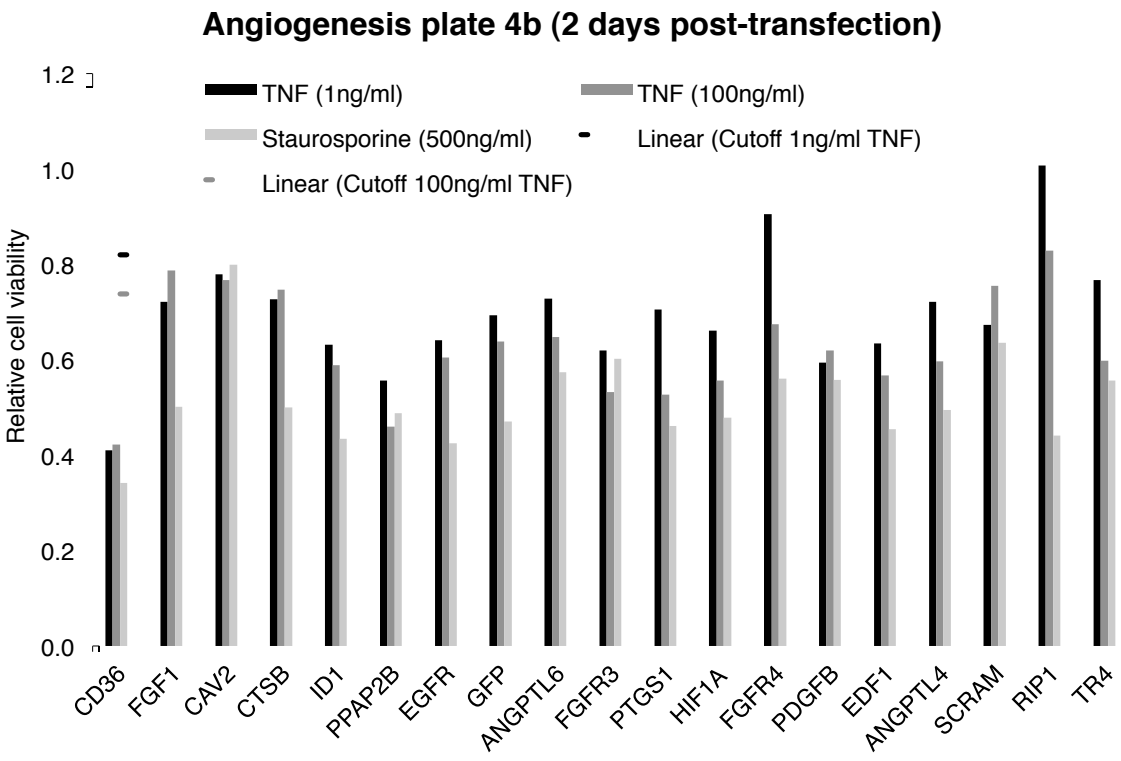
Angiogenesis plate 4b (2 days post-transfection)
TNF (1ng/ml)
TNF (100ng/ml)
Staurosporine (500ng/ml)
Linear (Cutoff 1ng/ml TNF)
Linear (Cutoff 100ng/ml TNF)
Relative cell viability
1.2
1.0
0.8
0.6
0.4
0.2
0.0
CD36
FGF1
CAV2
CTSB
ID1
PPAP2B
EGFR
GFP
ANGPTL6
FGFR3
PTGS1
HIF1A
FGFR4
PDGFB
EDF1
ANGPTL4
SCRAM
RIP1
TR4

REFERENCES

Ahmed, N., M. Zeng, et al. (2011). "The E3 ligase Itch and deubiquitinase Cyld act together to regulate Tak1 and inflammation." Nat Immunol 12(12): 1176-1183.

An, J., D. Mo, et al. (2008). "Inactivation of the CYLD deubiquitinase by HPV E6 mediates hypoxia-induced NF-kappaB activation." Cancer Cell 14(5): 394-407.

Annunziata, C. M., R. E. Davis, et al. (2007). "Frequent engagement of the classical and alternative NF-kappaB pathways by diverse genetic abnormalities in multiple myeloma." Cancer Cell 12(2): 115-130.

Bertrand, M. J., S. Lippens, et al. (2011). "cIAP1/2 are direct E3 ligases conjugating diverse types of ubiquitin chains to receptor interacting proteins kinases 1 to 4 (RIP1-4)." PLoS One 6(9): e22356.

Bertrand, M. J., S. Milutinovic, et al. (2008). "cIAP1 and cIAP2 facilitate cancer cell survival by functioning as E3 ligases that promote RIP1 ubiquitination." Mol Cell 30(6): 689-700.

Bignell, G. R., W. Warren, et al. (2000). "Identification of the familial cylindromatosis tumour-suppressor gene." Nat Genet 25(2): 160-165.

Bonnet, M. C., D. Preukschat, et al. (2011). "The adaptor protein FADD protects epidermal keratinocytes from necroptosis in vivo and prevents skin inflammation." Immunity 35(4): 572-582.

Brummelkamp, T. R., S. M. Nijman, et al. (2003). "Loss of the cylindromatosis tumour suppressor inhibits apoptosis by activating NF-kappaB." Nature 424(6950): 797-801.

Ch'en, I. L., J. S. Tsau, et al. (2011). "Mechanisms of necroptosis in T cells." J Exp Med 208(4): 633-641.

Chae, H. J., J. S. Kang, et al. (2000). "Molecular mechanism of staurosporine-induced apoptosis in osteoblasts." Pharmacol Res 42(4): 373-381.

Challa, S. and F. K. Chan (2010). "Going up in flames: necrotic cell injury and inflammatory diseases." Cell Mol Life Sci 67(19): 3241-3253.

Chan, F. K., H. J. Chun, et al. (2000). "A domain in TNF receptors that mediates ligand-independent receptor assembly and signaling." Science 288(5475): 2351-2354.

Chan, F. K., J. Shisler, et al. (2003). "A role for tumor necrosis factor receptor-2 and receptor-interacting protein in programmed necrosis and antiviral responses." J Biol Chem 278(51): 51613-51621.

Cho, Y. S., S. Challa, et al. (2009). "Phosphorylation-driven assembly of the RIP1-RIP3 complex regulates programmed necrosis and virus-induced inflammation." Cell 137(6): 1112-1123.

Conze, D. B., L. Albert, et al. (2005). "Posttranscriptional downregulation of c-IAP2 by the ubiquitin protein ligase c-IAP1 in vivo." Mol Cell Biol 25(8): 3348-3356.

Degterev, A., J. Hitomi, et al. (2008). "Identification of RIP1 kinase as a specific cellular target of necrostatins." Nat Chem Biol 4(5): 313-321.

Degterev, A., Z. Huang, et al. (2005). "Chemical inhibitor of nonapoptotic cell death with therapeutic potential for ischemic brain injury." Nat Chem Biol 1(2): 112-119.

Deng, W. G., H. Kawashima, et al. (2007). "Synergistic tumor suppression by coexpression of FUS1 and p53 is associated with down-regulation of murine double minute-2 and activation of the apoptotic protease-activating factor 1-dependent apoptotic pathway in human non-small cell lung cancer cells." Cancer Res 67(2): 709-717.

Deng, W. G., G. Wu, et al. (2008). "Enhancement of antitumor activity of cisplatin in human lung cancer cells by tumor suppressor FUS1." Cancer Gene Ther 15(1): 29-39.

Dynek, J. N., T. Goncharov, et al. (2010). "c-IAP1 and UbcH5 promote K11-linked polyubiquitination of RIP1 in TNF signalling." EMBO J 29(24): 4198-4209.

Ea, C. K., L. Deng, et al. (2006). "Activation of IKK by TNFalpha requires site-specific ubiquitination of RIP1 and polyubiquitin binding by NEMO." Mol Cell 22(2): 245-257.

Eckelman, B. P. and G. S. Salvesen (2006). "The human anti-apoptotic proteins cIAP1 and cIAP2 bind but do not inhibit caspases." J Biol Chem 281(6): 3254-3260.

Enari, M., H. Sakahira, et al. (1998). "A caspase-activated DNase that degrades DNA during apoptosis, and its inhibitor ICAD." Nature 391(6662): 43-50.

Espinosa, L., S. Cathelin, et al. (2010). "The Notch/Hes1 pathway sustains NF-kappaB activation through CYLD repression in T cell leukemia." Cancer Cell 18(3): 268-281.

Feoktistova, M., P. Geserick, et al. (2011). "cIAPs Block Ripoptosome Formation, a RIP1/Caspase-8 Containing Intracellular Cell Death Complex Differentially Regulated by cFLIP Isoforms." Molecular Cell 43(3): 449-463.

Friedman, C. S., M. A. O'Donnell, et al. (2008). "The tumour suppressor CYLD is a negative regulator of RIG-I-mediated antiviral response." EMBO Rep 9(9): 930-936.

Fujikura, D., M. Ito, et al. (2012). "CLIPR-59 regulates TNF-alpha-induced apoptosis by controlling ubiquitination of RIP1." Cell Death Dis 3: e264.

Gao, J., L. Huo, et al. (2008). "The tumor suppressor CYLD regulates microtubule dynamics and plays a role in cell migration." J Biol Chem 283(14): 8802-8809.

Gentle, I. E., W. W. Wong, et al. (2011). "In TNF-stimulated cells, RIPK1 promotes cell survival by stabilizing TRAF2 and cIAP1, which limits induction of non-canonical NF-kappaB and activation of caspase-8." J Biol Chem 286(15): 13282-13291.

Gunther, C., E. Martini, et al. (2011). "Caspase-8 regulates TNF-alpha-induced epithelial necroptosis and terminal ileitis." Nature 477(7364): 335-339.

He, S., Y. Liang, et al. (2011). "Toll-like receptors activate programmed necrosis in macrophages through a receptor-interacting kinase-3-mediated pathway." Proc Natl Acad Sci U S A 108(50): 20054-20059.

He, S., L. Wang, et al. (2009). "Receptor interacting protein kinase-3 determines cellular necrotic response to TNF-alpha." Cell 137(6): 1100-1111.

Hellerbrand, C., E. Bumes, et al. (2007). "Reduced expression of CYLD in human colon and hepatocellular carcinomas." Carcinogenesis 28(1): 21-27.

Hitomi, J., D. E. Christofferson, et al. (2008). "Identification of a molecular signaling network that regulates a cellular necrotic cell death pathway." Cell 135(7): 1311-1323.

Holler, N., R. Zaru, et al. (2000). "Fas triggers an alternative, caspase-8-independent cell death pathway using the kinase RIP as effector molecule." Nat Immunol 1(6): 489-495.

Hovelmeyer, N., F. T. Wunderlich, et al. (2007). "Regulation of B cell homeostasis and activation by the tumor suppressor gene CYLD." J Exp Med 204(11): 2615-2627.

Hutti, J. E., R. R. Shen, et al. (2009). "Phosphorylation of the tumor suppressor CYLD by the breast cancer oncogene IKKepsilon promotes cell transformation." Mol Cell 34(4): 461-472.

Jin, W., M. Chang, et al. (2008). "Deubiquitinating enzyme CYLD negatively regulates RANK signaling and osteoclastogenesis in mice." J Clin Invest 118(5): 1858-1866.

Kaiser, W. J., J. W. Upton, et al. (2011). "RIP3 mediates the embryonic lethality of caspase-8-deficient mice." Nature 471(7338): 368-372.

Kanayama, A., R. B. Seth, et al. (2004). "TAB2 and TAB3 activate the NF-kappaB pathway through binding to polyubiquitin chains." Mol Cell 15(4): 535-548.

Kang, T. B., G. S. Oh, et al. (2008). "Mutation of a self-processing site in caspase-8 compromises its apoptotic but not its nonapoptotic functions in bacterial artificial chromosome-transgenic mice." J Immunol 181(4): 2522-2532.

Kang, T. B., S. H. Yang, et al. (2013). "Caspase-8 blocks kinase RIPK3-mediated activation of the NLRP3 inflammasome." Immunity 38(1): 27-40.

Kawahara, A., Y. Ohsawa, et al. (1998). "Caspase-independent cell killing by Fas-associated protein with death domain." J Cell Biol 143(5): 1353-1360.

Keats, J. J., R. Fonseca, et al. (2007). "Promiscuous mutations activate the noncanonical NF-kappaB pathway in multiple myeloma." Cancer Cell 12(2): 131-144.

Komander, D., C. J. Lord, et al. (2008). "The structure of the CYLD USP domain explains its specificity for Lys63-linked polyubiquitin and reveals a B box module." Mol Cell 29(4): 451-464.

Komander, D., F. Reyes-Turcu, et al. (2009). "Molecular discrimination of structurally equivalent Lys 63-linked and linear polyubiquitin chains." EMBO Rep 10(5): 466-473.

Kovalenko, A., C. Chable-Bessia, et al. (2003). "The tumour suppressor CYLD negatively regulates NF-kappaB signalling by deubiquitination." Nature 424(6950): 801-805.

Laster, S. M., J. G. Wood, et al. (1988). "Tumor necrosis factor can induce both apoptic and necrotic forms of cell lysis." J Immunol 141(8): 2629-2634.

Lee, A. J., X. Zhou, et al. (2010). "Regulation of natural killer T-cell development by deubiquitinase CYLD." EMBO J 29(9): 1600-1612.

Legarda-Addison, D., H. Hase, et al. (2009). "NEMO/IKKgamma regulates an early NF-kappaB-independent cell-death checkpoint during TNF signaling." Cell Death Differ 16(9): 1279-1288.

Li, G., H. Kawashima, et al. (2011). "Frequent absence of tumor suppressor FUS1 protein expression in human bone and soft tissue sarcomas." Anticancer Res 31(1): 11-21.

Li, J., T. McQuade, et al. (2012). "The RIP1/RIP3 necrosome forms a functional amyloid signaling complex required for programmed necrosis." Cell 150(2): 339-350.

Li, M. and A. A. Beg (2000). "Induction of necrotic-like cell death by tumor necrosis factor alpha and caspase inhibitors: novel mechanism for killing virus-infected cells." J Virol 74(16): 7470-7477.

Li, W., Z. Chen, et al. (2011). "PP2A inhibitors induce apoptosis in pancreatic cancer cell line PANC-1 through persistent phosphorylation of IKKalpha and sustained activation of the NF-kappaB pathway." Cancer Lett 304(2): 117-127.

Lin, J., T. Sun, et al. (2007). "Oncogenic activation of c-Abl in non-small cell lung cancer cells lacking FUS1 expression: inhibition of c-Abl by the tumor suppressor gene product Fus1." Oncogene 26(49): 6989-6996.

Lin, Y., S. Choksi, et al. (2004). "Tumor necrosis factor-induced nonapoptotic cell death requires receptor-interacting protein-mediated cellular reactive oxygen species accumulation." J Biol Chem 279(11): 10822-10828.

Lu, J. V., B. M. Weist, et al. (2011). "Complementary roles of Fas-associated death domain (FADD) and receptor interacting protein kinase-3 (RIPK3) in T-cell homeostasis and antiviral immunity." Proc Natl Acad Sci U S A 108(37): 15312-15317.

Mahoney, D. J., H. H. Cheung, et al. (2008). "Both cIAP1 and cIAP2 regulate TNFalpha-mediated NF-kappaB activation." Proc Natl Acad Sci U S A 105(33): 11778-11783.

Mahul-Mellier, A. L., E. Pazarentzos, et al. (2012). "De-ubiquitinating protease USP2a targets RIP1 and TRAF2 to mediate cell death by TNF." Cell Death Differ 19(5): 891-899.

Masoumi, K. C., G. Shaw-Hallgren, et al. (2011). "Tumor Suppressor Function of CYLD in Nonmelanoma Skin Cancer." J Skin Cancer 2011: 614097.

Massoumi, R., K. Chmielarska, et al. (2006). "Cyld inhibits tumor cell proliferation by blocking Bcl-3-dependent NF-kappaB signaling." Cell 125(4): 665-677.

Massoumi, R., S. Kuphal, et al. (2009). "Down-regulation of CYLD expression by Snail promotes tumor progression in malignant melanoma." J Exp Med 206(1): 221-232.

Micheau, O. and J. Tschopp (2003). "Induction of TNF receptor I-mediated apoptosis via two sequential signaling complexes." Cell 114(2): 181-190.

Nenci, A., C. Becker, et al. (2007). "Epithelial NEMO links innate immunity to chronic intestinal inflammation." Nature 446(7135): 557-561.

O'Donnell, M. A., H. Hase, et al. (2012). "NEMO inhibits programmed necrosis in an NFkappaB-independent manner by restraining RIP1." PLoS One 7(7): e41238.

O'Donnell, M. A., D. Legarda-Addison, et al. (2007). "Ubiquitination of RIP1 regulates an NF-kappaB-independent cell-death switch in TNF signaling." Curr Biol 17(5): 418-424.

O'Donnell, M. A., E. Perez-Jimenez, et al. (2011). "Caspase 8 inhibits programmed necrosis by processing CYLD." Nat Cell Biol 13(12): 1437-1442.

Oberst, A., C. P. Dillon, et al. (2011). "Catalytic activity of the caspase-8-FLIP(L) complex inhibits RIPK3-dependent necrosis." Nature 471(7338): 363-367.

Oliveira, J. B. and S. Gupta (2008). "Disorders of apoptosis: mechanisms for autoimmunity in primary immunodeficiency diseases." J Clin Immunol 28 Suppl 1: S20-28.

Osborn, S. L., G. Diehl, et al. (2010). "Fas-associated death domain (FADD) is a negative regulator of T-cell receptor-mediated necroptosis." Proc Natl Acad Sci U S A 107(29): 13034-13039.

Oshima, S., E. E. Turer, et al. (2009). "ABIN-1 is a ubiquitin sensor that restricts cell death and sustains embryonic development." Nature 457(7231): 906-909.

Reed, J. C. (2006). "Drug insight: cancer therapy strategies based on restoration of endogenous cell death mechanisms." Nat Clin Pract Oncol 3(7): 388-398.

Reiley, W., M. Zhang, et al. (2004). "Negative regulation of JNK signaling by the tumor suppressor CYLD." J Biol Chem 279(53): 55161-55167.

Reiley, W., M. Zhang, et al. (2005). "Regulation of the deubiquitinating enzyme CYLD by IkappaB kinase gamma-dependent phosphorylation." Mol Cell Biol 25(10): 3886-3895.

Reiley, W. W., W. Jin, et al. (2007). "Deubiquitinating enzyme CYLD negatively regulates the ubiquitin-dependent kinase Tak1 and prevents abnormal T cell responses." J Exp Med 204(6): 1475-1485.

Rock, K. L., J. J. Lai, et al. (2011). "Innate and adaptive immune responses to cell death." Immunol Rev 243(1): 191-205.

Saito, K., T. Kigawa, et al. (2004). "The CAP-Gly domain of CYLD associates with the proline-rich sequence in NEMO/IKKgamma." Structure 12(9): 1719-1728.

Skaletskaya, A., L. M. Bartle, et al. (2001). "A cytomegalovirus-encoded inhibitor of apoptosis that suppresses caspase-8 activation." Proc Natl Acad Sci U S A 98(14): 7829-7834.

Skaug, B., J. Chen, et al. (2011). "Direct, noncatalytic mechanism of IKK inhibition by A20." Mol Cell 44(4): 559-571.

Srinivasula, S. M., R. Hegde, et al. (2001). "A conserved XIAP-interaction motif in caspase-9 and Smac/DIABLO regulates caspase activity and apoptosis." Nature 410(6824): 112-116.

Srokowski, C. C., J. Masri, et al. (2009). "Naturally occurring short splice variant of CYLD positively regulates dendritic cell function." Blood 113(23): 5891-5895.

Staal, J., Y. Driege, et al. (2011). "T-cell receptor-induced JNK activation requires proteolytic inactivation of CYLD by MALT1." EMBO J 30(9): 1742-1752.

Stegmeier, F., M. E. Sowa, et al. (2007). "The tumor suppressor CYLD regulates entry into mitosis." Proc Natl Acad Sci U S A 104(21): 8869-8874.

Sun, L., J. Gao, et al. (2010). "Tumour suppressor CYLD is a negative regulator of the mitotic kinase Aurora-B." J Pathol 221(4): 425-432.

Sun, L., H. Wang, et al. (2012). "Mixed lineage kinase domain-like protein mediates necrosis signaling downstream of RIP3 kinase." Cell 148(1-2): 213-227.

Sun, S. C. (2010). "CYLD: a tumor suppressor deubiquitinase regulating NF-kappaB activation and diverse biological processes." Cell Death Differ 17(1): 25-34.

Takeuchi, M., M. Rothe, et al. (1996). "Anatomy of TRAF2. Distinct domains for nuclear factor-kappaB activation and association with tumor necrosis factor signaling proteins." J Biol Chem 271(33): 19935-19942.

Temkin, V., Q. Huang, et al. (2006). "Inhibition of ADP/ATP exchange in receptor-interacting protein-mediated necrosis." Mol Cell Biol 26(6): 2215-2225.

Tenev, T., K. Bianchi, et al. (2011). "The Ripoptosome, a signaling platform that assembles in response to genotoxic stress and loss of IAPs." Mol Cell 43(3): 432-448.

Trompouki, E., E. Hatzivassiliou, et al. (2003). "CYLD is a deubiquitinating enzyme that negatively regulates NF-kappaB activation by TNFR family members." Nature 424(6950): 793-796.

Uno, F., J. Sasaki, et al. (2004). "Myristoylation of the fus1 protein is required for tumor suppression in human lung cancer cells." Cancer Res 64(9): 2969-2976.

Upton, J. W., W. J. Kaiser, et al. (2008). "Cytomegalovirus M45 cell death suppression requires receptor-interacting protein (RIP) homotypic interaction motif (RHIM)-dependent interaction with RIP1." J Biol Chem 283(25): 16966-16970.

Upton, J. W., W. J. Kaiser, et al. (2010). "Virus inhibition of RIP3-dependent necrosis." Cell Host Microbe 7(4): 302-313.

Upton, J. W., W. J. Kaiser, et al. (2012). "DAI/ZBP1/DLM-1 complexes with RIP3 to mediate virus-induced programmed necrosis that is targeted by murine cytomegalovirus vIRA." Cell Host Microbe 11(3): 290-297.

Uzhachenko, R., N. Issaeva, et al. (2012). "Tumour suppressor Fus1 provides a molecular link between inflammatory response and mitochondrial homeostasis." J Pathol 227(4): 456-469.

Vanden Berghe, T., G. van Loo, et al. (2004). "Differential signaling to apoptotic and necrotic cell death by Fas-associated death domain protein FADD." J Biol Chem 279(9): 7925-7933.

Vandenabeele, P., L. Galluzzi, et al. (2010). "Molecular mechanisms of necroptosis: an ordered cellular explosion." Nat Rev Mol Cell Biol 11(10): 700-714.

Vanlangenakker, N., T. Vanden Berghe, et al. (2011). "cIAP1 and TAK1 protect cells from TNF-induced necrosis by preventing RIP1/RIP3-dependent reactive oxygen species production." Cell Death Differ 18(4): 656-665.

Varfolomeev, E., T. Goncharov, et al. (2008). "c-IAP1 and c-IAP2 are critical mediators of tumor necrosis factor alpha (TNFalpha)-induced NF-kappaB activation." J Biol Chem 283(36): 24295-24299.

Vercammen, D., R. Beyaert, et al. (1998). "Inhibition of caspases increases the sensitivity of L929 cells to necrosis mediated by tumor necrosis factor." J Exp Med 187(9): 1477-1485.

Vince, J. E., D. Pantaki, et al. (2009). "TRAF2 must bind to cellular inhibitors of apoptosis for tumor necrosis factor (tnf) to efficiently activate nf-{kappa}b and to prevent tnf-induced apoptosis." J Biol Chem 284(51): 35906-35915.

Wang, L., F. Du, et al. (2008). "TNF-alpha induces two distinct caspase-8 activation pathways." Cell 133(4): 693-703.

Wang, Z., H. Jiang, et al. (2012). "The mitochondrial phosphatase PGAM5 functions at the convergence point of multiple necrotic death pathways." Cell 148(1-2): 228-243.

Welz, P. S., A. Wullaert, et al. (2011). "FADD prevents RIP3-mediated epithelial cell necrosis and chronic intestinal inflammation." Nature 477(7364): 330-334.

Wickstrom, S. A., K. C. Masoumi, et al. (2010). "CYLD negatively regulates cell-cycle progression by inactivating HDAC6 and increasing the levels of acetylated tubulin." EMBO J 29(1): 131-144.

Wright, A., W. W. Reiley, et al. (2007). "Regulation of early wave of germ cell apoptosis and spermatogenesis by deubiquitinating enzyme CYLD." Dev Cell 13(5): 705-716.

Xu, G., X. Tan, et al. (2010). "Ubiquitin-specific peptidase 21 inhibits tumor necrosis factor alpha-induced nuclear factor kappaB activation via binding to and deubiquitinating receptor-interacting protein 1." J Biol Chem 285(2): 969-978.

Xu, M., B. Skaug, et al. (2009). "A ubiquitin replacement strategy in human cells reveals distinct mechanisms of IKK activation by TNFalpha and IL-1beta." Mol Cell 36(2): 302-314.

Young, A. L., R. Kellermayer, et al. (2006). "CYLD mutations underlie Brooke-Spiegler, familial cylindromatosis, and multiple familial trichoepithelioma syndromes." Clin Genet 70(3): 246-249.

Zhang, D. W., J. Shao, et al. (2009). "RIP3, an energy metabolism regulator that switches TNF-induced cell death from apoptosis to necrosis." Science 325(5938): 332-336.

Zhang, H., X. Zhou, et al. (2011). "Functional complementation between FADD and RIP1 in embryos and lymphocytes." Nature 471(7338): 373-376.

Zhang, M., A. J. Lee, et al. (2011). "Regulation of antiviral innate immunity by deubiquitinase CYLD." Cell Mol Immunol 8(6): 502-504.

Zhao, J., S. Jitkaew, et al. (2012). "Mixed lineage kinase domain-like is a key receptor interacting protein 3 downstream component of TNF-induced necrosis." Proc Natl Acad Sci U S A 109(14): 5322-5327.